SSD

SCIENCE FOR A SUSTAINABLE DEVELOPMENT

BELGIAN OCEAN ENERGY ASSESSMENT

"BOREAS"

P. MATHYS, J. DE ROUCK, L. FERNANDEZ, J. MONBALLIU,
D. VAN DEN EYNDE, R. DELGADO, A. DUJARDIN

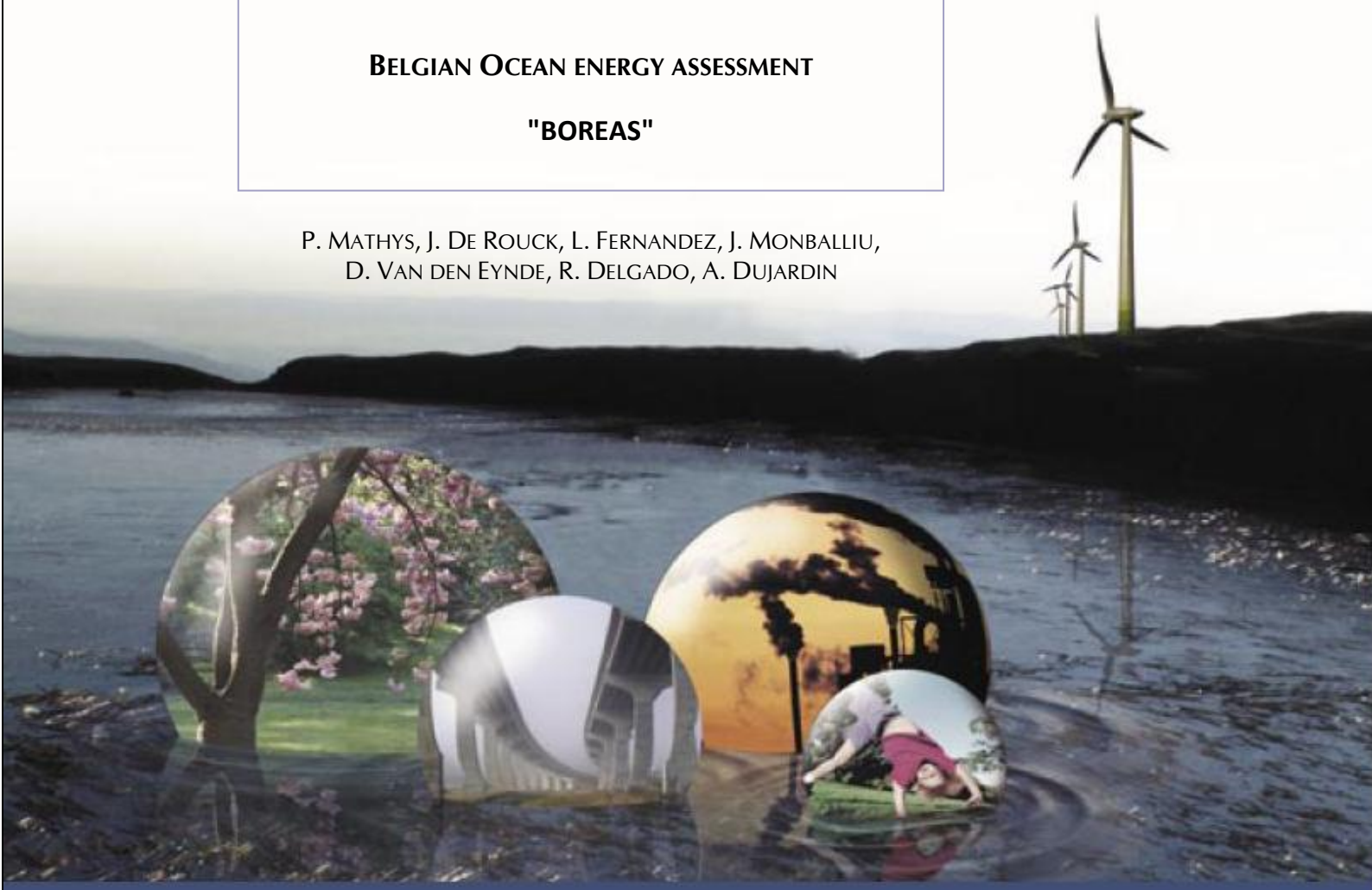

ENERGY

TRANSPORT AND MOBILITY

AGRO-FOOD

HEALTH AND ENVIRONMENT

CLIMATE

BIODIVERSITY

ATMOSPHERE AND TERRESTRIAL AND MARINE ECOSYSTEMS

TRANSVERSAL ACTIONS

.be

SCIENCE FOR A SUSTAINABLE DEVELOPMENT

(SSD)

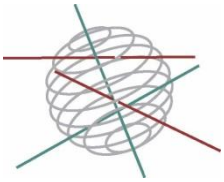

North Sea

FINAL REPORT

BELGIAN OCEAN ENERGY ASSESSMENT

BOREAS

SD/NS/13

Promotors

Julien De Rouck
UGent, Technologiepark 904
9052 Zwijnaarde

Jaak Monbaliu
K.U.Leuven,
Kasteelpark Arenberg 40, postbus 2448
3001 Heverlee

Dries Van den Eynde
Management Unit of the North Sea Mathematical Models
Gulledelle 100, B-1200 Brussel

Toon Verwaest
Flanders Hydraulics Research
Berchermlei 115
2140 Borgerhout

Authors
Mathys Pieter (UGent)
De Rouck Julien (UGent)
Fernandez Leandro (KULeuven)
Monbaliu Jaak (KULeuven)
Van den Eynde Dries (MUMM)
Delgado Rosalia (Flanders Hydraulics Research)
Dujardin Arvid (Flanders Hydraulics Research)

The authors were supported by the following contributors:
Muñoz Maria Liste (KULeuven)
Komijani Homayoon (KULeuven)
Loffredo Layla (KULeuven)
Ozer José (MUMM)
Vanlede Joris (Flanders Hydraulics Research)
Verwaest Toon (Flanders Hydraulics Research)
Mostaert Frank (Flanders Hydraulics Research)

D/2012/1191/11
Published in 2012 by the Belgian Science Policy Office
Avenue Louise 231
Louizalaan 231
B-1050 Brussels
Belgium
Tel: +32 (0)2 238 34 11 – Fax: +32 (0)2 230 59 12
http://www.belspo.be

Contact person: M. David Cox
+32 (0)2 238 34 03

Belgian Ocean Energy Assessment (BOREAS). Final Report. P. Mathys, J. De Rouck, L. Fernandez, J. Monballiu, D. Van den Eynde, R. Delgado, A. Dujardin - Brussels : Belgian Science Policy Office 2012 – 171 p. (Research Programme Science for a Sustainable Development).

Table of Contents

List of Figures

1 Introduction and scope

1.1 Rationale behind the BOREAS project

The new Climate Action – Energy for a Changing World of the European Commission proposed several measures to fight climate change and promote renewable energy. One of those measures includes legally enforceable targets to increase the share of renewable in the energy mix of each Member State. The target of the renewable share in the European Union is set to 20% by the year 2020, and the European Commission has set individual targets for every Member State. In the case of Belgium, the target is set to 13%, whereas the renewable share in 2008 was only 3.3 % (Eurostat, 2010).

Basically, this is the consequence of the (post)-Kyoto-agreements. But apart from this, consumption of energy is increasing year by year whilst it is proving increasingly difficult to find and extract sufficient fossil fuels to cover the annual increase in consumption. Contributions to the share of renewables are required from various sources, such as biomass, wind, hydropower and solar energy. In particular, offshore wind has boosted during recent years.

Offshore wind energy is now at a stage where it is becoming a competitive energy source. The cost of power generated from onshore wind farms in the most interesting locations is now reaching the level of most fossil fuel sources. During recent years a number of wind farms have been developed in shallow seas around the European coasts. Offshore developments give larger sites and the advantages of economies of scale. Offshore sites also have the advantage of being “out of sight, out of mind“, in addition to providing higher and more regular wind energy resources. However, offshore wind developments are facing a number of technological challenges specifically related to turbine tower foundations, and maintenance of the installations.

Ocean energy is an unexploited source of offshore energy, and is getting more attention of technology developers and policy makers. The main forms of ocean energy are wave energy and tidal current energy. They both have several advantages over wind energy such as: higher energy density, more predictable resources and less visible than windmill farms. Wave energy is also more persistent than wind: waves will transfer energy from windier areas to coastal zones and remain long after the wind has dropped. Tidal current energy is extremely predictable, as the most important driving force is the astronomical tide.

Consequently, a number of different technologies for wave and tidal current energy conversion have been developed, but up to now few of them have resulted in commercial development beyond the prototype stage. BOREAS (Belgian Ocean Energy Assessment) made an overview of the current technologies, and their possible applications on the Belgian Part of the North Sea (BPNS).

1.2 BOREAS project

1.2.1 Main themes

So far, the OPTIEP report (Mathys *et al.* 2010), also funded by BELSPO, was the only study to made a first assessment of the resource of the wave and tidal current energy climate on the entire (BPNS). BOREAS is building further on this study and aims at being a comprehensive study regarding wave and tidal energy applications on the BPNS.

This project assessed this potential and involved 5 main themes:

- Making an overview of existing wave or tidal current converters ("long-list") based on scientific literature and publically available information provided by the device developers or third parties such as, Ocean Marine Energy Centre (EMEC), Ocean Energy Systems Implementing Agreement (IEA-OES), Electric Power Research Institute (EPRI) and The Carbon Trust. A selection of the most appropriate converters for the specific conditions on the BPNS ("short-list") will be discussed in detail.
- Assessing the wave and tidal current climate, and hence the *available* potential. This assessment will be based on numerical results from the coupled WAM-COHERENS model, that allows both wave and tidal current modelling. Based on a 10 year hind cast, it will be possible to determine yearly, seasonally and monthly variations. Furthermore, the results will be verified against other numerical models (both for wave and tidal energy).
- Selection of interesting sites. Based on the current or expected space claims on the BPNS (either fixed, such as navigation ways or non-fixed such as fishery) and the knowledge of the *available* ocean energy potential, a selection and description of the most promising sites on the BPNS can be made.
- Assessing the *extractable* potential, based on the limitations of the converters (the "short-list") and the optimal sites. Starting from the extractable potential, an estimation of the cost of the electricity for several converters can be established. Based on the extractable potential, a possible synergy between offshore wind, wind and/or tidal current energy can be assessed.
- Further recommendations for the further deployment and potential exploitation of wave and tidal current energy on the BPNS.

UGent Afdeling Weg- en Waterbouwkunde (hereafter 'AWW') was the overall coordinator of the BOREAS-project. Together with the expertise of the Management Unit of the North Sea Mathematical Models (hereafter 'MUMM'), the Katholieke Universiteit Leuven (hereafter 'KUL') and Flanders Hydraulics Research (hereafter 'FHR'), the project consortium can present a broad expertise in hydrodynamic knowledge.

Every individual Work Package (hereafter 'WP') was led by a so called WP-leader, who was the contractor and main responsible for a specific task. Every WP also had at least one WP-reviser. The task of the WP-reviser was mainly to internally verify the methodology and results (Figure 1).

The numerical modelling with the state-of-the-art coupled WAM-COHERENS and SWAN-COHERENS models (operated by K.U.Leuven and MUMM) formed the core of the assessment of the potential ocean energy. The prefix 'coupled' indicates the fact that the wave models SWAN and WAM interacted in both ways with the hydrodynamic model COHERENS. The numerical approach was clearly the most appropriate, as it could provide a continuous and coherent dataset, both in time and in space.

The wave model WAM used a grid of approximately 1 km by 1 km, which is quite coarse in the near-shore area. It is clear that this near-shore area was quite interesting, since visual nuisance of wave and tidal current energy converters is not an issue compared to windmill farms. So, a complementary numerical model or method to quantify the wave climate in the near-shore was used. These complementary methods or numerical models were executed by the project partner FHR. In order to verify the near-shore wave climate (ranging from approximately 20km offshore to the nearshore region), FHR operated the so-called Transformation Matrix.

The hydrodynamic model COHERENS was not optimized for the Scheldt Estuary, as the grid is too coarse, not curvilinear and the model physics did not take into account the salt gradient due to the fresh water discharges. Once again, a complementary numerical model or method, which was capable of describing the local effects in the Scheldt Estuary was used. In order to verify the tidal current climate in the Scheldt-Estuary, FHR operates the hydrodynamic-morphological Long-Term-Vision Mud (LTV Mud) model.

The model results were then processed by AWW (Ghent University) to calculate the resources and to perform the economical models.

1.2.2 BOREAS reports

This final report is a summary of the following reports:

1. BOREAS Intermediate report – Wave and tidal energy convertors and their suitability fof the Belgian Part of the North Sea (Mathys *et al.* 2011a);
2. BOREAS Technical report – Wave modelling (Fernández *et al.* 2010);
3. BOREAS Technical report – A comparison of numerical wave data at the Belgian Coast (Delgado *et al.* 2010);
4. BOREAS Technical report – Tidal current modelling (Van den Eynde *et al.* 2010);
5. BOREAS Technical report – A comparison of numerical tidal models of the Belgian Part of the North Sea (Dujardin *et al.* 2010b);
6. BOREAS Technical report - Summary of model set-up and validation (Mathys *et al.* 2011c);
7. BOREAS Technical report – Wave and tidal current resource assessment (Mathys *et al.* 2011b);

Only this final report is publically available.

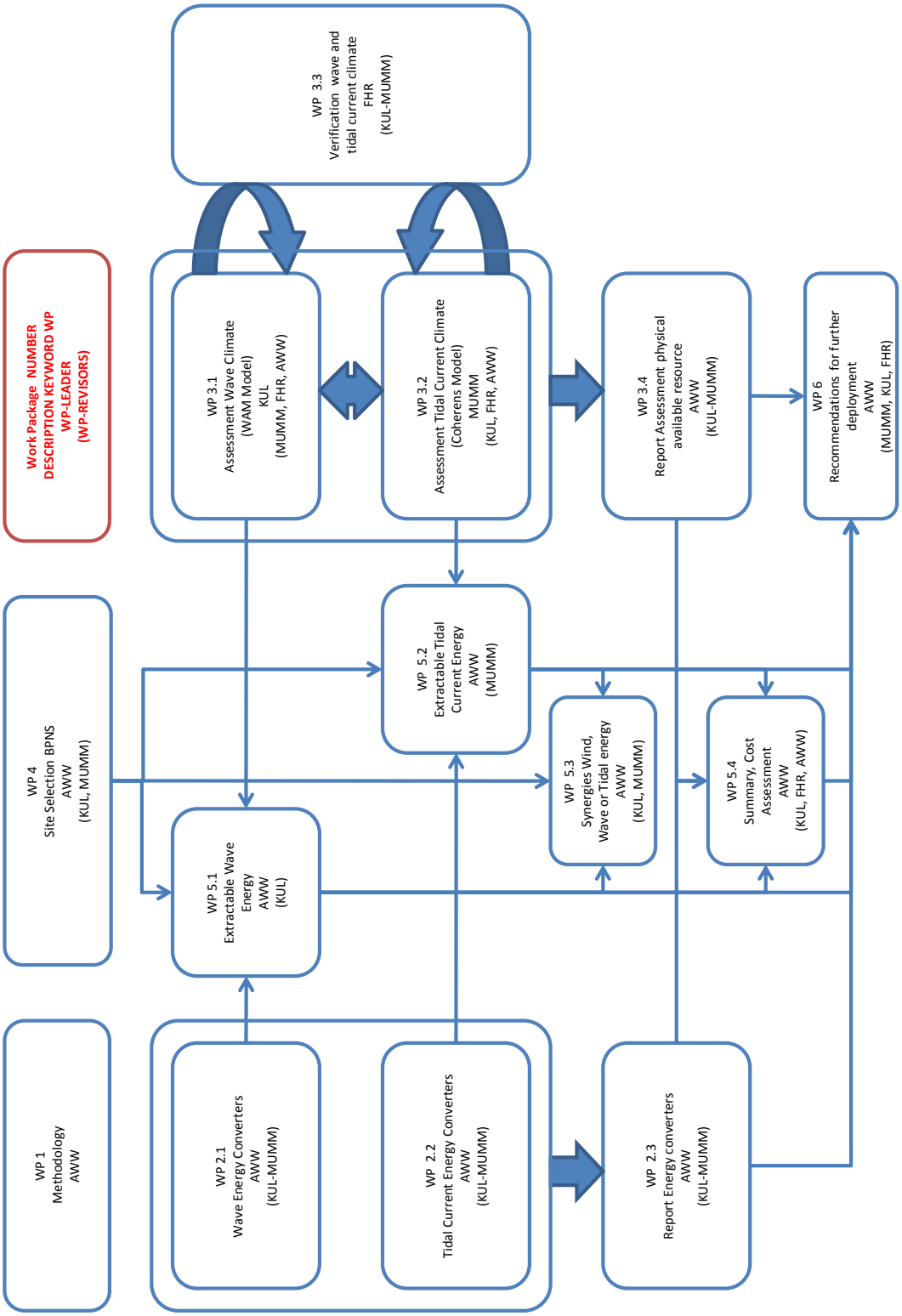

Figure 1: Boreas workpackages and project overview, indicating the WP leaders and revisors and the interaction between the different workpackages.

1.2.3 Link international programmes

Since wave and tidal energy technologies are new technologies, there were intensive and simultaneous, but independent, research projects during the execution of the BOREAS project. These were financed both by the private as well as the public sector. In the latter case, two European funded projects are worthwile mentioning within the BOREAS framework. These projects are Equimar and Waveplam.

The EquiMar website states (EquiMar 2010): *"The aim of EquiMar was to deliver a suite of protocols for the equitable evaluation of marine energy converters (based on either tidal or wave energy). These protocols have harmonised testing and evaluation procedures across the wide variety of devices presently available with the aim of accelerating adoption though technology matching and improved understanding of the environmental and economic impacts associated with the deployment of arrays of devices. EquiMar has assessed devices through a suite of protocols covering site selection, device engineering design, the scaling up of designs, the deployment of arrays of devices, the environmental impact, in terms of both biological & coastal processes, and economic issues. The series of protocols has be developed through a robust, auditable process and disseminated to the wider community. Results from the EquiMar project will establish a sound base for future marine energy standards. The project had a formal liaison with IEC TC 114[1] and many of the protocol authors are technical experts on the teams developing individual standards*".

During the execution of BOREAS, two reports were of particular interest since they presented protocols for wave and tidal current resource assessment (EquiMar *et al.* 2010; EquiMar *et al.* 2011).

The website of the other relevant European funded project, Waveplam, defines the project as follows: "*The purpose of WAVEPLAM is to develop tools, establish methods and standards, and create conditions to speed up introduction of ocean energy onto the European renewable energy market, tackling in advance non-technological barriers and conditioning factors that may arise when these technologies are available for large-scale development, by means of a series of activities geared towards supporting creation of an ocean energy market that will harness the great potential of this kind of energy that exists in Europe, contributing to decrease European external energy dependency and leading to a reduction in greenhouse gas emissions."* Waveplam furthermore made a template to describe wave energy convertors, this was used as well for the BOREAS project (Waveplam 2009).

1.3 Report structure

Chapter 1 of this report describes the context of the BOREAS (Belgian Ocean Energy Assessment project) and states the main themes and the expected results and outcomes of the project.

Chapter 2 introduces the reader to wave energy convertors (WEC) and tidal current energy convertors (TEC). An overview of the design requirements for marine energy convertors is given, both wave and tidal. The concept of the Technology Readiness Levels (TRLs) is explained, including the difficulties experienced when assessing different technologies based on partial information when no standards or protocols are developed yet. In the last part of this chapter,

[1] International Electrotechnical Commission – Technical Commitee 114 on Marine Energy, which is setting out standards for the marine energy technologies.

WEC and TEC that show interesting features for deployment on the Belgian Part of the North Sea (BPNS) are listed. Furthermore, the efficiencies of the devices are discussed in the form of the power matrix (WEC) and power curve (TEC). These will be used in chapter 5 to assess the extractable resource.

Chapter 3 provides an overview of a previous study on the wave power resource based on buoy data. It gives the reader an introduction in the methodology and also provides wave powers at buoy locations in the southern part of the North Sea.

Chapter 4 introduces the reader briefly to the main numerical models that were used for the resource assesment, and the main results of the validation excercises.

Chapter 5 is summarizes the results of the available and extractable wave and tidal current resource assessment. The methodology is described and the assumptions are discussed. In the case of wave power, yearly and monthly trends are presented.

Chapter 6 makes a quantitative economical feasibility study of a hypothetical wave or tidal current project. The methodology is the same as in the OPTIEP study for offshore wind (Mathys *et al.* 2010), but adapted for wave and tidal current energy, based on the results from chapter 5.

Chapter 7 describes qualitatively possible synergies between wave and tidal current energy with e.g. offshore wind.

Chapter 8 concludes this report (and the other BOREAS reports) and gives recommendations to support the wave and tidal current energy sector in Belgium.

The last 3 chapters are giving supplementary information. Chapter 9 is an appendix with yearly or monthly wave power maps that were not listed in the main report. Chapter 10 describes the economical formulas used in chapter 6. Chapter 11 contains the references that were used for this report.

2 Wave and Tidal Energy Convertors on the BPNS

This chapter briefly introduces wave and and tidal current energy convertors (respectively WECs and TECs) and their conversion mechanisms. Some WECs and TECs that show interesting features for deployment on the BPNS are presented. In order to calculate the extractable ressources, the power matrices for 3 different WECs and one power curve for a generic TEC are presented and discussed.

2.1 Introduction Wave Energy Convertors (WEC)

The main classification in WECs is based on their conversion technology. This conversion technology transfers the hydrodynamic energy of the waves over mechanical or hydraulic energy into electrical energy.

2.1.1 Conversion Technology

Before the description of the conversion technologies, the 6 so called *degrees of freedom* of floating objects are explained. The motion of a rigid body is characterised by six components corresponding to six degrees of freedom or modes of (oscillatory) motion (Figure 2). These modes describe for example the 6 forms of ship movements (elongated body, with the main axis according to x). For an axi-symmetric body (like most point absorber buoys), surge and sway are ambiguous, just like roll and pitch. However, in order to remove this ambiguity, the x-axis can be orientated along the incident wave. Note that with long crested waves, coming from the same direction, a 2D approximation can be used by neglecting the y-movement. The resulting 3 degrees of freedom are surge, heave and pitch (Falnes 2002). These 3 modes describe several WECs. Examples are: oscillating wave *surge* convertor (e.g. Aquamarine Oyster), a *heaving* point absorber (e.g. Wavebob) or the *pitching* absorbers (e.g. the Salter Duck, which was one of the earliest WECs developed in the early 80's).

The 6 main conversion types for WECS are shown in Table 1. The variety amongst these technologies is again clear. Examples of the devices can be found in the factsheets in the Appendix (§ 9.1 and 9.2).

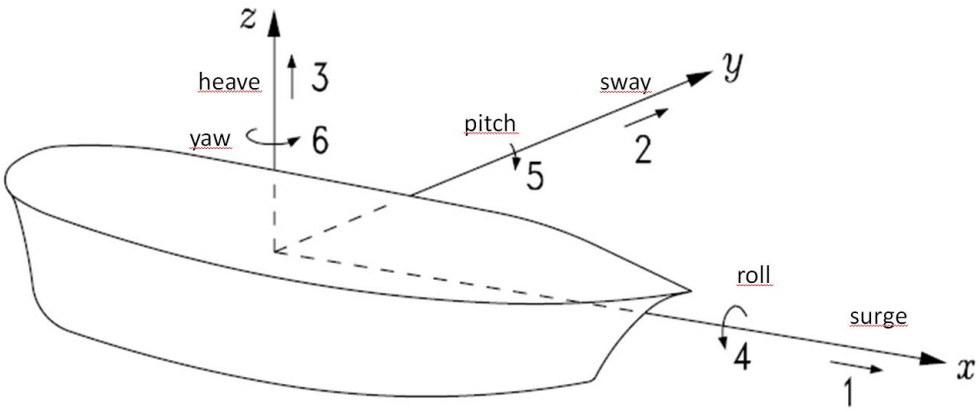

Figure 2: The six degrees of freedom of a ship, and by extension of a floating object (Falnes 2002).

Table 1: Conversion Technologies of Wave Energy Convertors, definitions and pictures cited from (CarbonTrust 2005; Aquaret 2008; EMEC 2010).

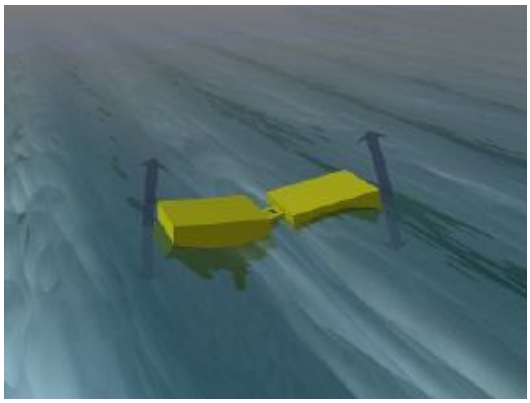	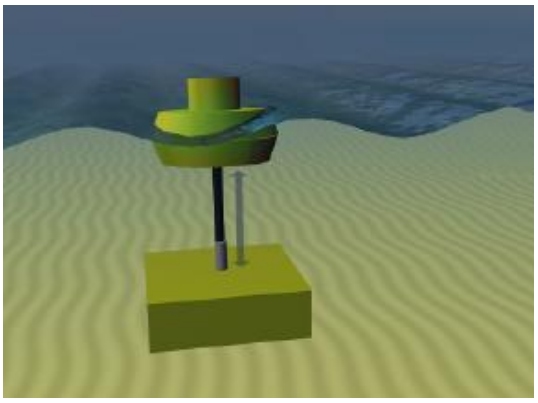
Attenuator – This is a long floating device which is aligned perpendicular to the wave front. The device effectively rides the waves and captures the energy as the wave moves under the floaters or tubes of the device, forcing the hinges to flex. A current example for the attenuator is the Pelamis.	(Axisymmetrical) Point Absorber – This is a floating structure that absorbs wave energy in all directions by virtue of its movements at or near the water surface. It has small dimensions compared to the typical wavelength, tending to have diameters of a few meters. One crucial aspect of a point absorber is its ability to focus energy onto itself. To do this the device radiates waves, which in part cancels the incoming waves (Falnes 2002), this effect is called the antenna effect.
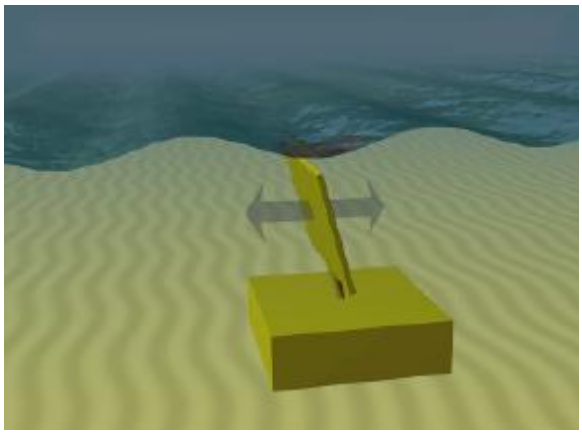	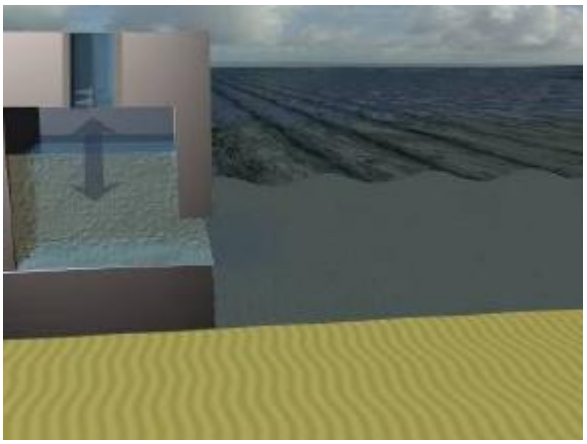
Oscillating Wave Surge Converters (OWSC) – This is a near-surface collector, mounted on an arm pivoted near the seabed. The arm oscillates as an inverted pendulum due to the movement of the water particles in the waves.	Oscillating Water Column (OWC) – This is a partially submerged, hollow structure, which is open to the sea below the water surface so that it contains air trapped above a column of water. Waves cause the column to rise and fall, acting like a piston, compressing and decompressing the air inside the chamber. This air is channeled through an air turbine to produce power. When properly designed for the prevailing sea state, OWCs can be tuned to the incident wave period in order to resonate.

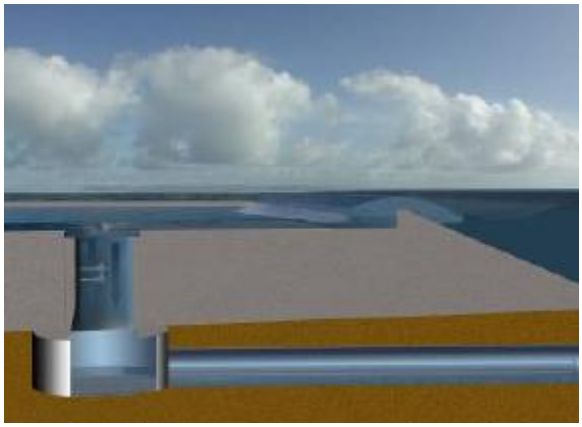	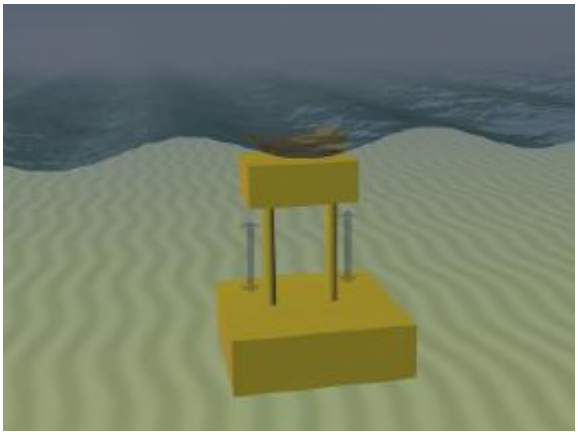
Overtopping Device – This consists of a slope that maximizes the wave overtopping. The water is collected in a storage reservoir. The incoming waves create a head of water, which is released back to the sea through conventional low-head turbines installed at the bottom of the reservoir. An overtopping device may use collectors to concentrate the wave energy. Overtopping devices are typically large structures due to the space requirement for the reservoir, which needs to have a minimum storage capacity.	Submerged Pressure Differential – This is a submerged device typically located near shore and attached to the seabed. The motion of the waves causes the sea level to rise and fall above the device, inducing a pressure differential which causes the device to rise and fall with the waves.

Based on these conversion technologies, WECs convert the hydrodynamic energy of the waves over mechanical or hydraulic energy into electrical energy. Depending on the conversion technology and Power Take Off (PTO), several options are possible. Figure 3 shows some options of the conversion of the energy.

Notice the variety of technologies, and the introduction of storage of energy early in the conversion chain. Storage of electricity is necessary both on the short term (order of wave periods 5-12 seconds) and in the long term (minutes, up to hours). The short term storage (in the order of 20-100 seconds) is typically integrated into the device by means of build up of hydraulic pressure (e.g. Pelamis) or hydraulic head (e.g. WaveDragon), by using mechanical solutions (like flywheels) or using electrical capacitors.

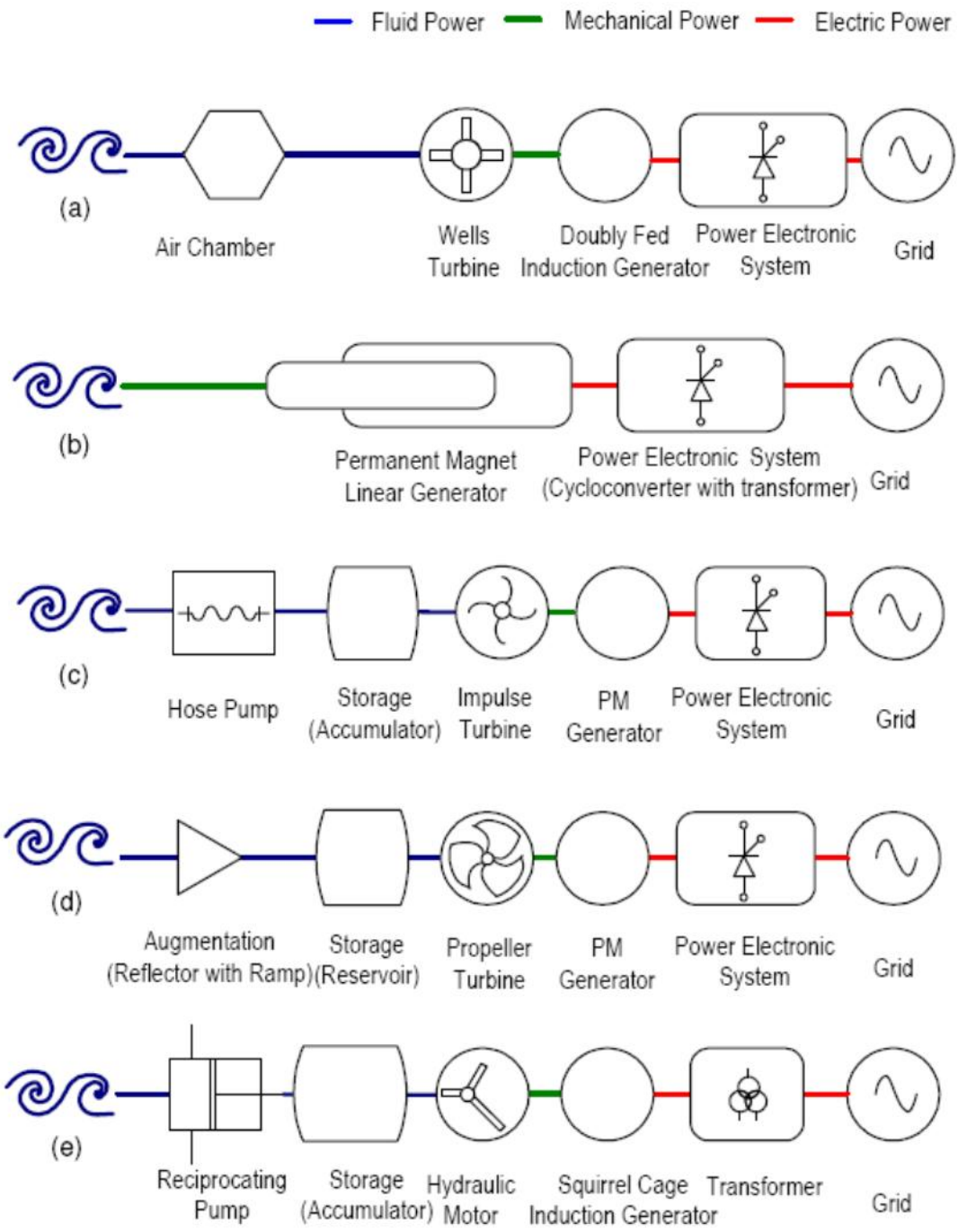

Figure 3: Converter schematics (a) Pico Oscillating Water Column WEC of IST (b) the original submerged pressure differential WEC (2004) of AWS (c) Point Absorber WEC of Finavera AquaBuOY (d) Overtopping WEC of WaveDragon (e) Attenuator WEC of Pelamis. Abbreviations: PM: Permanent Magnet (IEA-OES *et al.* 2009b).

2.1.2 PTO (Power Take Off)

The second conversion step, from mechanical or hydraulic energy into electricity, is determined by the PTO. A PTO exists out of many individual components, but not all components listed below are present in one PTO.

This is again an illustration of the variety of the different concepts that developers can use. The main possible components of the PTO are:

- The driveshaft
- Gearbox
- Freewheel
- Permanent magnet (linear or cage) generators;
- Turbines:
    - Air turbines (OWC), a Wells turbine (which rotates in the same direction independent of the air flow);
    - Hydraulic turbine (hydraulic motor);
    - Low head water turbines (Kaplan or propeller type);
- Storage systems:
    - Flywheel (rotating systems)
    - Reservoir (water or hydraulic) to keep the head or the pressure respectively stable
    - Capacitors
- Electronic components
    - Transformator
    - Capacitor
- Connection plug for grid connection.

2.1.3 Mooring or anchoring

The mooring is the connection between a reference point and the PTO of the WEC. Fixing a WEC to a certain reference point is a design issue that has a strong mutual influence on the power absorption.

Let's consider a point absorber, that always moves up and down. In this case, there is no resulting force and hence, no power production. However, in the case where the wave created by the buoy cancels out the incident wave, the power absorption (and hence power production) is maximal. The moorings and the PTO play an important role to achieve this so-called resonance state.

WECs can be:

- Moored to the seabed, different mooring options exist (Figure 4):
    - Catenary or slack moored: the mooring cables have a slack, the weight of the cable provide freedom of movement for the WEC until the cable becomes under tension;
    - Taut-moored: the mooring cables have a pretension, the elasticity of the cable provides freedom of movement for the WEC;
- The mooring cable fixed at the seabed can be attached to:
    - Directly to the floating WEC;
    - A submerged inertia plate, this inertia plate is then connected to the floating WEC;
    - A submerged buoy, which is then connected to the floating WEC.

- The anchoring in the seabed can be:
    - A gravity based anchor, mostly made of concrete;
    - A monopile or jacket structure;
    - A specific type of anchor, depending on the bottom substrate.

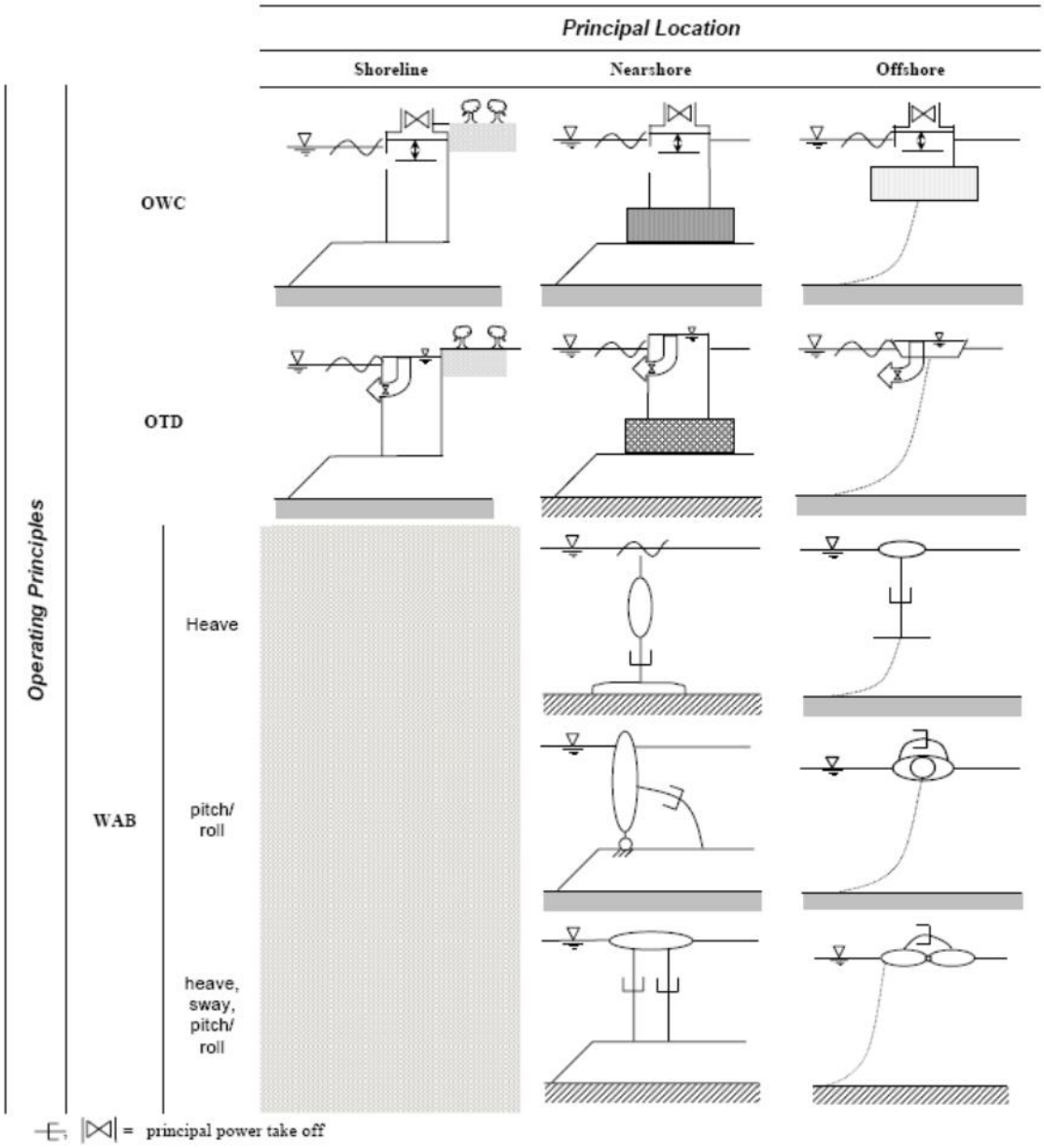

Figure 4: Mooring options for WECs, depending on their location (see § 2.1.4). Abbreviations: OWC: oscillating Water Column, OTD: overtopping devices, WAB: Wave Activated Bodies, these might be point absorber- , attenuator- or submerged pressure differential-WECs (Harris *et al.* 2008).

2.1.4 Location

According to the characteristics of their deployment sites, wave energy technologies are frequently divided into shoreline (or coastal), near-shore and offshore devices. The physical conditions (e.g. water depth, power level, directionality, and hydrodynamics) relevant for wave energy conversion are different according to the water depth and distance from shore.

The waves travel in deep water almost without energy loss across the ocean, which is why floating technologies moored in deep water are expected to have the largest potential for large-scale implementation. Typical water depths for offshore technologies are in the range of 50m. These water depths cannot be found on the BPNS. In shallower water, the waves suffer increasingly from bottom friction, making such sites less interesting from an energetic viewpoint. However as these are closer to shore ('near-shore'), mooring and grid connection costs decrease, and become more viable. Finally shoreline devices, which are typically integrated in the shoreline or into an artificial coastal defense structure, have lower incident power levels available but facilitated access and different structural solutions. They can be integrated in new breakwaters, like the OWC in Mutriku in Spain.

2.2 Introduction Tidal current Energy Convertors (TEC)

Like WECs, it is difficult to classify TECs based on one single criterion. The main criterion is again the conversion technology.

2.2.1 Conversion technology

TECs show a wide range of conversion technologies. The main technologies are based on turbine design, but other, non-turbines designs exist. A classification based on a review of the conversion technologies identified 10 conversion technologies (Khan *et al.* 2009), see Table 2 for examples:

- Turbine Systems:
    1) Axial (Horizontal): Rotational axis of rotor is parallel to the incoming water stream (employing lift or drag type blades), better known as Horizontal Axis Tidal Turbine (HATT);
    2) Vertical: Rotational axis of rotor is vertical to the water surface and also orthogonal to the incoming water stream (employing lift or drag type blades), better known as Vertical Axis Tidal Turbine (VATT), see also Figure 5 for subclasses of the VATT;
    3) Cross-flow: Rotational axis of rotor is parallel to the water surface but orthogonal to the incoming water stream (employing lift or drag type blades);
    4) Venturi or ducted systems: Accelerated water resulting from a choke system (that creates pressure gradient) is used to run an in-built or on-shore turbine;
    5) Gravitational vortex: Artificially induced vortex effect is used in driving a vertical turbine;
- Non-turbine Systems:
    6) Flutter Vane: Systems that are based on the principle of power generation from hydroelastic resonance (flutter) in free-flowing water, flutter is basically a resonance phenomenon with 2 degrees of freedom;
    7) Piezoelectric: Piezo-property of polymers is utilized for electricity generation when a sheet of such material is placed in the water stream;
    8) Vortex induced vibration: Employs vibrations resulting from vortices forming and shedding on the downstream side of a bluff body in a current;
    9) Oscillating hydrofoil: Vertical oscillation of hydrofoils can be utilized in generating pressurized fluids and subsequent turbine operation. A variant of this class includes biomimetic devices for energy harvesting;

10) Sails: Employs drag motion of linearly/circularly moving sheets of foils placed in a water stream.

Of these 10 conversion technologies, the VATT, (ducted) HATT, cross-flow or hydrofoils (Table 2 and Figure 5) are common and several device developers use this principle. Some TECs are developed not only for tidal currents, but also for river currents (sometimes with small modifications in the design or anchoring).

Table 2: Main conversion technologies of TECs (Aquaret 2008; Blanco 2009; IEA-OES *et al.* 2009a; EMEC 2010).

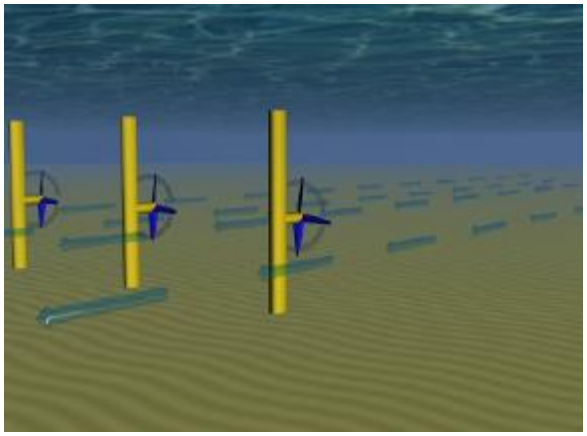	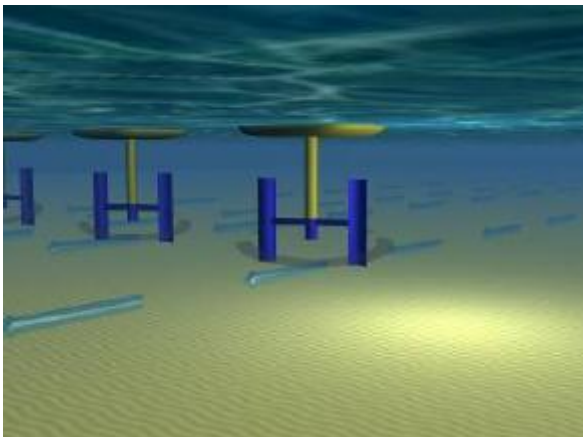
Horizontal axis turbines work much the same as a conventional wind turbine and some look very similar in design. A turbine is placed in a tidal stream which causes the turbine to rotate and produce power. This is achieved by pitching the blades to a certain angle, whereby an incoming current creates a lift force.	Vertical axis turbines use the same principle as the horizontal axis turbines (the lift force), but the blades are placed parallel with the axis instead of perpendicular. A turbine is placed in a tidal stream which causes the turbine to rotate and produce power. Originally developed for capturing wind energy, these device are also called Darrieus turbines.
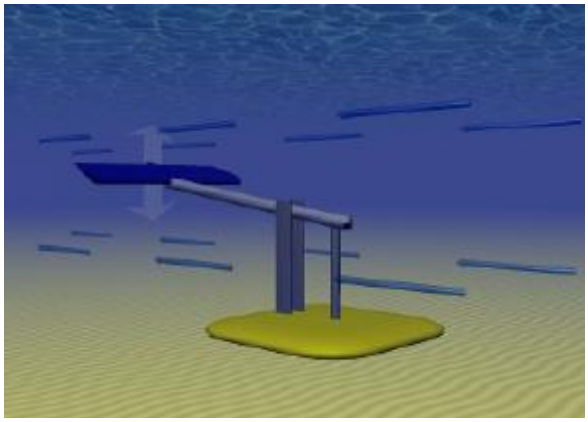	
Reciprocating devices (oscillating hydrofoils) have	Venturi effect (ducted) tidal stream devices – The

hydrofoils which move back and forth in a plane normal to the tidal stream, instead of rotating blades. The oscillation motion used to produce power is due to the lift created by the tidal stream flowing in either side of the wing. One design uses pistons to feed a hydraulic circuit, which turns a hydraulic motor and generator to produce power.	tidal flow is directed through a duct, which concentrates the flow and produces a pressure difference. This causes a secondary fluid flow through a turbine. The resultant flow can drive a turbine directly or the induced pressure differential in the system can drive an air-turbine.
	
Open centre tidal turbine. This device relies on the same principle as the HATT, but it has a 'virtual' horizontal axis, whereby the blades are connected at the tips with the foundation. Developers of these devices claim this concept has two advantages: the blades are located to generate a higher torque on the PTO and it facilitates the passing marine species without damaging them.	Cross-Flow turbine. This device relies on the same principle as the VATT, but it can differ in 2 ways: the axis can be placed horizontally and/or the blades can be curved along the periphery of the device. In the latter case, this device is then called a Gorlov turbine.

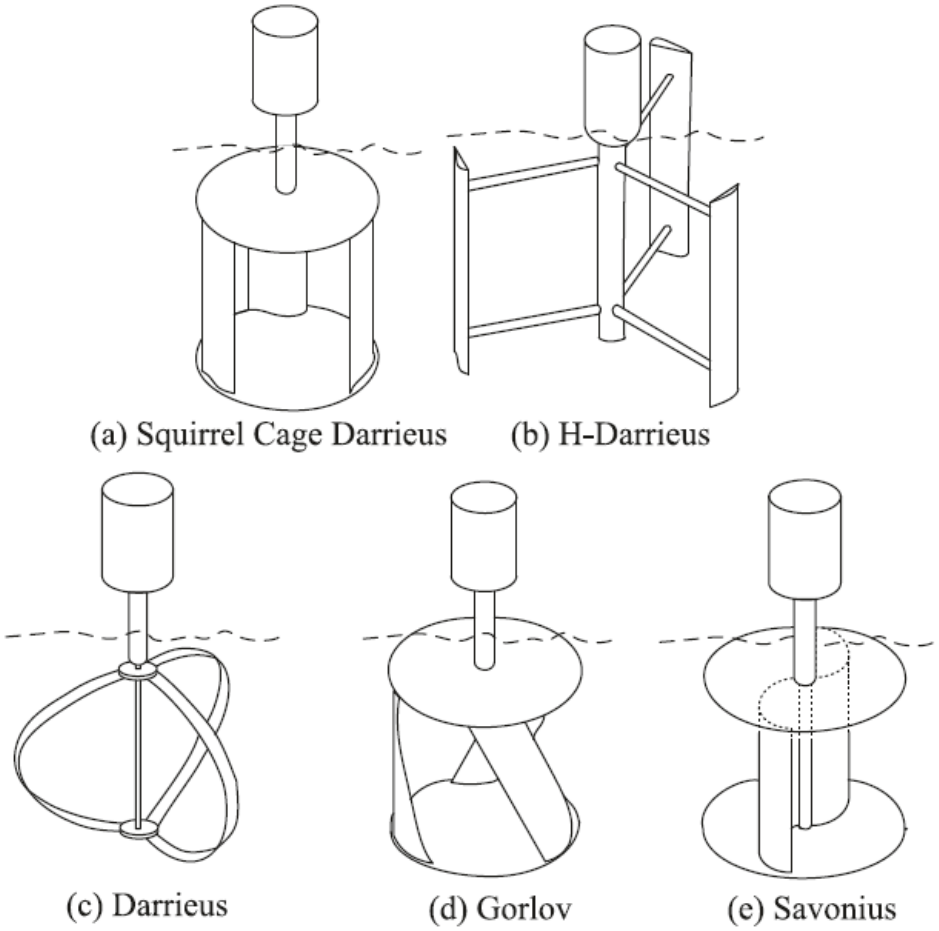

Figure 5: Different types of VATT (vertical axis tidal turbines) (Khan *et al.* 2009) .

2.2.2 Power take off (PTO)

Similar to wave energy, the conversion to electricity is a multistep conversion from hydrokinetic power over mechanical into electrical power. Hydraulic conversion steps are rare in TECs. Figure 6 represents some possible conversion steps of TECs (refer to Figure 3 for WECs).

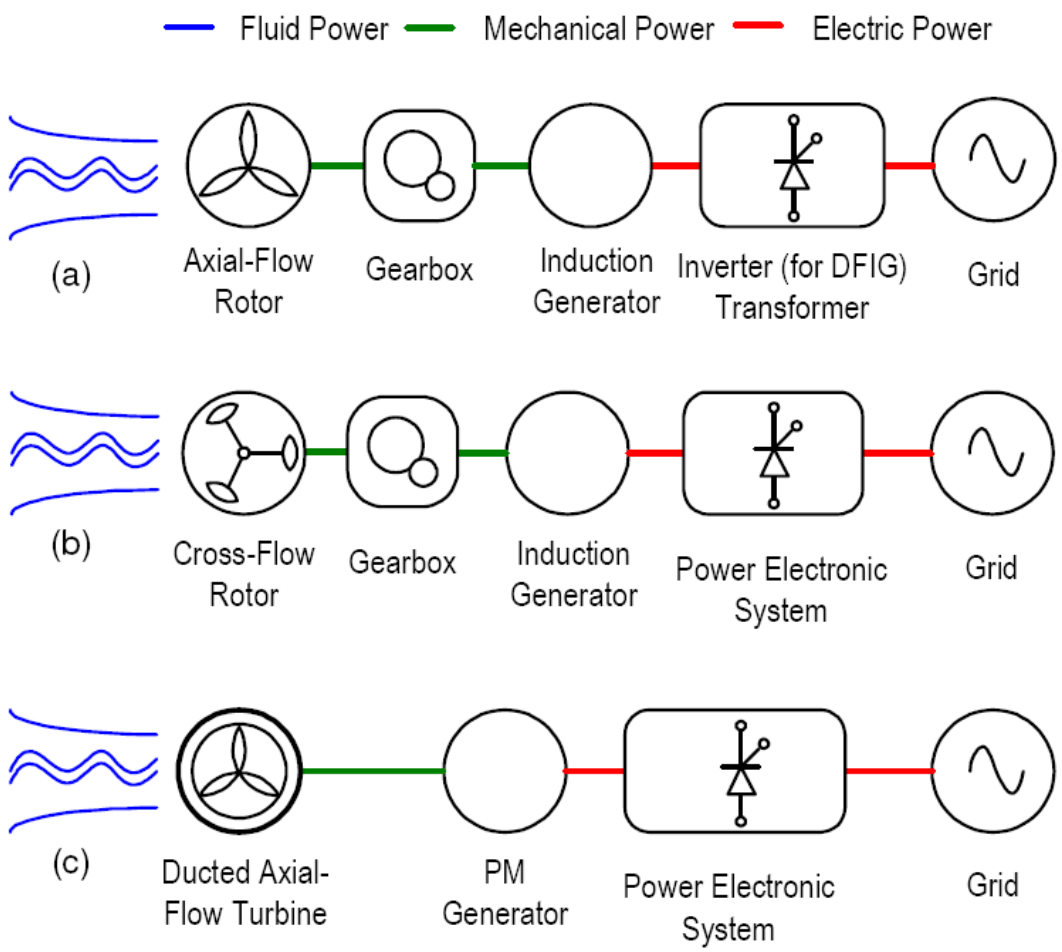

Figure 6: Possible conversion steps for TECs a) HATT (SeaGen, Marine Current Turbines), b) Cross-flow turbine (Kobold), c) Ducted HATT (Clean Current). Abbreviations: PM: permanent magnet generator; DFIC: Double Fed Induction Generator (IEA-OES *et al.* 2009b).

Most TECs use PTO technologies similar to the ones that are used in wind turbines. They can consist out of a shaft, gearbox, freewheel, generator as the main components.

2.2.3 Mooring or anchoring

TECs can be fixed to the seabed in different ways (EMEC 2010):

- Seabed Mounted / Gravity Base: the TEC is physically attached to the seabed or is fixed by virtue of the weight of the foundation. In some cases there may be additional fixing to the seabed.
- Pile Mounted: This principle is analogous to that used to mount most large wind turbines, whereby the device is attached to a pile penetrating the ocean floor. Horizontal axis devices will often be able to yaw about this structure. This may also allow the turbine to be raised above the water level for maintenance.
- Floating (with three sub-divisions):
    - Flexible mooring: The device is tethered via a cable/chain to the seabed, allowing considerable freedom of movement. This allows a device to swing as the tidal current direction changes with the tide.

  - Rigid mooring: The device is secured into position using a fixed mooring system, allowing minimal leeway due to the absence of cable slack.
  - Floating structure: This allows several turbines to be mounted to a single platform, which can move in relation to changes in sea level.
- Hydrofoil Inducing Downforce: This device uses a number of hydrofoils mounted on a frame to induce a downforce from the tidal current flow. Provided that the ratio of surface areas is such that the downforce generated exceeds the overturning moment, the device will remain in position.

2.3 Design requirements

2.3.1 Generic requirements for WECs and TECs

The design criteria for marine energy convertors (WECs or TECs) are quite extensive. The reason for this is the character of the resource, which is variable, and the harsh environment for operation (corrosive seawater, wave impact during storms). This is a big difference with conventional power plants, where the process control is not always easy, but at least more predictable and controllable.

Of course, every design criterion comes with a cost. Although it is difficult to give generic requirements, the following basic design criteria are valid for all marine energy convertors:

- Cost of electricity (CoE) needs to be low, the CoE is of course the prime driver;
- Survivability and structural design has to take into account the extreme wave forces: due to the high impact of waves (and to a lesser extent, currents), the structural integrity is of extreme importance. Special attention should be given to the effects of corrosion, biofouling and tear & wear to maintain the structural integrity and hull worthiness at sea.
- Quality, smoothing and storage of electricity output: due to the temporal variability of these energy resources (wave periods in the order of 6-10 seconds but also seasonal variability, tidal currents in the order of 6 hours) energy storage and smoothing is critical for injection into the grid;
- Easy installation and maintenance; preferably with existing infrastructure (existing tug boats and barges, in order to keep mobilisation/demobilisation costs low). If possible, keep critical components easily accessible or removable (“cartridge” system) to do as much as possible onshore.
- Tuneable to a wide range of power conditions: being able to exploit a wide range of wave heights or tidal currents optimally;
- In order to assure an efficient manufacturing and good operation and maintenance, the supply chain of components needs to be secured. Limiting the use of newly developed components will benefit operation and maintenance. Using components from maritime, offshore oil and gas industry is an advantage.
- Compatible with exisiting grid infrastructure, but ready for new grid developments, such as offshore interconnectors, coupling with energy storage, new trends in ‘intelligent’ grid,...
- Synergies with other energy technologies, such as offshore wind, but also parallel production of e.g. potable water, or aquaculture.
- Visible (marker buoys) for navigation purposes and to avoid damage due to ship collisions;

- Low environmental impact, which has quite a broad meaning:
    - Use of environmentally friendly materials like biodegradable oils, or anti fouling devices that do not have toxicological effects;
    - Small footprint or space occupation, both at the surface or at the seabed bottom in case of pile or anchors;
    - Avoidance of underwater noise during installation, operation and maintenance (marine mammals).

2.3.2 Requirements specific for WEC

Most WECs are placed at the sea surface, in order to capture the wave forces as much as possible. However, in storms, the wave forces are extremely high and the WEC has to withstand these forces. This consideration brings us to the first design requirement:

- Survivability at the sea surface during storms . This can be achieved in several ways . Some devices have inherent different characteristics (like Pelamis, which 'dives' under the big waves due to hydrostatic clipping (Cruz 2008)), others are controlled by their PTO, either passive or active, others are (partially) submerged in order to avoid the spil and impact forces of breaking waves.
- Flexibility to the tidal range: in regions with a high tidal range, the mooring has to flexible to account for the tidal variation.

2.3.3 Requirements specific for TEC

In the framework of this project, only tidal energy current convertors based on *kinetic energy* (so current energy) are considered, and not the ones based on *potential energy* (head difference due to low and high water). Further in this report, TECs are defined as tidal energy *current* convertors, unless stated otherwise. TECs differ fundamentally from WECs in the fact that the blades need to submerged to extract the energy. TECs have the most of their components underwater. This is a disadvantage for maintenance: maintenance has to be done by (expensive) divers or Remotely Operated Vehicles (ROVs) or the components have to be lifted above the water. However, the advantage is that TECs will experience lower wave impacts, since the wave forces decrease with depth. The following requirements are specific to TECs:

- Easily accessible for maintenance, by lifting the whole TEC above the water line (like Marine Current Turbines); by lifting the critical components of the TEC above the water line with a barge or maintenance ship and do maintenance onshore; by ROVs (highly depending on tidal windows, since these ROVs have to operate in strong currents), or otherwise.
- Avoidance of cavitation: typically, WECs have rotating blades. The speed at the tips of these wings can be high enough to induce cavitation. This induces vibrations and material fatigue and hence decreases the lifespan of the blades.
- Avoidance of biofouling: Many devices installed in the sea become artificial reefs, attracting a wide variety of marine organisms. These cover the structures and can cause significant fouling. Fouling of moving parts could affect the performance of devices. This can be especially an issue in the shallow waters of the BPNS. Beside the obviuous disadvantage that shallow waters provide less place for a tidal turbine, it is also more exposed to sunlight, which promotes biological growth.

2.4 The long list factsheet

In the Boreas intermediate report *'Wave and tidal energy energy convertors and their suitability for the Belgian Part of the North Sea'* (Mathys *et al.* 2011a) an overview of the most common WECs and TECs is presented, based on information template that was adapted and extended from the Waveplam project (Waveplam 2009). This template enables a standardized and synoptic way of describing the devices (see Table 3 for the template and Appendices 9.1 and 9.2), instead of describing it in full text. Notice that not all fields are as detailed across the different devices for two reasons:

- Some developers give more detailed information than others;
- Some devices are still in a conceptual phase, whereas others are further developed, up to level of demonstration or pre-commercial phase.

The authors chose to describe some WECs or TECs that are industry leaders or WECs or TECs which show interesting features for deployment on the BPNS. In the latter case, these devices will form the basis of the further short list. Contrarily, some developers give so little information about their device or concept, that it is hard to make any assessment. These devices were identified, but not necessarily described in the long list.

Environmental effects were not defined as a criterion, for several reasons. All the device developers make claims about environmental friendliness, such as the use of biodegradable oils, but these claims are difficult to assess in such an early development status. The most obvious (local) environmental impact is the additional presence of hard substrate such as steel and concrete (Langhamer 2009). These effects are likely to be similar to the effect of the introduction of offshore windmill farms that were observed for the C-Power offshore windmill farm (Degraer S. *et al.* 2009). An important aspect is however the spatial occupation or footprint, this is given in the dimension field. Some device developers have published environmental reports (enquiry taken at the end of 2008, (USDOE 2008), these are:

- TECs: Marine Current Turbines, Ocean Renewable Power Company, Tocardo BV Tidal Energy, IHC Engineering business, Verdant Power;
- WECs: AW Energy, Ocean Power Technologies, Seabased, Wavedragon.

The long list factsheet does not pretend to be exhaustive, and doesn't want to criticize nor judge any of the devices that are currently under development and are solely based on information that is available in the public domain.

Table 3: Template for the description of the WEC/TEC longlist.

Current corporate profile	
Name of the company	Name of the WEC or TEC
Official website of the company	Foundation year and nation
Company profile: describing the company (e.g. small independent research groups, contains sometimes historical facts, etc.)	Projected Cost of Electricty, as given by the developper (No third party verification)
Origin, and if possible names, of investors	

Pictures	
Pictures of the device, concept or installation (in most cases official pictures from websites)	Additional picture
Caption of the picture	Caption of the picture

Device specifications		
Conversion technology	Power Take off (PTO) information	Mooring or anchoring characteristics
•Unique features according to the developpers (no third party verification)		Required water depth
		Dimensions of Full prototype (size and weight)
		Information about the Power Matrix (no third party verification)

Device Development history and future strategy
Field describing the history and prospects of the convertor, by means of their phases as defined by the Technology Readiness Levels (TRLs), see explanation below

Device evaluation
Device evaluation by the authors of this report

Suitability for the BPNS
Suitability for the BPNS, according to the authors of this report (partially based on the requirements that the device developers provide on their website, partially based on own judgement)

The wave and tidal current energy market experienced a high pressure to produce electricity. Due to this high pressure and the lack of standards, developers sometimes went too fast to the open sea, with sometimes disastrous consequences. Examples are the sinking of the 2MW Archimedes Wave Swing in 2004, the Finavera Aquabuoy 2.0 in 2007 and more recently the sinking of the Oceanlinx precommercial prototype in 2010.

Although marine energy can only become a reality following full scale testing of WECs or TECs at sea it is important that the correct engineering procedures are followed leading up to the first sea trials. Although difficult, political and business concerns must resist applying pressure to deploy new devices prematurely. Therefore, the Hydraulics and Maritime Research (HMRC) applied the TRL (Technology Readiness Level) schedule to Wave energy (Holmes 2009).

This approach is becoming more popular as it provides the current “best practices” in marine energy development. TRL development programmes are standard approaches for product advancement in established industries such as NASA and American military equipment industry. It must be stated that HMRC is not the only institution that is involved in the development of the TRLs. Furthermore, the TRLs can provide a blueprint for the international standards. However, it is unsure if these TRLs as such will be integrated in the international standards (Nadeau 2010). The 5 main TRL phases are (Holmes 2009):

1. TRL 1: Proof of concept: provide the basic concept of the proposed WEC in regular waves and obtain an estimate of its power performance in irregular, real sea waves.
2. TRL 2: Part-scale (Tank): Testing of 1:10 (approximately) scale model in a wave flume that allows component testing in more seaways, including those expected to be used at the sea trial test. There are less design options to investigate than in TRL1.
3. TRL 3: Part-scale (Sea): Testing of 1:4 scale model in a benign offshore location. This device should be a fully operational unit, but the required budget should be an order of magnitude less.
4. TRL 4: Full-scale – Prototype model: Prototype testing, which enables a full assessment of the so called ‘wave-to-wire’ performance. At this stage, the required investment rapidly increase. It is however not expected here that for this single (or perhaps 2-3) unit(s), the project can make profit at this stage. Test centers and external funding are almost essential to pass this TRL.
5. TRL 5 : Full-scale – Precommercial model: when a device successfully completes the rigorous technical sea trials, the solo pre-production converter of TRL 4 should have evolved into a pre-commercial machine ready for economic demonstration in TRL 5.

2.5 Conversion efficiencies: power matrix (WEC) and power curve (TEC)

2.5.1 Power Matrix for WEC

The translation from wave climate (wave height and period), and hence *available* wave power, to produced *extractable* power is done by the so-called power matrix (see also § 5.2.1). The power matrix gives the relation between the wave height and period with the produced power. If the produced power is at its maximum, the so-called ‘rated power’ is achieved.

This power matrix can thus be used to translate the resource into produced power. An example is given in Table 4 (Pelamis WEC). The rated power is achieved at 750 kW. Below 0.5 m wave height, no power is produced. Below 1 m wave height a small amount of power is produced between a wave period of 5.5 and 11.5 seconds. The wave height is clearly the dominant factor, the period is of secondary importance (this is also reflected in the available wave power calculation, see § 5.1). Table 5 and Table 6 give the power matrices for the Prote ch Straumekraft 25 kW point absorber and a single floater of a Wave Star WEC.

Table 4 : Power matrix used for Pelamis,rated 750 kW. (Dalton *et al.* 2009; Pelamis Wave Power 2010)

$T_{m-1,0}$ / H_{m0}	3	4	5	6	7	8	9	10	11	12	13
0.5	0	0	0	0	0	0	0	0	0	0	0
1.0	0	0	0	29	37	38	35	29	23	0	0
1.5	0	0	32	65	83	86	78	65	53	42	33
2.0	0	0	57	115	148	152	138	116	93	74	59
2.5	0	0	89	180	231	238	216	181	146	116	92
3.0	0	0	129	260	332	332	292	240	210	167	132
3.5	0	0	0	354	438	424	377	326	260	215	180
4.0	0	0	0	462	540	530	475	384	339	267	213
4.5	0	0	0	544	642	628	562	473	382	338	266
5.0	0	0	0	0	726	707	670	557	472	369	328
5.5	0	0	0	0	750	750	737	658	530	446	355
6.0	0	0	0	0	750	750	750	711	619	512	415
6.5	0	0	0	0	750	750	750	750	658	579	481
7.0	0	0	0	0	0	750	750	750	750	613	525
7.5	0	0	0	0	0	750	750	750	750	686	593
8.0	0	0	0	0	0	0	750	750	750	750	625
8.5	0	0	0	0	0	0	0	750	750	750	750
9.0	0	0	0	0	0	0	0	0	750	750	750
9.5	0	0	0	0	0	0	0	0	0	750	750
10.0	0	0	0	0	0	0	0	0	0	0	750
10.5	0	0	0	0	0	0	0	0	0	0	0

It is important to stress that this extractable resource is valid for a single WEC at a specific site, since the current methodology doesn't allow to take into account the interaction between a WEC and waves, or between one WEC with another WEC (like in a WEC farm).

The Prototech Straumekraft WEC is based on a computer model, and thus doesn't represent experimentally proved power production. In the original reference for Wave Star (Marquis *et al.* 2010a; Marquis *et al.* 2010b), not the power matrix but a power curve (produced electricity in function of the wave height for an average wave period of 4.5 seconds) is given.

There are already some remarkable differences when comparing power productions based on typical wave conditions for an average day on the BPNS (assume a H_s of 1.25 m and a T_e of 5 seconds, which corresponds with a common sea state at Westhinder (Beels 2009)). Pelamis would be producing 16kW (interpolated value), whereas the Straumekraft would produce 3.1 kW and the Wave Star 7.75 kW. The Pelamis is clearly developed for higher wave climates than the BPNS.

Table 5 : Power Matrix for Protech Straumekraft. (rated 25 kW, based on computer simulations by the developer and Prototech (Straume 2010).

$T_{m-1,0}$ / H_{m0}	0	2.5	3.5	4.5	5.5	6.5	7.5	8.5	9.5
0	0	0	0	0	0	0	0	0	0
0.25	0	0	0	0	0	0	0	0	0
0.75	0	0.1	0.3	0.4	0.4	0.3	0.3	0.3	0.3
1.25	0	0.5	2.1	3.2	3	2.7	2.3	2.1	2
1.75	0	1.6	6.8	10	9.7	8.6	7.4	6.9	6.6
2.25	0	0	8.7	15	15	14	13	12	10
2.75	0	0	9.9	19	20	20	18	16	14
3.25	0	0	0	22	24	25	23	20	18
3.75	0	0	0	22	25	25	25	23	21
4.25	0	0	0	24	25	25	25	25	24
4.75	0	0	0	0	25	25	25	25	24
5.25	0	0	0	0	25	25	25	25	25
5.75	0	0	0	0	25	25	25	25	25
6.25	0	0	0	0	25	25	25	25	25
6.75	0	0	0	0	0	25	25	25	25
7.25	0	0	0	0	0	25	25	25	25
7.75	0	0	0	0	0	25	25	25	25
8.25	0	0	0	0	0	25	25	25	25
8.75	0	0	0	0	0	0	25	25	25
9.25	0	0	0	0	0	0	0	0	0

Table 6 : Power Matrix for a Wave Star (37 kW rated for a single buoy the only data given by Wave Star are the produced power for a period with 4.5 seconds (indicated in bold, (Marquis et al. 2010a)). The other values of the power matrix are filled in by the authors based on the comparison with the Protech Straumekraft and Pelamis Power Matrix trends).

$T_{m-1,0}$ / H_{m0}	0	2.5	3.5	4.5	5.5	6.5	7.5	8.5	9.5
0	0	0	0	0	0	0	0	0	0
0.5	0	0	0	1	1	1	1	1	1
1.0	0	1	2	4.5	6	8	6.5	4.5	4.5
1.5	0	2	6	9.5	11	12	11	9.5	9.5
2.0	0	5	13	17	17	17	14	11	9
2.5	0	0	20	27	27	27	25	20	15
3.0	0	0	0	37	37	37	37	37	37
3.5	0	0	0	0	37	37	37	37	37
4.0	0	0	0	0	0	37	37	37	37
4.5	0	0	0	0	0	0	37	37	37
5	0	0	0	0	0	0	0	0	0

The power matrix is thus a crucial aspect to assess the power production. However, only a few device developers have published their power matrices. Furthermore, since no standards exist to make this power matrix, it is extremely difficult to compare these power matrices over different devices and evaluate them. Applying these power matrices to the wave conditions on the BPNS is necessary to obtain an *extractable* wave power, but Pelamis was never developed to be installed in wave conditions that are similar to the ones at the BPNS.

2.5.2 Efficiency & power curve for TECs

The power curve[2] for a TEC gives the relation between the current velocity and the electrical output power (see also § 5.3.2). It is the multiplication of the kinetic power associated with the undisturbed flow at the centre of the device with the efficiency curve. The mathematical formulation of the available tidal current energy is discussed further in the paragraph of the calculation of the available tidal power (§ 5.3).

Figure 7 shows an idealized efficiency curve for a generic tidal kinetic energy converter (neglecting the influence of the current direction and thus assuming a 0° angle of attack). The term efficiency curve is used here to refer to the relationship between the power generated by the device and the kinetic power associated with the undisturbed flow at the centre of the device. For this hypothetical device, the efficiency is zero for flow speeds below 0.5 m/s and above 3.6 m/s, and varies between 30% and 43% over the range in velocity from 1.5 to 3.5 m/s. The peak efficiency of 43% coincides with a flow speed of 2.75 m/s. This idealized efficiency curve was developed for high velocities to demonstrate the prediction of generated power from the time series of current speed (Cornett *et al.* 2010). It might not be the idealized efficiency curve for the conditions on the BPNS, because the maximum currents determined by previous studies indicate relatively low flow currents at spring tide, in the order of 1.7 m/s (Van Lancker *et al.* 2007)

The term 'cut-in' speed can be easily derived from Figure 7. It is the threshold speed to start the turbine and generator (or more general the PTO). Similarly, the 'cut-off speed' is the upper limit to produce electricity. Above this upper limit, the TEC tries to avoid possible damage due to high forces and torques and does not produce electricity. Similar efficiency curves exist for wind energy turbines.

[2] Note the term 'curve' here instead of 'matrix': for tidal energy the power curve is a fuction of only one variable (the current velocity), whereas the power for wave energy is a function of both wave height and wave period.

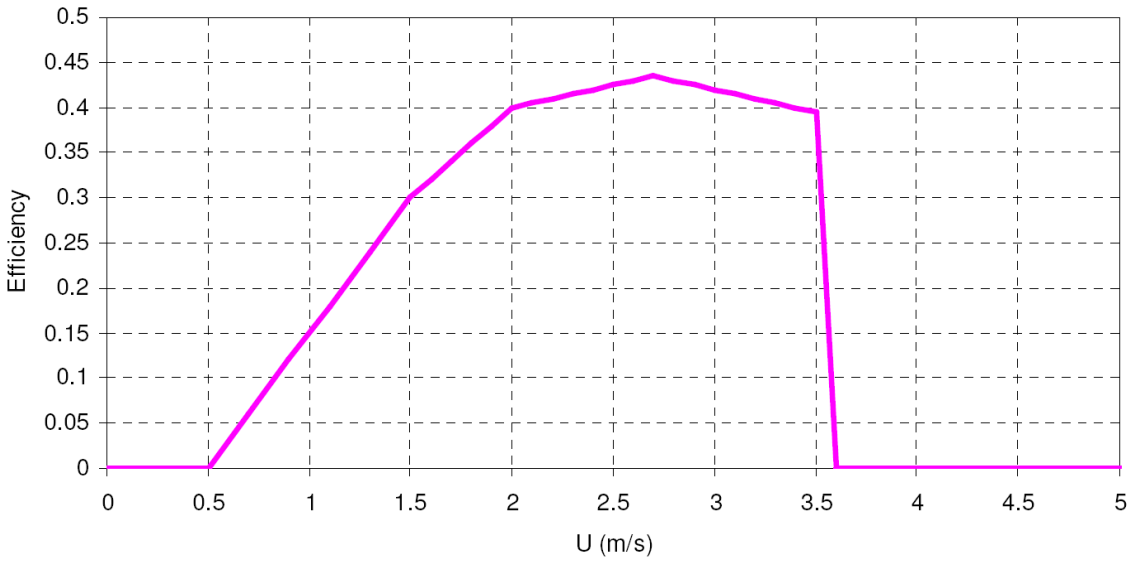

Figure 7: Efficiency curve for a generic energy convertor (so developed for higher currents than that occur at the BPNS). Source: (Cornett *et al.* 2010).

2.6 Suitable WECs for the BPNS

As mentioned in § 2.5, 3 WECs were selected due to the availability of their power matrix, without specifically taking the suitability for the BPNS into account (Pelamis is not suited, Wave Star and Protech Straumekraft are better). In this paragraph, WECs that show interesting characteristics for deployment on the BPNS are briefly discussed. However, no currently existing WEC can be taken 'off the shelf' for deployment on the BPNS, therefor the conditions on the BPNS are too specific.

In the OPTIEP-BCP report, 3 WECS were presented that showed interesting features for deployment on the BPNS (Mathys *et al.* 2010). These were Wave Star, Power Buoy and the B1 of Fred Olsen. After the analysis of BOREAS, other WECs were selected, due to new concepts, developments or insights. Wave Star is still discussed here and the B1 of Fred Olsen is replaced by the FlanSea buoy (which is an indirect continuation of the project SEEWEC). Power Buoy is however replaced by Seabased and Wavetreader (Point Absorbers). Seabased was preferred due to the simple concept and development in the Swedish coast (with similar wave powers as on the BPNS) and Wavetreader was selected due to their synergetic effects with offshore wind foundations. This is again an example of the rapid development that characterizes this market. The WECs presented here are:

1. Seabased: a PA buoy developed by the Electrical department of Uppsala University Sweden. It is a simple mechanical system, putting more design effort in the electrical design and control;
2. Wave Treader: a point absorber which is explicitly designed to be attached to monopile foundations of windmill farms;
3. Wavegen: an OWC integrated in a breakwater in Mutriku, Spain.
4. Wave Star: a jack-up structure with individual point absorbers attached.
5. FlanSea: a point absorber buoy that is explicitly designed for low too moderate wave conditions. The project team consist of DEME Blue Energy, Electrawinds, Cloostermans, Spiromatic, the harbour of Oostende, Contec and 4 research groups of the Ghent University;

2.6.1 Seabased WEC – Lysekill (Sweden)

2.6.1.1 *Introduction*

Seabased is a spinoff of the Uppsala University from Sweden. They developed a point absorber with a linear generator, without gearboxes and few moving parts. The developers thus chose to have a very simple mechanical system, but a rather advanced electrical system (since it was the Electrical department of Uppsala who started the development).

2.6.1.2 *Concept and design*

A unique feature of their design is the fact the PTO module is not situated in the buoy, instead it is mounted directly on the gravity based anchor plate. The PTO is a direct-driven, linear, synchronous three-phase generator. The technology of the linear generator was assumed to be somewhat depth independent and the unit size of 10 kW for power conversion was assumed to match a significant wave height in the range of 2 m, found in near shore and sheltered waters typical for Swedish conditions. However, the generator and the mechanical structure of the generator are designed to handle great over-loads in terms of electrical power and mechanical strains. This makes it possible to e.g. change the buoy to a buoy with larger diameter in the offshore experiments without damaging the WEC (Leijon *et al.* 2008).

The PTO is a linear generator with little moving parts apart from a cable and a permanent magnet. The concept of the PTO remained the same during the test period, but the shape and draft of the buoys did change. Four different buoys were tested, one of them was a donut shaped buoy.

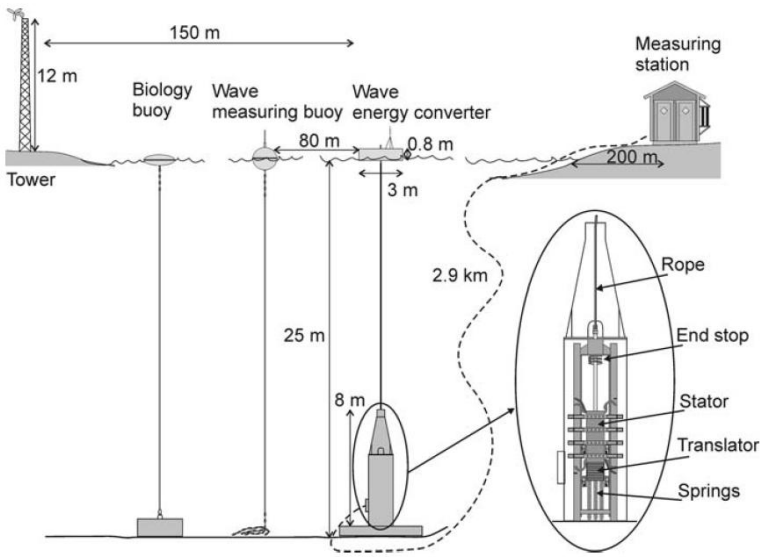

Conceptual drawing of the Seabased PA WEC deployed at Lysekill, Sweden (Leijon *et al.* 2008)

The linear generator, mounted on a gravity based anchor.

Figure 8: Concept (left) and picture (right) of the PTO of Seabased.

Furthermore, the Lysekill project executed environmental studies from the beginning of the project, and all the results of the environmental monitoring are documented (Langhamer 2009).

2.6.1.3 *Considerations for deployment on the BPNS*

The Lysekill testsite has similar wave conditions of those on the BPNS. The Lysekill testsite has an average wave power of 2.6 kW/m, a depth of 25 m, a significant wave height with 100 year return period of 4m, and a maximum wave height with a return period of 100 years of 6.2 m (Waters *et al.* 2009). These characteristics, especially the wave power, are representative for the conditions on the BPNS. The developers chose this site because of the existing research infrastructure nearby Lysekill: "*Due to its relatively low energy flux, the wave climate at the Lysekil test site would not be ideal for commercial wave power production. That was, however, not the motive for choosing the site; it was chosen due to its proximity to the marine research."* (Leijon *et al.* 2008).

However the tidal range is less than 25 cm, which is in sharp contrast with the BPNS where the tidal range is up to 4.5m. The latter is a disadvantage for deployment on the BPNS, as the tidal range uses the full stroke length of the generator. An alternative could be to install a drum in the buoy to account for the stroke length differences caused by the tidal range.

Other problems that can expected based on their design are:

- the friction and heating of the cable, and consequently, tear and wear of this cable;
- the sealing of the chamber has to be extremely good, since maintenance is only possible with divers, ROVs, or lifting the whole PTO with its foundation outside the water.

2.6.2 Wave Treader WEC (Green Ocean Energy 2010)

2.6.2.1 *Introduction*

Wave Treader is a unique wave energy device which is attached to the supporting pile of an offshore wind turbine. Combining Wave Treader to an offshore wind farm shares the offshore infrastructure and also increases the yield from the sea area. According to Green Ocean Energy, Wave Treader also assists in power smoothing in the offshore wind farm and offers improved personnel access to the turbine (claim by developer), both of which are major benefits to site developers.

2.6.2.2 *Concept and design*

Wave Treader concept utilizes a fore and after arm and sponson which react through an interface structure onto the foundation of an offshore wind turbine (Figure 9). Between the arms and the interface structure hydraulic cylinders are mounted and as the wave passes the machine first the forward sponson will lift and fall and then the after sponson will lift and fall each stroking their hydraulic cylinder in turn. This pressurizes hydraulic fluid which is then smoothed by hydraulic accumulators before driving a hydraulic motor which in turn drives an electricity generator. The electricity is then exported through the cable shared with the wind turbine.

Figure 9: Conceptual design of the Wave Treader of Green Ocean Energy, attachted to the monopole of an offshore windmill..

Periodically the interface structure moves vertically to allow for the effects of tidal range, and it also can rotate to ensure that the sponsons are optimally aligned with the wave direction.

An initial study[3] commissioned by the company indicates that the additional loads placed on the foundation of an Offshore Wind Turbine from Wave Treader are relatively small, and therefore Wave Treader will not adversely affect the stability of the Wind Turbine. However, this point will certainly need further 3rd party verification.

2.6.2.3 *Future market deployment*

Wave Treader is primarily aimed at the UK Round 3[4] and Scottish Territorial Water offshore wind farm sites. The company estimates that between 2015 and 2023 7,500 to 8,300 offshore wind turbines will be installed in the UK waters and claims that their device can also be retrofitted to existing windmill foundations. The company is building a full scale prototype in 2011-2012 for deployment at a UK test centre. The Green Ocean Energy indicates on their website that they want to develop the same technology further for standalone WECs, so independent of the pile of offshore windmills.

2.6.2.4 *Considerations for deployment on the BPNS*

The Wave Treader device has one obvious advantage: it connects to an offshore windmill pile, but, although the Green Ocean Energy claims to make an easily accessible Wave Treader, they do not specify how they would implement this.. According to the BOREAS authors, adding a

[3] Wave Treader did not mention the reference for this study.
[4] This is the new tender round for granting offshore windmill parks in Scottish waters.

structure to an existing windmill foundation would just make accessibility harder. So, the claim by Green Ocean Energy of enhanced accessibility needs further verification. Wave Treader does make use of the infrastructure of windmill farms (foundation, grid connection, etc.). Furthermore, it also can profit from the time lag and intermittent character of both wave and wind energy. High windspeeds and big waves do not always occur simultaneously, especially in exposed locations. However, even in the sheltered BPNS, the waves continue to go on after the wind drops. Equally important in a Belgian context, is the fact that it makes an optimal use of space possible.

However, some disadvantages need to be mentioned as well. This device is developed for, highly energetic, Scottish seas and has a rated power of 500 kW, so scaling down will be necessary. How much scaling down is hard to tell, but the Wavetreader should be more or less in equilibrium with the installed power of a windmill. Combining a 10 kW Wavetreader with a 5 MW windmillfarm does not seem very logical, because it adds complexity to the structure, operation and maintenance (boat access) with only a little marginal energy production. Adding the Wavetreader to existing piles ('retrofitting') will most likely not be possible, as the added geotechnical and structural requirements were not foreseen in the design of the current windmills.

2.6.3 Wavegen Voith OWC WEC– Mutriku breakwater

2.6.3.1 *Introduction*

In the Basque county in Spain, a new breakwater was designed for the small harbour. EVE (Ente Vasco de la Energia) chose to integrate 16* 18.5 kW OWC turbines into the design of the breakwater, by building the air compression chambers in front of the breakwater (Figure 10).

Figure 10: Construction of the Mutriku breakwater and air compression chambers (left).

2.6.3.2 *Concept*

The Mutriku breakwater is a nice example of a combined use of a breakwater: on the one hand it protects the harbour against waves, on the other hand it is a 300 kW OWC wave energy converter. Originally the plan for the breakwater was a 'normal' breakwater, without the OWC, but soon after the first concept, the idea of an OWC was integrated.

The waves at a location in front of Mutriku in deep water contains approximately 26 kW/m of wave energy, with a seasonal variation of 44 kW/m in winter, 19 kW/m in spring or autumn and 9 kW/m in summer. Just in front of the breakwater (30 m deep) the wave climate is 18 kW/m in winter, 8.8 in spring or autumn and 4.4 in summer. It is expected that this installation can produce 600 MWh/year, corresponding to the energy requirements of 250 households in the Mutriku town. According to the investor, the civil costs are estimated at 4.4 mio €, the electromechanical costs at 1.5 mio €, and the other costs (licensing, etc.) are estimated at 0.5 million € (Yago 2009).

2.6.3.3 *Considerations for deployment on the BPNS*

The double function of a combined breakwater and energy production is in principle an interesting feature for deployment on the BPNS. However, the capital cost of these projects are high. It is therefore unlikely that these projects can be retrofitted to the existing coastal defence structures nearshore. An interesting and somehow visionary project is the project 'Vlaamse Baaien'. It is an integrated future vision on the development of the BPNS in terms of (navigational and coastal) safety, sustainability, attractiveness, environmental and general development (Vlaamse Baaien 2010). Ten projects were presented as ideas to support this future vision. One of them, the idea of a multifunctional island at the Gootebank, could be combined with this technology. It is conceived as a test site for sustainable marine energy, a shelter harbor, offshore services or transfer of bulk materials. The integration of different functions is interesting and can only be achieved if the initial design does take into account this function. Furthermore, the Gootebank is situated in a zone outside the Flemish banks, and experiences higher wave energy than nearshore. The project team behind the Vlaamse Baaien gives an indicative framework of 2020-2050 for this island.

2.6.4 Wave Star WEC

2.6.4.1 *Introduction*

Wave Star is currently one of the very few devices that actually provides electricty to the grid with a 2 float (each 5m diameter) 110 kW test unit. The price of the electricity produced is not yet competitive to the market according to Wave Star, but the next steps, two full scale units (Marquis *et al.* 2010b), one 600 kW with 20 floats of 5m diameter (for water depths from 10-15m and a H_s of 2.5m) and the second a 6 MW unit with 20 floats of 10 m diameter (for water depths from 20-30m and a H_s of 5m) each should significantly drop the electricity price (Figure 11). This price projection is based on 3 parameters: increasing energy production, decreasing investment cost and decreasing maintenance. Interesting to see in the roadmap is that in 2010 Wave Star is producing electricity at around 1000 €/MWh, whereas in 2019 it drops below 100 €/MWh (although the latter comes of course with higher uncertainties).

Furthermore, Wave Star has a very transparant and open communication strategy. According to Wave Star, over 500 visitor visited the Wave Star test unit at Roshage, in close collaboration with the Danish Wave Energy Center.

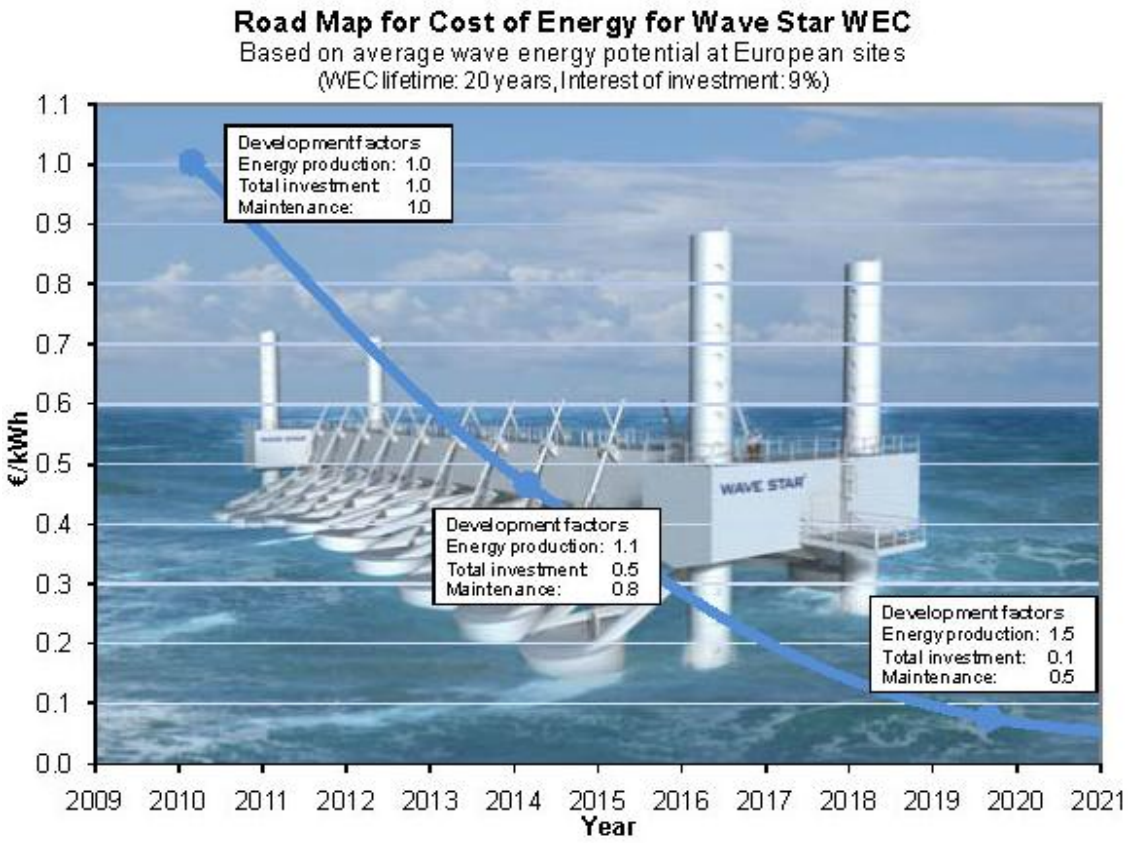

Figure 11: Road map for cost of energy for Wave Star WEC (based on average energy potential at European sites, WEC lifetime: 20 years, interest of investment: 9%). Source: (Marquis *et al.* 2010b).

2.6.4.2 *Concept and design*

Wave Star is using the point absorber technology, but integrates it in a unique jack-up platform. Most other 'clustered' wave point absorbers (like the old SEEWEC Buldra platform) are based on floating platforms which are moored and anchored to the seebed. In the full scale design, it is the intention that a jack-up platform will hold 2 rows of 10 floats each (acting as 20 point absorbers). All electromechanical moving parts are located on the platform, which remains at all time above the waterline. In storm survival mode, the Wave Star can lift the floaters also out of the water into a safety position. The PTO system is hydraulic, whereby each float is pumping hydraulic fluid to a hydraulic motor, which drives a generator. Instead of having 20 small hydraulic circuits for each float, a combined hydraulic PTO is used, to smooth out hydraulic peak pressures.

2.6.4.3 *Considerations for deployment on the BPNS*

A general disadvantage for deployment on the BPNS, is the jack-up structure to hold the floaters, because it increases capital cost. It is unlikely that these devices can be combined with with offshore windmill foundations, and Wave Star have not explicitely released information about research in that direction.

Remark that Wave Treader (§ 2.6.2) and Wave Star share similar concepts. However, Wave Star uses an array of buoys instead of a sponson. Another company, the Israeli company SDE, uses a similar technology but attaches its sponsons to breakwaters instead of windmill monopiles. They tested a 40 kW prototype in Jaffa, Israel for 1 year. However, since 2007, the company has not released any news so it is unclear if the development stopped or not.

2.6.5 FlanSea

2.6.5.1 *Introduction*

Although the development of the FlanSea point absorber buoy just started in 2010, it is worthwhile to mention this technology because it will be specifically developed for low to moderate wave climates, like the conditions that can be found on the Southern North Sea (and thus the BPNS). The FlanSea project is an indirect continuation of the SEEWEC project (which was coordinated by AWW - Ghent University). The project team consists of both industrial partners, as well as 4 research groups of Ghent University. The industrial partners are DEME Bleu Energy, Cloostermans, Electrawinds, Spiromatic, the Harbor of Ostend and Contec. The project has received funding from the Flemish Agency for Innovation and Technology.

2.6.5.2 *Concept and design*

The FlanSea wave energy converter is based on the so-called “point absorber” technology. These point absorbers keep track of and react in synchronization with wave motions, whereby their movements relative to the seafloor as a fixed point of reference can be converted to electrical power. The generator will be mounted on/inside the buoy itself. Moreover, inside the buoy there is a winch with a cable wind around it. The other, far end, of the cable is fixed into the seafloor. The buoy will use the rising and falling motions of the waves to wind or unwind the cable on the winch, thus producing electrical power (Figure 12).

During the first two years of the project, the expertise within the team will be directed towards conducting a thorough study (hydraulic, mechanical, electrical) of developing and building a wave energy converter, and conducting tests in laboratory conditions. During the 3rd and final year of the project, a wave energy converter will be positioned at approximately 1 km outside the port of Ostend. This wave energy converter will feature different measurement and registration devices meant to provide scientists with insights into production capabilities (efficiency) and the loads and the strength and resistance (survivability) of the system. During this phase, the converter will not be connected to the electrical distribution grid.

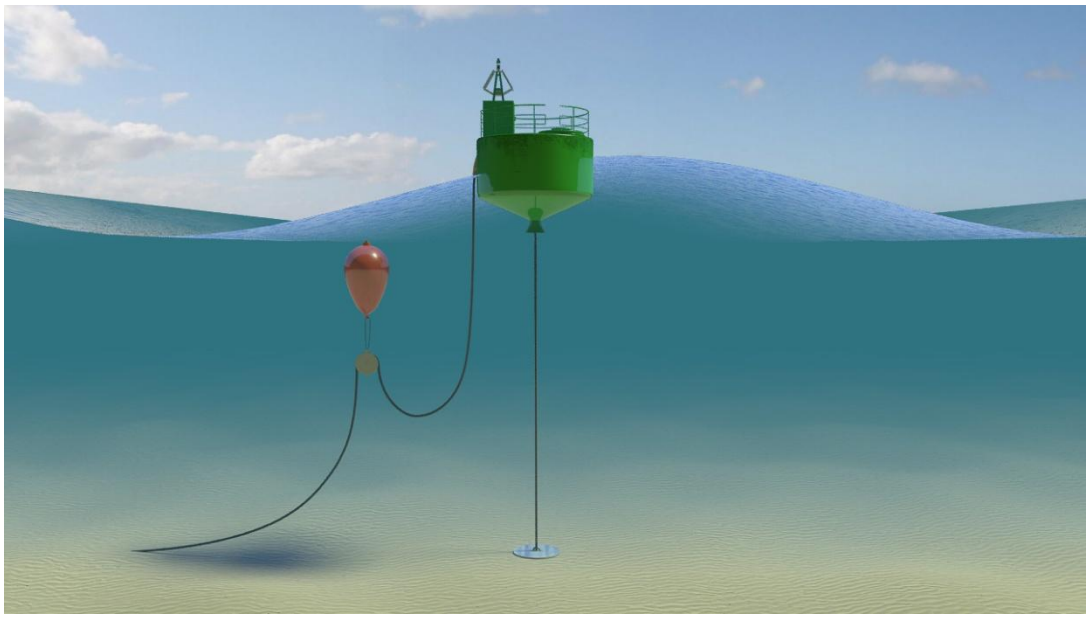

Figure 12: Concept of the FlanSea point absorber WEC, specifically designed for low to moderate wave climate conditions found on sheltered seas, like on the BPNS.

2.6.5.3 *Considerations for deployment on the BPNS*

Although the FlanSea buoy is still in an early development phase, it is one of the very few devices known to the authors that is explicitly designed for low to moderate wave climates. The Seabased technology (see § 2.6.1) is perhaps the direct competitor, as it is also conceived as a simple and robust design, but it cannot account for the different water levels causes by the tidal range found on the BPNS.

2.7 Suitable TECs for the BPNS

As mentioned in § 2.5, one 'generic' TEC was selected due to the absence of device specific power curves. In this paragraph, TECs that show interesting characteristics for deployment on the BPNS are briefly discussed. However, no currently existing TEC can be taken 'off the shelf' for deployment on the BPNS, therefore the conditions on the BPNS are too specific.

In the OPTIEP-BCP report, 3 TECS were presented that showed interesting features for deployment on the BPNS (Mathys *et al.* 2010). These were Davis Hydro Turbine, the cross flow TGU Turbine from Ocean Renewable Power and the SmarTurbine from Free Flow Power. After the analysis of BOREAS, only the Davis Hydro Turbine remained of these three. TGU Turbine has changed its concept and is no longer a cross flow turbine. Free Flow Power is now focussing on river applications (and classical hydro-energy and storage) and no longer on open sea applications. Just, as in the case with the changed WEC selection, this is again an example of the rapid development that characterizes this market.

For the TECs, only some 'niche' devices were selected. The majority of the TEC market consists of HATTs (Horizontal Axis Tidal Turbines). The HATTs that are currently developed aims for high tidal current climates, and is therefore less suitable for the deployment on the BPNS today. The TECs presented here are:

1. VIVACE: a special TEC,based on resonance effect instead of using a turbine.

2. Ecofys: a Dutch 'wave rotor', which is a hybrid technology to capture both wave and tidal current energy.
3. Davis Hydro: a VATT which is designed for construction e.g. with bridges.

2.7.1 VIVACE TEC (Vortex Hydro Energy)

2.7.1.1 *Introduction*

Vortex Hydro Energy (VHE) is a spinoff of the Michigan University and developed a TEC based on vortices, which absolutely need to be avoided in classical (civil) engineering constructions. Vortices are vibrations that can cause accelerated material fatigue in industries like civil and maritime construction. The system of VHE is based to *maximize* these vortices in a way that they induce a controlled up and down movement of cylinders that are orientated perpendicular to the incident flow.

2.7.1.2 *Concept and design*

The physical phenomenon of the Vortex Induced Vibrations (or VIVs as they are called by VIVACE) and the concept is shown in Figure 13. The interaction between the fluid and the structure occurs because of nonlinear resonance of cylinders or spheres through 'vortex shedding lock-in'. That is, the period at which vortices are formed and shed becomes synchronized with the side-to-side motion of the bluff body, and thus the motions become amplified over time. As a reflection of this, the phenomenon can be characterized as vortex induced vibration, wake synchronization, vortex shedding lock-in, or nonlinear resonance.

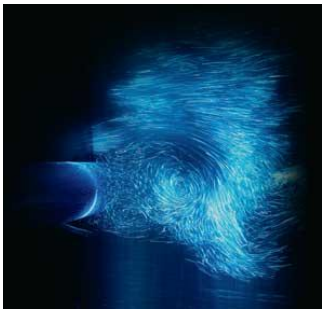

Visualization of the induced vortices behind a cylinder in a laboratory wave flume.

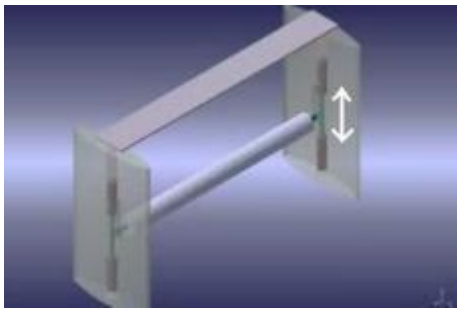

Concept of the VIVACE, with the cylinders moving up and down.

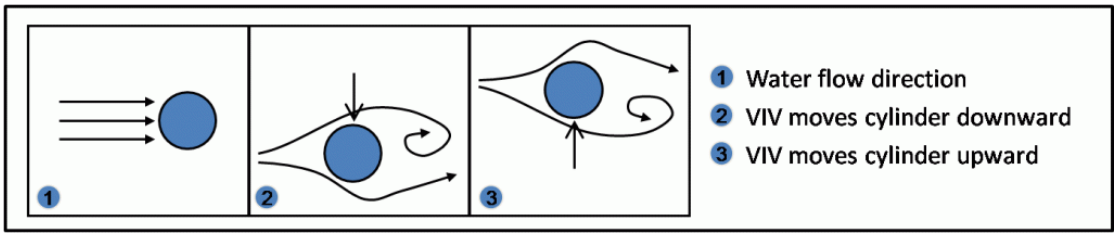

Working principle and the 'vortex lock in' phenomenon in the wake of cilinder, which forms the basis of the power production for VIVACE

Figure 13: Vortices induced by a cilnder placed in a current (left) and concept of VIVACE (right).

A small converter with 180 5-meter cylinders operating in 5 meters of water could generate 100 kW at 1.5 m/s. Such a converter would have a footprint of about 300 m². The design parameters that Vortex Hydro is now focusing on, are the diameter/length ratio, and the optimal configuration of multiple cylinders in order to maximize the energy production.

2.7.1.3 *Market and future development*

VIVACE already deployed a single test unit in a river to test in real conditions (Port Huron, Michigan in 2010). They are aiming both at the river currents and tidal current market. Although their website does not mention projected prices of the COE, the Chief Technology Officer (CTO) of the company said in an interview that the estimated price would vary around $ 55/MWh (Schwartz 2008).

2.7.1.4 *Considerations for deployment on the BPNS*

VIVACE is interesting for deployment on the BPNS for several reasons:

- VIVACE has a very low cut-in speed: from 0.5m/s on, the cylinders start moving and the electricity production starts, most turbine based TECs (HATTs of VATTs) have cut-in speeds of 0.7 – 1.0 m/s;
- Despite the fact that is has no gearbox or pitching blades (like HATTs of VATTS typically have), they can still produce energy in a wide range of operational conditions. This is due to the vortex-shedding synchronization (the physical phenomenon that drives the cylinder up and down) occurs over a broad and continuous range of frequencies, not just at natural frequency, as in linear resonance (Raghaven *et al.* 2007). This in sharp contrast with e.g. point absorber WEC, where resonance and hence the control algorithm is an absolute condition to optimally extract power.
- Although it is not the primary research focus at this moment, Vortex Hydro is one of the many developers who are looking synergies with offshore wind; their concept is shown in Figure 14.

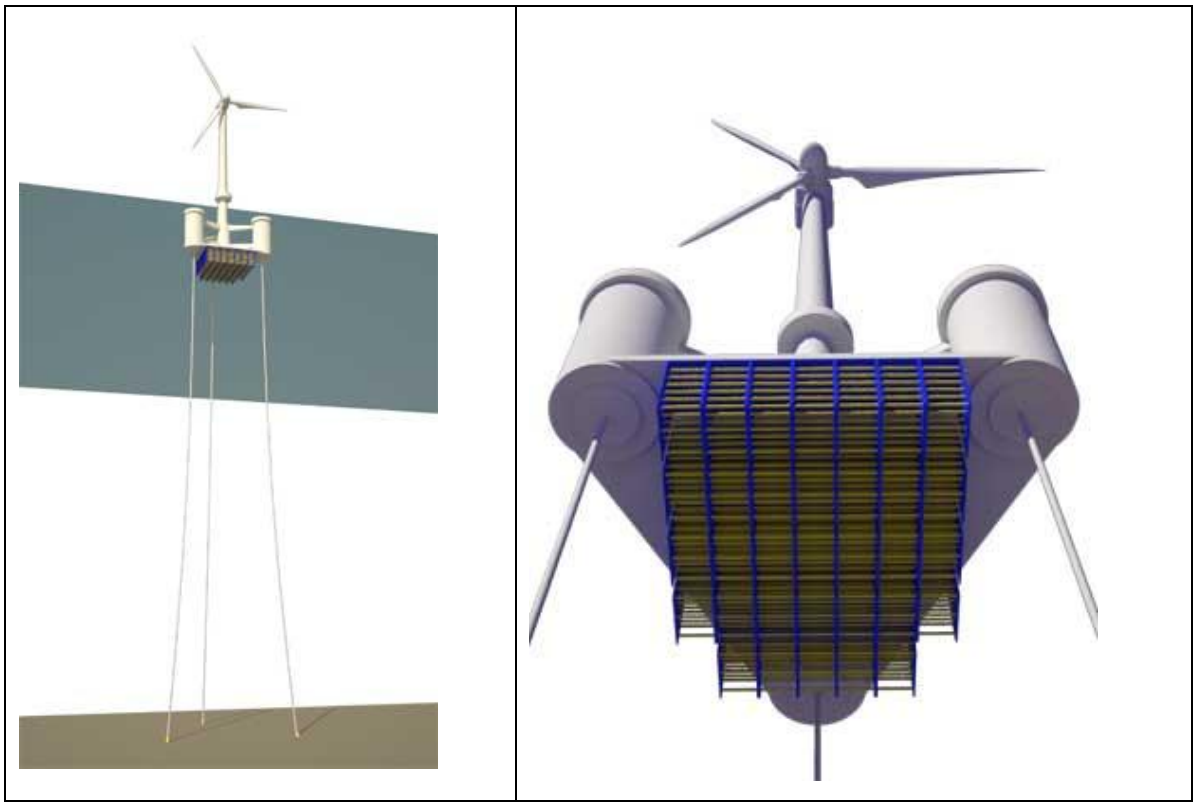

Figure 14: Vivace technology combined under a floating windmill (ASME 2010).

2.7.2 Ecofys waverotor (combined TEC/WEC)

2.7.2.1 *Introduction*

Ecofys is a Dutch company specialized in sustainable energy and energy efficiency is currently test a unique grid-connected 'wave rotor' at Borssele in the Scheldt Estuary. Note that this is a combination of a WEC and TEC, which will be explained further. The original concept came from a Danish partner Eric Rossen and was tested in Nissum Bredning, Denmark.

2.7.2.2 *Concept and design*

The Wave Rotor works based on simple wind turbine principles and is capable of converting wave and tidal energy directly into electrical power. This is realized without the need of intermediate transmission steps.

Ecofys' wave rotor has the unique feature that it can exploit both wave and tidal energy. Although the name says wave rotor, it is listed here as a TEC since the deployment at the pier at Borssele is conceived as a TEC. Rather than looking at the up and down movements of waves there is also considerable energy to be captured from the circulating water particles in the waves creating local currents. The waverotor uses the circular currents to directly drive a rotor to produce electricity directly (without a hydraulic circuit or other intermediate step). In order to tap energy directly from both the up and down and back and forward currents, two types of rotors were combined on the same axis of rotation(Figure 15):

- Darrieus rotor (see Figure 6), consisting of the vertical blades on the figure. The tidal currents in the horizontal direction make the rotor turn;

- Wells rotor, consisting of the horizontal and inclined blades on the figure. The Wells rotor is turned by the up- and downward component of the orbital movement of the water particles;

These are respectively omni- and bi-directional rotors, which can operate in currents of changing directions. Another advantage of this simple, light but strong structure is that it is expected to better withstand storm conditions than other systems, because of the minimal exposed surface area. The 'swept' area is approximately 25 m².

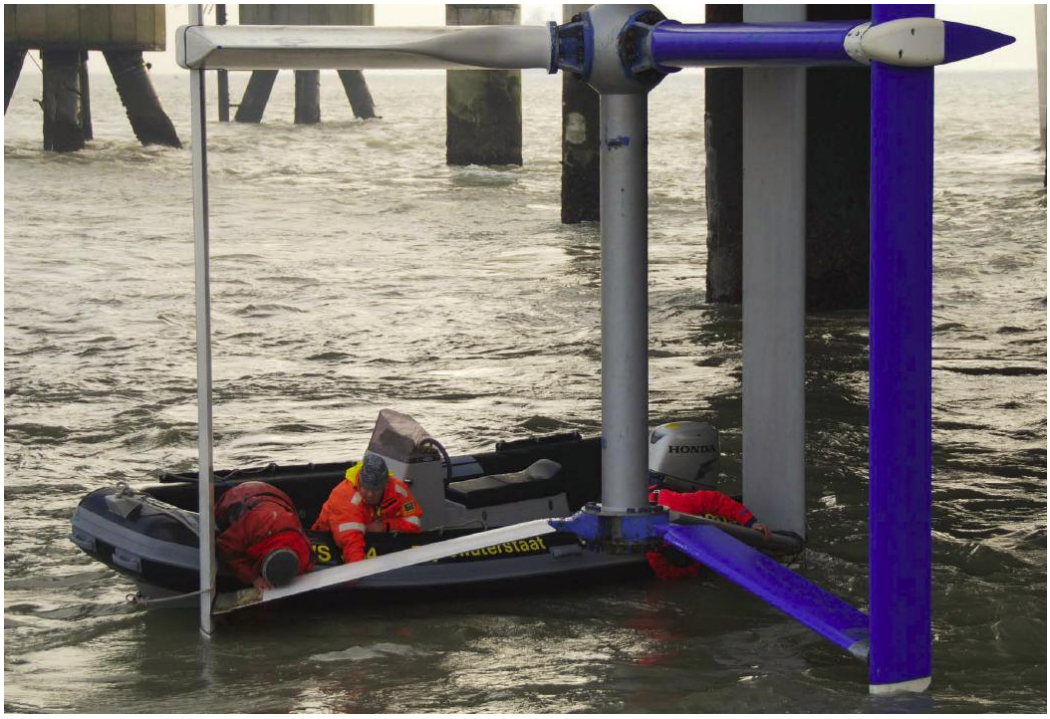

Figure 15: Inspection of the Ecofys Waverotor blades (Borssele, the Netherlands), Picture by Peter Scheijgrond.

2.7.2.3 *Considerations for deployment on the BPNS*

Ecofys waverotor has some interesting features for deployment on the BPNS:

- It is the only device that combines the energy from both wave and tidal currents. This combination has both advantages and disadvantages.
  Disadvantages are:
  - One can argue that the individual efficiency of one of the rotors may be low compared with a device that is a pure TEC or WEC.
  - Locations where both the tidal current and the wave current are high, are rare. High currents typically occur at locations with disturbances in the geometry or depth, whereas high waves typically occur at deep water.

  Advantages are:
  - The joint wave and tidal current energy extraction could provide benefits in reducing capital and operational costs. This can be even increased by using windmill foundations, thus combining 3 types of renewable energy (Figure 16).
  - More constant energy producing by relying on 2 energy sources.

- The current testsite is located at Borssele in the Scheldt estuary at a location where the currents are high. Although this zone belongs to the Dutch Continental Shelf, the vicinity of this test site is useful in term of contact with the developers and ease of access.

If the results are promising, a pre-commercial 50 kW demonstration unit will be built. Meanwhile the ideas have been patented. In the future 0.5 MW mono-pile units are envisioned which are mounted in arrays on the seabed.

	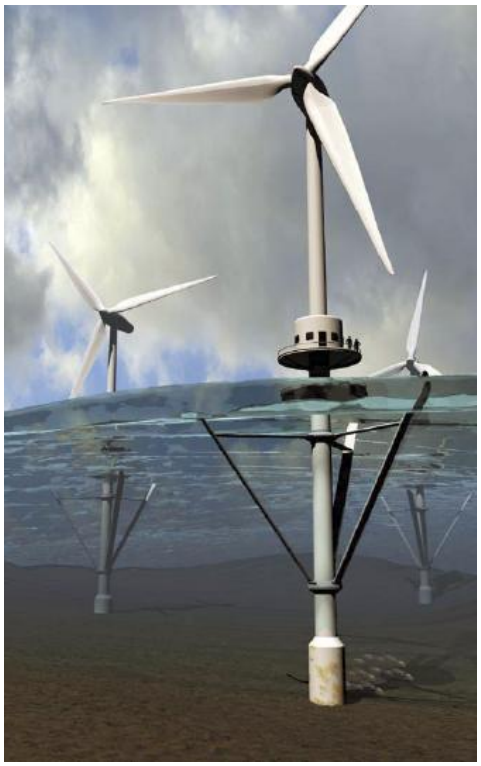
Configuration with the main focus on the Darrieus rotors, and consequently, tidal energy.	Configuration with the main focus on the Wells rotors (with the blades just below the surface, where the orbital velocity of the waves, and consequently, wave energy is the highest).

Figure 16: Two conceptual Ecofys waverotor configurations attached to a monopile windmill farm.

2.7.3 Davis hydro (TEC Blue Energy Canada)

2.7.3.1 *Introduction*

Cross-flow turbines are a good option to be placed in shallow waters, due to the compact rotors. These turbines have in general lower cut-in speeds than propeller type turbines, and can be placed in ducts or be attached to floating structures. Most of them are highly modular, due to the rectangular cross-sections, whereas propeller type turbines typically have circular cross sections. Here the Davis Hydro turbine is presented, but it is stressed that other devices with similar characteristic are under development, like the Gorlov Helical Turbine of Lucidenergy and the Proteus of Neptune Renewable Energy. Furthermore, the same group that developed the

Seabased WEC (the electrical department of the Uppsala University), is currently developing a cross flow turbine in collaboration with Current Power AB. They use a very basic design for the rotor and the blades and put more development focus in the generator. This approach is quite unique, since most developers try to design new blades or rotors for a given (commercially available) generator.

2.7.3.2 *Concept and design*

The basic idea of the Davis Hydro Turbine is a VATT, combined in an array to be mounted under a bridge over an estuary, or the 'Blue Energy Tidal Bridge Power System', as Blue Energy calls it themselves. A specific advantage is the accessibility, since the bridge will provide easy access for all kinds of equipment. Not only Davis Hydro seeks such a synergy, Teamwork technology, a Dutch company, tested their Tocardo HATT on the 'Afsluitdijk'.

This synergy is not directly useful for the BPNS, but Davis Hydro is presented here based on the conversion technology, and the fact that the PTO or generator are above the waterline, and thus easily accessible. Furthermore, a floating unit with ducts is possible, as indicated in Figure 17.

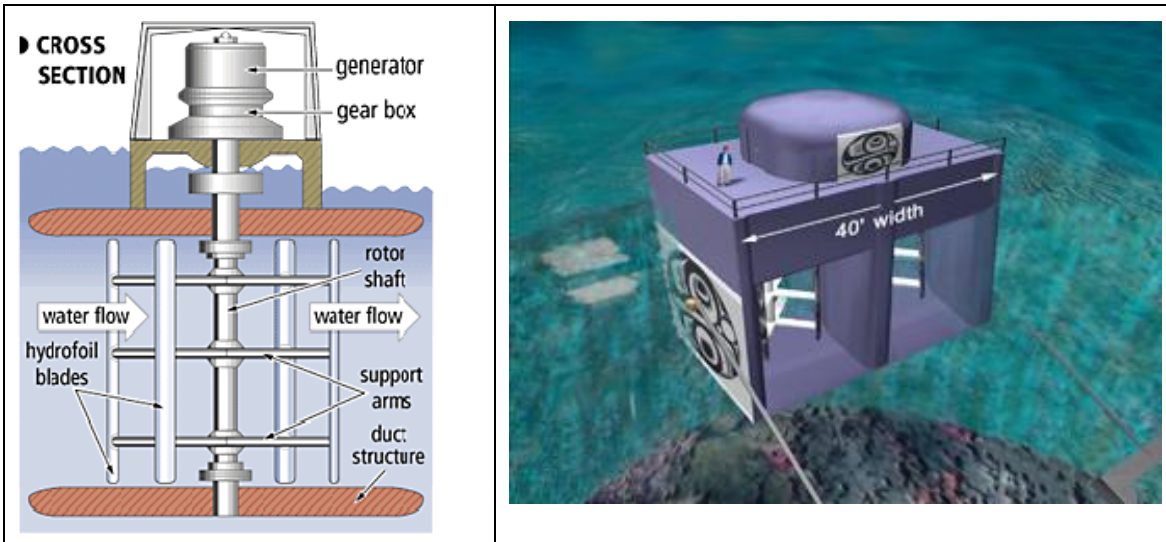

Schematic design	Floating Davis Hydro turbine

Figure 17: Conceptual designs of the Davis Hydro Turbine.

2.7.3.3 *Considerations for deployment on the BPNS*

As mentioned above, the Davis Hydro turbine is a vertical axis (ducted) floating turbine. All the critical components can be located above the water, making the installation and maintenance rather easy. Blue Energy Canada claims to have a lower cut-in speed than a typical HATTs. However, little information is available on their overall performance and efficiency.

2.8 Conclusion

Most WECs and TECs described here have interesting characteristics for the BPNS, but none of them can be taken 'off the shelf' for immediate deployment on the BPNS. Most of them were

just not developed for the specific conditions on the BPNS, with the exception of the FlanSea concept. The latter is however still in an early development phase, so reaching pre commercial demonstration projects (TRL-5) will take some years.

3 Overview of previous wave energy resource assessment based on buoy data.

3.1 Data source and methodology

The Belgian Part of the North Sea (BPNS) is small part (0.5 %) of the whole North Sea. Waves are modified when they travel to the coast and enter in shallower waters. The direction of waves changes when approaching the coast oblique to the depth contours. Furthermore, waves loose energy through bottom friction and depth induced wave breaking. In order to characterize the wave climate on the North Sea, and the Belgian Part of it, several national hydrographic institutes deployed buoys. The BPNS has a high density of buoys and some of them were already deployed in the mid 80's. The analysis of these buoy data makes the assessment of the wave climate - and hence the wave power resource - for a specific point location, reliable and straightforward.

The first calculations of the wave power resource based on buoy data for the BPNS were performed by dr. ir. Beels (Beels 2009). The following paragraphs present a short overview of the methodology and results obtained.

On the BPNS wave measurement buoys were deployed in varying water depths on various distances from the coast. The properties of six wave measurement buoys (Westhinder, ZW-Akkaert, Trapegeer, Oostende, Wandelaar and Bol van Heist) are given in Table 7.

Table 7: Properties of wave measurements on the BPNS. The wave data intervals represent the availability of the wave data which where used in the study of Beels 2009).

Name of location	Type of buoy	Longitude (WGS 84)	Latitude (WGS 84)	Wave data interval
Westhinder	Wavec	2 ° 26 ' 52 "E	51 ° 23 ' 12 "N	1990-2004
ZW-Akkaert	Waverider	2 ° 48 ' 12 "E	51 ° 24 ' 29 "N	1984-2004
Trapegeer	Waverider	2 ° 34 ' 59 "E	51 ° 08 ' 15 "N	1994-2004
Oostende(1)	Waverider	2 ° 55 ' 14 "E	51 ° 14 ' 34 "N	1997-2002
Oostende(2)	Directional Waverider	2 ° 55 ' 14 "E	51 ° 14 ' 34 "N	2002-2005
Wandelaar	Waverider	3 ° 03 ' 02 "E	51 ° 23 ' 32 "N	1995-2004
Bol van Heist	Wavec	3 ° 11 ' 43 "E	51 ° 23 ' 25 "N	1985-2004

In the case of the time domain analysis, the mean wave period (T_m) is determined by dividing a certain time of observations over the total number of down crossings of the water surface during that period. The significant wave height is the average of the 33% highest wave heights during this time (Figure 18).

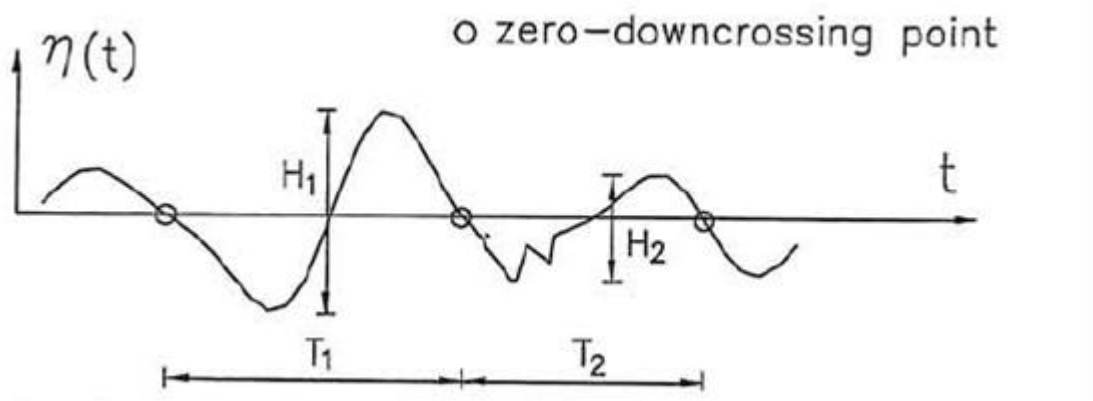

Figure 18: Determination of the mean wave period and significant wave height (based on zero-down crossing) on a water surface time series.

The measurements of a Wavec and Directional Waverider are analyzed in the spectral domain, whereby the calculation of the integral wave parameters (height and period) is based on the moments of the spectral density (Eq 1).

$$m_n = \int_0^\infty f^n S(f) df \qquad \text{Eq. 1}$$

With m_n is the n^{th} moment of spectral density
f= frequency (Hz)
n = order (-)
$S_{(f)}$= the spectral energy distribution (which gives the energy density for a certain frequency)

In the North Sea, the spectral density for developed sea states is characterized by a Jonswap spectral density. An example is given in Figure 19.

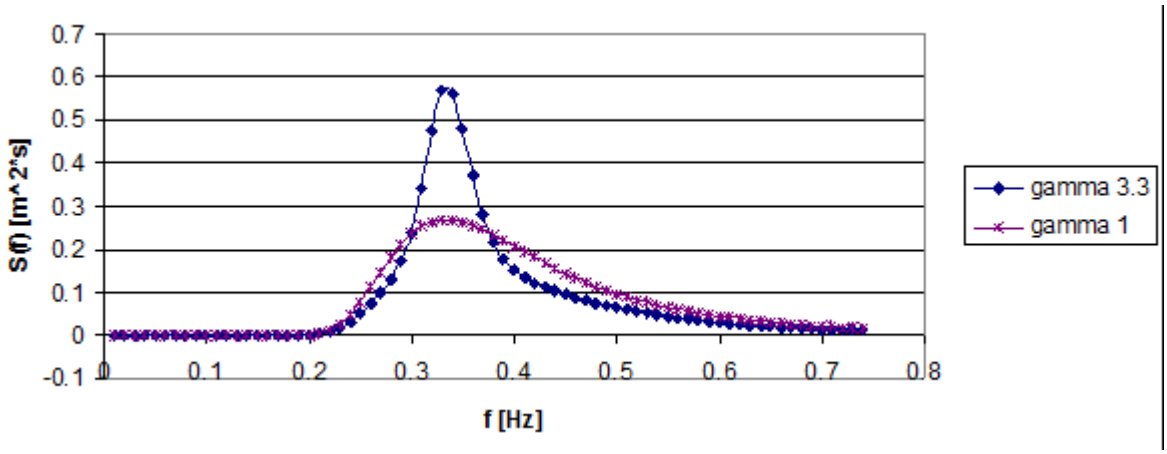

Figure 19: Theoretical shape of the spectral energy distribution of a Jonswap spectrum with different peak enhancement factors (gamma). Note that the m_0, the zeroth order moment, represents the area under the spectrum (Beels 2007).

Thus, in the frequency domain $H_s = H_{m0}$ and $T_m = T_{m0,2}$ as defined in the following equations (Eq. 2 and 3).

$$H_{m0} = 4\sqrt{m_0}$$ Eq. 2

$$T_{m0,2} = \sqrt{\frac{m_0}{m_2}}$$ Eq. 3

$T_{m0,2}$ is obtained with the second moment of spectral density (Eq. 3) and as a result may be sensitive to high-frequency (low period) low energy variations in the wave spectrum. Therefore sometimes T_p or T_e, instead of $T_{m0,2}$, is given in a scatter diagram. The energy period T_e is defined as equation Eq. 4, and is equal to the spectral wave period $T_{m-1,0}$.

$$T_e = T_{m-1,0} = \frac{m_{-1}}{m_0}$$ Eq. 4

T_e depends mainly on the lower frequency band of the spectrum (that contains most of the energy) and is therefore a more stable parameter than the traditional mean period $T_{m0,2}$. The peak period T_p is the inverse of the peak frequency that corresponds to the highest spectral density.

The relation between T_e and $T_{m0,2}$ is depending on the shape of the energy spectrum and T_p . For a Jonswap spectrum with the peak enhancement factor γ = 3.3. For a T_p between 3 and 15 s the average relationships are given by Eq. 5a and b:

$$T_e = 1.155 T_{m0,2}$$ Eq. 5a

$$T_p = 1.286 T_{m0,2}$$ Eq. 5b

Buoys typically measure directly movement parameters, like heave, pitch, roll, etc. based on a sensors like a gyrocompass or accelerometers. These raw measurements are transformed by means of on board processing into integral wave characterizing parameters like wave height and period (based on time domain analysis) or wave spectra (based on the frequency domain analysis). The integral wave characterizing parameters are further verified by Flemish Ministry of Transport and Public Works (Agency for Maritime and Coastal Services - Coastal Division) and transformed into directional or omni-directional scatter diagrams, for the total measurement period of each buoy. The scatter diagrams show the average frequency of occurrence (in %) of different sea states for one or more year(s), or one specific month, and a given directional sector (or omnidirectional if they are averaged over all the directions). A sea state derived from buoy data measurements is defined by a combination of significant wave height H_s and mean wave period, T_m (time domain analysis) or H_{m0} and $T_{m0,2}$ (frequency domain analysis). Notice that for wave power calculations, $T_{m-1,0}$ is the recommended wave period parameter, however historically most scatter diagrammes contain $T_{m0,2}$ (Table 8).

For every combination of H_s and T_m, the wave power is calculated with the correct formulation based on the energy spectrum (Eq. 6). This is done by assuming a parameterized Jonswap spectrum. Further background and details of this methodology is described in (Beels 2009)[5].

$$P = \rho g \int_0^\infty c_g S(f) df \qquad \text{Eq. 6}$$

Table 8: Average annual scatter diagram for all wind directions at Westhinder, based on measurements from 1-7-1990 until 30-6-2004 (Source: Flemish Ministry of Transport and Public Works (Agency for Maritime and Coastal Services – Coastal Division)), cited from (Beels 2009).

T_m [s] / H_s [m]	**0-2.5**	**2.5-3.5**	**3.5-4.5**	**4.5-5.5**	**5.5-6.5**	**6.5-7.5**	**7.5-8.5**	**>8.5**	Sum
0.0-0.5	0.05	4.52	12.33	4.07	0.55	0.06	0.01	-	21.58
0.5-1.0	0.01	6.12	20.51	8.38	1.91	0.3	0.02	-	37.25
1.0-1.5	-	0.29	11.63	8.98	1.83	0.27	0.02	-	22.02
1.5-2.0	-	-	1.89	6.46	2.02	0.27	0.01	-	10.65
2.0-2.5	-	-	0.04	2.67	2.00	0.42	0.01	-	5.14
2.5-3.0	-	-	-	0.57	1.17	0.5	0.02	-	2.26
3.0-3.5	-	-	-	0.04	0.46	0.26	0.04	-	0.8
3.5-4.0	-	-	-	-	0.09	0.07	0.05	-	0.21
4.0-4.5	-	-	-	-	0.02	0.03	0.02	-	0.07
4.5-5.0	-	-	-	-	-	0.01	-	-	0.01
>5.0	-	-	-	-	-	-	-	-	-
Sum	0.06	10.93	45.4	31.17	10.05	2.19	0.2	-	100

The analysis of these buoy data makes the assessment of the wave climate, and hence the wave power resource, reliable and straightforward. Unfortunately, it only provides information at the location of the buoy itself.

3.2 Results

Table 9 shows the average annual available wave power for different locations in the North Sea and surroundings. On the BPNS, the average annual available wave power ranges from 1.5 kW/m, approximately 3 km offshore, until 4.6 kW/m, approximately 30 km offshore. Characteristic sea states for Westhinder and ZW-Akkaert are given in Table 10 and Table 11. For Westhinder, the most representative sea state is sea state 3 (see Table 10), with a wave power of 4.29 kW/m.

Furthermore, monthly and yearly variations were assessed, which is shown in Figure 20 and Figure 21 respectively. As expected, the winter months, with January on top, yield the highest wave powers. The yearly results also show variations, ranging from 2.6 to 6.8 kW/m.

[5] Further this formula will be generalized for the two dimensional case (see eq. 11).

The primary reason is the occurance of big storms, with low probability but with high wave power; so increasing the wave power. A secondary reason is missing buoy data. For some years, buoy data is missing in winter (e.g. 2003), in other years buoy data is missing in summer (e.g. 2007). Table 12 gives an overview of the missing buoy data per year and month during the period 2000-2008.

Table 9: Wave power resource at different locations over the North Sea and surrounding based on buoy data with the exception of the 'points' on the Danish and the Norwegian Continental Shelf, and all locations of the UK Continental Shelf (Beels 2009).

Name of location (N°)	Average annual available wave power [kW/m]	Mean water depth [m]	Shortest distance to shore [km]
Belgian Continental Shelf			
Westhinder (1)	**4.64**	**29**	**32**
ZW-Akkaert (2)	3.64	23	20
Trapegeer (3)	1.51	7	4
Oostende (4)	1.66	6	1
Wandelaar (5)	2.63	13	10
Bol van Heist (6)	2.54	12	7
Dutch Continental Shelf			
ELD (7)	**9.86**	**26**	**31**
EUR (8)	7.04	32	36
K13 (9)	10.80	30	88
LEG (10)	6.13	21	15
MPN (11)	5.42	18	8
SON (12)	7.44	19	16
SWB (13)	5.57	20	20
YM6 (14)	8.68	21	32
German Continental Shelf			
Fino-Borkumriff (15)	**11.60**	**27**	**35**
Helgoland (16)	5.91	20	43
NSB II (17)	17.55	42	118
Westerland (18)	4.47	18	44
Danish Continental Shelf			
Point 1 (19)	7	20	64
Point 2 (20)	12	31	100
Point 3 (21)	**16**	**39**	**150**
Point 4 (22)	17	40	150
Point 5 (23)	14	58	100
Point 6 (24)	11	166	68
Fjaltring (25)	7	20	4
Norwegian Continental Shelf			
Point1160 (32)	23.60	200	57
Point1261 (33)	32.52	270	43
Utsira (34)	**23.12**	**200**	**21**
Ekofisk (26)	24	71	300
UK Continental Shelf			
Shetland (27)	42	200	30
Orkney (28)	33	90	27
Moray Firth (29)	19	112	55
Marr Bank (30)	**11**	**57**	**52**
Fair Isle (31)	61.47	100	70

Table 10: Characteristic sea states for Westhinder.

Location			Westhinder			
Mean water depth [m]			29			
Distance to shore [km]			32			
Average annual available wave power [kW/m]			4.64			
H_s with a return period of 25 years [m]			5.29			
Sea State	1	2	3	4	5	6
H_s [m]	0.25	0.75	1.25	1.75	2.25	2.75
T_e [s]	4.69	4.87	5.35	5.89	6.45	6.93
Wave power p [kW/m]	0.15	1.39	4.29	9.42	17.48	28.86
Frequency of occurrence FO [%]	21.58	37.25	22.02	10.65	5.14	2.27

Table 11:Characteristic sea states for ZW-Akkaert.

Location			ZW-Akkaert			
Mean water depth [m]			23			
Distance to shore [km]			20			
Average annual available wave power [kW/m]			3.64			
H_s with a return period of 25 years [m]			5.01			
Sea State	1	2	3	4	5	6
H_s [m]	0.25	0.75	1.25	1.75	2.25	2.75
T_e [s]	3.59	4.08	4.73	5.32	5.88	6.37
Wave power p [kW/m]	0.11	1.16	3.80	8.59	16.02	26.73
Frequency of occurrence FO [%]	24.02	38.46	20.97	9.81	4.23	1.66

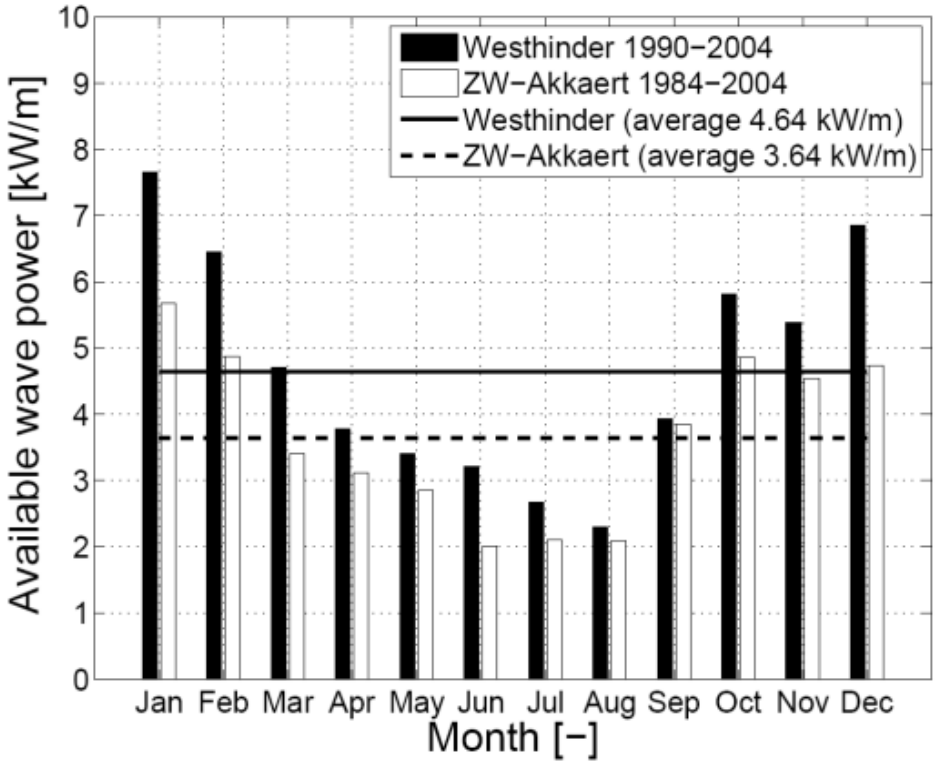

Figure 20: Variation of the monthly available wave power for Westhinder and ZW-Akkaert (1990-2004), (Beels 2009).

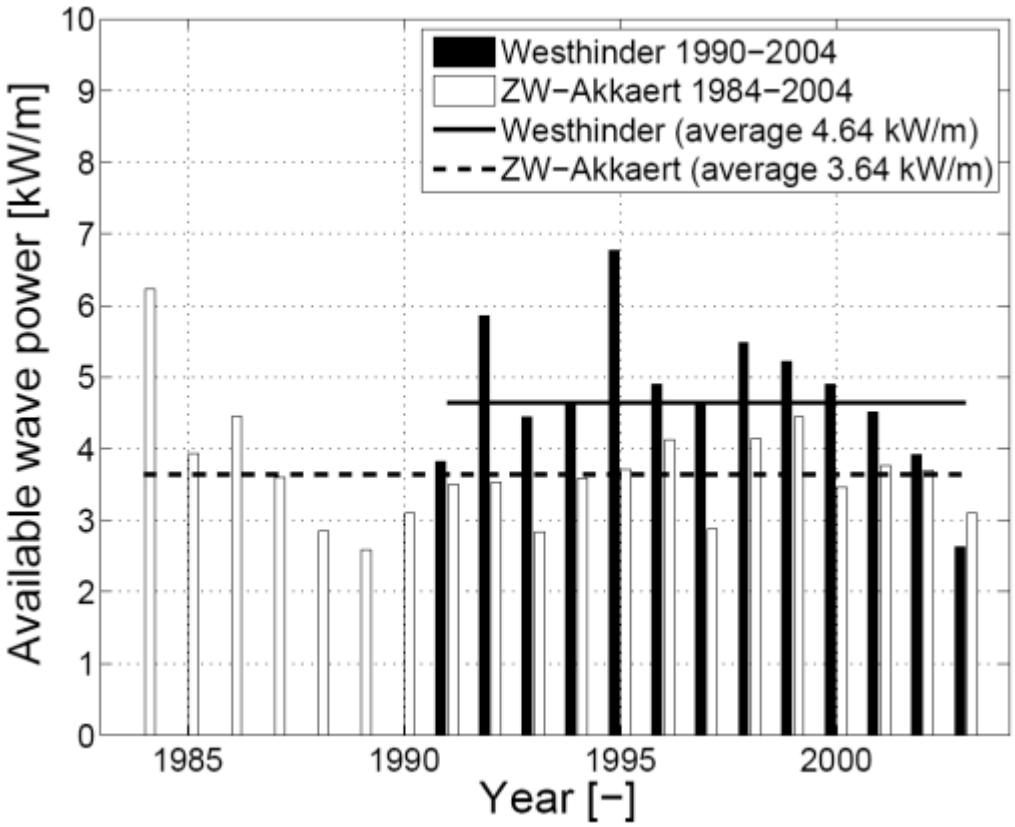

Figure 21: Variation of the yearly available wave power for Westhinder and ZW-Akkaert (1990-2007), (Beels 2009).Summary and main conclusions of technical notes

Table 12: Overview of the percentage of time where buoy data is missing in the buoy dataset. 100% indicates no buoy data during that month, 1% indicates no buoy data during 1% of the time.

Month/ Year	1	2	3	4	5	6	7	8	9	10	11	12	Total
2000	1.2	6.9	1.2	3.3	2.8	7.5	4.0	1.2	0.4	0.8	4.6	40.7	6.3
2001	52.4	35.3	21.0	17.9	12.9	10.0	12.9	6.5	2.5	2.0	0.0	3.2	14.6
2002	2.0	9.4	95.2	79.2	31.0	5.4	6.5	1.6	5.4	21.4	23.8	22.2	25.3
2003	30.6	53.6	45.2	72.1	71.8	27.5	45.6	4.0	0.0	4.4	28.8	61.7	37.0
2004	37.9	64.7	8.9	1.7	0.4	0.8	1.2	0.8	6.3	3.2	4.2	0.8	10.7
2005	1.6	17.0	26.2	12.5	11.7	5.0	13.7	17.3	7.1	8.5	26.3	8.1	12.9
2006	28.2	9.8	14.9	13.3	0.0	1.3	32.3	51.2	0.8	2.4	1.3	0.0	13.1
2007	22.2	14.3	54.8	100.0	100.0	100.0	100.0	63.3	0.4	9.7	1.3	0.0	47.4
2008	13.3	7.3	13.7	8.8	7.3	9.6	4.4	20.2	2.1	13.7	14.2	12.1	10.6
Total	19.0	21.9	28.1	30.9	23.8	16.7	22.1	16.6	2.5	6.6	10.4	14.9	17.8

4 Wave and tidal current numerical models

In the previous chapter, an overview was presented how buoy data can be used to assess the wave climate at specific locations. However, having a full geographical coverage of the wave climate is not possible with only buoy data. Therefore the numerical models, validated with buoy data come into place. The original set-up of the models, the calibration and validation and performance are described in detail in the following separate reports.

- The set-up, simulation and model results of the wave energy climate (performed by KULeuven (Fernández *et al.* 2010));
- The set-up, simulation and model results of the tidal current energy climate (performed by MUMM (Van den Eynde *et al.* 2010));
- The validation of the Wave model by means of the Transformation Matrix (performed by Flanders Hydraulics Research (Delgado *et al.* 2010));
- The validation of the Tidal current model by means of the LTV (Long Term Vision) Scheldt model, (performed by Flanders Hydraulics Research (Dujardin *et al.* 2010b)).

In this chapter, the main conclusions of these reports are presented. The first paragraph shows an overview of the points of interest. The second paragraph provides the reader with an overview of the different numerical models and tools, and their intermittent relationship. From there on the wave model results and validation are presented, followed by the tidal model results.

4.1 Zones of interest

BOREAS is investigating the wave and tidal current climate on 2 geographical scales. The first is a general overview of the whole Belgian Part of the North Sea. The results of the analysis on the whole BPNS will be maps with available and technical resources. However since some zones are more interesting than other zones[6], it was decided to define points of higher interest, for which 2D wave spectra were stored (Figure 22). In total 50 points were selected, of which 46 are located on the finest wave model (BSB model). The 4 points outside this model were the Dutch buoy locations Euro, LEG, K13 and an output point of the Anemoc database. Out of of the 46 points that were located on the finest grid, 28 points were selected of primary interest (domain concession zone, location of buoy data, etc…).

[6] Furthermore, saving all the ouput information (especially the timeseries of the full 2D wave spectra for all the grid points) was not possible, due to storage (and processing) limitations.

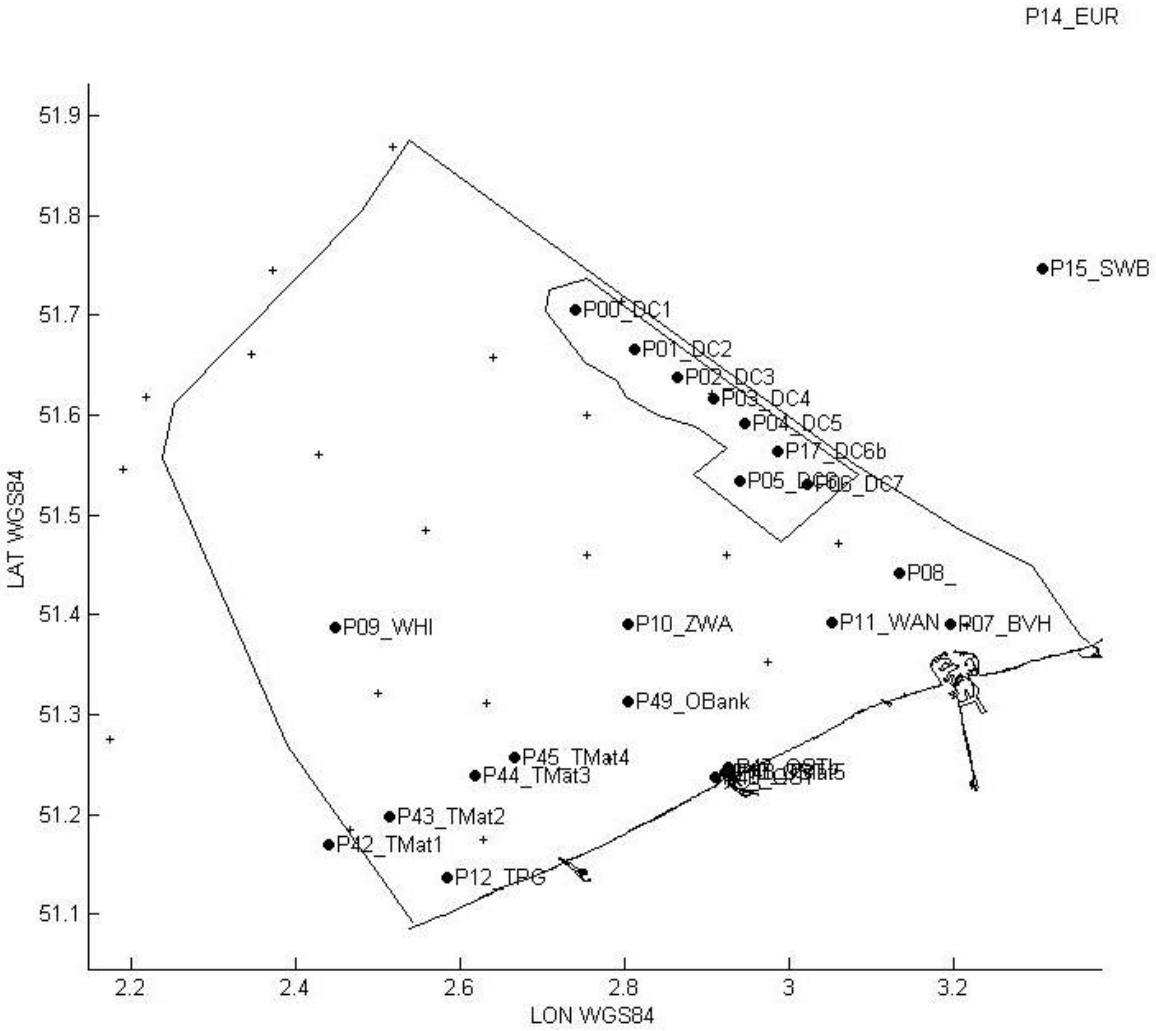

Figure 22: Points of interest for the wave modeling. The big dots with the indication of names are identified as zones of interest within this project, the small crosses were chosen for other reasons, like comparison with other models.

4.2 Introduction to the numerical models

Nine numerical models (10 if one also takes into account the Transformation Matrix as a numerical model) were used to set up the full model train and validation, but the further analysis was based on the 2 most detailed models. The wave model train consists of 3 nested models. The finest model, BOREAS-SWAN-BCS, is validated with buoy data and the Transformation Matrix. The tidal current model train consists of 4 models. The finest model, BCF-Fine, is validated against ADCP measurement and the independent hydrodynamic model LTV (Long Term Vision) Scheldt. An overview of the relationship between all the models, and their spatial resolution is given in Figure 23.

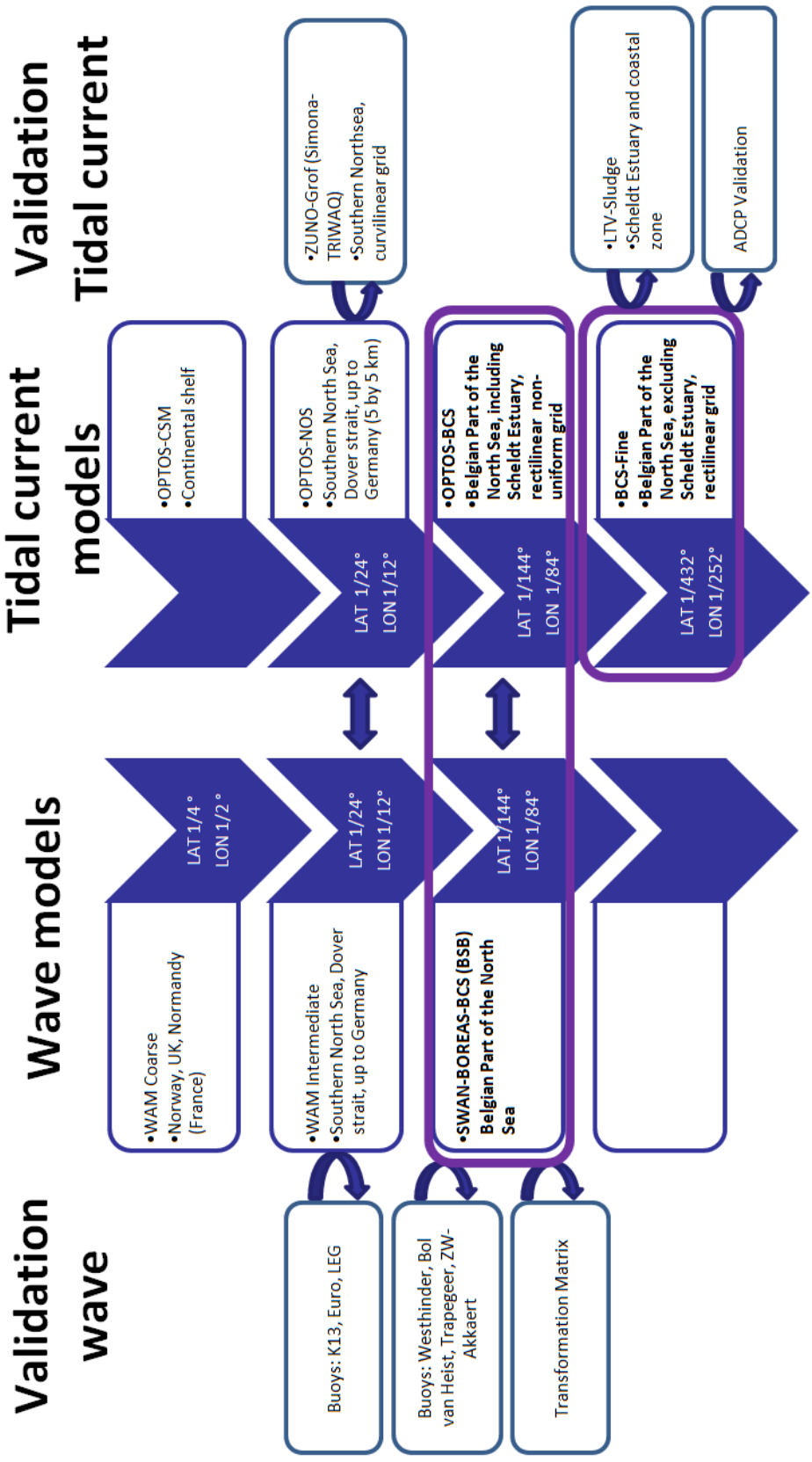

Figure 23 : Overview and interaction of the different numerical models that were used for the BOREAS project. The purple boxes indicate the models on which resource assessment was based (the BSB model for waves and the BCS-Fine for tidal currents).

4.3 Wave Modeling BOREAS-SWAN-BCS ('BSB' operated by K.U.Leuven)

4.3.1 Model set up

In order to have sufficient spatial coverage, it was decided to use a suite of numerical wave models in order to come up with wave information on a grid of about 1kmx1km. Wave boundary conditions for the zone of interest (Belgian Part of the North Sea) were generated using a nested WAM-model set-up. On the BPNS itself, an implementation of the wave model SWAN was preferred. SWAN (Delft University of Technology 2008) is a third-generation wave model for obtaining realistic estimates of wave parameters in coastal areas, lakes and estuaries from given wind, bottom and current conditions. The SWAN version 40.72 has been used for all of the computations in this study. The model is based on the wave action balance equation. Wave action is conserved in the presence of currents, which makes this model formulation very suitable for applications where current field information is available. Although there is still active development, this model is considered as the standard model for shallow water applications and is the most widely used model for such applications. It also has a more extensive list of model options and output parameters compared to the WAM model.

4.3.1.1 *Wave model grid in space and bathymetry used*

The bathymetry used for the SWAN grid, is the same grid as the OPTOS-BCS-Fine model of the COHERENS v2 code (Giardino *et al.* 2000). To make clear that this bathymetry is used, this SWAN model implementation is called BOREAS-SWAN-BCS (BSB).

4.3.1.2 *Boundary conditions and/or model trains*

In order to provide the wave boundary conditions for the BOREAS-SWAN-BCS model a set of nested wave model grids has been set up (Figure 24).

First a coarse WAM grid (CMS or Continental Shelf Model) provides boundary conditions for an intermediate resolution nested WAM model (the intermediate WAM model grid N1_24_SWANB). The coarse grid WAM model extends until 70°N in order to catch the waves that are generated in this area and travel (as swell) towards the Belgian coast. Westward extension is limited since the Southern North Sea is sheltered by the British Isles. The Intermediate WAM model grid (N1_24_SWANB) then in turn provides boundary conditions for the BOREAS-SWAN-BCS model.

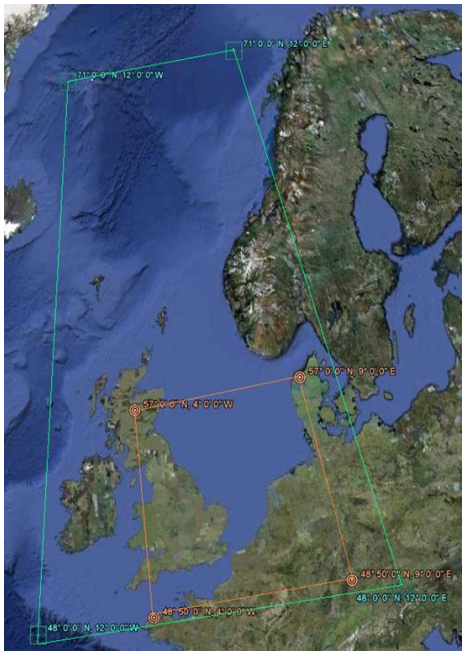

Coarse and intermediate grid

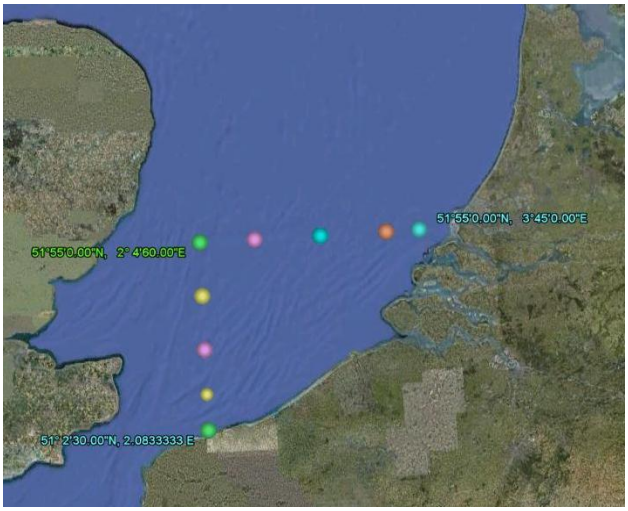

Boundary output points from the intermediate grid to the fine grid, which forms the model grid for the BSB model.

Figure 24: Overview of the coarse, the intermediate and the fine wave model grids.

The WAM-model version used, is the WAM Cycle 4.5 version (Günther, personal communication). It permits use of parallel computing and also allows a number of the features introduced in the WAM-Cycle4 (Monbaliu *et al.* 2000). However it does not allow dynamic coupling with a hydrodynamic model as described in (Ozer *et al.* 2000) and was therefore considered less suitable for wave modeling in the Belgian Coastal Zone. To drive the WAM wave models, 6-hourly UKMO wind data received from MUMM were used.

4.3.1.3 *Modeled processes*

The SWAN model (version 40.72) has been set up to run with a spectral grid of 25 frequencies logarithmically spaced between 0.05 and 0.5 Hz and with 30 directions (with a resolution of 12^0). The SWAN model was run in third generation stationary mode using the Westhuysen formulation for white-capping together with the corresponding wind input term. A JONSWAP bottom friction term was used (with coefficient 0.067). Default breaking conditions were applied. The triads were not activated.

Since tidal influence on the BPNS is substantial, varying water levels and currents need to be taken into account. To that end the SWAN model has been coupled to a hydrodynamic model on the BPNS. The water levels and currents obtained from the Coherens optos_bcz model implementation have been used as input to the wave model.

The BOREAS-SWAN-BCS implementation takes into account all important processes including varying water level and currents. It is therefore well suited to assess the wave climate on the Belgian Part of the North Sea.

4.3.1.4 *Temporal resolution*

As mentioned above, the SWAN model is used in stationary mode. This means that it is assumed that the boundary conditions supplied by the WAM model can be considered as quasi-steady. The model was run every 3 hours. This is sufficient to get a reliable estimate of the wave climate, and still feasible in terms of data storage.

Note that the wind speed and direction is kept constant over the domain. The values used are the wind speed and direction at the WHI location as used in the WAM model.

4.3.2 Model output

4.3.2.1 *Full grid output: integral parameters*

The main important parameters like significant wave height Hs, frequency weighted periods and wave power in W/m are saved at every spatial grid point and at every (3-hourly) time step. The native dimension for wavepower for the model is W/m, further results are presented in kW/m.

4.3.2.2 *28 Points of interest*

Full 2D spectra were stored at about 50 points. However, only 46 of them were on the BSB grid (see Figure 22). They were saved to assess the difference between the correct spectral calculation of the wave power with the approximation of the deep water assumption (see § 5.2.1). Of these 46 points, 28 were defined as points with a high interest (see Figure 22).

4.3.2.3 *Problems encountered and workarounds*

As mentioned, UKMO wind data were received from MUMM for the above period. There were problems with a limited number of wind records. The problematic records were replaced with the nearest 'non-problem' wind field in time. Since just a few records are affected (on average about 1 day per year or less than 0.3%), this replacement procedure was considered acceptable. It should have no consequences for the accuracy of the wave climate to be determined from the simulation. Processing of the large amount of data required a considerable amount of extra programming effort.

4.3.3 Model performance/validation with buoys

Buoy data were obtained in two ways: 1) wave buoy spectra from Monitoring Network Flemish Banks (received directly from Maritieme Dienstverlening en Kust, Afdeling Kust); these data have been transformed in Statistical Moment data for comparing with models results and will be called *'buoy-moments'* in the following graphs, and 2) Integral parameters from the Monitoring Network Flemish Banks downloaded via the VLIZ website, which will be called *'MNFB'*. Data from Westhinder and Bol van Heist buoys have been used for comparison processes.

The raw buoy data were used to compute the different moments, which were then compared with the obtained buoy integral parameters and with the model (WAM and SWAN) results. The main reason to do this is that through the VLIZ interface only a limited number of integrated parameters are available.

The following widely used statistical parameters were considered for comparisons between model results and buoy data (Eq. 7 till 10):

- The Root Mean Square Error (RMSE) provides information about the average magnitude of the error arising from the deviation of buoy data ('y') with respect to the model results ('x'). The smaller the RMSE is the better the prediction.
- The Bias is an evaluation of the difference between the model data and the buoy data. Positive values indicate that the model data is higher than the buoy data, negative values indicate that the buoy data is higher than the model data.
- The Scatter Index is a normalization of the RMSE with the absolute value of the mean observed or reference value. In other words, it is the ratio of the RMSE to the average value of the series considered. Therefore, the higher the Scatter Index the more uncertainty in the results.
- The Correlation Coefficient measures the direction and consistency of a possible linear relationship between two variables, in this case, predicted vs. measured or reference values. In an ideal case, the correlation coefficient should be equal to one. Negative values indicate that the values of one variable increase as the values of the other variable decrease.

$RMSE = \left\{ \frac{1}{N} \sum_{i=1}^{N} (x_i - y_i)^2 \right\}^{\frac{1}{2}}$	Root Mean Square Error	Eq. 7
$BIAS = \frac{1}{N} \sum_{i=1}^{N} (x_i - y_i)$	BIAS	Eq. 8
$SI = \frac{RMSE}{\lvert \bar{y} \rvert}$	Scatter Index	Eq. 9
$r_{x.y} = \frac{\sum_{i=1}^{N} \left(x_i - \bar{x} \right) \cdot \left(y_i - \bar{y} \right)}{\left\{ \sum_{i=1}^{N} \left(x_i - \bar{x} \right)^2 \right\}^{\frac{1}{2}} \cdot \left\{ \sum_{i=1}^{N} \left(y_i - \bar{y} \right)^2 \right\}^{\frac{1}{2}}}$	Correlation coefficient	Eq. 10

With: 'x' is the model data and 'y' is the buoy data. The index '$_i$' indicates individual model or buoy data, the overline indicates the average of all corresponding model or buoy points. 'N' indicates the total number of points.

In the next figures the results for the BOREAS-SWAN-BCP (BSB) are given at Westhinder for January 2005. The good agreement of H_{m0} at Westhinder (Figure 25) illustrates that the boundary conditions between the 3 wave models are properly transferred. The model is capable of

reproducing the integral parameters (wave heights and periods). Some deviations on the wave period can occur as illustrated in the last figure (Figure 26), in particular for the wave period at low wave heights. Locally generated waves in the SWAN run can introduce some energy at higher frequencies, which would lower the wave period. The statistical indicators at the Westhinder location are typical for wave hind cast calculations using the 6-hourly UKMO wind fields.

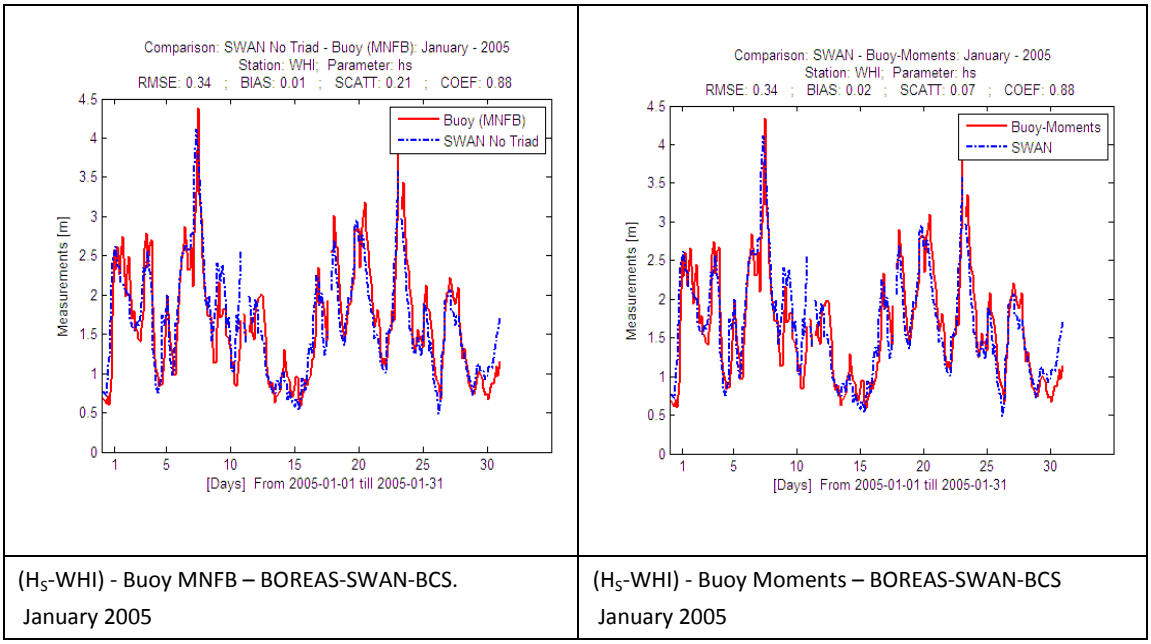

(H_S-WHI) - Buoy MNFB – BOREAS-SWAN-BCS. January 2005	(H_S-WHI) - Buoy Moments – BOREAS-SWAN-BCS January 2005

Figure 25: Comparison of the significant wave height (H_{m0}) between the model data ('SWAN') and the buoy measurements (Westhinder).

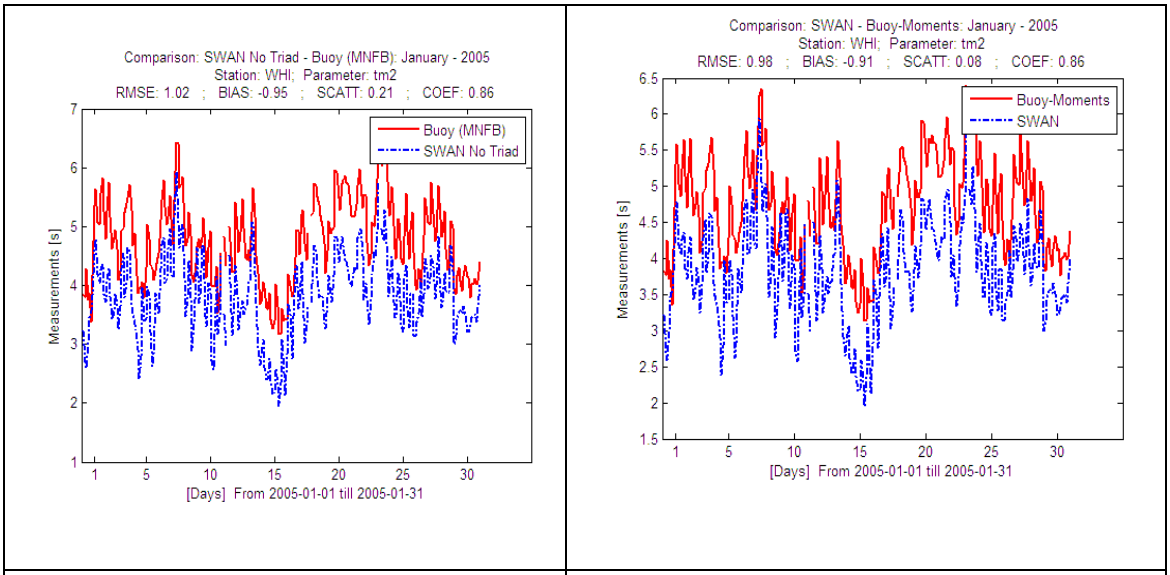

(TM_{02}-WHI) - Buoy MNFB – BOREAS-SWAN-BCS. January 2005	(TM_{02}-WHI) - Buoy Moments – BOREAS-SWAN-BCS January 2005

Figure 26: Comparison of the wave period (T_{m02}) between the model data ('SWAN') and the buoy measurements (Westhinder).

For the location Bol van Heist , the statistical indicators are still acceptable, but not as good as at Westhinder (results not shown). There are a number of reasons for this. First of all the

deviations at Westhinder, will also be transferred to near shore locations such as Bol van Heist. An additional 'error' at near shore locations will be introduced due to the time lag between the measurements and the arrival of the waves applied at the boundary (violation of the quasi-steady assumption). It is believed that this violation is on the one hand relatively small and on the other hand not systematic. This should therefore have little or no influence when model output is used to look at the wave climate.

Overall, one can conclude that the wave height Hm0 is modeled very well, with an overall bias for the 10 year period of -3.7 cm. The wave period Tm-1,0 is modelled with an overall bias for the 10 year period of -0.25 seconds. These results are considered as acceptable and comparable to other numerical model results. In the later analysis of the wave power resource, these biases will be used to correct the model results to better reflect the wave buoy data. This means that the modeled wave height and period will be increased by 3.7 cm and 0.25 seconds respectively.

4.3.4 Transformation Matrix: characteristics (operated by FHR)

The transformation matrix is a database containing results of wave calculations initially based on the third-generation wave propagation model SWAN (version 40.11, TUDelft). The original goal of the transformation matrix was to speed-up the conversion of off-shore wave conditions to near-shore conditions, at the -5 and -10m TAW depth line, using wind measurements obtained also at the coast. The wave characteristics at Westhinder, the input area, are transformed to wave characteristics at other locations of the Belgian coast by means of a so called transformation matrix (which is based on SWAN model results). Other inputs are the water levels, measured at Oostende, and the wind speeds, 90 minutes averaged using measurements at Wandelaar. It is important to notice that the Transformation Matrix itself is not a numerical model, but a rather a multilinear interpolation tool based on a numerical model[7].

The differences in wave characteristics calculated with the Transformation Matrix depend on the imposed conditions, namely, wave conditions at input area (Westhinder), wind and water levels. Any combination of these three is obtained by applying a multi linear interpolation between the parameters contained in the transformation matrix. The transformation includes a structured discretization of significant wave height (H_s), peak periods (T_p), wave direction (°), wind speed and direction, and water levels. For each combination of these variables, a SWAN simulation is performed and the results brought together in the matrix and linked to a particular location. For further information the reader is referred to the technical reports of the Transformation Matrix (Doorme *et al.* 2006; IMDC 2006; IMDC 2008; IMDC 2009).

The Transformation Matrix was compared with the —independent— BSB model of this study as a supplementary validation besides the wave buoy data validation (Delgado *et al.* 2010). This was done for 5 selected points, as shown in Table 13. Bias results for the H_s (H_{m0}) and for the T_m (= $T_{m-1,0}$) are given (Figure 27). The results for the other periods (T_{m01} and T_{m02}) have a larger bias (results not shown), but are not used for the calculation of the wave power and therefore less relevant.

[7] The Transfomation Matrix entry values were used as boundary condition for a SWAN model run; model output was stored for these conditions and afterwards measured conditions were used to know the interpolation weights in the multilinear interpolation.

Table 13: The 5 output locations for the comparison between the wave model and the transformation matrix.

Name	ID Location	Type	Depths (m)	Easting	Northing
-	10west_123	Point	7.55	507563	5697875
Akkaert	P10_ZWAkkaert	Buoy	20.55	486324.4	5695221.9
Bol van Heist	BVHD08	Buoy	9.38	513579.6	5693213.9
Oostende	OSTG	Buoy	5.71	494516.2	5676794.6
Trapegeer	TRGG08	Buoy	4.14	470825.9	5665198.3

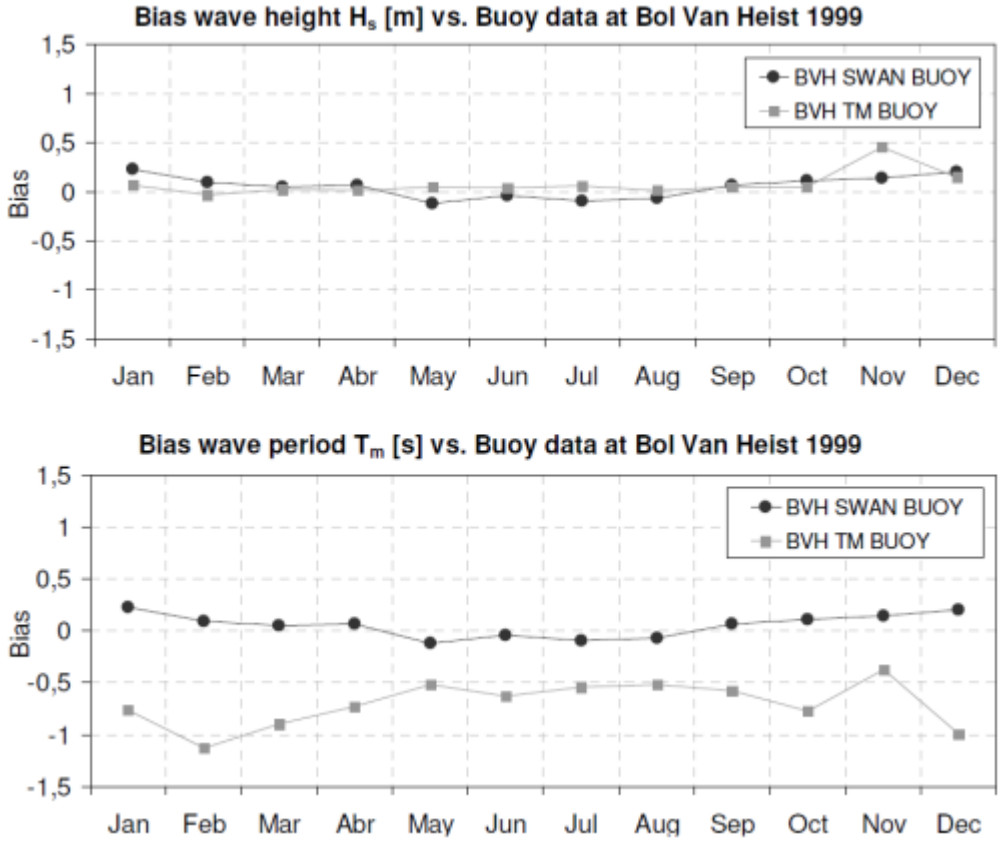

Figure 27: Bias for the SWAN-BSB model and Transformation Matrix in comparison with the wave buoy data (H_{m0} and $T_{m-1,0}$).

Both the Transformation matrix and the BOREAS-SWAN-BCS (BSB) model give an accurate approximation to wave conditions at the Belgian Coast. The agreement between the Transformation Matrix and the results from the BOREAS-SWAN-BCS model is good, especially for the wave height H_s, the most important parameter for the assessment of wave energy. The bias in this case is only 5 cm for year 1999. These good results explain the excellent agreement with the results of the Transformation Matrix, presenting a deviation of only 1 cm from measured data for the same year. Such a low bias is not surprising if we take into account that actual wave data is used as input for the Transformation Matrix at Westhinder. For this point, located inside the domain of interest, the correlation is 100% and includes extreme conditions which are difficult to calculate by spectral models. This fact can explain many of the differences observed between the transformation Matrix and the BOREAS-SWAN-BCS.

The Transformation Matrix is proven to be a good validation tool that can provide quickly accurate estimations of the wave conditions at the Belgian Coast. The main disadvantage of this tool for operational resources assessment is the need of wave conditions input at the input location inside the area of interest. This is required to perform the multilinear approximation resulting in wave parameters at the different output locations.

The BOREAS-SWAN-BCS (BSB model) does not depend on discrete points of the area of interest and therefore can provide accurate wave parameters with full spatial coverage without needing actual area specific wave data as input. The model outputs do not present data gaps. These facts, together with the good results presented and discussed in the comparison report (Delgado *et al.* 2010) make the BOREAS-SWAN-BCS (BSB) model, together with the buoy data, a suitable tool for the resource assessment.

4.3.5 Conclusion Wave modeling

A numerical wave database has been set-up for the whole Belgian Part of the North Sea. The period covered is 1999-2008. Wave information is available every 3 hours with a spatial resolution of the order of 1 km x1 km. The model results of the BSB model provides a coherent dataset with 10 year of wave modeling, with a consistent temporal and spatial resolution

The model results have been validated using buoy data from the Monitoring Network of the Flemish Banks. The model data compare quite well with the buoy data (good agreement with H_{m0}, slight underestimation of $T_{m0,2}$). Main advantages of the model data are 1) that they provide a continuous and consistent data record, and 2) that they provide information on all the locations on the BPNS whereas buoy data often have gaps. Still great care and caution is needed when using the wave model data, especially in locations with limited water depth (close to the coast). The resolution (and accuracy) of the bathymetry used, is not sufficient to provide accurate estimates in the shallow areas and deviations from real conditions have to be expected in these shallow areas.

The comparison with both buoy data and the Transformation Matrix, indicate a reasonable level of accuracy, which makes it a very powerful and useful tool to further assess the wave energy resource. Since the buoy data are considered as the reference point, the biases for H_{m0} and $T_{m-1,0}$ will be used and a correction will be made for the different effect of the bias at wave heights above 1m.

There are however, some limitations. Although the grid is quite fine local effects like time varying bathymetry (sand dunes) can influence waves. The dataset also provides an estimate of the wave climate before the implementation of wave energy convertor farms. A - hypothetical- massive WEC farm placed at the BPNS, would influence the waves due to wave interactions like absorption, diffraction, refraction, etc... In the assessment of the extractable wave energy resource, this must be approached in a pragmatic way.

4.4 Tidal Current modeling

4.4.1 OPTOS-BCS-Fine (operated by MUMM)

This paragraph gives an overview of the tidal current modeling. The two finest models, BCF and BCF-fine, are discussed (Figure 23), the two coarser models are not discussed here (see Figure 23 for the overview of the models). These models, which are operated by MUMM and implemented in the Coherens software, were validated with a numerical model operated for the Scheldt Estuary (operated by FHR and implemented in Simona software, see (Dujardin *et al.* 2010a)).

4.4.1.1 *Model set up*

The state-of-the-art three-dimensional hydrodynamic model COHERENS (Luyten *et al.* 1999; Luyten *et al.* 2011) calculates the currents and the water elevation under the influence of the tides and the atmospheric conditions. A train of models is set up to provide good boundary conditions for the model, applied at the Belgian Part of the North Sea (see Figure 23).

4.4.1.2 *Grid and bathymetry*

The OPTOS-BCS-S is implemented on the Belgian Continental Shelf on a grid with a resolution of 42.86" = 1/84° in longitude (817 – 833m) and of 25" = 1/144° in latitude (772m). The extent and the bathymetry of the model are presented in Figure 28. The model has 20 σ-depth layers (σ indicates evenly distributed over the height).

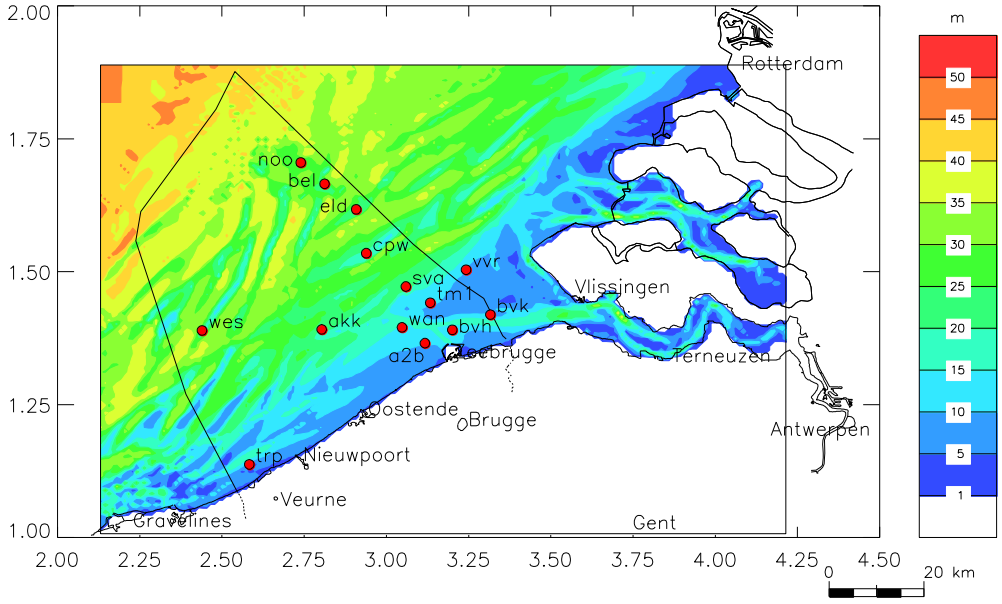

Figure 28: Bathymetry and extent of the BCS model, with an indication of the output points that were used.

4.4.1.3 *Boundary conditions and/or model trains*

Along the open boundaries, the BCS model is coupled with two regional models. The OPTOS-CSM model comprises the entire Northwest European Continental Shelf and is driven by the water elevation at the open sea boundaries, at the 200m isobaths. The model takes into account four semi-diurnal and four diurnal constituents. The OPTOS-CSM model calculates the boundary conditions of the North Sea model OPTOS-NOS, which has the same resolution but only covers the North Sea. This model OPTOS-NOS is a three-dimensional model with 20 σ-layers over the vertical. The boundaries of the OPTOS-BCS model are calculated from the OPTOS-NOS model results (Figure 23).

4.4.1.4 *Modeled processes*

The hydrodynamic model solves the momentum equations and the continuity equation with, if activated by the model, equations for the sea water temperature and salinity. For the BOREAS project, however, the calculation of sea water temperature and salinity is not taken into account. COHERENS disposes over several turbulent closures. A good description of the turbulence is necessary for a good simulation of the vertical profile of the currents. In the current application, an equation for the turbulent kinetic energy is combined with a length scale formulation.

4.4.1.5 *Temporal and spatial resolution*

The time step of the two-dimensional model of the OPTOS-BCS-fine model is 4 seconds, while the time step of the three-dimensional model is 120 seconds. The rather small time step in the model is due to the explicit numerical scheme, used in the model. When atmospheric conditions are taken into account, the model is using the 6-hour UKMO wind data that MUMM is receiving in operational mode.

4.4.1.6 *Model output*

The main output of the model are the water elevation, or total actual water depth, and the current profiles. In the framework of this project, also the tidal energy is important. This tidal energy can be calculated from the current as:

$$\frac{P}{A} = \frac{1}{2}\rho \mathrm{v}^3$$

With P the tidal energy through a water section of 1 m², ρ the water density, A the vertical swept area and v the current speed. To verify the results of the model, the tidal energy is calculated at the water surface, (*i.e.* using the current speed in the highest level in the water column), at the bottom (*i.e.* using the current speeds in the lowest level in the water column) and using the depth-averaged current speeds. Note that in the final tidal current energy assessment, the average tidal current power over the 4th till 9th depth layer was used (so the upper half layer of the water column, but with a top clearance layer, see § 5.3.2.1). Also the total tidal energy, integrated over the entire water column, is calculated.

4.4.2 OPTOS-BCS-fine (operated by MUMM)

The OPTOS-BCS-fine (short: BCS-Fine) model is a finer version of the OPTOS-BCS model described above, but with only 10 depth layers instead of 20 due to computational limitations. The model set-up is similar to the OPTOS-BCS model, which provides the boundary conditions for the BCS-fine model.

4.4.2.1 *Grid and bathymetry*

The OPTOS-BCS-fine is implemented on the Belgian Continental Shelf with on a grid with a resolution of 14.28" = 1/252° in longitude (272 – 278 m) and of 8.33" = 1/432° in latitude (257 m). The extent and the bathymetry of the model are presented in Figure 29. The model has 10 σ-depths layers.

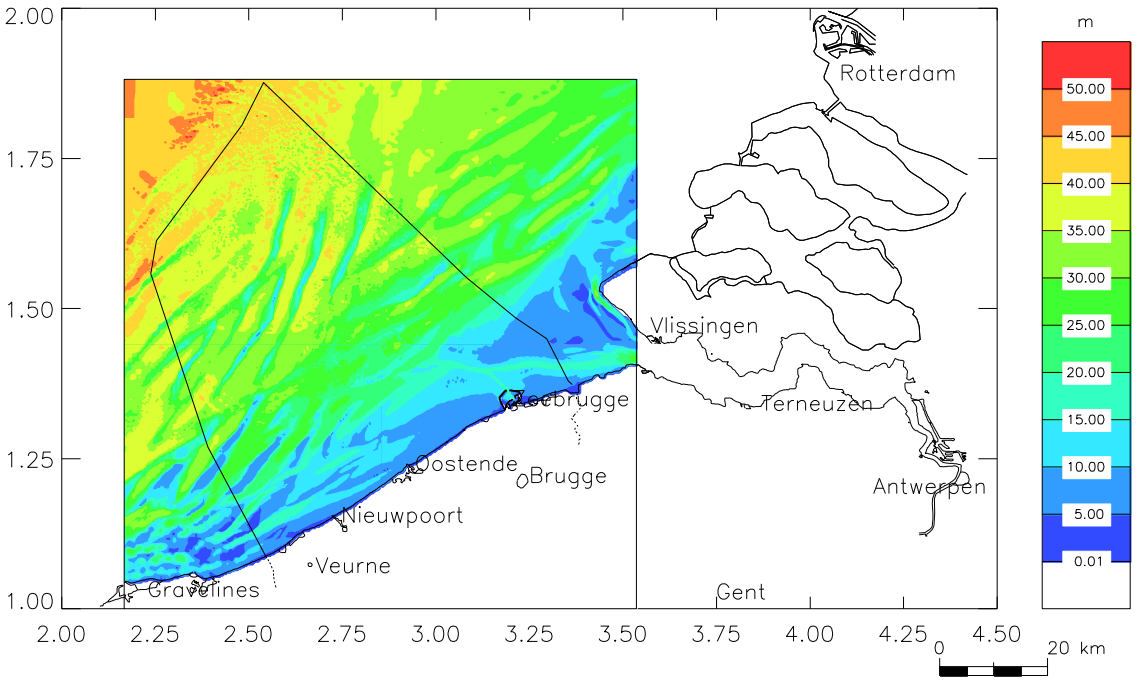

Figure 29: Bathymetry of the OPTOS-BCS-fine model.

4.4.2.2 *Boundary conditions and/or model trains*

Along the open boundaries, the OPTOS-BCS-fine model is coupled with the OPTOS-BCS model, which is described above.

4.4.2.3 *Modeled processes*

The same processes are modeled as in the OPTOS-BCS model, with a higher spatial resolution.

4.4.2.4 *Temporal and spatial resolution*

The 2D time step op the OPTOS-BCS model is 4 seconds, while the 3D time step of the model is 120 seconds. The rather small time step in the model is due to the explicit numerical scheme, used in the model. When atmospherically conditions are taken into account, the model is using the 6-hour UKMO wind data that MUMM is receiving in operational mode.

4.4.2.5 *Model output*

The same output is provided as the OPTOS-BCS model.

4.4.3 Results for the OPTOS-BCS and OPTOS-BCS-fine models

The validation of the OPTOS-BCS model has been executed, amongst others, in the framework of the MAREBASSE project (Van Lancker *et al.*, 2004). The main conclusions are presented here again. First some general figures are presented. Figure 30 shows the maximum velocities that occur during 2 consecutive spring neap cycles, whereas Figure 31 shows the average velocities. Maximum velocities are found around the harbor of Zeebrugge and up to 1.8 m/s. Figure 32 shows the time series for the Belwind output point (indicated bel in Figure 28) for respectively the depth averaged velocity current. Note the difference between the 2 tidal cycles. The further analysis was based on these 2 tidal cycles. Considering more than 2 tidal cycles took more processing time and did not increase the accuracy (results not shown, but available in the technical note (Van den Eynde et al. 2010)).

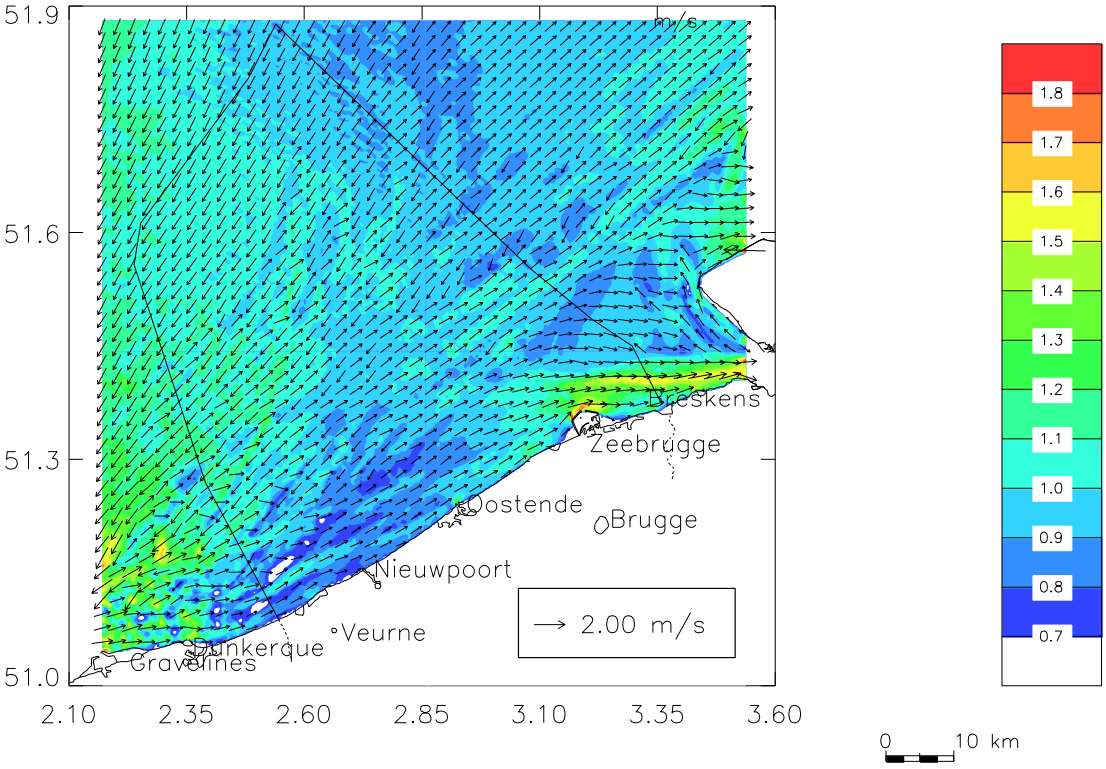

Figure 30: Depth-averaged, maximum (over 2 tidal cycles velocity) vectors and magnitude, as modeled with the BCS-fine model. One vector of 64 (8*8 output points) is shown in the plot.

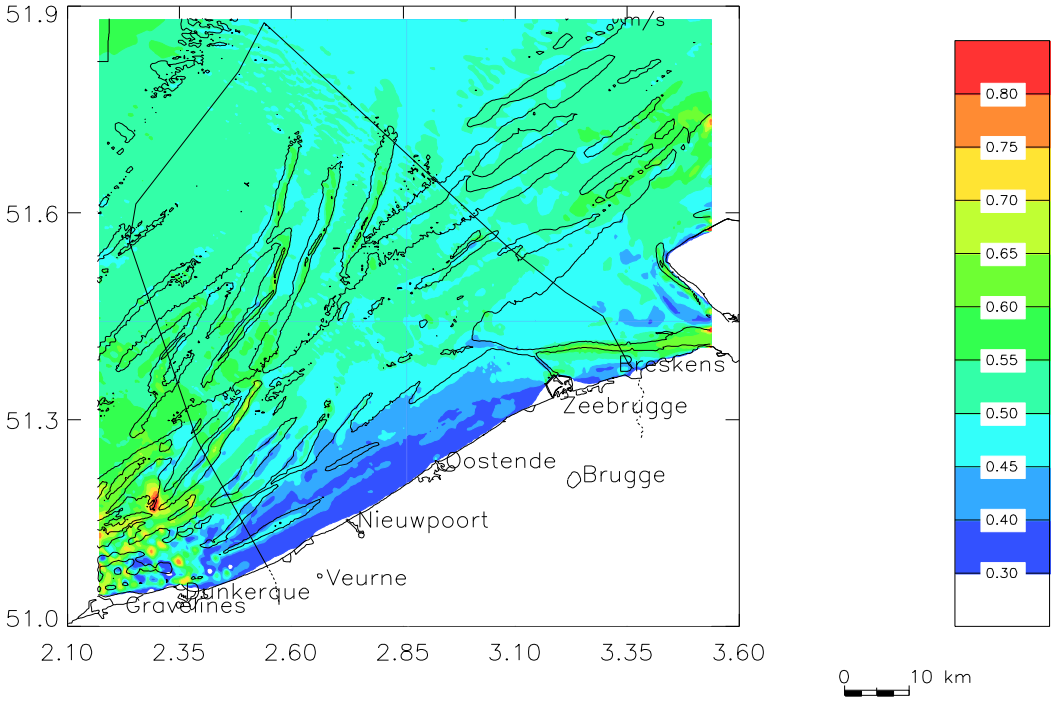

Figure 31: Mean current speed, averaged over two spring-neap tidal cycles, as calculated with the BCS-fine model.

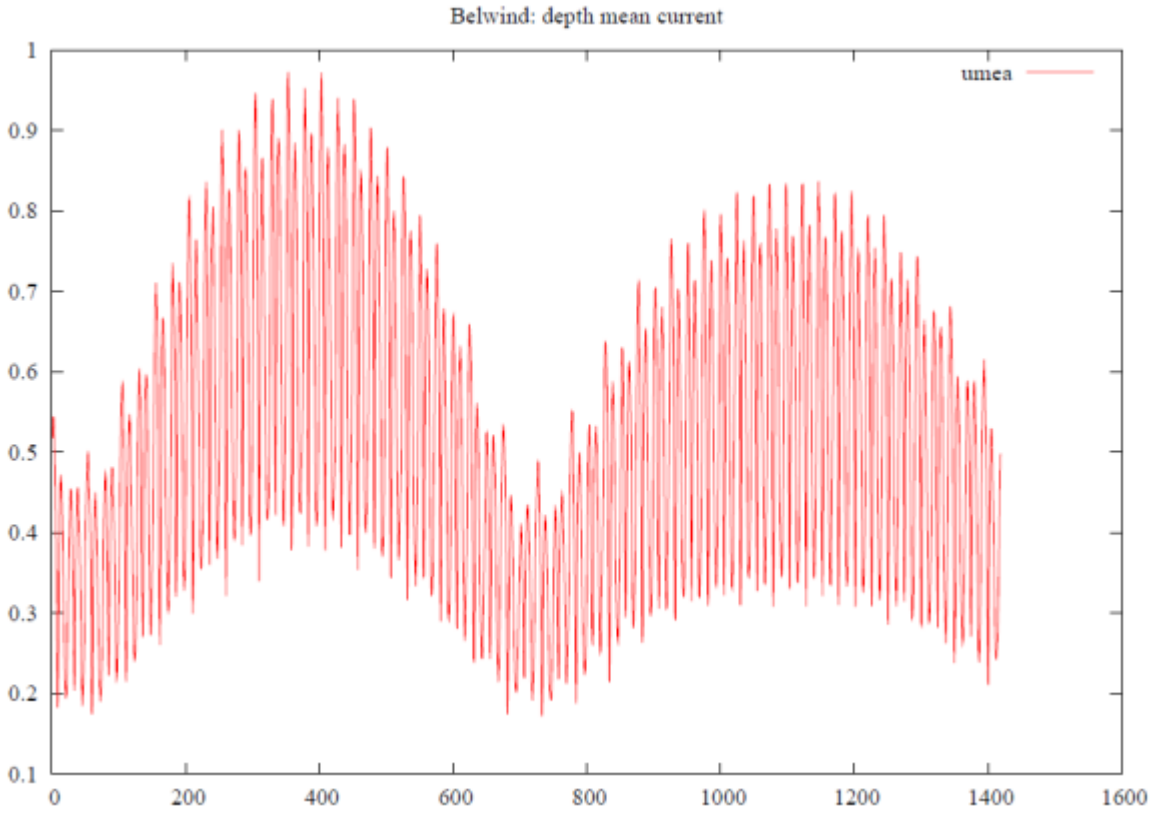

Figure 32: Depth average current velocity at Belwind during 2 spring-neap tidal cycles (m/s on y-axis, time step for every 30 minutes on the x-axis).

4.4.4 Model performance/validation with ADCP

4.4.4.1 *OPTOS-BCS*

The BCS model was validated extensively, using 400 hours of current profiles on the Belgian Part of the North Sea, measured with a bottom mounted Acoustic Doppler Current Profiler (ADCP). These ADCP data were taken over various places on the Belgian Part of the North Sea, near the coast (*e.g.* B&W Oost, Zeebrugge Oost), or more offshore (Kwintebank, Vlakte van de Raan, Sierra Ventana).

Some statistical calculations, like the Root-Mean-Square-Error (RMSE), bias, correlation, and scatter index, have been carried out in order to apprehend the differences in the absolute value (or modulus[8]) and direction of the currents between model simulation results and ADCP measurement data. The RMSE, which gives a global indication of the error, of the amplitude of the currents is situated between 5 and 15cm/s (except for campaign 2003/04 where it attains 30cm/s). The error varies in general relatively little with water depth. There exist however significant differences between the campaigns. The currents in the 'deep' water campaigns are, particularly well represented by the model, whereas in shallow waters the results are less good. These areas are usually characterized by highly variable bathymetry on small horizontal scale (sand dunes), which cannot be represented accurately on the model grids. The precision of the model results depends also on the precision of the meteorological data used in the model run.

The validation exercise led to the conclusion that the magnitude and the direction of the current profiles are satisfactory represented by the 3D hydrodynamic model. The RMSE of the modulus of the currents is usually less than 15cm/s and the error in direction usually is less than 20°, except during some of the simulation where specific problems occurred.

4.4.4.2 *OPTOS-BCS-fine*

A validation of the OPTOS-BCS-fine model was executed in the framework of the Marebasse project (Van Lancker *et al.* 2007). The model was used for the calculation of the effects of sand extraction on the sediment transport on the Kwintebank and a validation was performed. The results are reported in a separate technical report (Van den Eynde *et al.* 2010).

For the validation, measurements from a bottom mounted ADCP were used, which were executed on the Kwintebank, during two measuring campaigns. The RMSE are presented in Table 14. For the longer March 2004 period, the RMSE of the modulus of the depth-averaged currents calculated by the BCS-fine model is around 0.072 m/s, which is clearly satisfying.

Table 14: RMSE of the U-component (RMSE U), RMSE of the V-component (RMSE) and RMSE of the modulus of the depth-averaged current (RMSE) for the BCS-fine model.

Start of campaign	Period	RMSE U (m/s)	RMSE V (m/s)	RMSE (m/s)
11/06/2003	25h	0.140	0.119	0.127
02/03/2004	216h	0.069	0.083	0.072

[8] Since the velocities are given in x, y (and in case of 3D modelling, z direction), taking the modulus (this is the absolute value of a vector) of the x and y direction gives the overall velocity magnitude.

An additional validation was executed in the framework of the BOREAS project by comparison with the LTV model and with ADCP measurement.

4.4.5 Model performance/validation with LTV-Sludge model (operated by FHR)

The LTV model is a three-dimensional hydrodynamic model consisting of six layers with an approximate logarithmic distribution (top to bottom 10, 20, 30, 20, 15 and 5% of total water depth). This gives the model results the necessary vertical resolution near the bottom, while maintaining a sufficiently small layer at the top for comparison with satellite measurements (van Kessel et al. 2010). The model is nested in the ZUNO-grof model, as shown in Figure 33. The nesting is performed using a combination of two velocity boundaries perpendicular to the coast, and a Riemann boundary parallel to the coast. The 3D hydrodynamic model is implemented in TRIWAQ, a module of SIMONA (Spee 2010) . Meteorological influences are taken into account, both in the LTV model as in the ZUNO-grof model. The grid is curvilinear, whereas the two models of MUMM are rectilinear grids. For a comprehensive description of the hydrodynamic model, the reader is referred to (van Kessel et al. 2010).

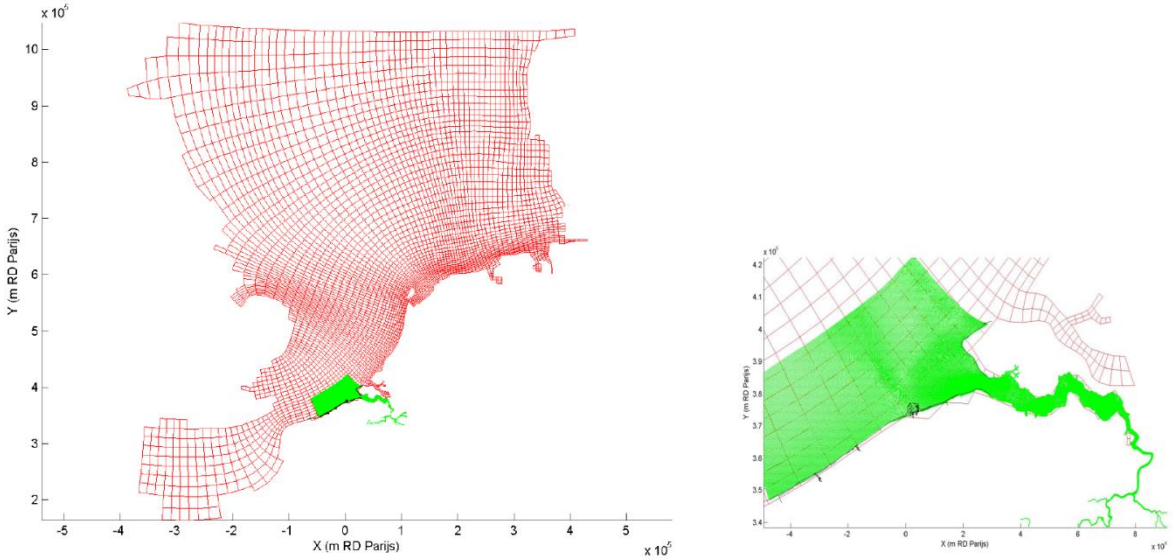

Figure 33: Geographical extent and nesting of the LTV Scheldt in the ZUNO-grof model.

4.4.5.1 *Comparison OPTOS-BCP-fine and LTV sludge with ADCP measurements*

The main conclusions are given in brief. For a full discussion, the reader is referred to the full report (Dujardin *et al.* 2010b).

4.4.5.1.1 Results: ADCP measurements in comparison with LTV and the OPTOS models.

The ADCP profiles at the stations “MOW0 – Wandelaar” and “MOW3 – Bol van Heist” have been processed by the “Vlaamse Hydrografie” in such a way that time series with a 10 minutes interval are obtained in 6 bins. These are:

- Bin 1: 10 minutes averaged surface velocity;
- Bin 2: 10 minutes averaged velocity between 2.5 and 5.0m below the water surface;
- Bin 3: 10 minutes averaged velocity between 5.0 and 7.5m below the water surface;
- Bin 4: 10 minutes averaged velocity between 7.5 and 10.0m below the water surface;

- Bin 5: 10 minutes averaged velocity between 10.0 and 12.5m below the water surface;
- Bin 6: 10 minutes averaged velocity between 12.5 and 15m below the water surface.

In a separate technical BOREAS report (Dujardin *et al.* 2010b) it is shown that the current in the upper bin is significantly higher than in the other bins and has a high variability (standard deviation). On the other hand, the current in bin2 is significantly lower than the current in all other layers. The same behaviour was already reported (Doorme *et al.* 2006) or measurements at the Thornton bank, and could only partially be explained by the influence of waves. Therefore, the velocity data in the upper two bins, describing the upper 5m of the water column, will not be taken into account for this comparison.

Still, for these two stations, measurement data at four levels in the water column will be used in this report: at 6.25m, 8.75m, 11.25m and 13.75m below the water surface, in accordance to the centre of the bin locations. It is possible, especially at low water, that there is not enough water above the sensor to calculate averaged velocities in bin6, and sometimes even in bin5 (Dujardin *et al.* 2010b).

However, during data processing it has been noticed that during certain moments in the tidal cycle ADCP measurements exist on depths up to 13.75m under the free surface, while the bathymetry in the models is shallower (see table 15).

Table 15: Depth at the monitoring station in the different models

	OPTOS-BCS	OPTOS-BCS-fine	LTV
Bol van Heist	10.90m	11.32m	11.56m
Wandelaar	12.80m	12.01m	13.56m

These differences in depth are not unexpected. The bathymetry in the models gives one mean value for an area of approximately 825 by 775 meters for the OPTOS-BCS model and approximately 250 by 250 meters for the OPTOS-BCS-fine and LTV models, while the ADCP equipment is placed at a precise location. As the area around these measurement locations ("MOW0 – Wandelaar" and "MOW3 – Bol van Heist") is characterised by the appearance of large dunes (Lanckneus *et al.* 2001), local bathymetry can easily vary up to two meters on a horizontal scale much shorter than the grid resolution of the models. Unfortunately the actual depth, as measured by the ADCP, is not included in the data files delivered by the "Vlaamse Hydrografie".

In order to make an extensive comparison of modelled and measured velocities possible, a vertical shift has been applied on the ADCP measurements in such way that the lower bin of the ADCP is matched with the bathymetry of the models..

Even with this vertical shift applied, it was found that the results, obtained in this test, are not as good as the results obtained in previous validation exercises with the OPTOS-BCS and the OPTOS-BCS-fine models.

4.4.5.1.2 Results: Water levels

The LTV model underestimates the water levels. The modelled water levels for the OPTOS-BCS and OPTOS-BCS-fine models are nearly identical (results not shown here).

Both BCS models have a smaller bias in water level than the LTV model. The LTV model underestimates the water level, with biases between -14cm and -4cm.

On the other hand, the LTV model shows slightly better RMSE values, which could indicate that the LTV model reproduces the intra-tidal water level variations better. Although both BCS models have quasi identical biases (between -6cm and +2cm), the OPTOS-BCS-fine model has consistently higher RMSE values than the coarser OPTOS-BCS model.

The reproduction of high water is better in the LTV model than in the other two models, both for level and timing. On the other hand, the LTV model shows a clear underestimation of the low water. Whereas the RMSE of the low water levels in the LTV model is slightly better than in both BCS models, the timing of the low water is reproduced better by the latter.

4.4.5.1.3 Current velocities

Only three velocity measurement locations are available. Unfortunately, run simG19 of the LTV model only produces output at the locations “MOW0 – Wandelaar” and “MOW3 – Bol van Heist”, reducing the number of stations usable for comparison between measurements and the different models. A vertical shift was applied on the ADCP measurements at these locations.

In almost all models and all stations, bias (absolute values) and RMSE values increase with depth. Only in “A2B-boei” RMSE values clearly show the opposite behaviour (result not shown here, for technical note for further reference (Dujardin *et al.* 2010a)) .

In general, all models underestimate the velocities. The OPTOS-BCS model produces the smallest bias, followed by OPTOS-BCS-fine and LTV. RMSE values are similar in all models, ranging from 0.15m/s up to 0.22m/s for “Bol van Heist” and “A2B-boei” and 0.12m/s up to 0.16m/s at “Wandelaar”. Overall the OPTOS-BCS-fine model seems to give the best results at “Bol van Heist”, while the LTV model give better results at “Wandelaar”.

The results, obtained in this test, are clearly not as good as the results obtained in previous validation exercises with the OPTOS-BCS and the OPTOS-BCS-fine models. Together with the uncertainty about the vertical level of the measurements bins, this can raise some questions on the quality and practicability of the measurements at locations “MOW0 – Wandelaar” and “MOW3 – Bol van Heist” for the validation of numerical models. Remark that when the vertical shift in the measurements in these stations is not applied, both the bias and RMSE values increase, as should be expected.

4.4.6 Overall conclusion tidal current modeling

Biases between measured and modelled water levels are between +8cm and -2cm for the OPTOS-BCS and OPTOS-BCS-fine models. Although the underestimation of the water levels is (on average) stronger in the LTV model, it shows slightly better RMSE values than both OPTOS-BCS and OPTOS-BCS-fine models (Table 16).

Table 16: Bias and $RMSE_0$ between observed and modelled water levels for all stations (straight setup).

	range of bias [m]		$RMSE_0$ [m]
OPTOS-BCS	+0.07	-0.02	0.27
OPTOS-BCS – fine	+0.08	-0.02	0.29
LTV	+0.14	-0.04	0.24

The underestimation of the water levels in the LTV model is presumably due to the way meteorological conditions are taken into account. Harmonic analysis shows a slight overestimation of the amplitude in the LTV model, for all major harmonic components.

In general, all models underestimate the velocities, bias (absolute values) and RMSE values increase with depth. On average, RMSE values range from 0.12m/s at “Wandelaar” to 0.21m/s at “Bol van Heist” (Table 17).

Table 17: Bias and RMSE between observed and modelled tidal velocities (straight setup).

	range of bias [m/s]		range of RMSE [m/s]	
OPTOS-BCS	**+0.12**	**-0.03**	**0.12**	**0.21**
OPTOS-BCS – fine	**+0.14**	**-0.02**	**0.12**	**0.22**
LTV	**+0.15**	**-0.04**	**0.12**	**0.21**

These values are not as good as the results obtained in previous validation exercises with the OPTOS-BCS and the OPTOS-BCS-fine models. Together with the problems concerning the measured velocities in bin1 and bin2 (upper layers of the ADCP measurements) and the uncertainty about the actual vertical level of the measurements bins, this can raise some questions on the quality and practicability of the measurements at locations “MOW0 – Wandelaar” and “MOW3 – Bol van Heist” for the validation of numerical models.

The harmonic analysis of the currents (results not shown) shows that the model results of the OPTOS-BCS, OPTOS-BCS-fine and LTV models give similar results in the open sea stations (results not shown). The velocity output in the stations near the coasts has not been considered here because the different grid setups (curvilinear for the LTV model, Cartesian for the OPTOS-BCS and OPTOS-BCS-fine models) near the model boundaries influences the results too much.

At the location at Belwind windmill park, the modelled velocity currents in the upper half of the water column vary between 0.2 and 1.05 m/s. The OPTOS-BCS model was validated with ADCP measurements during the MAREBASSE project, showing RMSE between 5 to 15 cm/s for most measuring campaigns.

Overall, one can conclude that the OPTOS-BCS, OPTOS-BCS-fine and LTV model give satisfactory results and that the models are well suited to be used for the calculation of the tidal current climate on the Belgian Part of the North Sea and can be used for the assessment of good sites for exploitation of tidal current energy. In the case of specific project location, it is however advisable to verify velocity currents with ADCP measurement over longer periods.

5 Wave and tidal current resource

5.1 Protocols for wave and tidal resource assessment and BOREAS methodology

At the start of the BOREAS project, there was no international consensus, guidelines or standardization for the protocols or methodologies for wave and tidal resource assessment. Many different methodologies and criteria existed, making an intercomparison between resources, and the expected energy production by convertors difficult. The different approaches that were used weren't beneficial for the credibility of the claims that were made by potential investors. Many research groups (amongst them the Hydraulic Maritime and Research Centre of Cork University, EMEC and DTI) emphasized the importance of a generalized protocol to asses both the wave and tidal energy climate, and the performance of wave and tidal current convertors.

To tackle this, the European funded Equimar was launched. Its main focus was the equitable testing and evaluation of marine energy extraction devices in terms of performance, cost and environmental protection.

Although most of the (final) Deliverables were only launched at the end of 2010 or 2011 (and thus the end phase of the BOREAS project), the BOREAS project methodology is in line with the recommendations. It is therefore that the recommendations from Equimar are used here to provide an introduction and rationale for the wave and tidal energy resource assessment.

Equimar defined 3 levels of operational resource assessment steps (Figure 34), which are: the early stage, the project development & project feasibility and the operational phase. The definition for the early stage wave energy assessment is (EquiMar *et al.* 2011):

> *'Resource characterization should provide an estimate of the annual resource along with quantification of the seasonal and inter-annual variability. This assessment should be conducted over a period of 10 years with the data provided by hind cast modeling and/or existing data.'*

For tidal wave energy assessment it is:

> *'Resource characterization should estimate the peak resource along with the seasonal variability. This may be achieved using tidal stream atlases or shelf tidal models. Coarse grid models and area models may also be utilized'.*

BOREAS is clearly set up as an initial assessment (early phase), with some aspects towards a – generic – project development. The main summary methods that are required during the early (and later) phase(s) are outlined in Figure 35.

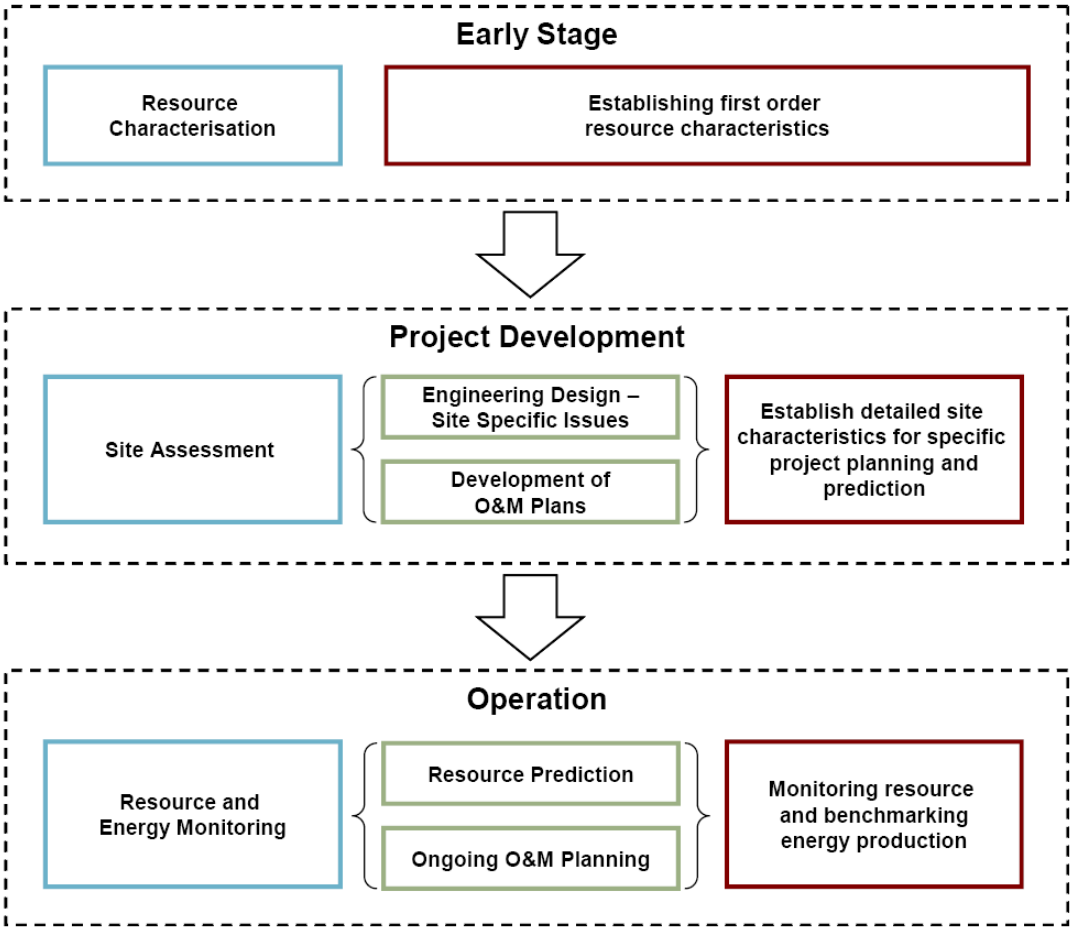

Figure 34 : The stages of a marine energy project, and how resource assessment will be utilised during each stage (EquiMar *et al.* 2010; EquiMar *et al.* 2011) .

				Early	Development			Operation		
		Modelling	Measurement	Resource Characterisation	Engineering Design	Site Assessment	Operational Planning	Level of Resource	Ongoing Operation & Maintenance	Prediction & Tuning
Summary statistics		•	•	✓	✓	✓	✓	✓	✓	
Spectra	Directional	•	•		✓	✓		✓		✓
	Non-directional	•	•		✓	✓		✓	✓	✓
Elevation Time series	Directional		•		✓					✓
	Non-directional		•		✓					✓
Extremes		•			✓	✓				
Long-term temporal variation		•		✓		✓				
Mean and maximum currents		•	•	✓	✓	✓	✓		✓	✓
Tidal level		•	•	✓	✓	✓	✓		✓	
Wind (model input)		•	•	✓		✓	✓		✓	✓

Figure 35 : Summary of the methods and data required for resource assessment at each stage of a wave energy development (EquiMar *et al.* 2010; EquiMar *et al.* 2011).

It should be emphasized that Equimar doesn't necessarily suggest the use of spectral wave information for an early wave energy assessment[9]. The wave power, or energy flux per unit of crest length, is described by its directional variance spectrum and is given by Eq. 11 (which is basically the two dimensional version of the one-dimensional spectral density as given by Eq. 6):

$$P_{sp} = \rho g \int_0^{2\pi} \int_0^{\infty} c_g(f,d) E(f,\theta) df d\theta \qquad \text{Eq. 11}$$

With: ρ= density of sea water (1025 kg/m³)

g= gravitational acceleration (m/s²)

c_g = group velocity (= 'celerity'), m/s

f = frequency

d= depth

E =directional variance density spectrum (m²/Hz/rad)[10]

However, as Equimar suggests, deep water approximations, based on the integral parameters H_{m0} and $T_{m-1,0}$, are sufficient for a first order wave resource assessment. H_{m0} and $T_{m-1,0}$ can be derived based on the spectrum by spectral moment analysis.

$$P_{dp} = \frac{\rho g^2}{64\pi} H_{m0}^2 T_{m-1,0} \qquad \text{Eq 12}$$

Notice that (Beels 2009) based the wave resource analysis on scatter diagrammes and did not have the directional variance density spectrum E. Furthermore Beels (2009) used the same method of (Goda 2000), but with the formula of Eckart instead to solve c_g (see also § 3.1). Therefore the author assumed a parametric Jonswap spectrum (Beels 2009).

However, since a big part of the Belgian Part of the North Sea is rather shallow (especially the nearshore location), Eq 12 isn't always valid under any circumstances. The two-dimensional spectral data were saved at 46 points, due to storage and processing limitations. Consequently, the resource was based on the integral parameters for the full grid (Eq 12), but with a correction factor based on 46 points where the full 2D spectra were available and the correct formulation of Eq. 11 could be used.

[9] For further (mathematical) background the reader is referred to reference books like Holthuijsen, L. H. (2007). Waves in Oceanic and Coastal Waters.

[10] Note that *S* in eq. 6 is used for the one dimensional variance density spectrum and that *S* is only a function of *f* and not of *Θ*.

5.2 Available wave power resource

5.2.1 Methodology

5.2.1.1 *BOREAS-SWAN-BCS numerical model (BSB) and the corresponding dataset*

The output of the BSB wave model is a database on 2 levels: data stored at the full grid and data stored at 46 specified points of interest.

On the full grid (131*141 rectilinear grid), every timestep (3 hours) contains the following relevant parameters: H_{m0} and $T_{m-1,0}$. This allows to use the deep water approximation for the wave power calculation as defined in Eq. 12.

For the points of interest as defined in Figure 22, the database contains the full two dimensional spectra. This allows to calculate the -correct- wave power as defined in Eq. 11. In order to solve this equation, the spectrum is first integrated over the direction (30 directional sectors, every 12°) to obtain the one dimensional spectrum. The actual depth for the point is obtained by linear interpolation of the depths that are given on the output grid. Then the group velocity c_g is calculated for every frequency bin based on the formula of (Goda 2000). Since the energy variance spectrum $E_{(f,\theta)}$ is given by the SWAN model, the integration over the 25 frequency bins can be executed. However, this information was only stored for 46 selected points of interest, due to storage and processing limitation. Hence, the integral parameters H_{m0} and $T_{m-1,0}$ were used to calculate the wave power by means of the deep water formula (Eq 12).

Wavepower is expressed in kW/m and should be interpreted as the amount of energy that is available per m wavecrest. However, just multiplying the width of a WEC with the available power does not yield in the extractable wave power. Conversion efficiencies and resonance effects (Falnes 2002) influence the extractable power to a large extent.

The maps with the wave power are based on H_{m0} and $T_{m-1,0}$ of the full grid and the 10 year timeseries and calculated using Eq 12, but 3 corrections were applied, which are discussed hereafter.

5.2.1.2 ***Buoy data correction***

In order to account for the difference between the observed buoy data and the numerical model, the bias[11] for Westhinder, both for H_{m0} and $T_{m-1,0,}$ was applied to the modeled SWAN results for the full grid and the 10 year dataset. The rationale behind is that Westhinder is the buoy with the most reliable and longterm results, and therefore is a reference point for the wave parameters, and hence the wave statistics. This correction provides good results at intermediate and deep waters offshore (like at Westhinder and the domain concession). Since the main focus is the domain concession zone, it was chosen to apply this correction. Thus, the model results H_{m0} were increased with +0.037 m and $T_{m-1,0}$ increased with +0.25 seconds (which correspond to the 10 year bias between buoy data and model results for Westhinder). This will be annotated in the titles of the figures with 'buoy data correction'.

[11] Missing buoy data was excluded for the determination of the bias.

5.2.1.3 *Deep to spectral correction*

In order to account for the difference in methodology between the correct spectral (Eq. 11) and the approximate deep water methodology (Eq 12), a correction map was based on the bathymetry and the correlation between the bathymetry and difference between deep and spectral wave power. For th e 46 points where the spectrum was available, both the wave powers based on equations 11 and 12 were calculated, and plotted in function of the bathymetry, whereby the correction factor is given by:

$$\text{Correction factor (\%)} = 100^* (WP_{sp}-WP_{deep})/WP_{deep}$$

With WP = wave power with the indices indicating the used equation ($_{sp}$ stands for Eq. 11 and $_{deep}$ stands for Eq 12). The correlation factor found was (Mathys *et al.* 2011b):

$$\text{Correction factor (\%)} = - 0.24^*\text{Depth(m)} +13$$

The obtained correction factor was in line the results of the French Anemoc Study (Mattarolo *et al.* 2008).

5.2.1.4 *Seventeen year correction*

Although the BOREAS project used a ten year wave hindcast (1999-2008), results for longer periods based on buoy data were available (Beels 2009). In the latter study, the covered period is longer (1991-2007) than in the BOREAS model (1999-2008), and is therefore assumed to be more reliable. The study of Beels (2009) assessed the wave period for Westhinder at 4.68 kW/m for the reported period (1991-2008). However, when this dataset was reanalyzed for the BOREAS period (1999-2007), the wave power dropped to 4.35 kW/m. Thus, taking a longer (and thus more reliable) period into consideration (17 years instead of 10 years), corresponds with an increase of 7.6%. Therefore, the results of the hindcast of the BOREAS model were increased with 7.6. This is indicated with the annotation ’17 year average wave power’ instead of ’10 year average wave power’.

5.2.2 Longterm

The wave power resources are given, as the original model results and the 3 corrections that were chronologically applied:

1. The model output (as described in § 5.2.1), at Westhinder, the wavepower is 3.98 kW/m, the average of all model points within the domain concession is 4.88 kW/m.
2. The model output, corrected with the buoy data correction (described in § 5.2.1.2), at Westhinder, the wavepower is then 4.37 kW/m, due to the higher wave height and period (positive biases applied to the whole time series) , the average of all model points within the domain concession is 5.32 kW/m;
3. The model output, corrected with the buoy data correction (applied first) and the deep to spectral correction (applied secondly), the wavepower at Westhinder is thus 4.37* 1.0665 (see § 5.2.1.3) = 4.66 kW/m, the average of all model points within the domain concession is 5.66 kW/m;

4. The model output, corrected with the buoy data correction (applied first), the deep to spectral correction (applied secondly) and the 17 year period correction (applied thirdly) give the final result shown in Figure 36. The wavepower at Westhinder is thus 4.66kW/m *1.076 (see § 5.2.1.4) = 5.01 kW/m, the average of all model points within the domain concession is 6.08 kW/m .

The final available resource map, taking into account these 3 corrections (Figure 36), shows consistently higher wave powers compared to previuos buoy data studies at Westhinder. The study from Beels (2009) found 4.64 kW/m, whereas in this study 5.01 kW/m was found (Table 18). The wave powers at ZW-Akkaert and Wandelaar are higher for the BOREAS study than for Beels (2009). At the domain concession zone, the wave powers are ranging from 5.5 (South) to 6.4 (North) kW/m.

Table 18: Comparison between the wave powers from BOREAS and (Beels 2009).

Buoy	BOREAS final wave power	Beels (2009)[12] with indication of the considered period
Westhinder	5.01	4.64 (’90-04) 4.68 (’90-’08)
ZW-Akkaert	4.95	3.64 (’84-’04) 3.68 (84’-’08)
Trapegeer	1.65	1.51 (’94-’04)
Oostende	2.00	1.66 (’97-’02)
Wandelaar	3.8	2.63 (’95-’04)
Bol van Heist	2.92	2.54 (’85-’04)
Average on domain concession	6.08[13]	NA

The difference between the results from the BOREAS study and the buoy data study from Beels (2009) could be explained by the following arguments:

- The buoy data study (Beels 2009) used discrete classes of wave height and periods in the scatter diagramme (see (Mathys *et al.* 2011b)for an example at Westhinder). In a sea state between 1 to 1.5 m all points are considered as having a wave height of 1.25m. However, the model data was based on continuous wave heights and periods, and used the actual modeled wave data and heights.
- Another possible source for the difference could be the data gaps in buoy data due to for example maintenance or transmission problems (as was shown in Table 12). The model results provide a continuous dataset.
- Lastly, the methodology of the buoy data study is different (assumption of parametrized Jonswap spectrum for (Beels 2009) versus the deep water approximation with corrections that was used in BOREAS).

12 The original study from Beels (2009) calculated the wave powers based on a paramatrized JONSWAP parameter, derived from the integral parameters. The deep to spectral correction was not applied on these values, but cited from the original reference.

13 Average of all the model output points within the domain concession zone.

These arguments are plausible to explain the difference. Concluding, one can state that the model results, with the corrections, give the best available wave power resource map with the current methodology.

The three available output points of the French Anemoc study (Anemoc 2011) gave comparable wave powers (indicated with white 'o' symbols) in Figure 37. The only point available from Anemoc in the domain concession zone gives a wave power of 6.68[14] kW/m, whereas in this study 6.48 kW/m was found. Another point (4.31 kW/m) lies just North of the 4 kW/m contourline and thus seems in line. A third point (4.42 kW/m), laying outside the BPNS, apparently underestimates the values obtained by the BOREAS project (5 kW/m contourline). The Anemoc study was based on a 23 year hindcast of waves with the spectral wave model TOMAWAC (Mattarolo *et al.* 2008).

The results from the UK Wave Atlas are also shown (indicitated with '*') in Figure 37. At the western zone of the model grid, the 5 kW/m contourline of the BOREAS study is in line with approximately kW/m of the UK Wave Atlas point. At the NE zone of the BPNS, the 6kW/m countourline of the BOREAS project is in line with the UK Wave Atlas points. The agreement with the UK Wave Atlas is strikingly good, although the latter used a much coarser grid than the BOREAS model. In the study of the UK WAVE Atlas a '*good agreement between modeled and observed data was found: within 10% of significant wave height and 20% of wave power*' (ABPMER Ltd *et al.* 2008b).

The Anemoc and UK wave Atlas points at the western part of the model grid (outside the BPNS) gives respectively 4.98 and 4.42 kW/m, which corresponds to a 11% difference, between the French and UK wave model.

Overall, one can conclude that the available wave power (Figure 37) is inline with the UK Wave Atlas and Anemoc study (Figure 37), and that the errors between the model results of BOREAS, Anemoc and UK Wave atlas studies are of a similar order of magnitude to the errors found between the numerical models and observations[15] within these 3 studies (Mattarolo *et al.* 2008).

14 This was calculated based on the scatterdiagrammas of H_{m0} and $T_{m-1,0}$ of the Anemoc study, using the deep water formulation (Eq. 12), without any corrections.

15 Observations are dependent on the study: in most cases buoy data where used, but also lightships were used as a measuring platform in the UK Wave Atlas study.

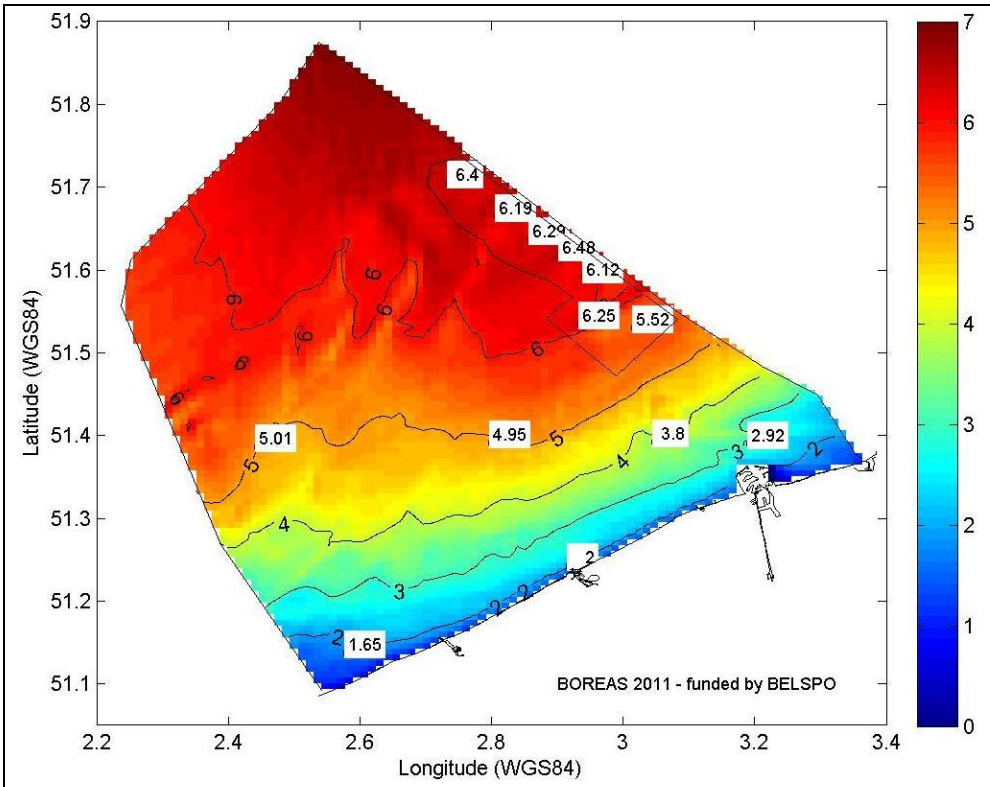

Figure 36: Final wave power resource: 17 year average wave power (kW/m) with buoy data and deep to spectral correction (all 3 corrections).

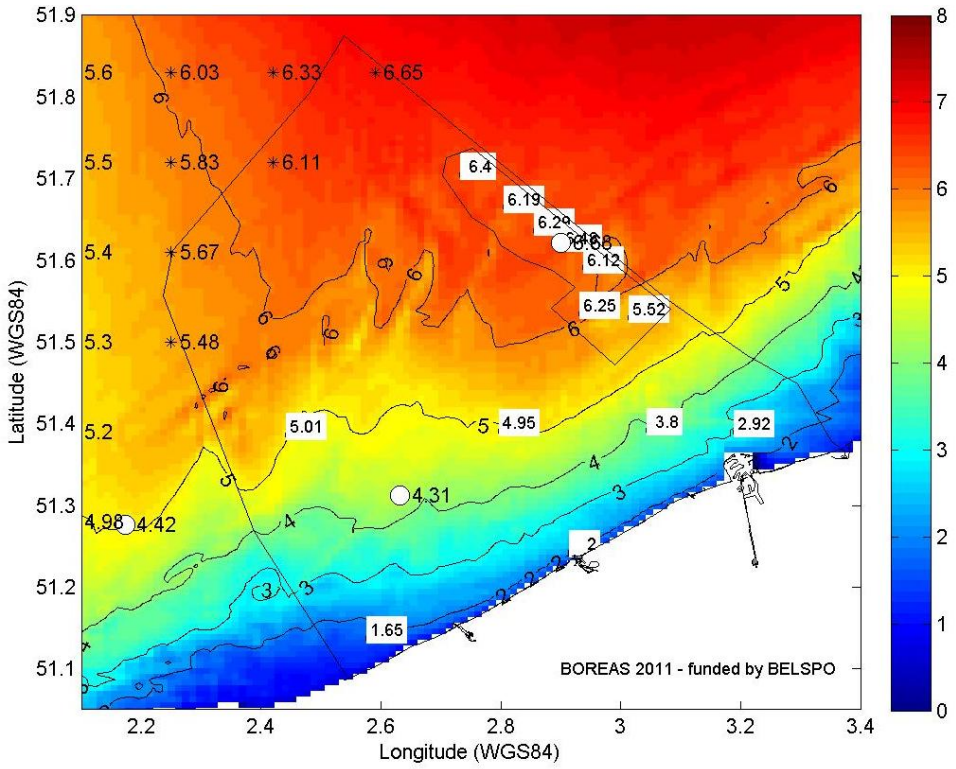

Figure 37: Comparison of the final wave power resource climate in kW/m of BOREAS (background, contourlines and white boxes, same as Figure 36,but extended to the full model grid), the French Anemoc data points (white o) and the UK Wave Atlas points (*). Sources: (ABPMER Ltd *et al.* 2008a; Anemoc 2011).

5.2.3 Monthly trends

The monthly available wave power resources are presented here in the 'final' way, thus with the 3 corrections applied.

The results for the Months January (Figure 38), April (Figure 39), July (Figure 40) and October (Figure 41) are given. The other months are given in the Appendix (§ 9.3). There is, as expected, a strong variation between the wavepowers. The maximum is obtained in January, where the wave power is about 10.7-9.03 kW/m in the domain concession zone, with the lower values in the Southern part of the domain concession zone. This monthly maximum is of course due to higher winds in the storm season. In the summer months July the wave power drops to values around 2.6-2.9 kW/m in the domain concession zone.

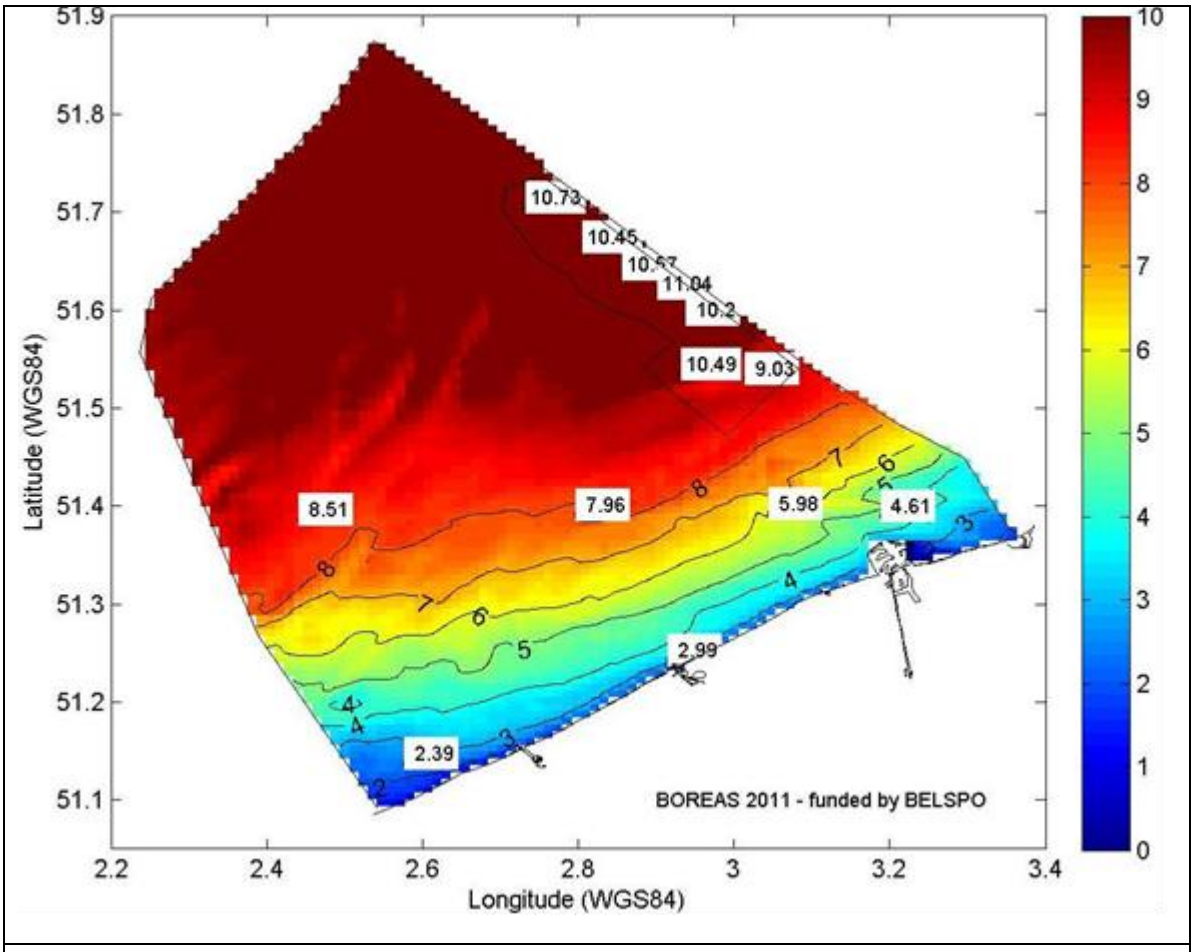

Figure 38: Final Average wave power (kW/m) for the month January (final, with the 3 corrections).

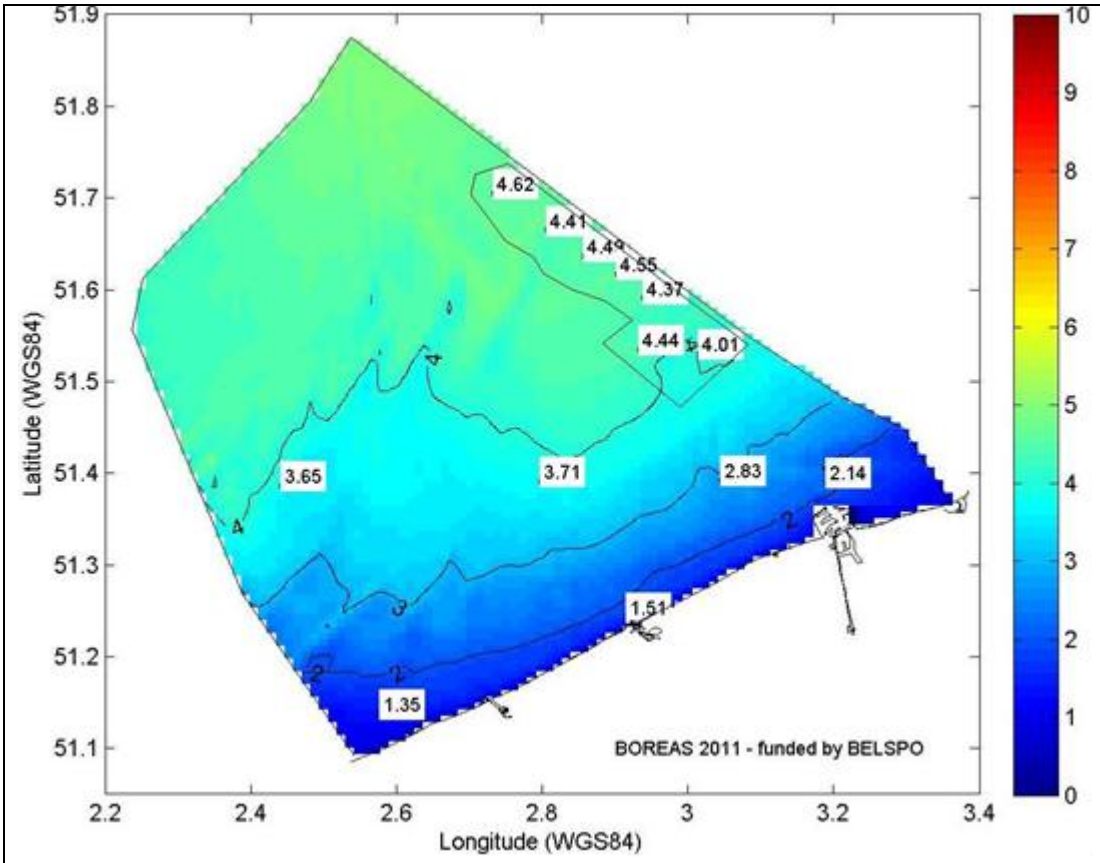

Figure 39: Final Average wave power (kW/m) for the month April (final, with the 3 corrections).

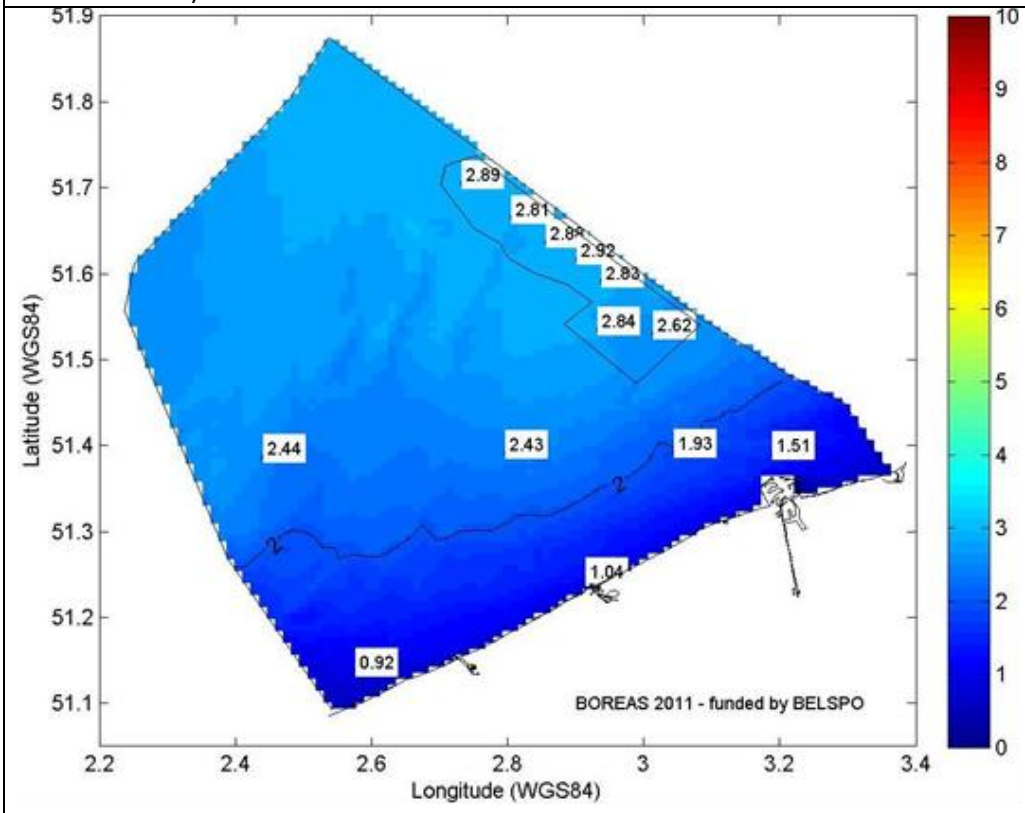

Figure 40: Final Average wave power (kW/m) for the month July (final, with the 3 corrections).

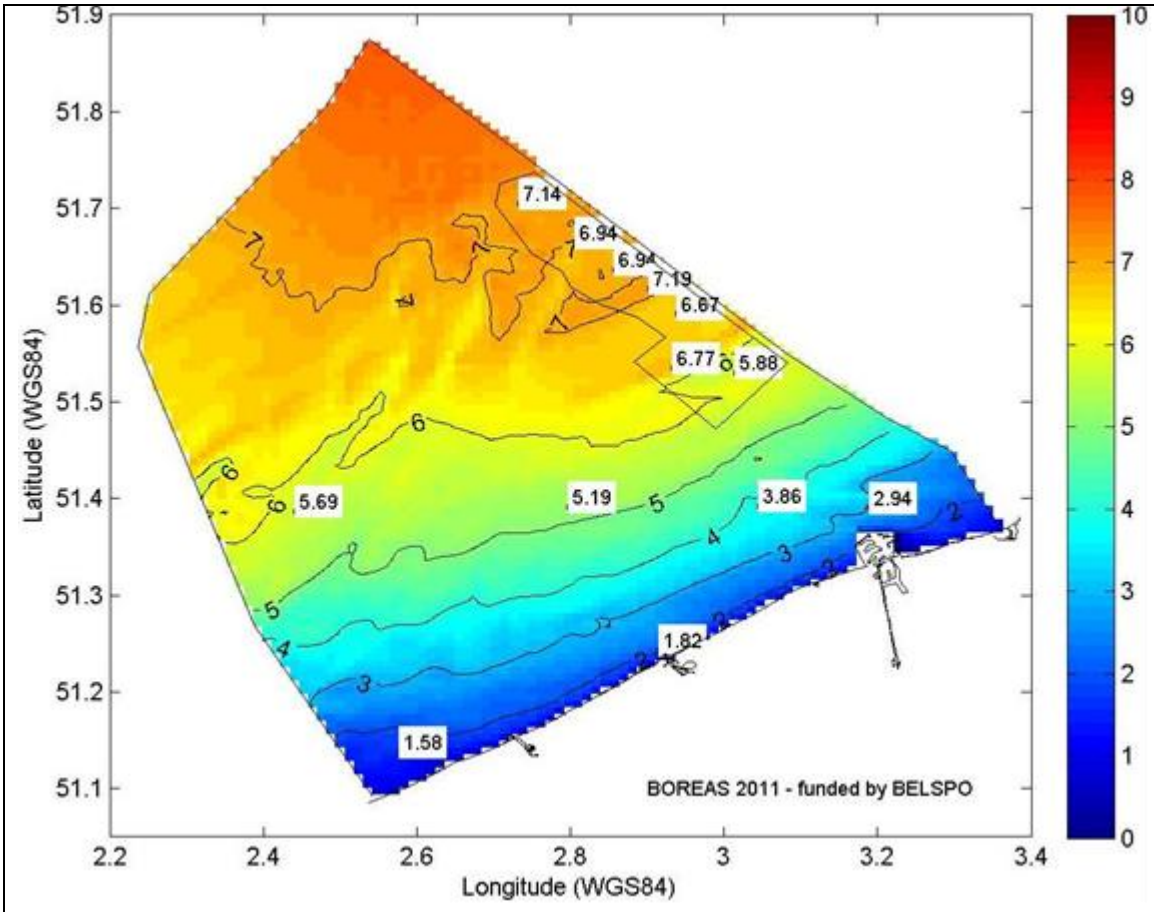

Figure 41: Final Average wave power (kW/m) for the month October (final, with the 3 corrections).

5.2.4 Yearly Differences

The yearly available wave power resources are presented here in the 'final' way, thus with the 3 corrections applied.

The year with the highest and lowest annual wave powers are given in Figure 42 (1999) and Figure 43 (2003) respectively (the other years are given in the Annex). For Westhinder, the long term yearly average is 5.01 kW/m, the yearly average is 5.82 kW/m in 1999 and the minimum 3.69 kW/m in the year 2003. The long term average for Westhinder is 5.01 kW/m and for ZW-Akkaert 4.95 kW/m.

For the years 2001 (Figure 78), 2003 (Figure 43), 2004 (Figure 80), 2005 (Figure 81) and 2007 (Figure 83) the wave power at Westhinder is lower than at ZWAkkaert.

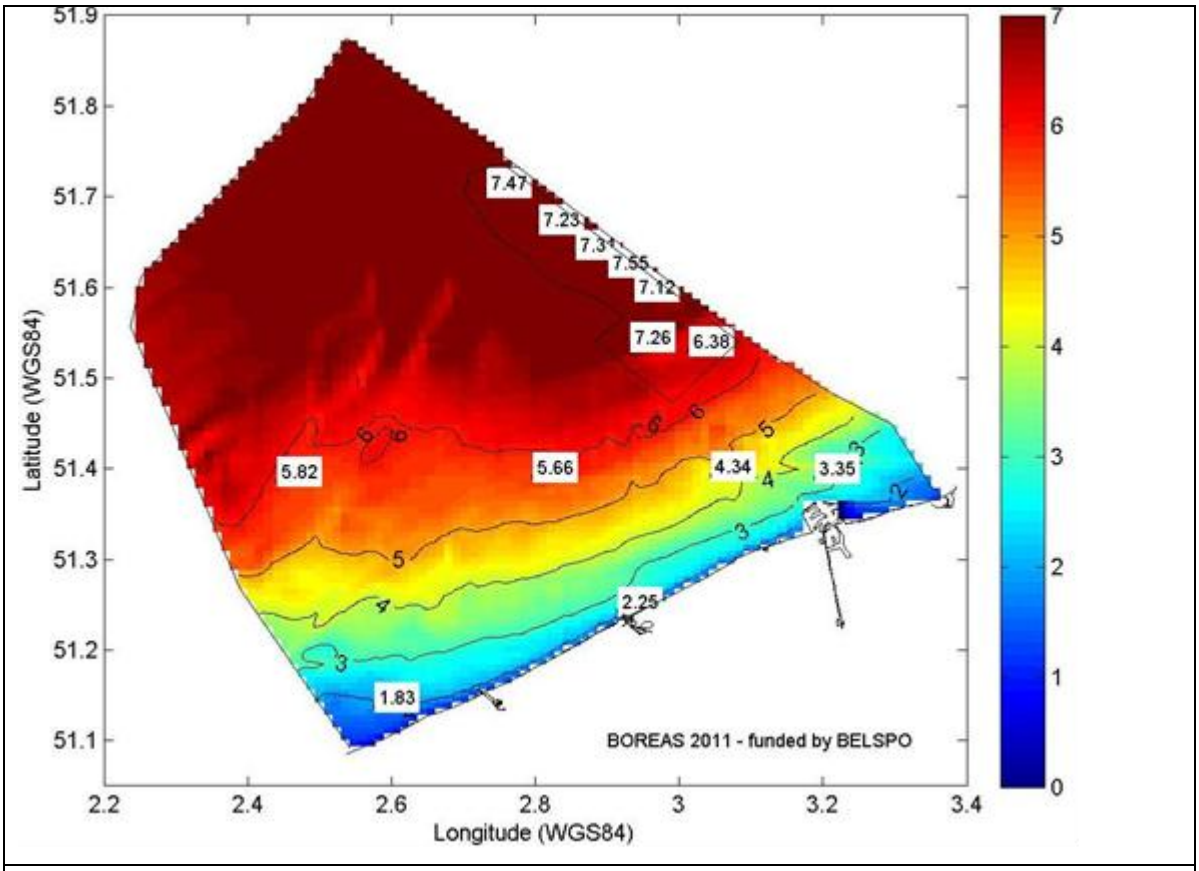

Figure 42 : Average wave power (kW/m) year 1999 (final, with the 3 corrections).

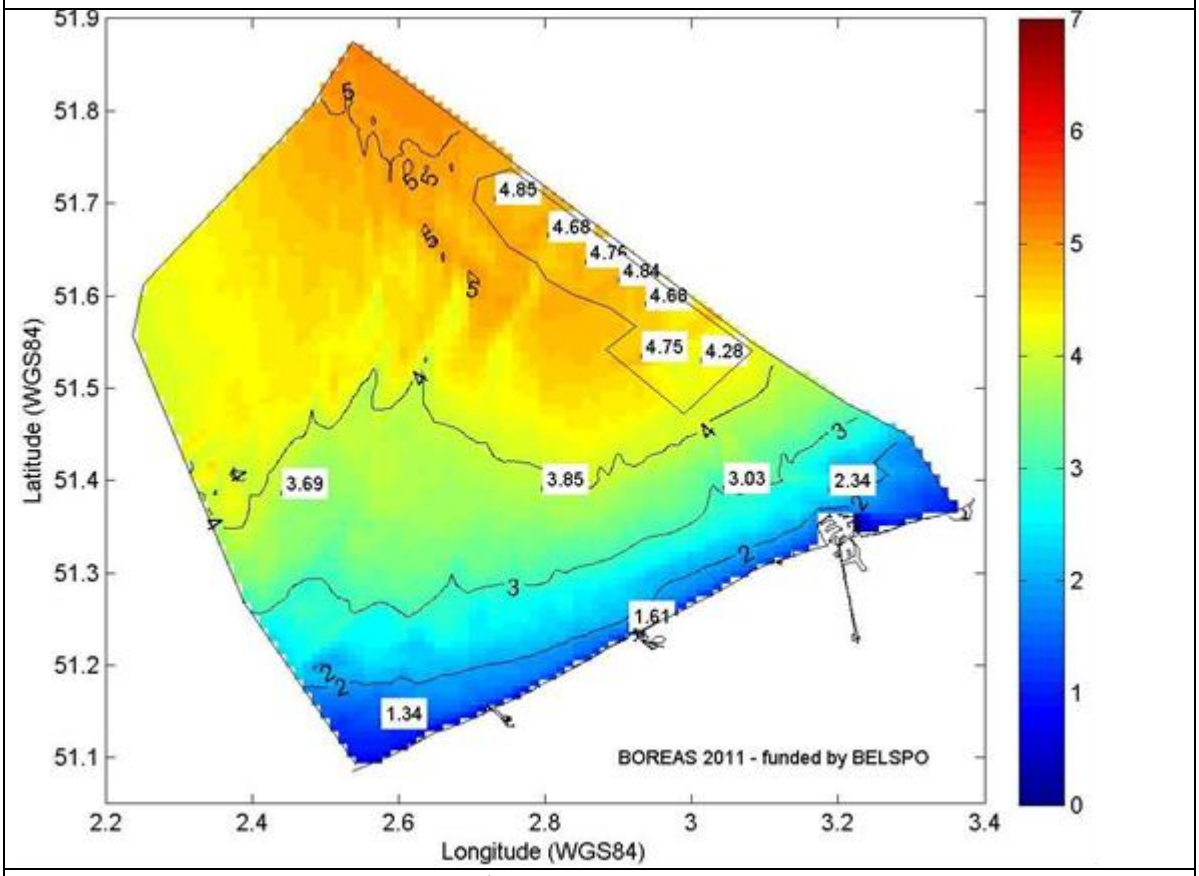

Figure 43 : Average wave power (kW/m) year 2003 (final, with the 3 corrections).

5.2.5 Extractable wave power resource

The assessment of the extractable wave power resource is based on the combination of the available resource and a conversion efficiency, in this case represented by a power matrix, which gives the relation between the wave height and period with the produced power.

5.2.5.1 *Methodology*

The extractable resource was calculated based on available power matrices for 3 WECs: the 750 kW Pelamis, the Protech Straumekraft 25 kW point absorber and a single 37 kW floater of a Wavestar WEC. The extractable resource was calculated by combining the power matrix of the respective WEC with the combination H_{m0} and $T_{m-1,0}$ (with the buoy data correction) for every timestep of the 10 year hindcast. For every combination of the wave height and period the produced power production was linearly interpolated on the given power matrices (Table 4, Table 5 and Table 6). Most power matrices just indicate H_s or T_e (respectively significant wave height and energy period). It is assumed here that H_{m0} as given by the model (frequency domain analysis) equals H_s (from the power matrix) and $T_{m-1,0}$ equals the period (from the power matrix). After this calculation, an extractable resource was produced (expressed in kW), after which the 10 to 17 year correction was applied.

The extractable power is thus based on H_{m0} and $T_{m-1,0}$ of the wave model. The buoy data correction was used, since this correction directly applies to H_{m0} and $T_{m-1,0}$. The deep to spectral correction was not applied. The 'deep to spectral' correction is not necessary as the power matrix requires the integral parameters H_{m0} and $T_{m-1,0}$ directly and not the spectral data. The 10 to 17 year correction was also applied.

It is important to mention that this extractable resource is valid on placing a single WEC at a specific site, since the current methodology doesn't allow to take into account the interaction between a WEC and waves, or between one WEC with another WEC (like in a Wave Energy Convertor farm).

The first available power matrix is the one of Pelamis, given in Table 4. The Pelamis is developed for higher wave climates than the BPNS. Two other power matrices are given for the Protech Straumekraft point absorber WEC (Table 5) and for a single floater of a Wave Star WEC (Table 6). The Protech Straumekraft is based on a computer model. Pelamis' power matrix was originally published before a full scale device was deployed, so their power matrix is also based on a computer model (it is likely however that it was validated by Pelamis themselves with scale model results, due to the long development track and scale testing Pelamis performed). For the Wavestar WEC, experimentally proven power outputs are given. However, not the power matrix but a power curve (produced electricity in function of the wave height for an average wave period of 4.5 seconds) is given (Frigaard *et al.* 2010).

In this study the term 'rated power' is assumed to be equal to the maximum produced power within the power matrix. Furthermore it is assumed that this 'rated power' equals the 'installed power', which will be used for the economical assessment in chapter 7.

5.2.5.2 *Results*

The average produced electricity during the 10 year hindcast of single WEC is given in Figure 44 (Pelamis), Figure 45 (Straumekraft Protech) and Figure 46 (single floater of a Wavestar).

The results for the Pelamis (Figure 44) , which is a 750 kW device and developed for high wave climates like the coast of Portugal, Ireland, UK, etc.., show that a Pelamis WEC is by a large extent overdimensioned for the conditions on the BPNS (which was expected). If the Pelamis would be placed in the domain concession zone (average on the domain concession zone is 45.5 kW), the capacity factor is only 45.5/750 = 6.1%. The annual production for a single unit would be 399 MWh (=45.5kW*365days *24hrs/day). This is approximately 2/3 of the lowest production found in another case study, which looked at higher energetic zones (Dalton et al. 2009).

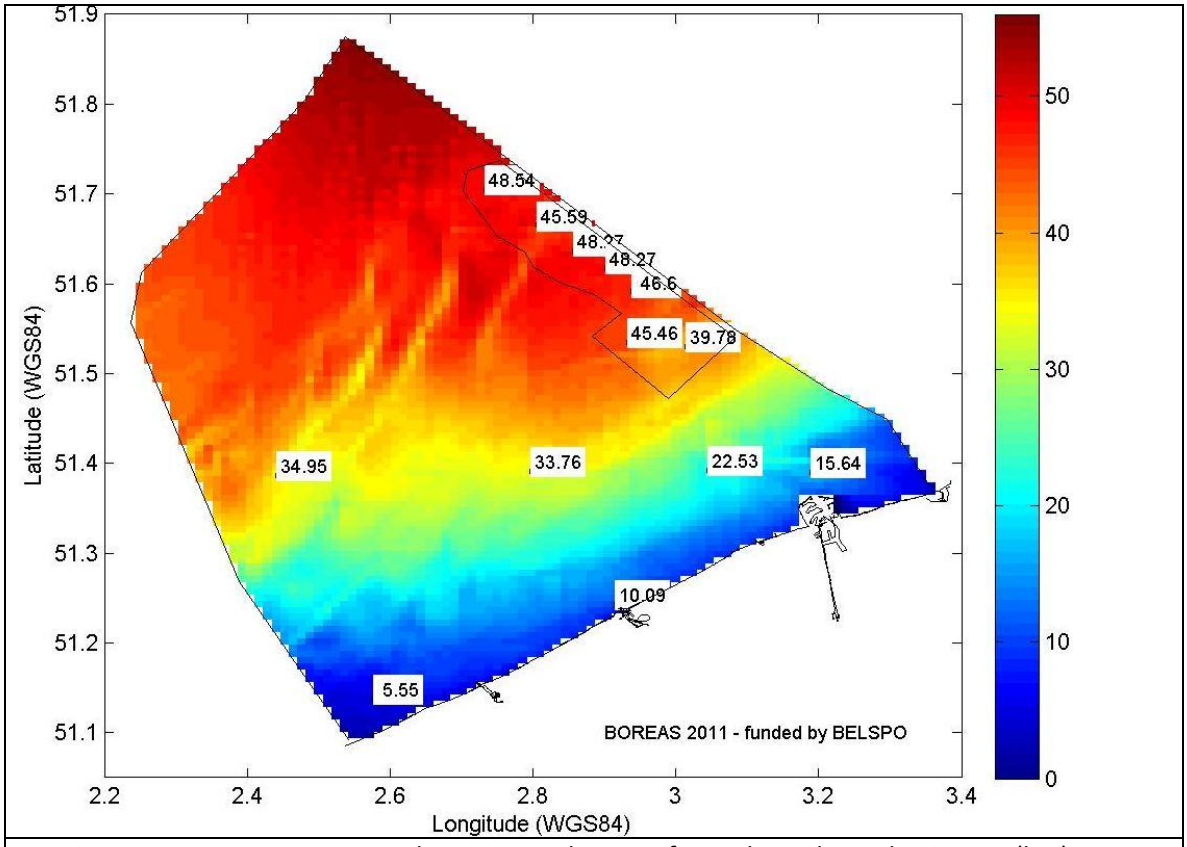

Figure 44 : Longterm average electricity production of a single 750kW Pelamis WEC (kW).

For the Straumekraft (Figure 45) which is a point absorber with a rated power of 25 kW, the capacity factors are higher. Straumekraft would produce in the order of 4.48 kW on average at the domain concession zone and hence the capacity factor would be 17.9% and the yearly produced electricity for a single unit would be 39.2 MWh (= 4.48 kW*365days*24hrs/day).

The results for a single floater of the Wavestar are shown in Figure 46. The capacity factor would then be 22.4% (8.28 kW on average on the domain concession/37kW), so higher than Straumekraft, corresponding with yearly 52.7 MWh production for a single floater But the power matrix of the Wavestar is already confirmed and therefore more reliable. Furthermore, Wavestar is trying to improve their production with advanced control strategies and optimal damping parameters. The results for a full Wavestar unit is easily obtained by multiplying the values in Figure 46 with a factor 20, since a complete jack-up platform consists of 20 floaters.

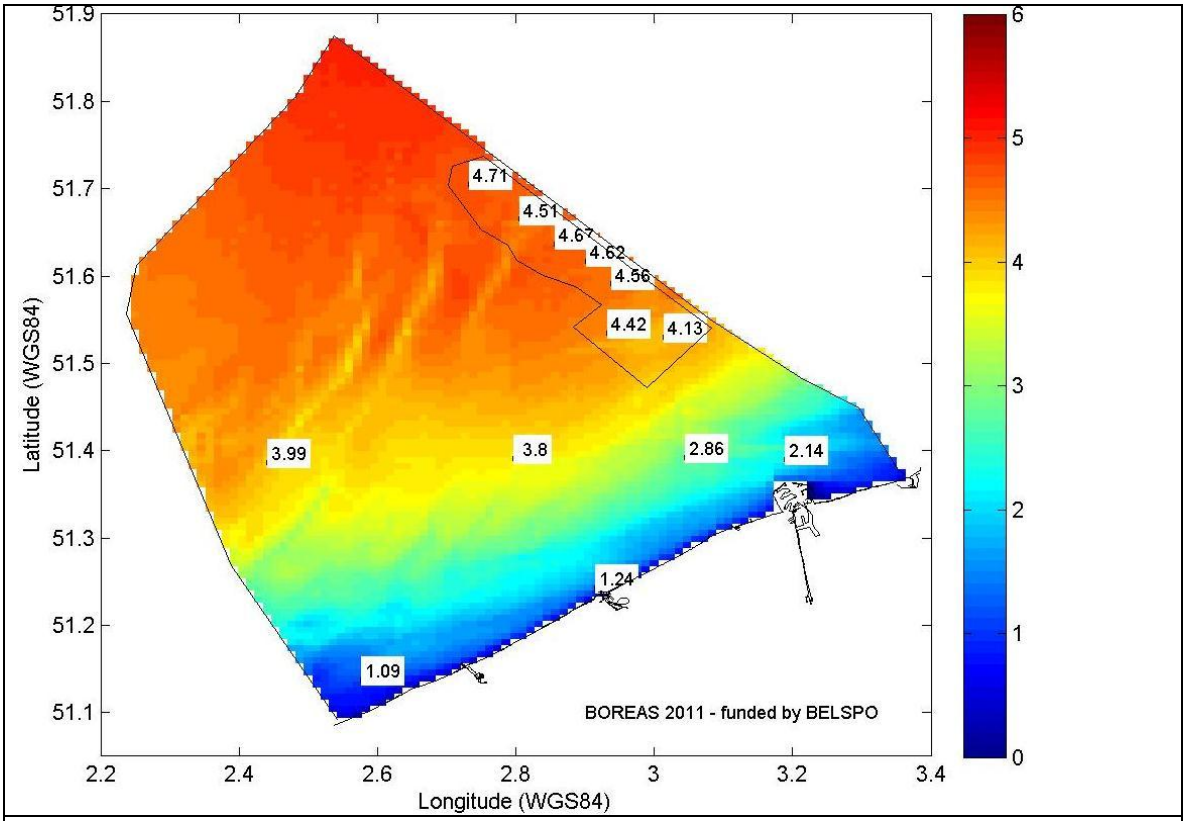

Figure 45 : Longterm average electricity production of a single 25kW Straumekraft WEC (kW).

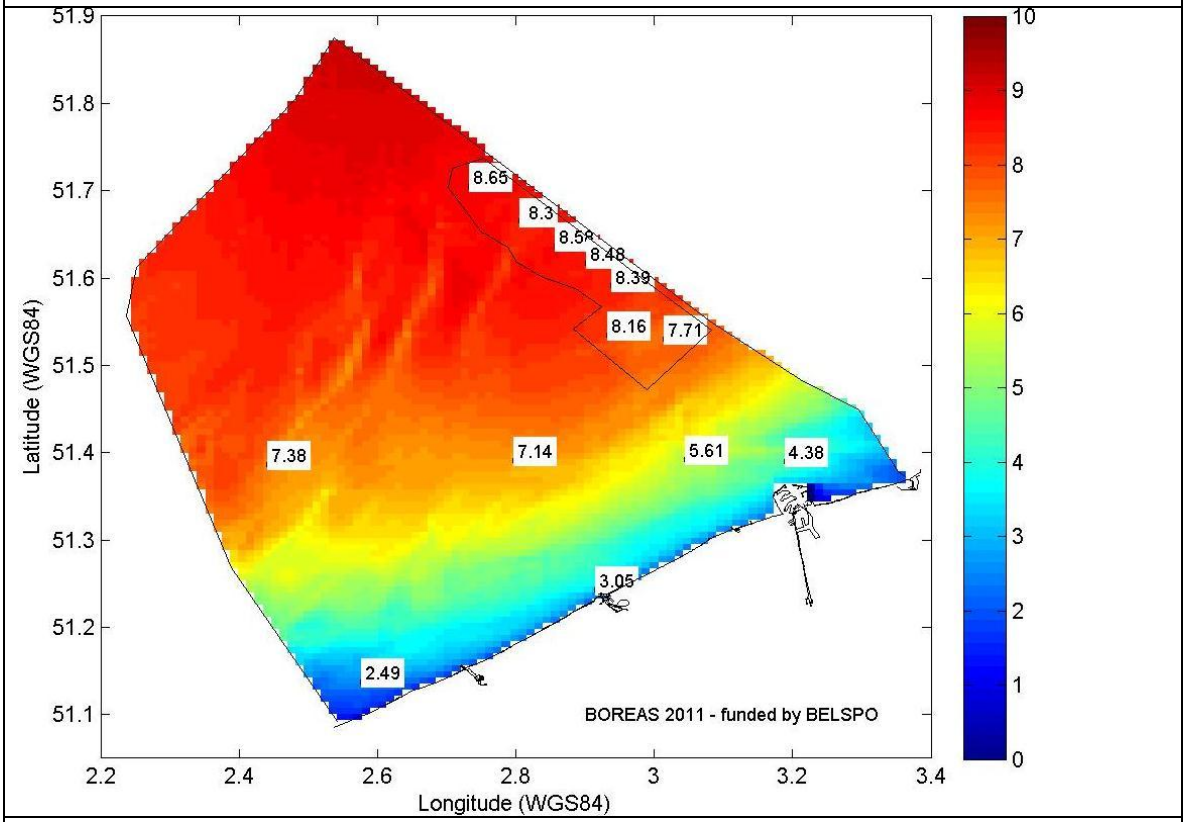

Figure 46 : Longterm average electricity production of a single 25-50kW floater of a Wavestar WEC (kW).

5.3 Tidal current resource

5.3.1 Physically available resource

5.3.1.1 *Methodology*

The calculation of the available tidal current resource is very straightforward. The current velocities are given in an x,y and z-component. The z-component is not considered as these velocities were not contributing to the wave power (< 0.001 m/s) in comparison with the x and y component. In a first step these velocities are converted to current velocities and directions, and centered and interpolated to the same gridpoint. This step is necessary to carry on with the next calculation steps, since the output grid is a staggered Arakawa C-grid (Luyten *et al.* 2011). Then, for all the gridpoints (381*345 gridpoints, including the dry land cells), all the half hourly timesteps and all the 10 depth layers, the tidal current resource is calculated by means of Eq. 13.

$$\frac{P}{A} = \frac{1}{2}\rho \mathrm{v}^3 \qquad \text{Eq. 13}$$

The results are then averaged over the total depth and time to obtain the available physical resource.

5.3.1.2 *Results*

The variations in the tidal currents are highly dependent on the bathymetry, and hence the available sandbanks. The bathymetry, and the names and location of these sandbanks is given in Figure 47. The available wave power is given in Figure 48. The results are in line with the expectations and previuous results from the OPTIEP study (Mathys *et al.* 2010). In general, the bathymetry, especially around the bigger sand banks offshore like Oostdyck, Noordhinder, Oosthinder and Blighbank can be distinguished. Furthermore, the harbor around Zeebrugge, and in a lesser extent the harbors of Ostend, Nieuwpoort and Blankenberge[16].

The model used for BOREAS has a finer grid than used for OPTIEP and is therefore more suited to give insight in local peaks of tidal current power. The peak tidal current resource is therefore higher than reported in the OPTIEP study. The OPTIEP study defined 4 zones:

1) Zone West, formed in the south by the Oostdyck bank, delimited at the west side by the border with the French Part of the North Sea. Whereas OPTIEP reported peaks at Westhinder around 140 and 194 W/m² at the Fairybank, the results found in BOREAS are higher (up to 250 W/m²). The higher values found in BOREAS are due to the finer grid of BOREAS (in comparison with the OPTIEP grid)., Local stronger currents are better detected in a finer grid and not lost in the geographical averaging over a coarser grid.

[16] The harbor of Ostend was modelled in the old version, so not with the new breakwaters that were under construction. It is expected that the new construction would increase the velocities at the breakwaters, similar to the observations in Zeebrugge. However, since the breakwater does not extend as far as in Zeebruges, the increase in current velocity, and hence tidal current power, will be in a lesser extent.

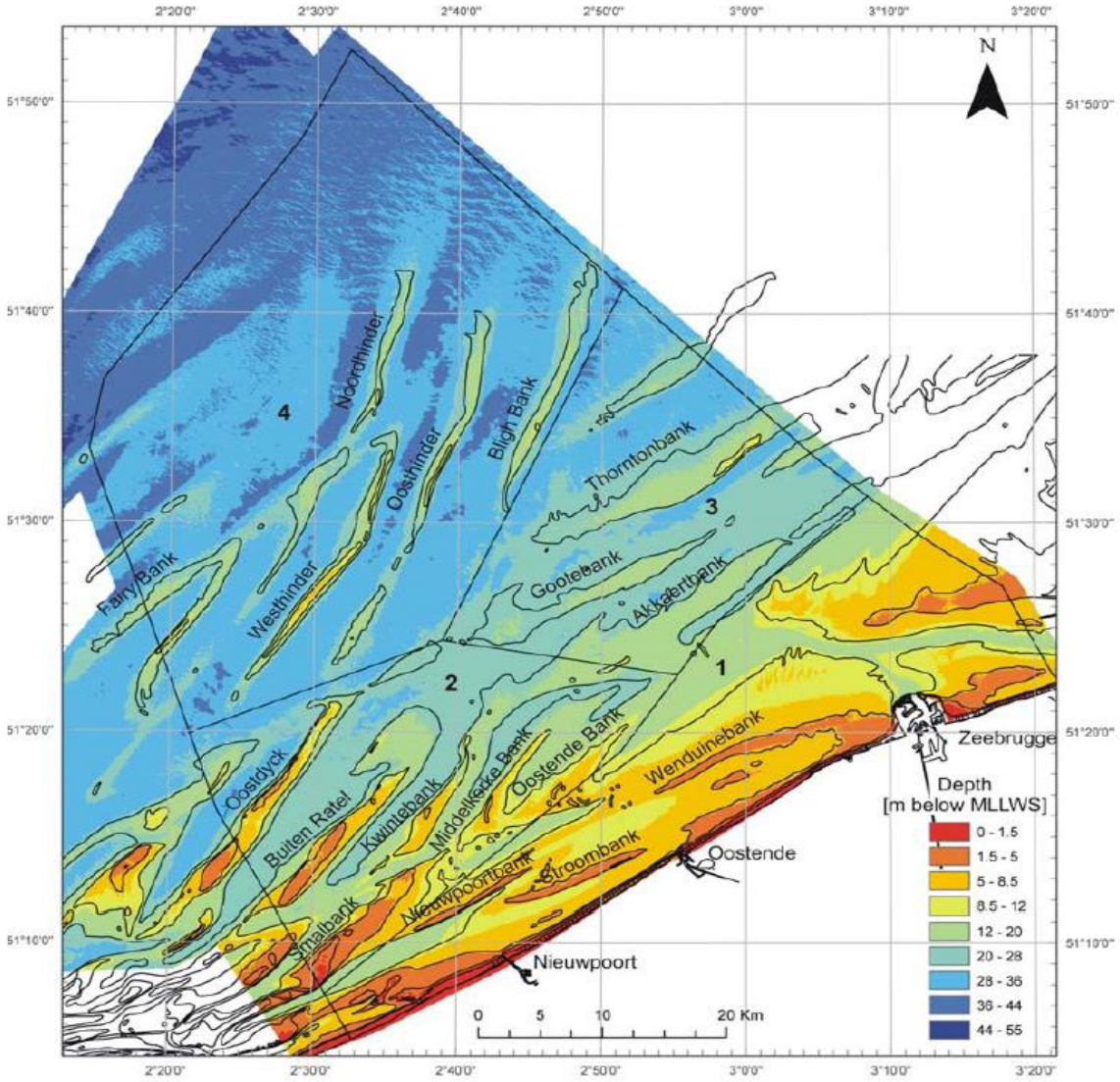

Figure 47: Overview of the sandbanks on the BPNS (Mathys 2009).

2) The two zones around the DC zone, one at NW part of the DC zone (between the westerly tips of Noord- en Oosthinder) and the other at the Bligh Bank. Whereas in OPTIEP these zones were questioned, they are now confirmed with a detailed bathymetry.

3) The harbor of Zeebrugge, and especially the zone around the NW breakwater (Figure 49), is identified as the zone with the highest tidal current potential. The tidal current ressource goes up locally to 330 W/m², whereas in OPTIEP an upper limit of 240 W/m² was detected (this is again due to the finer resolution of the BOREAS grid). However, the increased currents found here are very local, and the grid resolution of the model used was still too coarse to consider the harbor of Zeebrugge in full detail. A detailed model of the harbor of Zeebrugge, like the µ-Heist model from the BMM could provide very detailed information about where exactly the peak currents (and hence powers) occur (Van den Eynde *et al.* 2007). These peak currents then need to be confirmed by ADCP measurements.

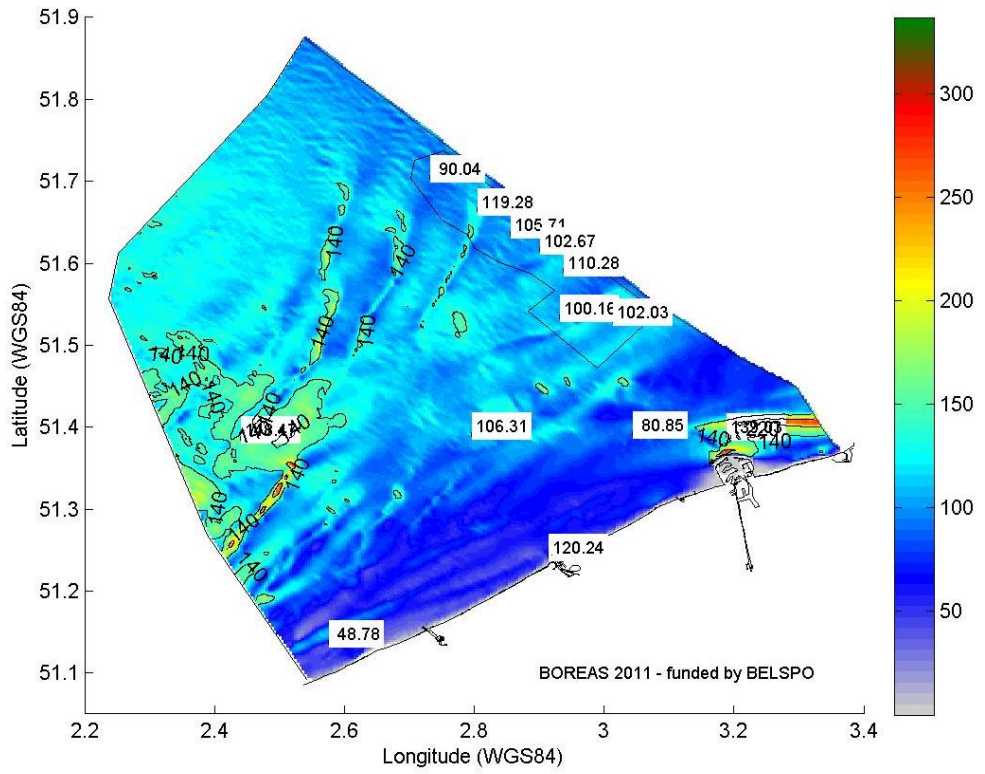

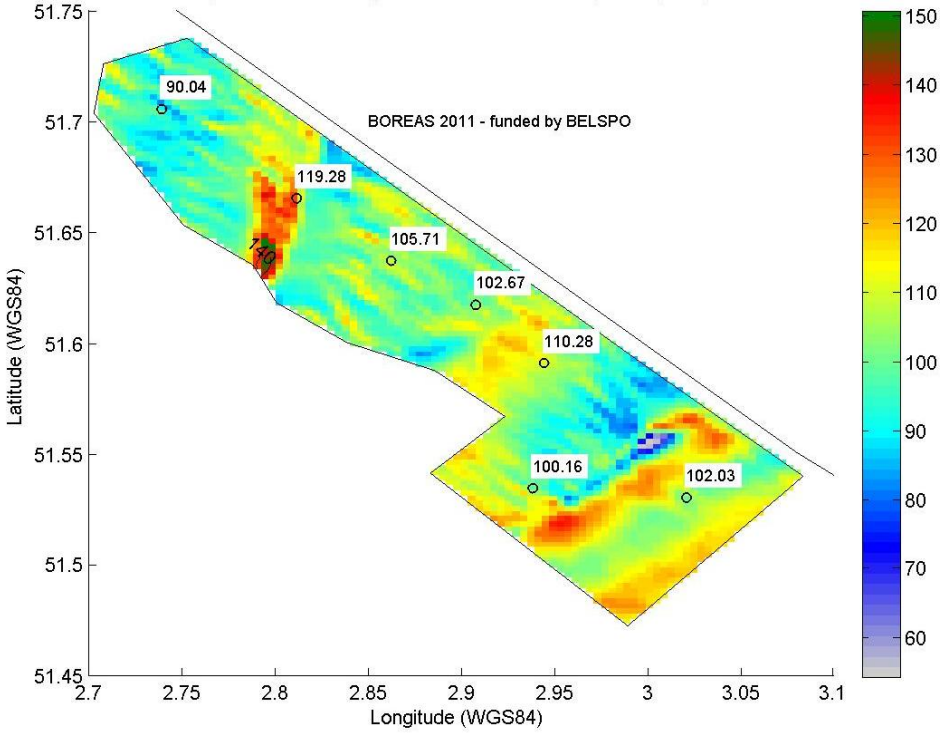

Figure 48: Depth (all depth layers) and time averaged available tidal (based on 2 spring-neap tidal cycles) current power for th BPNS and the DC zone (W/m²).

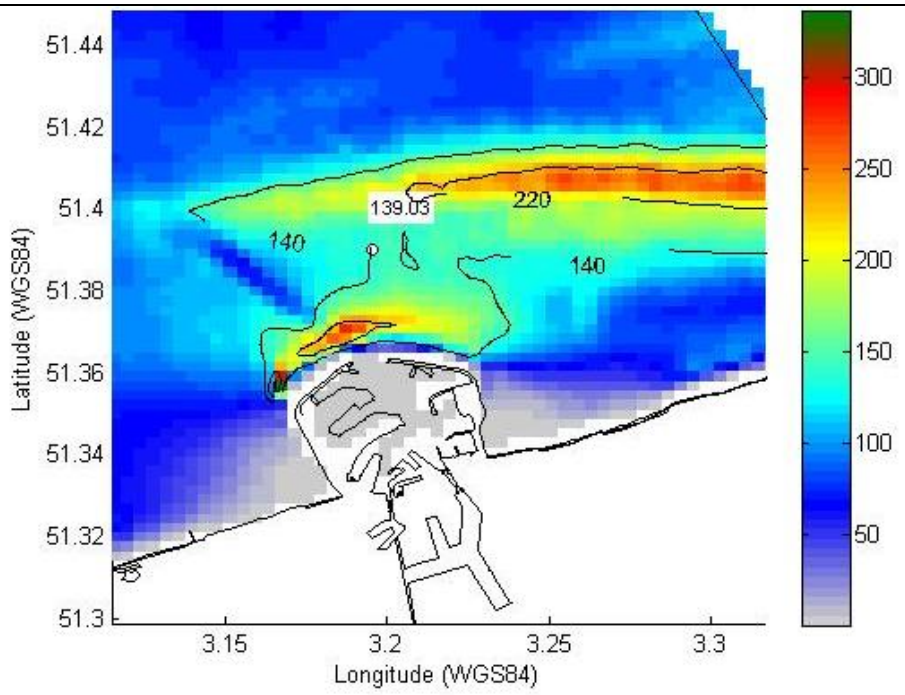

Figure 49: Depth (all depth layers) and time averaged available tidal (based on 2 spring-neap tidal cycles) current power for the region around the harbor of Zeebrugge (W/m²).

4) The navigation channel Scheur is confirmed as a zone with high energetic outputs. However,as this is a very dense shipping lane, this zone is excluded. The filling and emptying of the Scheldt Estuary, along with the presence of the shallow Vlakte van de Raan, is the cause of these higher tidal current powers.

The Domain concession zone has an available resource between 55 and 155 W/m² on most locations the resource varies between 90 and 110 (Figure 48). The highest available resource is found at the Bligh Bank (concession granted to Belwind) and varies between 130-140 with a peak of 155 W/m².

5.3.2 Extractable resource

5.3.2.1 *Assumptions*

The extractable tidal current resource is based on the available resource. In order to make a distinction between the total tidal current resource and the part that is extractable, the following assumptions are made:

- The turbine is horizontal axis tidal turbine with no in- or outlet structures to focus the tidal current stream. The effect of the angle of attack is neglected, so it is assumed that the currents are perpendicular to the blades.
- No wake interactions are considered, nor interactions with currents or waves.
- The generic efficiency curve is presented in Figure 50, which is essentially a smoothed version of the original efficiency curve presented in Figure 7 (Cornett *et al.* 2010). The available

power is indicated in the blue thick line (left axis), which is related to the cube of the current velocity. The efficiency curve (from TEC to wire, so overall TEC efficiency) is shown on the green dashed line on the right axis. Notice the cut-in speed: below 0.5 m/s no electricity is produced. Above 0.5 m/s the efficiency rapidly increases to a maximum of ca 43 % at 2.5 m/s. Notice that 2.5 m/s does not occur on the BPNS, the maximum speeds are to be found around Zeebrugge and going locally up to approximately 2 m/s. By multiplying the available power with the efficiency curve, the extractable power is achieved (thin blue line on right axis). Figure 51 illustrates this methodology for the location Westhinder for the upper half of the water column.

- The usable depth is given by the total bathymetry minus the half of the waveheight which is exceeded during 5% of the 10 year wave hindcast[17], minus the lowest low water. After obtaining this 'usable depth', 1.5m bottom and 1.5 top clearance is added. In this way the maximum diameter of a tidal turbine can be assessed and it is possible to determine the order of magnitude of the technically extractable resource (See Figure 52 and Figure 53) .
- Since the current velocities vary with the depth, either the depth averaged current in the upper half is used for the further calculations (from depth layer 4 till 9 and not 5-10 since this would involve the surface layer as well, which should be avoided to provide clearance for wave throughs, debris and ship hulls). It should be interpreted as the current velocity that is present in the water column from 40% to 90% above the bottom.

[17] The hindcast of the waves as described in the previuous chapter was used. The 5% percentile was chosen to allow enough clearance for the tips of the turbine to avoid exiting the water (with possible cavitation and damage to the blades).

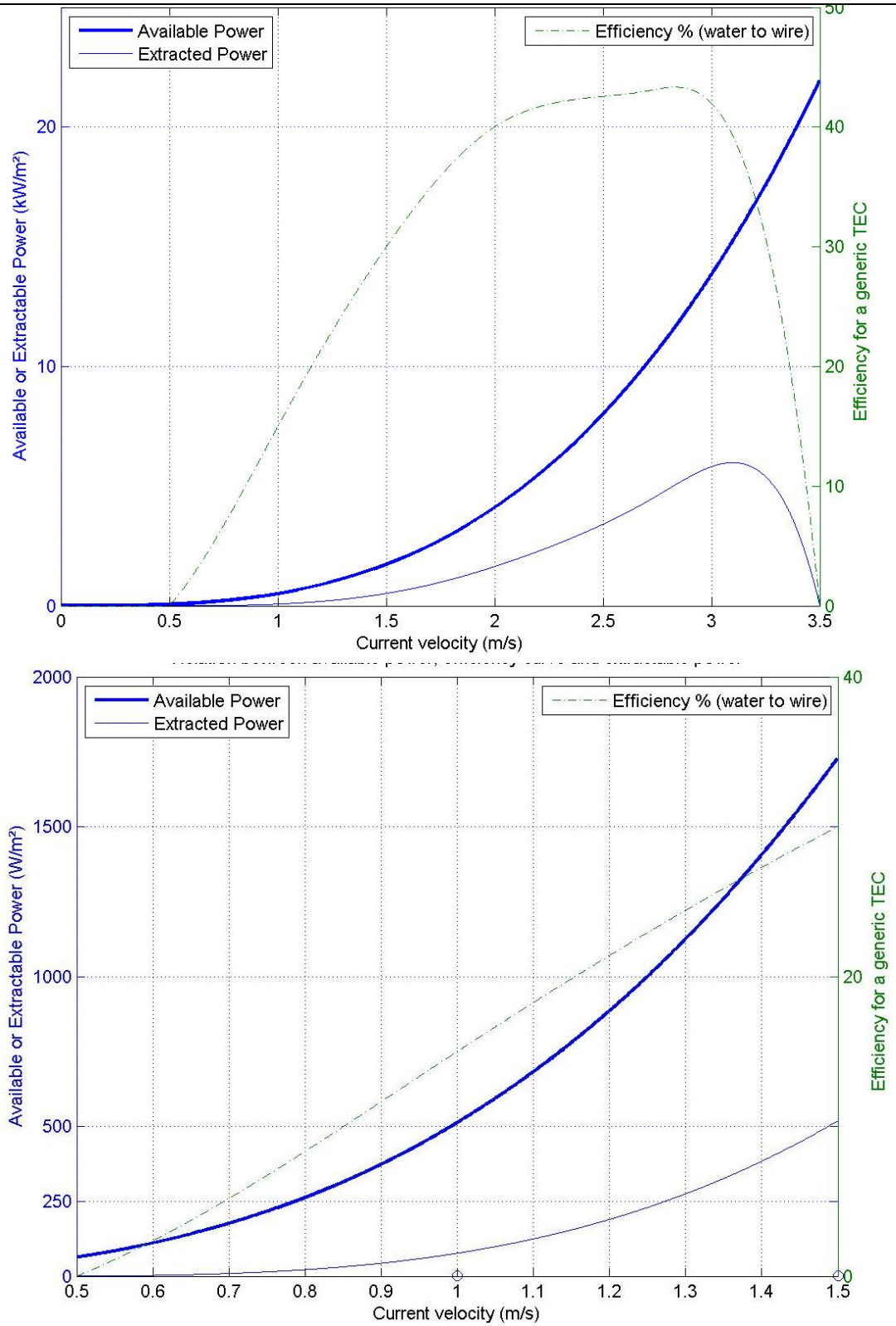

Figure 50: Relation between the available power (kW or W/ per m² swept turbine area), the efficiency (from water to wire, so overall efficiency, in %) and the extractable power (kW or W/m² swept turbine area). Top: overview; bottom: detail of current velocities between 0.5 and 1.5 m/s.

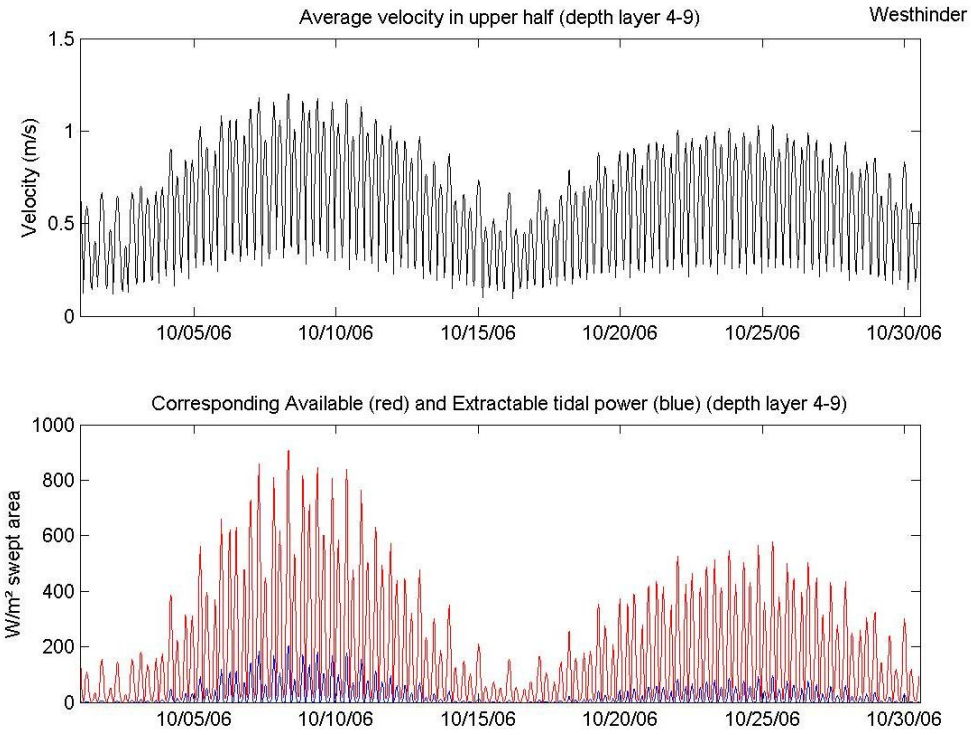

Figure 51: The current velocity (top figure) and available and extractable tidal current power (bottom figure), all for the 4th till 9th depth layer at Westhinder.

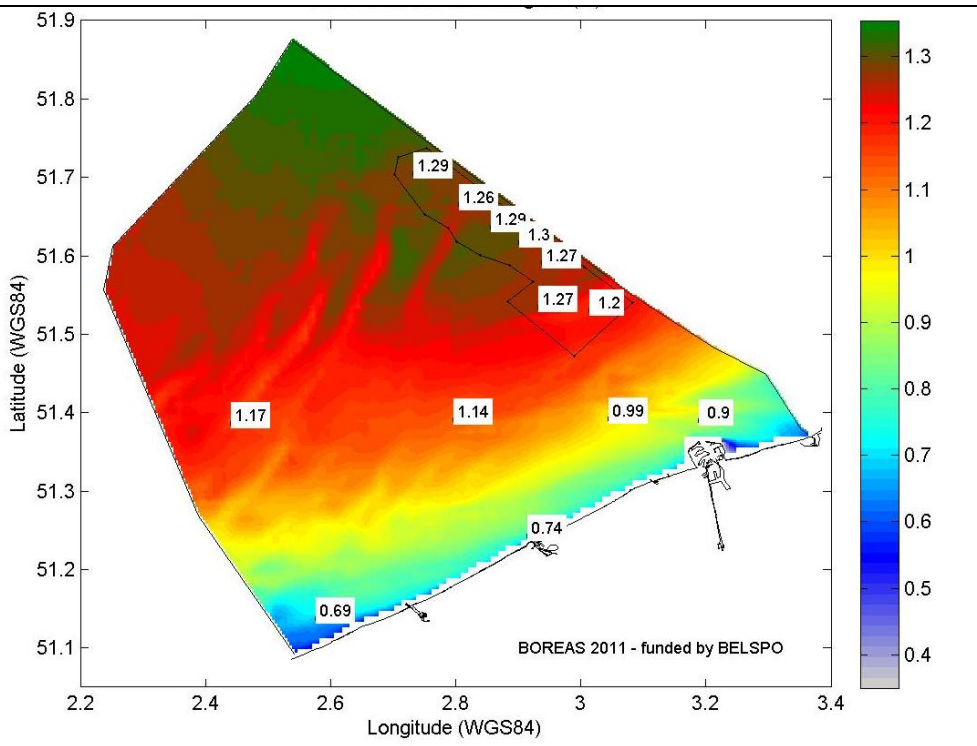

Figure 52: The half of the wave heights H_s exceeded during 5% of the 10 year wave hindcast (m).

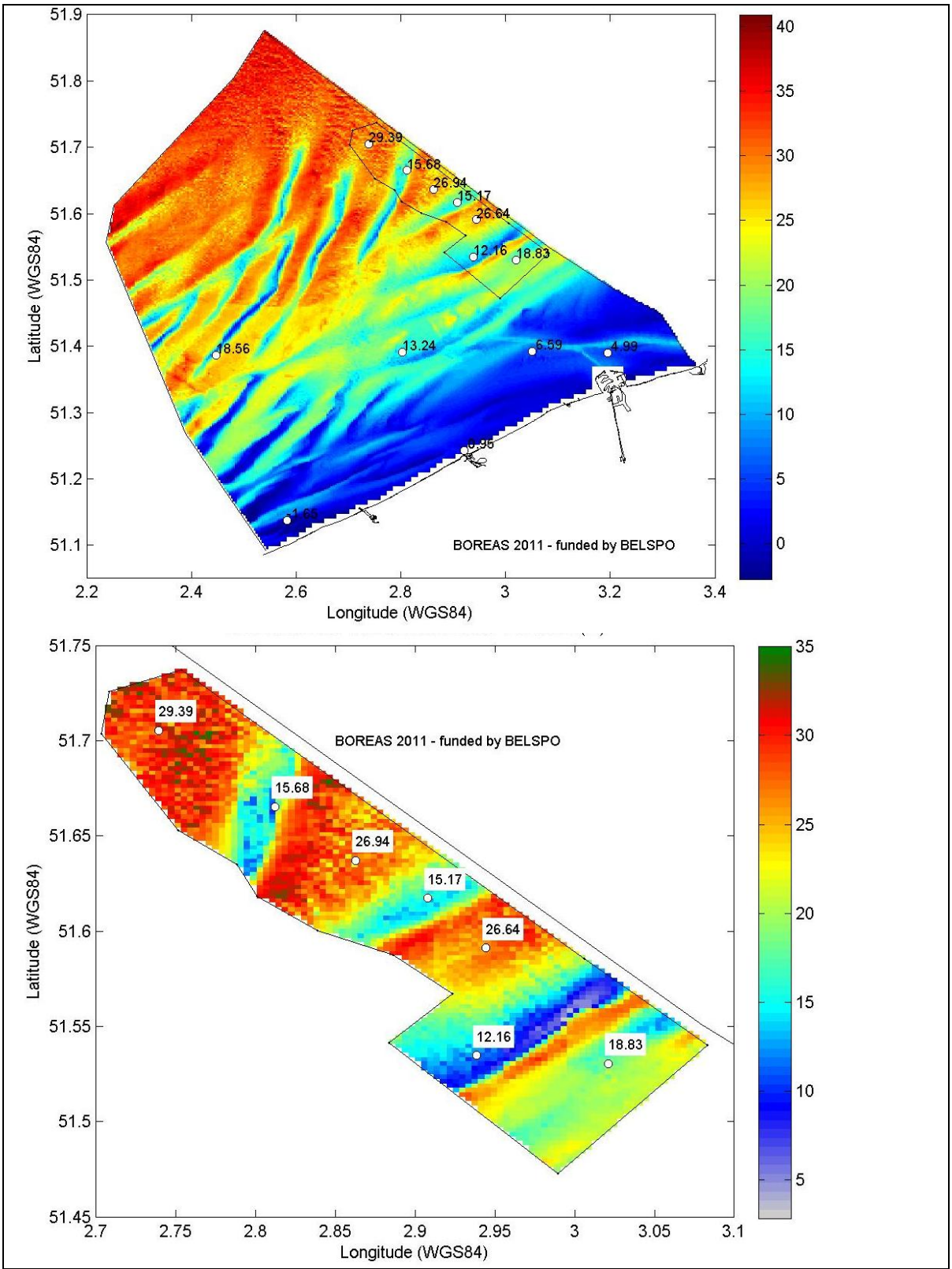

Figure 53: The absolute maximum turbine size diameters using the full wet height of the watercolumn, minus 1.5 m bottom clearance and 1.5 m top clearance.

5.3.2.2 *Results*

Figure 54 shows the result of the averaged extractable tidal current power under the assumptions mentioned in § 5.3.2.1. The result is low compared to the available tidal current power as presented in Figure 48. In the domain concession zone, the available tidal current resource on most locations (which was depth averaged over the full water column) is in the order of 90-110 W/m² (Figure 48), whereas the extractable tidal current power (averaged over the 4th till 9th depth layer) drops to 7-12 W/m² (Figure 55), which is drop by a rough factor of 10.. There is one big exception, which is the harbor of Zeebrugge. Due to the big disturbance in the current streamlines due to the harbor, high peak velocities are observed around the breakwaters (up till 110 W/m² extractable (Figure 55) of the 330 W/m² available at the very best location (Figure 49), which is a drop by a factor 3 only). A detail of the harbor of Zeebruges is shown in Figure 55. Previous studies reveiled high tidal currents around these breakwaters and showed the existence of an erosion gully at the western breakwater (Van Lancker *et al.* 2007; De Vos *et al.* 2009; Van Damme *et al.* 2009). Furthermore it is expected that, locally, even higher currents can be observed when using a finer resolution model or ADCP measurements, since the grid used to asses the local current around the breakwater of Zeebruges is still too coarse.

However the low result at the BPNS is remarkable and needs further explanation. When looking at the efficiency curve (Figure 50), no power is produced below 0.5 m/s and hence this part is not contributing to the average extractable power. Furthermore, just above 0.5 m/s, the efficiency remains low. Figure 56 shows the percentage of the time where the depth averaged current over layers 4 till 9 is below 0.5 m/s. This varies from 25 to 100%, an order of magnitude on most locations on the BPNS of 40 till 50%. The 100% values are found in the coastal zone and next to the harbor of Zeebrugge. The sandbanks are an exception with 25-30%. This means that on most locations a TEC is not producing electricity for 40-50 % of the time since the cut-in speed is not achieved. Even at the most feasible locations (in terms of operational time), like Oostdyck bank, TECs would not produce electricity for 25% of the time. Note that around Zeebrugge, the turbines are not delivering power for 35-45% of the time (although this is on the very edge of the model grid, so results should be carefully interpreted). A possible explanation could be that during ebb, the high energetic zones west of Zeebrugge are shielded by the breakwaters, whereas during flood, they are fully exposed. This causes high peak powers, after which a drop in peak power occurs.

Since the TECs would not be turning at standstill, algae growth and biofouling are very likely on the blades and the turbines, and thereby negatively influencing the hydrodynamic efficiency. This is clearly a design issue if the cut-in speed remains at 0.5 m/s, and if the TEC is deployed at shallow locations (due to the penetrating sunlight promoting biological growth).

To further illustrate the difference in available and extractable tidal power resource, the example of Westhinder is used:

- The available tidal power (full water depth) is 140 W/m² (Figure 48);
- The timeseries of the tidal current velocities and extractable power (Figure 51) show the variable power outputs depending on the flood-ebb and neap-springtide tidal cycles: the available power varies roughly 40 to 900 W/m², whereas the the extractable power varies from 0 (39% of the time, see Figure 56) to 180 W/m² (Figure 51),
- The average extractable tidal current power at Westhinder is then 18.4 W/m² (Figure 54). This is due to the observed velocities (Figure 51, top), the used effiency curve (Figure 50) and

only considering the 4th till 9th depth layer (representing the upper half layer of the watercolumn).

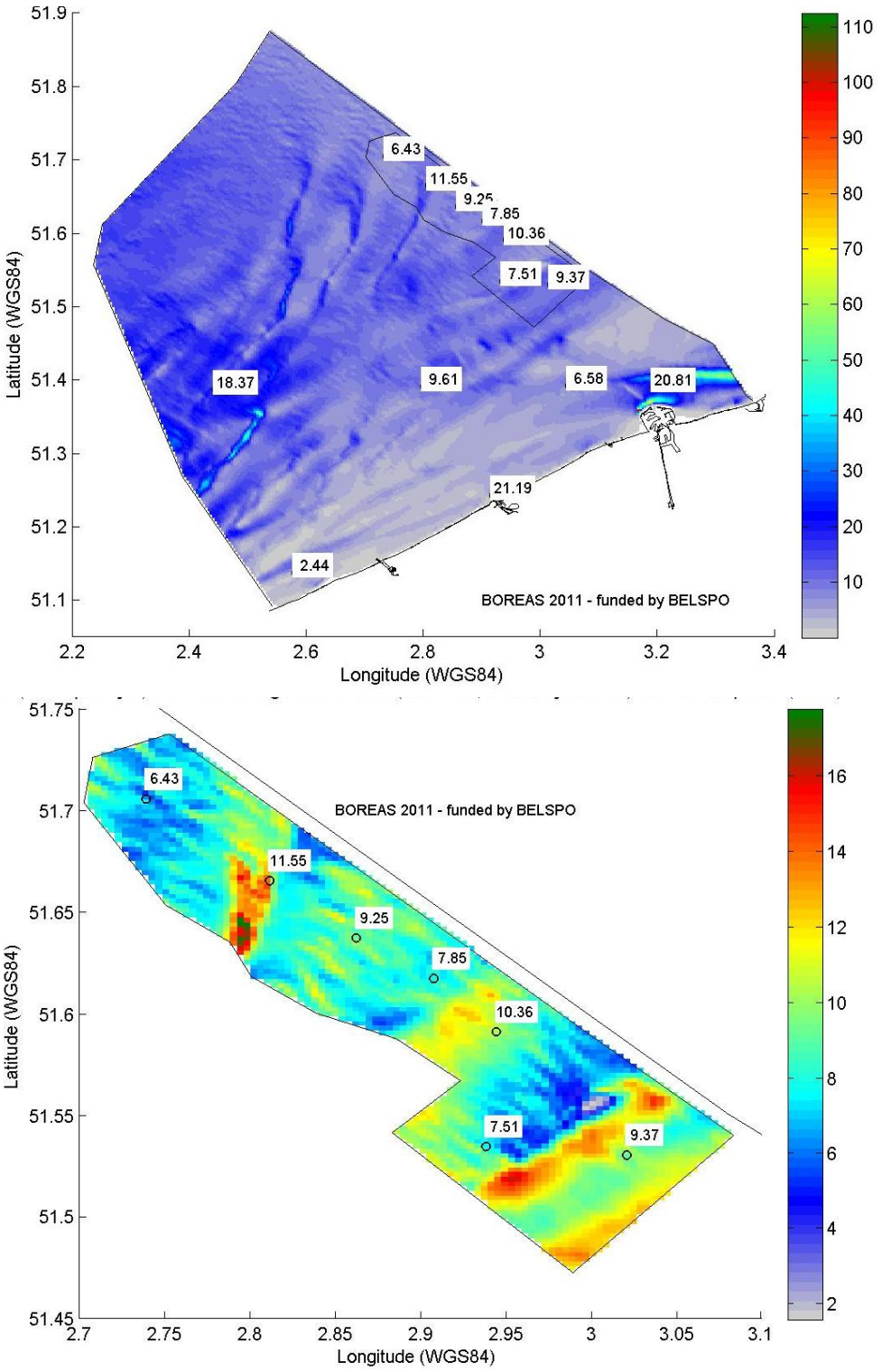

Figure 54: The extractable tidal current power (W/m²) in the upper half of the water column (depth layers 4 till 9), taking into account a cut-in speed of 0.5 m/s and the efficiency curve described in Figure 50 for the BPNS and the DC.

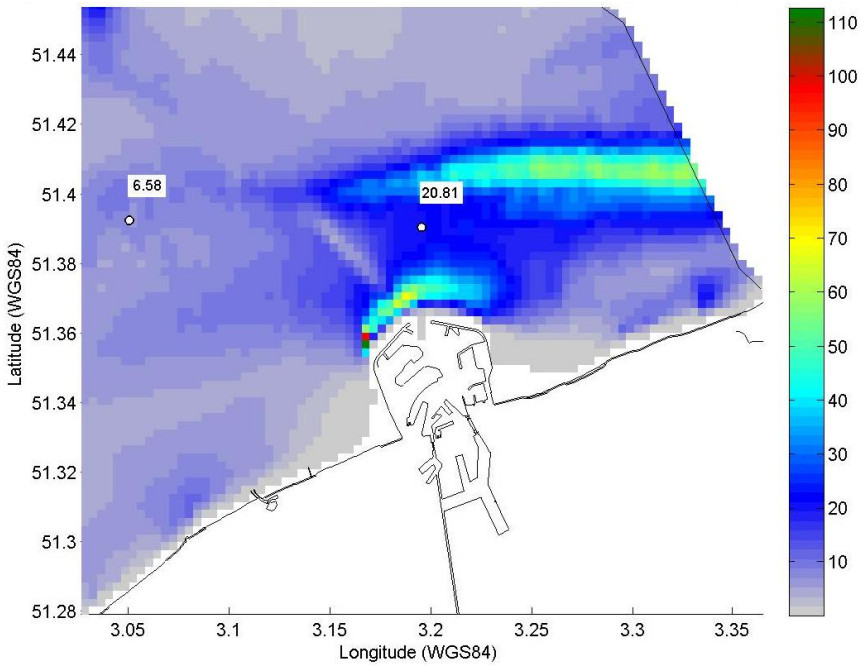

Figure 55: Detail of the extractable tidal current power around the breakwater of Zeebruges, maximum extractable tidal current power is 112 W/m².

By multiplying the tidal extractable current power (Figure 54) with the swept areas of the TECs, as calculated from the turbine diameters (Figure 53), the extractable tidal current power for a TEC taking the full water column is obtained (Figure 57). This figure should therefore be interpreted as the maximal average power produced for a single TEC with a maximal diameter for the turbines blades, and is therefore un upper limit of average production.

Figure 57 and Figure 58 show the average extracted tidal current power (W) for a turbine taking up the full usable depth of the watercolumn, respectively the yearly produced electricity (kWh).

However, taking the full usable watercolumn is not very realistic. Therefore,Figure 59 represent the same parameters for an (arbitray) swept area of 1m². In the Domain concession zone, the highest value can be found on the Bligh Bank with approximately 150 kWh/m² swept area (Figure 59). If a turbine of 10m diameter (and hence a swept are of 78.4m²) would be placed there, it would produce 11.8 MWh/year. The average produced power would be 17 W/m² (Figure 54) *78.4m² = 1333 W. But in order to capture this power, the TEC should be dimensioned to the peak loads, since these contain virtually all the energy. Therefore Figure 60 gives the ratio of the maximum extractable power and the average extractable power. For this region on the Blighbank, the ratio is approximately 10. Thus the installed capacity should be 1333*10 W =13.3 kW. Or in other words: in order to fully exploit the extractable tidal current resource at this site, the capacity factor would be roughly 1/10 or 10 %. Notice that due to the intermittent and peaked availability of the tidal resource, the dimensioning of the turbine was done on the peak load, in order to produce as much electricity as possible with one turbine. The more commonly used approach is however to find the economical optimum between power production and installed capacity.

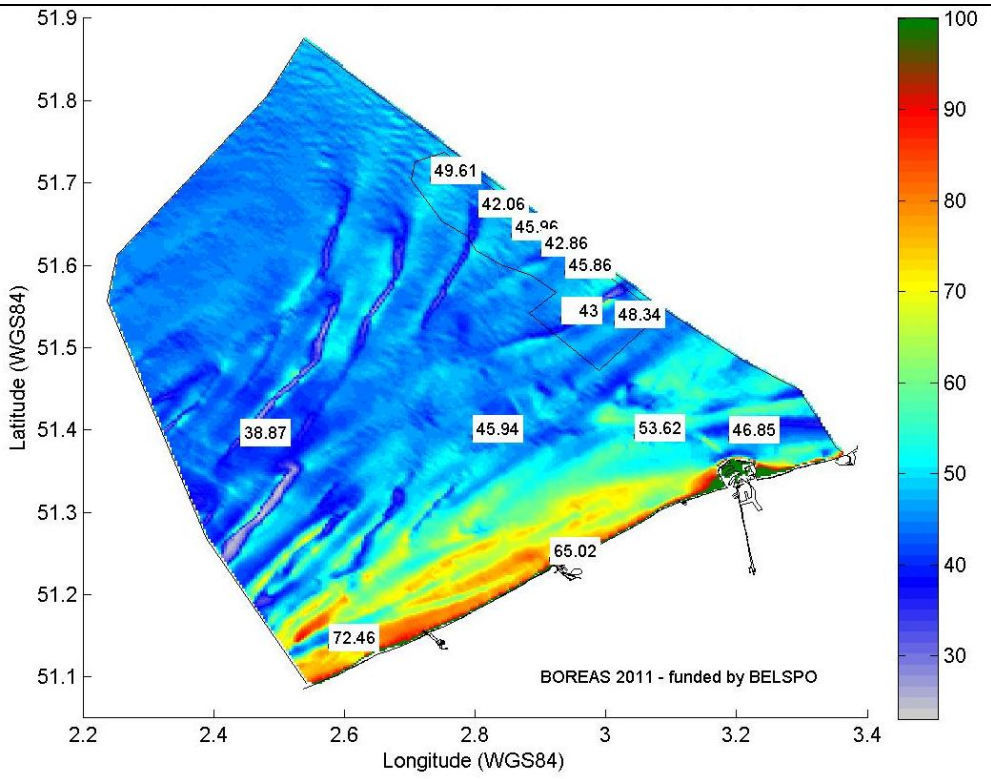

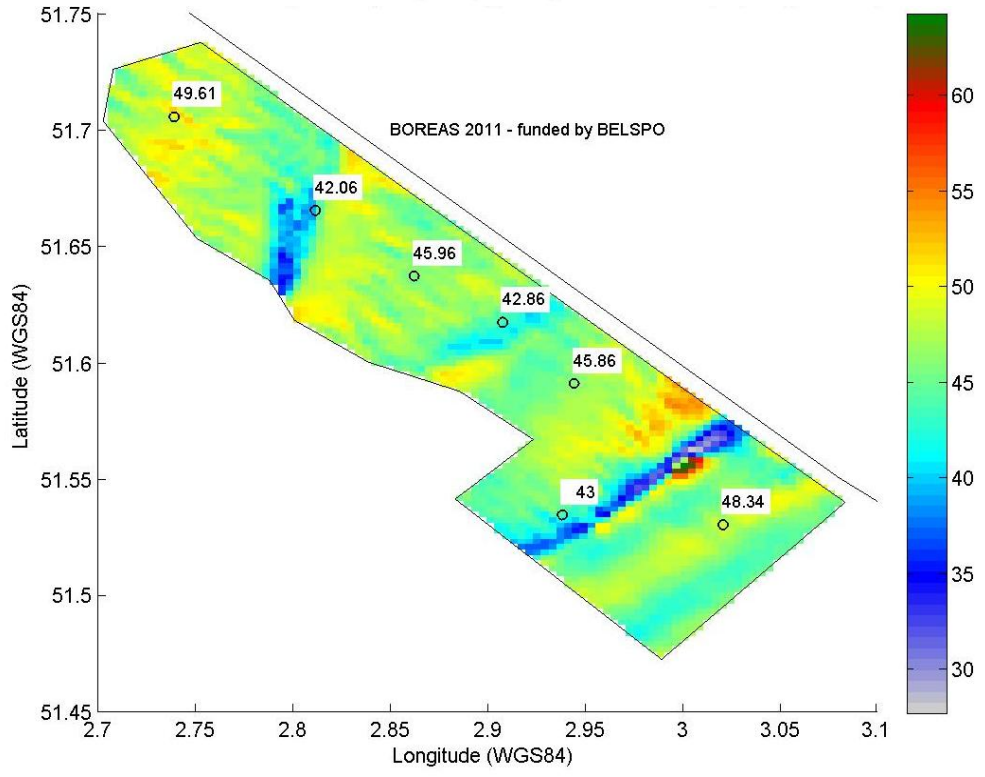

Figure 56: Percentage of the time where the velocity current in the upper half of the water column (depth layers 4-9) are below 0.5 m/s, and hence the generic TEC would not produce electricity.

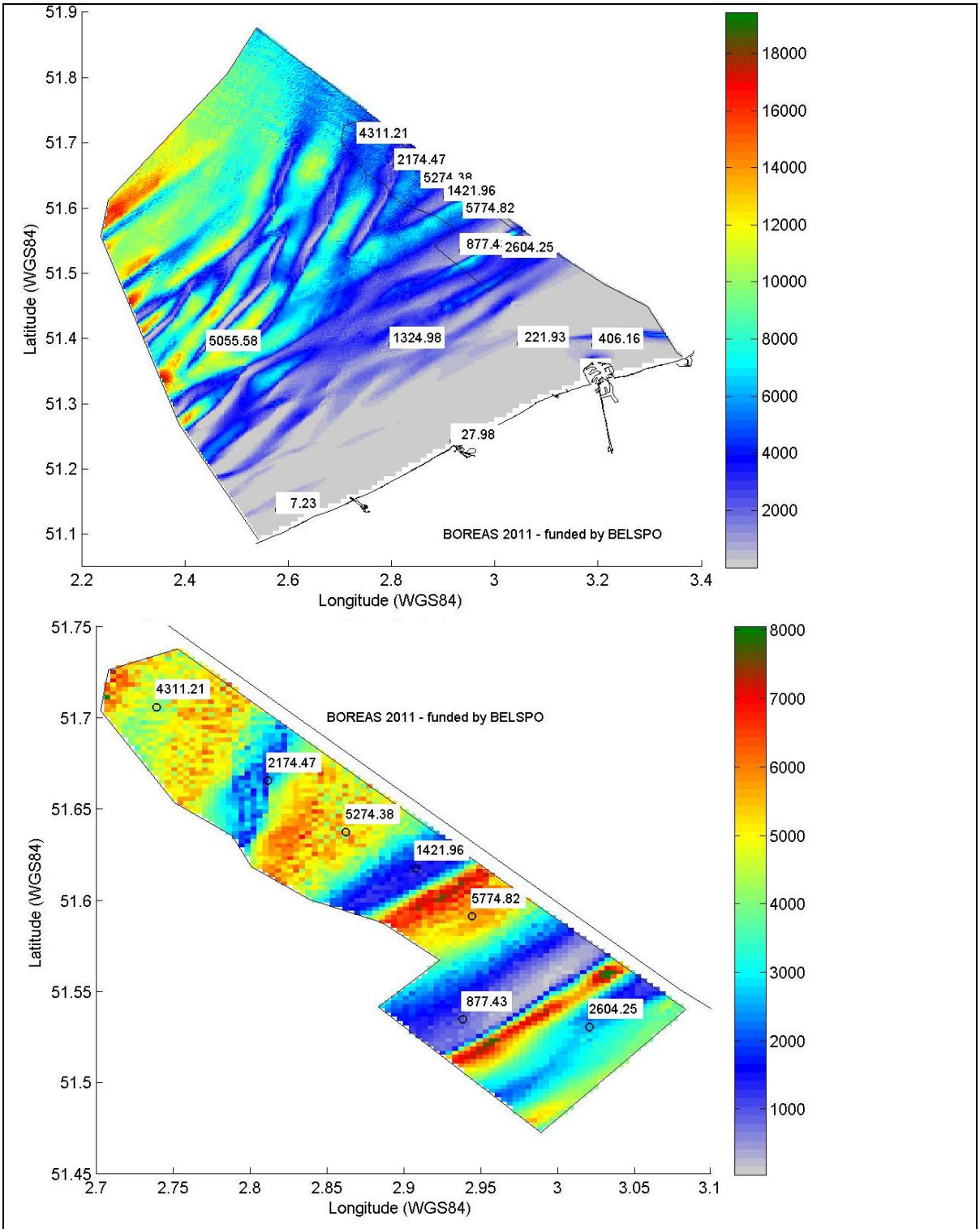

Figure 57: Average power production (W) for a TEC taking the full water column. This map is the product of the tidal current power from Figure 53 and the turbineareas given by Figure 54.

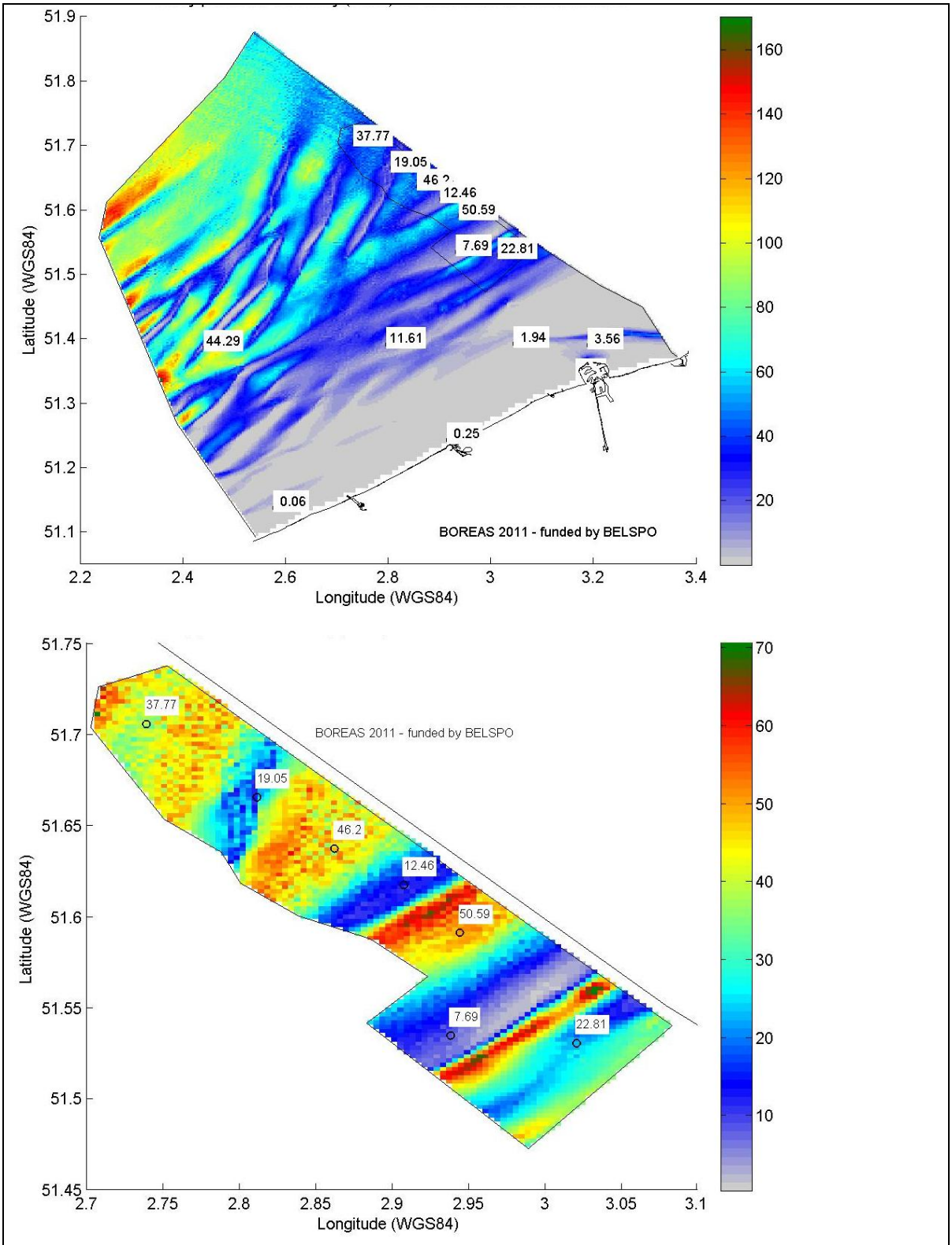

Figure 58: Yearly produced electricy (MWh) for a single TEC (varying turbinediameters depending on location), obtained by multiplying Figure 57 with 365*24 hours/1000000.

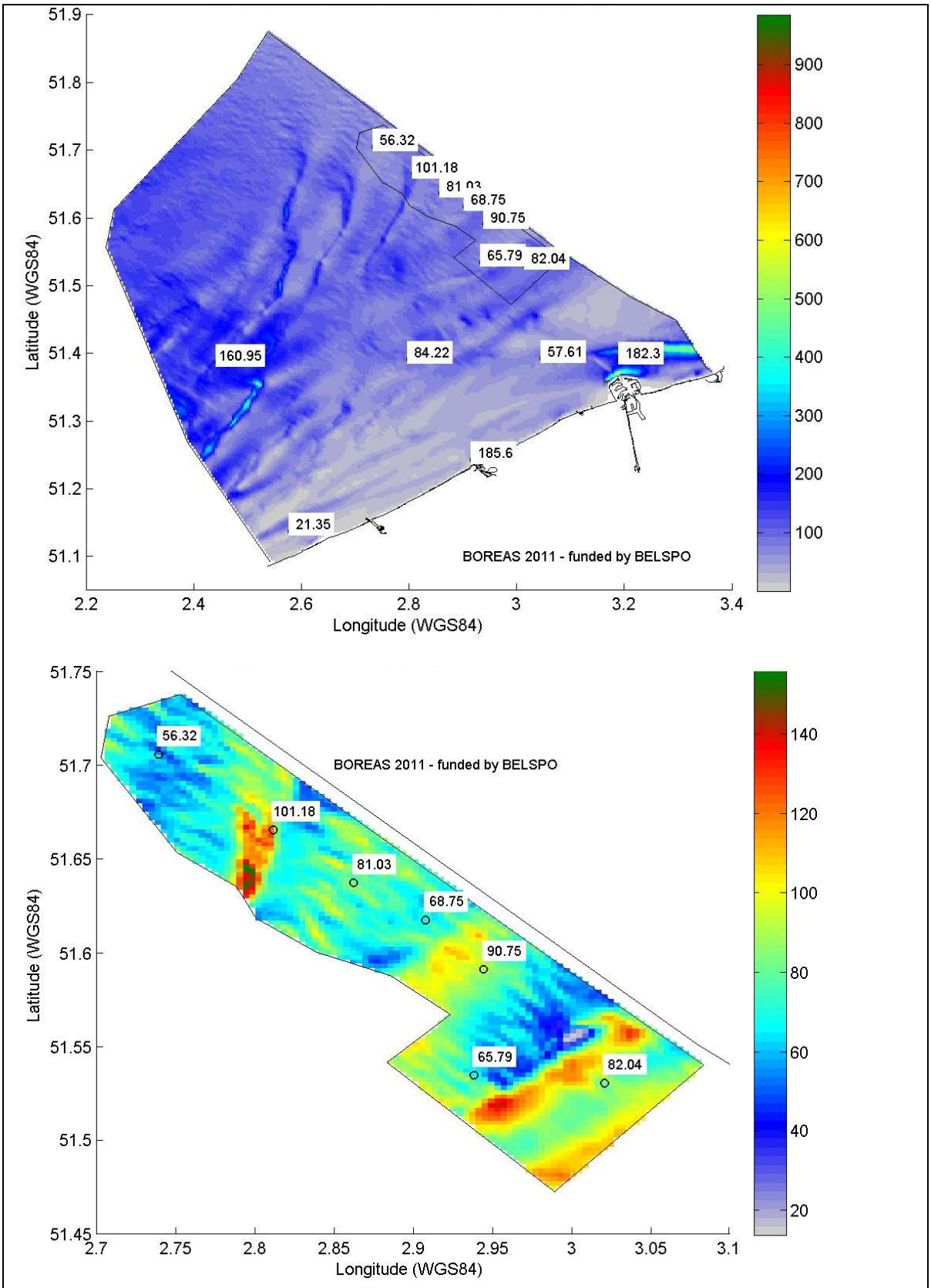

Figure 59: Yearly produced electricy (kWh) for a turbine with a swept area of 1m². Multiplying the values with the swept area gives the annually produced power.

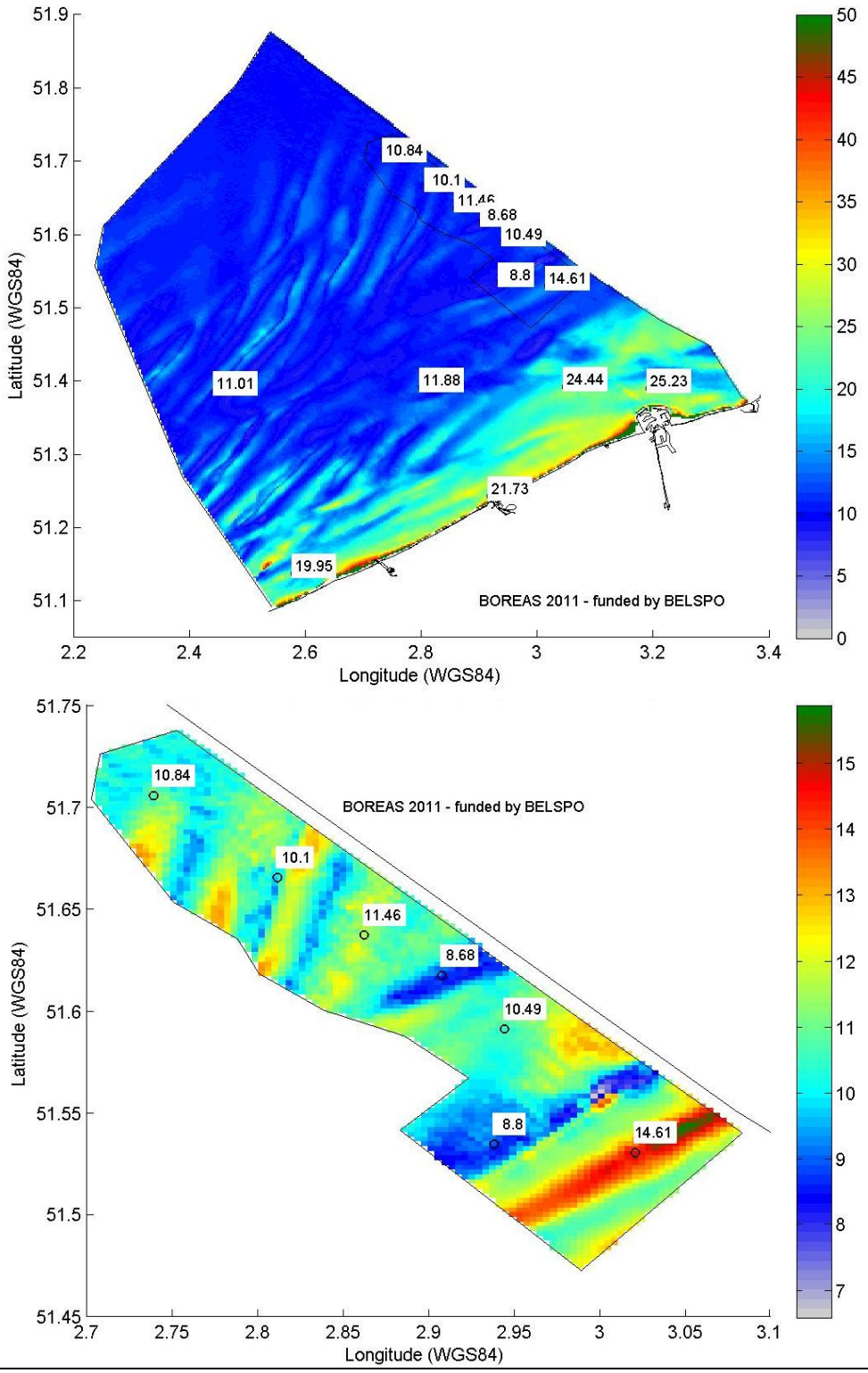

Figure 60: Ratio of the maximum/average extractable tidal current power in the upper half (depth layers 4-9) of the water column.

6 Economical analysis

In order to asses the feasibility of a wave or tidal current energy project on the BPNS, an economic analysis by means of the Net Present Value (NPV) is presented here. The methodology used in this chapter is analogue to the economical analysis for offshore wind that was performed in the OPTIEP study (Mathys *et al.* 2010). In the OPTIEP study the input parameters (both technical and economical) were taken from publically available literature. For tidal current and wave energy, economical relevant information concerning cost prices and revenues are much more scarce. If no update on the economical parameters was found, they were taken from the OPTIEP study, as will be discussed in § 6.1.1.

In this study, hypothetical WEC or TEC farms were placed on the domain concession zone. It was assumed that the implementation of the windmills did not impose restrictions on the placing of the WEC of TEC farm. The most obvious implementation would be to place the WEC or TEC in between windmill farms (staggered lay-out). Once more: in this first generic assessment, it is not possible to assess interactions between the foundations of windmills, the TECs or WECs, nor their interaction between the tidal current and or wave climate. This is a stringent assumption, but other studies had to base their economical analysis on the same assumption. The scope of this exercise is to provide order of magnitudes for the Net Present Value (NPV) of a hypothetical and *generic* WEC or TEC farm. In case of a *specific* project design, detailed information (finer bathymetry resolution, in-situ measurements and detailed geometry and design of the planned structures) and the efficiencies of the proposed devices are needed to look at the specific project feasibility.

6.1 Economic analysis WEC

6.1.1 Methodology

The input variables of the economical input parameters are taken over from the OPTIEP study and are listed in Table 19 (see Appendix for the definition of the economical parameters used). The Tradable Green Certificate or TGC is given by the Decree of 8 May 2009 regarding the general energy policy (90 €/MWh, guaranteed for 10 years). However, for this study 20 years was used, similar as the garantueed support period for offshore wind. The electricity price is taken over from the OPTIEP study and fixed during the project span at 55€/MWh (BELPEX 2009; Mathys *et al.* 2010).

Three WECs are considered for which publically available power matrices were available:

- The Pelamis (or 'sea snake'), which is an attenuator and one of the fore front runners in the WEC market, with a published power matrix that has been sited in many publications. The main costs were taken from another study (Dalton *et al.* 2009).
- Straumekraft: a Norwegian concept, based on the point absorber technology. This device was chosen due to the availability of their (projected) power matrix for a small point absorber buoy. No information was available on the costprice, but this was taken over from the SEEWEC study (SEEWEC *et al.* 2009), which uses a similar technology (but SEEWEC did not publish a power matrix for their B1 buoy).

- The Wavestar: a WEC consisting of a jack-up structure with floaters based on point absorber technology, with a well documented and excellent track record. Furthermore Wavestar published cost prices in term of the development of their WEC. These cost prices are amongst the highest that are publically available, and therefore Wavestar deserves credit as probably publishing the most realistic cost prices.

Table 19: Input variables for the economical analysis, cited from the OPTIEP study.

	Value		Value
TGC	90 €/MWh[18] , guaranteed for 20 years	CP (own capital)	25%
Electricity price	55 €/MWh	D (Debt share)	75%
Investment cost WEC or TEC	Variable €/kW	T (Corporate tax)	33,33%
Investment cost cable	k€ 433 /km[19] (10 kV), see Table 20	R (Interest rate)	6%
Depreciation (%)	60% (40%+20%)	k_{cp} (Return on equity)	13,5%
Maintenance cost	2% of investment cost	Inflation	2%
Park size	variabel MW	R (Disconto rate after inflation)	8,61%
Capacity factor	Variable, see § 5.2.5.2	Project duration	20 year

The evolution of the investment cost is variable and based on a previous study of the economical assessment of the Pelamis (Dalton *et al.* 2009). In the latter study a cost price of 1533 k€[20] for a single 750 kW Pelamis is given for the year 2004, for 2008 the costprice rose to 4599 k€ due to highly fluctuating steel prices. In 2011, the steel price (SBB word steel price tracker) is approximately in between the levels of 2004 and 2008 (SBB 2011), and therefore the average price is used for BOREAS. This corresponds with an initial price of 4088 €/kW installed at the 2011 level. Since steel is a major component of most WECS, especially for the large constructions like Pelamis, the steel price has a major influence on the WEC price. They used a sliding scale to estimate the costs with increasing number, based on the learning curve. A factor for the mass production was not introduced in the equation, since, according to the cited study, WEC production is not supposed to reach the scale of automotive mass production. The formula for the the learning curve is :

$$P_{scaling} = A^{(\ln(tf)/\ln(2))} \qquad \text{Eq. 14}$$

With $P_{scaling}$ the % scaling, A the number of WECs and *tf* the technology factor, chosen at 0.9 (Dalton *et al.* 2009). If the original unity price of the first unit would be 100%, 5 units would cost 78% of the unity price, 10 units would cost 70%, 50 units 55% and so on.

18 http://navigator.emis.vito.be/milnav-consult/consultatieLink?wettekstId=31931&date=06-05-2011&appLang=nl&wettekstLang=nl, Decree of 8 May 2009 concerning the general energy policy, Art. 7.1.6 (in Dutch), but the period was extended to 20 year instead of 10 year, similar to offshore wind.

19 For Pelamis and Wavestar, 4km was assumed to interconnect the 5-6 MW WEC farm. For Straumekraft 12km cable was assumed, due to the higher number of devices. Note that the cable cost price and grid lay-out together determine the total cable cost price. For the 50 and 200 MW WEC farm, a reduction of 33% in this cost price was assumed (based on €/kW).

20 This costprice was calculated originally from k$ 1565 for the WEC + k$ 850 for the steel sections, and converted to Euros with conversion rate of 1.57 in July 2008.

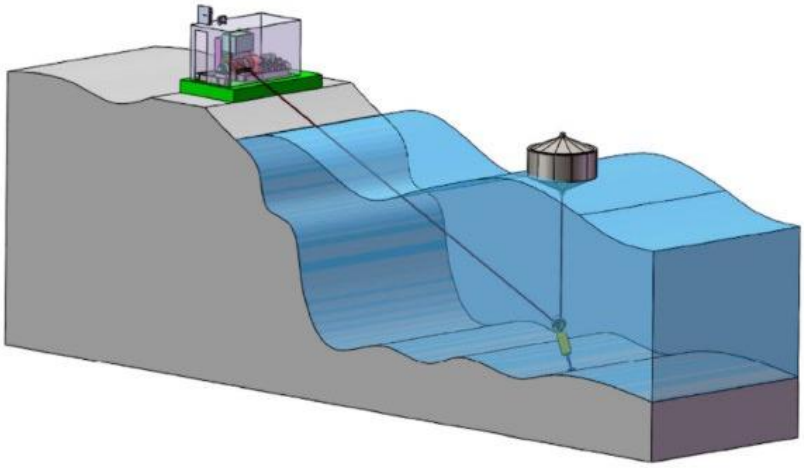

Figure 61: Overview of the Pelamis (top), the Straumekraft concept (middle) and the Wavestar (bottom).

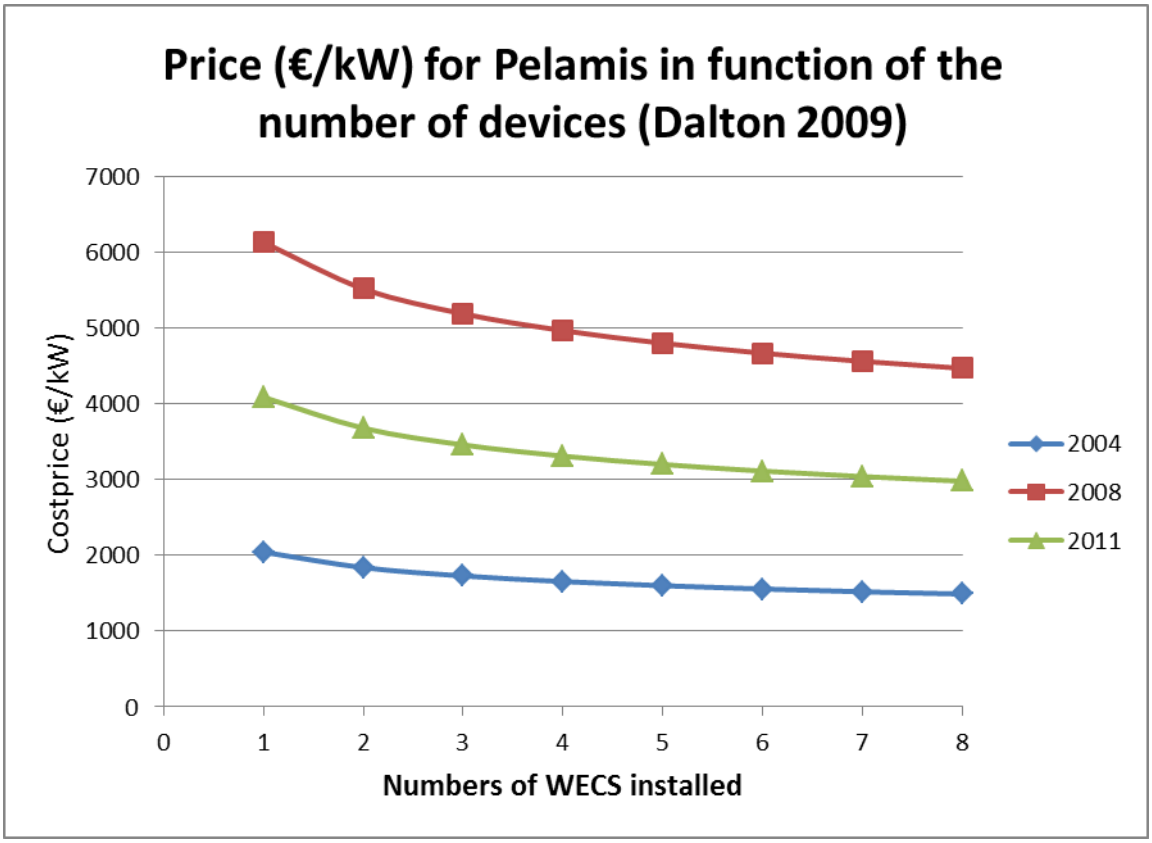

Figure 62: Unity price (expressed in €/kW) of a Pelamis in function of the number of devices (Dalton *et al.* 2009).

The cable cost is given by Table 20. Based on the capacity factors and choosing a park size of approximately 5 MW, 4 km of 10 kV cables should be sufficient to interconnect the WEC farm internally. This 4 km was pragmatically chosen to interconnect the WEC farm internally..The transport to land is assumed to take place by the existing offshore wind electricity cables. It is assumed that the cable is connected to the transformator of the offshore windmill foundations or transformation hub and that the (long distance) transport of electricity onshore are covered by this cable, and therefore, no additional cost is implemented.

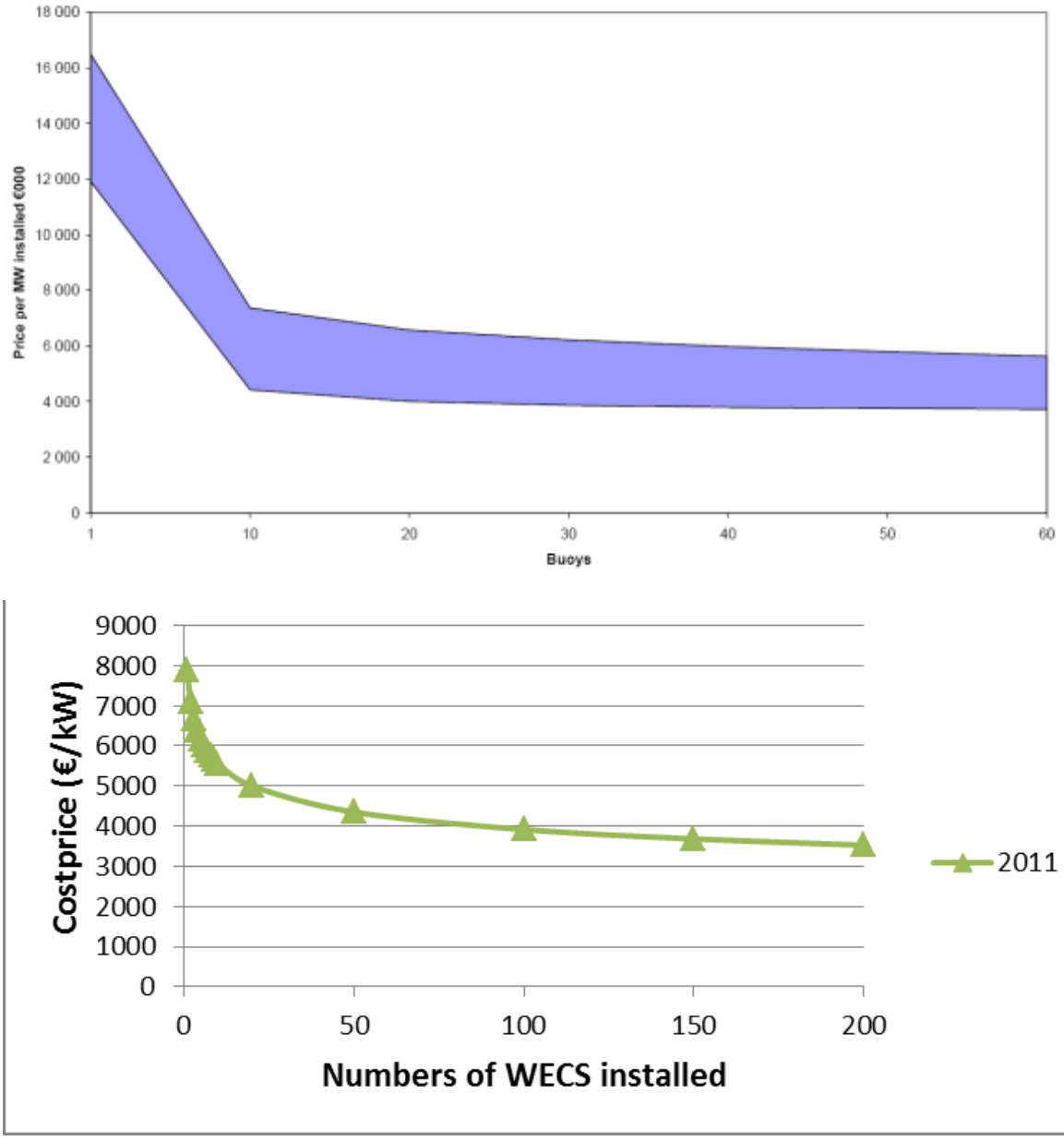

Figure 63: Unity price (expressed as €/kW) in function of the number of Straumekraft WECS. Since the Straumekraft point absorber uses as similar conversion technology as the SEEWEC device, the initial costprice was taken over from this study (5000 €/kW for 20 WECs produced in 2008). The same price was taken for 2011 and is presented in the top figure (SEEWEC *et al.* 2009). The unity price of 25 kW Straumekraft WECS in function of the number of devices is shown on the bottom figure.

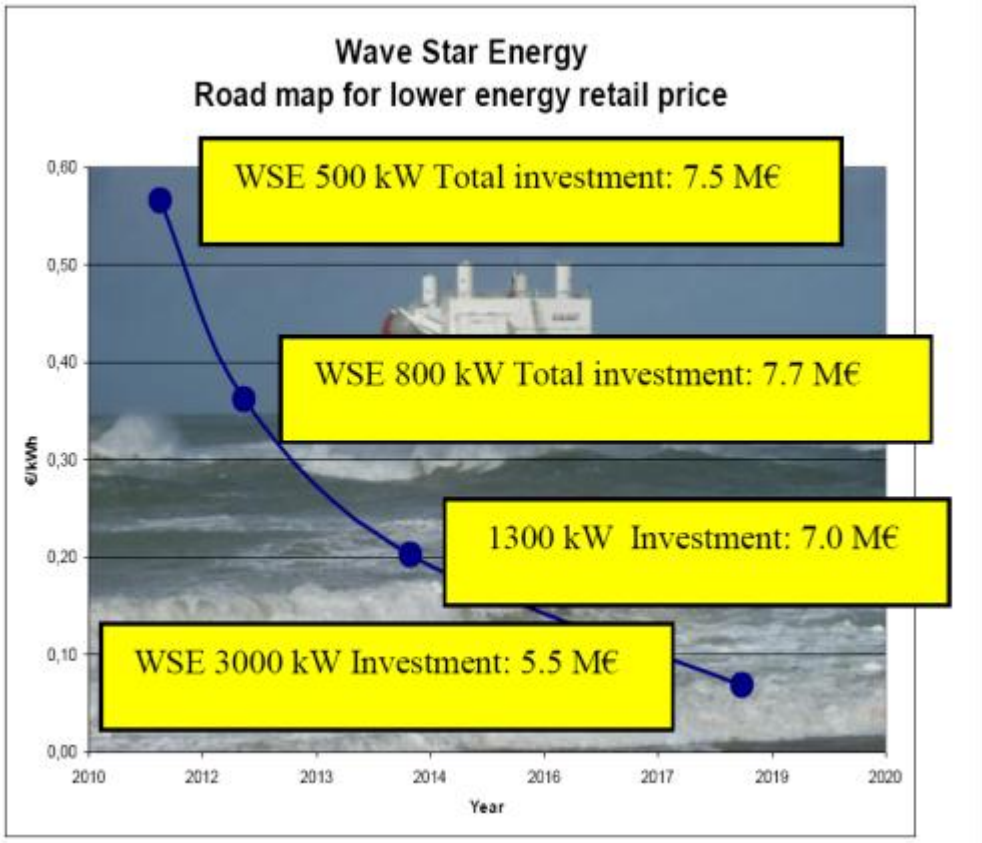

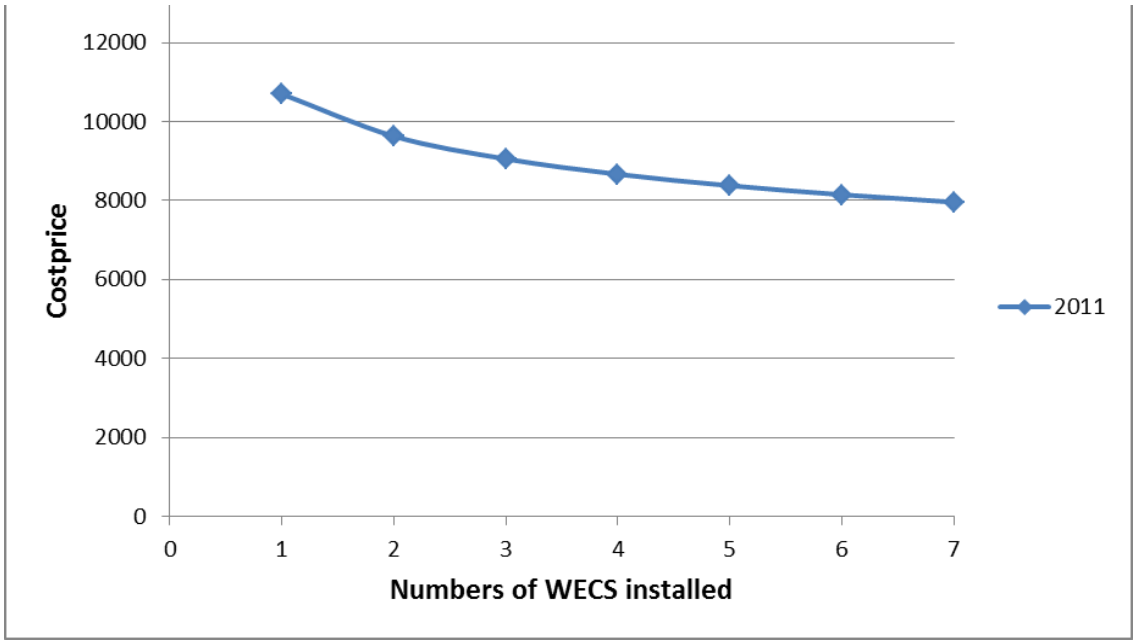

Figure 64: Projected cost price for a jackup platform with 20 floaters of the Wavestar (Frigaard *et al.* 2010) (top), and costprices used in this study (bottom). The platform would be rated at 20*37kW= 740 kW, and this lies between the first and second benchmarks on the Wave Star Energy Roadmap (top figure). The corresponding unity price for the 500 kW design is 15000€/kW, for the 800 kW it is 9625 €/kW. The corresponding 20*37kW (=740kW) can thus be interpolated and determined as 10700 €/kW for the first unit.

Table 20: WEC power output, corresponding cable kV and relevant cost in €/km (Dalton *et al.* 2009)

Range MW	kV	Cost per km	Number of kms	Cost
0.5–1.9 MW	10	€433,333	4	€1,733,333
2–5 MW	10	€433,333	4	€1,733,333
5–19 MW	30	€1,300,000	4	€5,200,000
Over 20 MW	110	€3,900,000	4	€15,600,000

In the same study (Dalton *et al.* 2009), the operation and maintenance cost was implemented as a percentage of the capital cost of 1,2 or 3%. In BOREAS, 2% was used. The used capacity factors were the capacity factors calculated from § 5.2.5.2 (6.1% of the Pelamis, 17.9 % for the Straumekraft, and 22.4% for the Wavestar). Size of the park is in the order of 5 MW, which is the order of magnitude of the first really commercial planned projects.

6.1.2 Results

The input parameters based on the WEC specific properties and the results (presented here as NPV or as the necessary TGC price for the project to achieve a zero NPV) are given in Table 21. The necessary TGC price to achieve a zero NPV can be interpreted as the break even point for feasibility *with the technology knowledge of today and the assumptions used in this report*.

It must be stressed that there is a big uncertainty on the initial cost prices of the WECs presented, as they are very hard to assess or verify (claims based on publically available data). However the expected produced power levels (used here in the form of capacity factors) are based on the 10 year hindcast and are the best possible capacity factors that could be used, if the power matrices of the devices are reliable (see § 5.2.5.2 and 5.3.2).

When looking at the results (Table 21), it is clear that Pelamis is well overdimensioned for application on the BPNS, which is no surprise. Even though the investment cost is only 39 % of the Wavestar, the necessary TGC to achieve a zero NPV (856 €/MWh) would be almost double the price of the initial Flemish TGCs for solar energy (450 €/MWh). The main reason is the low capacity factor of 6.1%, which is again caused by the fact that the Pelamis is dimensioned for higher wave climates.

Table 21: Results of the economic analysis of a Pelamis, Straumekraft and Wavestar arbitrary WEC farm in the order of 5-7MW with the expected power production in the domain concession zone. It is assumed that the cable cost is only in the order to connect the WEC park to the transformator hub of the offshore windmill parks, from whereon the transport to land is foreseen.

Value	Pelamis	Straumekraft	Wavestar
Size	8*750 kW= 6MW	200*25kW = 5 MW	7*(20*37kW)[21] = 5.18 MW
Capacity factor[22] at the domain concession zone (see § 5.2.5.2)	6.1 %	17.9 %	22.4 %
Initial Cost for the first WEC (€/kW)	4088[23] €/kW (Figure 62)	7883 €/kW[24] (Figure 63)	10700 €/kW (Figure 64)
Technology factor *tf,* $P_{scaling}$ *(%)* (according to Eq. 14) and resulting initial capital cost for the WEC park (€/kW)	0.9 (-) 72.9% 2980 €/kW	0.9 (-) 44.7% 3523 €/kW	0.9 (-) 74.4% 7960 €/kW
Cable cost	1733 k€	5200 k€[25]	1733 k€
Maintenance cost	2% of capital cost of WEC and mooring	2% of capital cost of WEC and mooring	2% of capital cost of WEC and mooring
Final investments cost, including O&M (based on the investment cost) and cable cost	3335€/kW	4654 €/kW	8460 €/kW
Net Present Value with a TGC of 90 €/MWh	- 15 639 k€	-14 150 k€	-29 752 k€
Necessary TGC for the NPV to become 0	856 €/MWh	379 €/MWh	575 € /MWh.

Wavestar has a high investment cost, but may be more realistic than the, perhaps, over optimistic initial investment costs of e.g. the Pelamis. This is noticeable when comparing the initial

[21] A single floater of a Wavestar is 'clustered' in a jack-up platform with 20 floaters, thereby reducing the cable cost for connecting to the grid.

[22] These capacity factors were based on the 10 year hindcast, assuming full time operationability.

[23] This price was cited from the study of Dalton 2009 but seems very low compared to other technologies.

[24] This was recalculated based, on a projected price of 5000€/kW for 20 SEEWEC devices and a *tf* of 0.9 (SEEWEC 2009).

[25] Connecting 200 small buoys with cables with less capacity would increase the cost for the overall grid connection (a factor 3 was used here in comparison with Pelamis and Wavestar).

cost prices for the maturing offshore wind energy. The range found in literature for offshore wind was 2300-3000 €/kW (Mathys *et al.* 2010), but an extra scenario with 3500 €/kW was assessed to better reflect the Belgian conditions. The necessary TGC level of support for Wavestar would be 575 €/MWh. This is due to the high investment cost (but fortunately Wavestar has a high capacity factor).

The small scale Straumekraft point absorbers achieve a zero NPV with a TGC of 379 €/MWh, which is high compared to offshore wind, but lower with the Flemish solar TGCs that were implemented until 2010. This assumes a constant technology factor of 0.9 up to 200 devices.

From the comparison between the 3 WECs, two important implementation criteria for WEC deployment on th BPNS can be derived:

- Big (support) structures are to be avoided (this is the case for Wavestar and Pelamis), since they increase the investment cost, more and smaller WECs seem to be favorable;
- The WEC needs to be able to capture the low energetic waves for the BPNS, and hence WECs should be specifically designed for these conditions, which would result in high capacity factors (Straumekraft and Wavestar have acceptable capacity factors for the early technology WECs).

In the case of the implementation of bigger wave energy farms (order from 50 to 200 MW), scale advantages are expected. A similar calculation was thus performed for a 50 MW wave energy farm (tf 0.91) and a 200 MW (tf 0.92). The results are shown in Table 22 and Table 23. The necessary TGCs to achieve a zero NPV drop to 278 and 420 €/MWh for Straumekraft and Wavestar respectively in the 50 MW scenario. In the 200MW scenario, the costs drop further to 265 and 376 €/MWh for Straumekraft and Wavestar respectively.

Designing and scaling a device to meet the conditions found on the BPNS should lead to an increase increase in the capacity factor of the device. Table 24 shows the economic parameters in case the capacity factor increases, which can be interpreted as a WEC that is more suited to the conditions on the BPNS, or alternatively: a sensitivity analysis of the capacity factor. So, if the costs would remain the same (200 MW park), but the capacity factor would increase to 25% or 30% the necessary TGC support for a zero NPV would drop to be respectively 331 and 267 €/MWh for WaveStar, and to 174 and 136 €/MWh for the Straumekraft.

Table 22: Results of the economic analysis of a Pelamis, Straumekraft and Wavestar arbitrary WEC farm in the order of 50MW with the expected power production in the domain concession zone. It is assumed that the *tf* factor changed to 91% instead of 90%. The capacity factors, initial costs remained the same as in Table 22.

Value	Pelamis	Straumekraft	Wavestar
Size	67*750 kW = 50.25 MW	2000*25kW = 50 MW	67*(20*37kW) = 49.6 MW
Technology factor *tf*, $P_{scaling}$ *(%)* (according to Eq. 14) and resulting initial capital cost for the WEC park (€/kW)	0.91 (-) 56.4% 2307 €/kW	0.91 (-) 35.6 2802 €/kW	0.91 (-) 56.4% 6038 €/kW
Cable cost[26]	10 780 k€	38 992 k€	11 113 k€
Maintenance cost	2% of capital cost of WEC and mooring	2% of capital cost of WEC and mooring	2% of capital cost of WEC and mooring
Final investments cost, including O&M (based on the investment cost) and cable cost	2550€/kW	3569 €/kW	6415 €/kW
Net Present Value with a TGC of 90 €/MWh	- 92 752 k€	-91 910 k€	-201 095 k€
Necessary TGC for the NPV to become 0	642 €/MWh	278 €/MWh	420 € /MWh.

[26] Cable Cost was assumed tob e 2/3 of the cost prices of the corresponding 5-6 MW wave farms due to enhanced cable lay-out.

Table 23: Results of the economic analysis of a Pelamis, Straumekraft and Wavestar arbitrary WEC farm in the order of 200 MW with the expected power production in the domain concession zone. It is assumed that the *tf* factor changed to 90% instead of 92%.

Value	Pelamis	Straumekraft	Wavestar
Size	267*750 kW = 200.25 MW	8000*25kW = 200MW	270*(20*37kW)[27] = MW=199.8 MW
Technology factor *tf*, $P_{scaling}$ *(%)* (according to Eq. 14) and resulting initial capital cost for the WEC park (€/kW)	0.92 (-) 55.7% 2277 €/kW	0.92 (-) 33.9% 2674 €/kW	0.92 (-) 50.9% 5456 €/kW
Cable cost	38 543 k€	138 646 k€	44 730 k€
Maintenance cost	2% of capital cost of WEC and mooring	2% of capital cost of WEC and mooring	2% of capital cost of WEC and mooring
Final investments cost, including O&M (based on the investment cost) and cable cost	2519€/kW	3434 €/kW	5793 €/kW
Net Present Value with a TGC of 90 €/MWh	- 363 921 k€	-343 049 k€	-703 907 k€
Necessary TGC for the NPV to become 0	633 €/MWh	265 €/MWh	376 € /MWh.

Table 24: Sensitivity analysis of the influence of the capacity factor on the NPV and TGC for the same assumptions as for the 200 MW WEC farm.

Capacity Factor (%)	Net Present Value (k€) with a TGC of 90 €/MWh		Necessary TGC for the NPV to become 0 (€/MWh)	
	Straumekraft	Wavestar	Straumekraft	Wavestar
25	-230 071	-666 877	174	331
30	-150 509	-583 101	136	267

[27] A single floater of a Wavestar is 'clustered' in a jack-up platform with 20 floaters, thereby reducing the cable cost for connecting to the grid.

6.2 Economic analysis TEC

6.2.1 Methodology

Initial investment costs of TECs are difficult to find, but in most studies the intial investement cost of a TEC is approximately 40-70 % of WEC costs (Carbon Trust 2006; Allan *et al.* 2011). This is represented in Figure 65. The first production models of initial TECs are expected to be around £ 1400-3000 £/kW installed, whereas for WECs these cost would vary around £1700 to 4300/kW installed. The ratio of the middle of these bandwidths would be 2200/3000 = 73% (Carbon Trust 2006). Another study mentions £ 1641/kW installed for TECs, and £ 3622/kW for WECs (2006 levels), giving a ratio of 45% (Allan *et al.* 2011). The latter study also breaks up the cost in different components (Table 25). For a WEC, the PTO or Power Take Off (PTO) takes 51% of the total capital cost, whereas for TEC the foundation and subsea cable installation takes up 48% of the cost. From this break-up, it can be derived that for a TEC, not the device itself, but the installation and grid connection is the big cost component.

From both studies, an initial cost price for a TEC of 57%[28] of a WEC seems logical. Thus averaging the costprice of the Pelamis, Straumekraft and Wavestar, and applying this 57% ratio, an initial cost for the first TEC of 4307 €/kW installed is used in the generic TEC cost assessment. In § 5.3.2.2, it was calculated that a turbine of 10 m diameter to be deployed on the Bligh Bank (highest tidal current power in the domain concession zone), would need a rated capacity of 13.3 kW. Installing a 5-7 MW TEC farm seems exaggerated, due to the small zone where these highest tidal currents occur. Therefore it is suggested to install 40 turbines of 13.3 kw each, giving an installed capacity of 0.532 MW. It is reminded that due to the high cut in speeds and low efficiencies, the capacity factor was 10 % (see § 5.3.2.2). Similar to the WEC cost assessment, a decreasing unity price was used based on the technology factor (Figure 66).

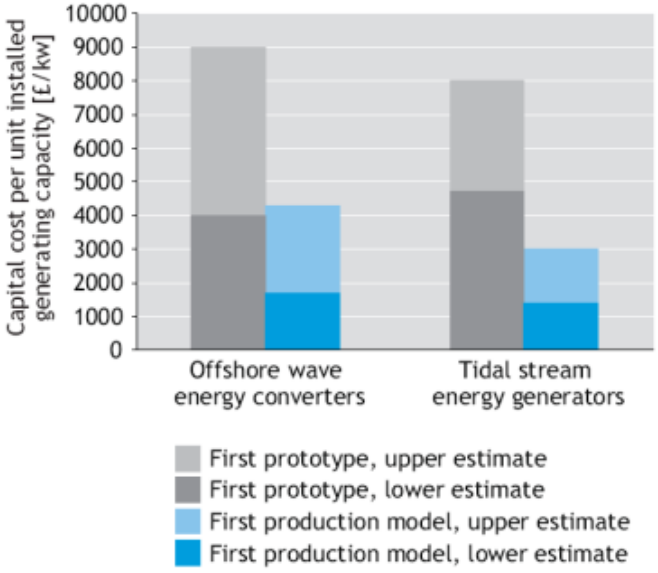

Figure 65: Capital costs of first prototypes and first production models (Carbon Trust 2006)

[28] Determined as the average of the bandwith of 40-70 and 45-73%.

Table 25: Components costs for a generic 1 MW WEC or TEC, in 2006 prices, and the % of the total costs (Allan *et al.* 2011)

(a) Component costs used for 1 MW wave generation, in 2006 prices, £000s and % of total costs.

	Total (£000s)	%
Onshore transmission and grid upgrade	36.22	1
Undersea cables	181.12	5
Spread mooring	362.24	10
Power conversion module	1847.44	51
Concrete structures	724.88	20
Construction facilities	144.88	4
Installation	144.88	4
Construction management	181.12	5
Total	3622.44	100

(b) Component costs used for 1 MW tidal generation, in 2006 prices, £000s and % of total costs.

	Total (£000s)	%
Power conversion systems	284.31	17
Mono-pile structural elements	174.30	11
Subsea cable cost	21.13	1
Assembly and transport	17.50	1
Mono-pile/turbine installation	458.20	28
Subsea cable installation	326.37	20
Onshore items and grid interconnection	24.46	1
Overheads and omitted items	334.28	20
Total	1640.54	100

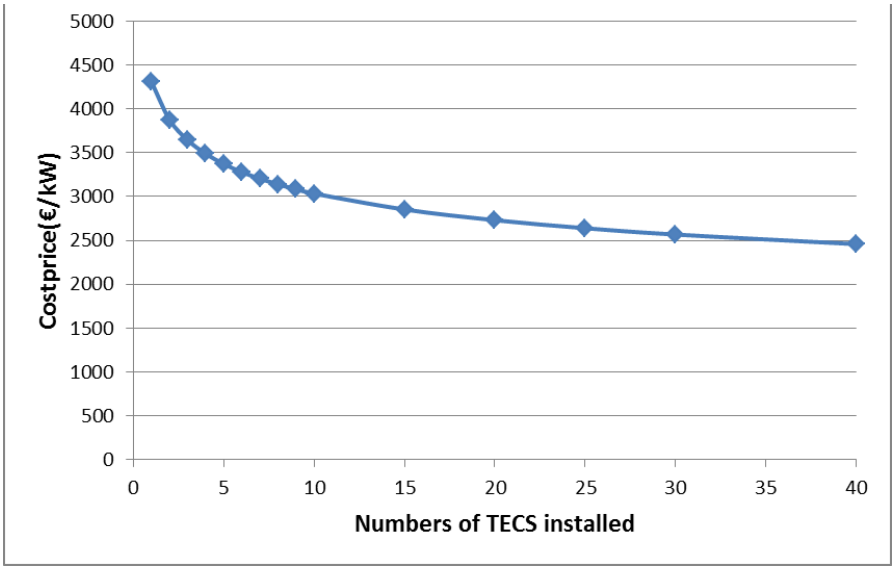

Figure 66: Unity price of a 36 kW generic TEC (expressed as €/kW installed)

6.2.2 Results

The result for a generic 40*13.3 kW TEC park to be deployed at the best location on the domain concession zone (Bligh Bank) is shown in Table 26. The swept area of this 10 m diameter turbine would be 78.5 m² and the combination of the swept area with the rated power of 13.3 kW was discussed in § 5.3.2.2. The ratio rated power/swept area is thus 0.17 kW/m². It should be noted however that the commercial SeaGen (Marine Current Turbines) has a twin rotor design with a total swept area of 2*200m² has a rated power of 1.2 MW, or equivalently 3kW/m². This reflects the high energetic zone where this SeaGen is located, namely at the inlet-outlet of Strangford Lough, with local currents up to 3m/s. This means that the blades of the generic TEC turbine for deployment on the BPNS would need larger swept areas (factor 17-18) for the same installed capacity than with the commercial available technologies (which makes smaller, but stronger blades as they are exposed to higher tidal currents).

When this TEC would be deployed under these conditions, the NPV would be -11 727 k€, and the TGC to achieve a zero NPV is 446 MWh, which is in the same order of magnitude for the initial Flemish TGC for solar energy and is in the same order of Straumekraft. Notice however that due to the high technology factor (0.9) and taking 40 units, a price reduction per unit of 43% (100-57%, see Table 26) can be expected.

Table 26: Results of the cost assessment of a generic 36 kW TEC to be deployed on the Bligh Bank.

Value	Generic 13.3 kW TEC (10 m diameter), see § 5.3.2.2
Size	40*13.3 kW =0.532 MW
Capacity factor at the DC Zone (see § 5.3.2.2)	10 %
Initial Cost for the first WEC (€/kW)	4307 (Figure 62)
Technology factor *tf, $P_{scaling}$ (%)* (according to Eq. 14) and resulting initial capital cost for the WEC park (€/kW)	0.9 (-) 57.7% 2458 €/kW
Cable cost	419 €/kW (20% of Investment cost, see Table 25)
Maintenance cost	2% of capital cost of TEC and mooring
Final investments cost, including 2% O&M (based on the investment cost)	3009 €/kW
Net Present Value with a TGC of 90 €/MWh	-11 727 k€
Necessary TGC for the NPV to become 0	446 €/MWh

6.3 Comparison with TGC support of other technologies

It is usefull to compare the necessary TGCs to obtain a zero NPV with the current legislation and the support level of offshore wind. For offshore wind, the first 206 MW within a single concession zone installed gets a TGC of 107 €/MWh (Table 27). Above the 206 MW, the TGC drops to 90 €/MWh. The guaranteed period is 20 years. In the current federal legislation, there is a TGC for ('waterpower') of 50 €/MWh guaranteed for 10 year, without specifying 'waterpower'. According to the knowledge of the authors, no claim has been made for wave or tidal energy on the BPNS, so it is unclear if 'waterpower' also covers wave or tidal current energy.

The Flemish Electricity Decree foresees a TGC of 90 €/MWh for tidal current or wave energy, garuanteed for 10 years. However the BPNS belongs to the federal jurisdiction, so it is unclear if these TGCs are applicable.

Table 27: Level and garanteed period of TGC support (Federal level)[29].

Energy source	TCG support level (€/MWh)	Guaranteed term (year)
Offshore-wind, first 216 MW	107	20
Offshore-wind, above 216 MW within the same concession zone	90	20
Onshore-wind	50	10
Solar	150	10
Waterpower	50	10
Others, (eg. Biomass)	20	10

Table 28: Level and garanteed period of TGC support (Flemish level)[30].

Energy source	TCG support level (€/MWh)	Guaranteed term (year)
Solar – fading out mechanism to 2016	350 ➔ 90	20/15 (?)
Hydropower, **wave, tidal**, earth heat, on shore wind, solid or liquid biomass, biomass waste, biogas	90	10
Biogas from wastewater sludge, incineration of waste	60	10
Biogas from manure, vegetables, fruits or garden waste	100	20
Others	60	10

[29] Federal law of *5 October 2005 (BS 14.10.2005) — Koninklijk besluit tot wijziging van het koninklijk besluit van 16 juli 2002 betreffende de instelling van mechanismen voor de bevordering van elektriciteit opgewekt uit hernieuwbare energiebronnen. In Dutch.*

[30] Flemish decree of 8 May 2009: Elektriciteitsdecreet (*Decreet van 17 juli 2000 houdende de organisatie van de elektriciteitsmarkt*), consolidated version Octobre 2011. *In Dutch.*

7 Synergies

The combination of different offshore renewable energies (wind, wave and tidal) can have multiple advantages.

- It can reduce cabling costs, due to the common grid connection;
- It can provide a more constant and smooth output, which is important of balancing the electricity grid
- It can make optimal use of the existing space.

Therefore the most promising locations to combine combinations of offshore wind, wave and tidal are presented. Therefore, one should combine the resource maps of wind, wave and tidal and detect possible zones with common high ressources. The available wind resource, shown as wind velocities, is cited from the OPTIEP study and shown in Figure 67.

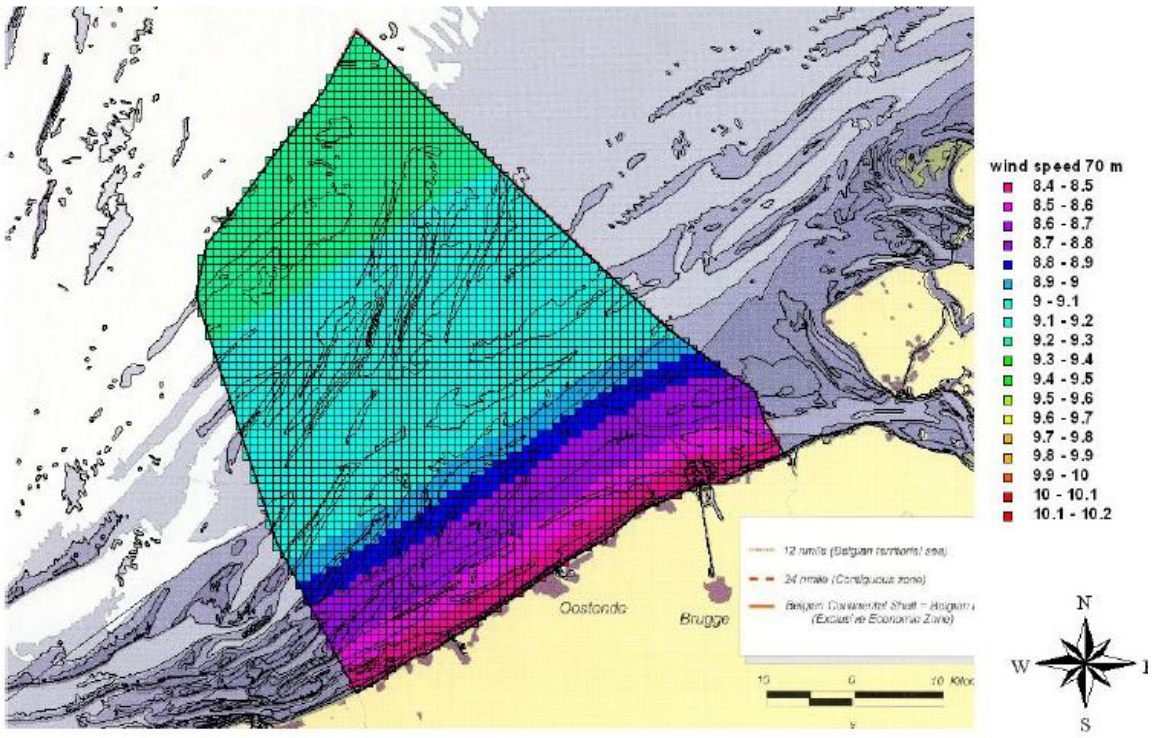

Figure 67: Average windspeeds at 70 m above sealevel (Mathys *et al.* 2010).

The *extractable* wave and tidal current resource are given in Figure 45 for the *extractable* power of the Straumekraft WEC (see Figure 46 for Wavestar) and Figure 57 for the *extractable* power of a generic TEC that exploits the full water depth. The situation of the sandbanks was shown in Figure 47.

For offshore wind (Figure 67) , the trend is very clear: the more offshore, the better, although the gain in wind speed beyond 15km of the coast line is small. But for reasons of visual hindrance, offshore wind is not accepted nearshore on the BPNS.

For wave, a similar trend is noticeable. But the *available* wave power resource shows that around the Westhinder-Oosthinder banks the influence of the British coastline becomes visible and wave power does not further increase with distance from shore.

This is however less noticeable for the *extractable* wave power resource, as Straumekraft and Wavestar can capture this smaller wave energy resource a bit more efficient, and in that way makes up the difference in wave power resource. The offshore sandbanks Oostdyck, Westhinder, Oosthinder and to a lesser extent the Fairybank and Noordhinder show a smaller extractable wave power resource then the immediate surroundings. Although smaller depths would make the installation and mooring easier, the wave climate is a bit lower. The highest wave powers are found in the north of the BPNS and the northern zone of the domain concession zone (up 6.4 kW/m).

For tidal current energy, the picture looks different. The location of the sandbanks is reflected very well in the *available* tidal current power, since these disturbances in the natural flow pattern make the current velocity increase. The nearshore sandbanks, like Wenduinebank, Stroombank and Nieuwpoortbank, show a slightly higher tidal current resource than the immediate surroundings. Since these banks are orientated along the coast (west-south-west to east-north-east), and hence along the major flood-ebb currents (Figure 68), a part of the tidal currents are going around these sandbanks instead of over (this is however a very local effect which cannot be seen on Figure 68). The offshore sandbanks, like Westhinder, Oosthinder, Noordhinder and especially Oostdyck are orientated more towards south-west to north-east, but most of the tidal ellipses are still orientated west-south-west to east-north-east, thereby forcing the flood-ebb currents (partially) over the sandbank instead of around. The currents over the sandbank increase the available tidal current resource, making them thus interesting for both installation of foundation and/or mooring (wind or tidal) and a possible combination of combining wind and tidal energy.

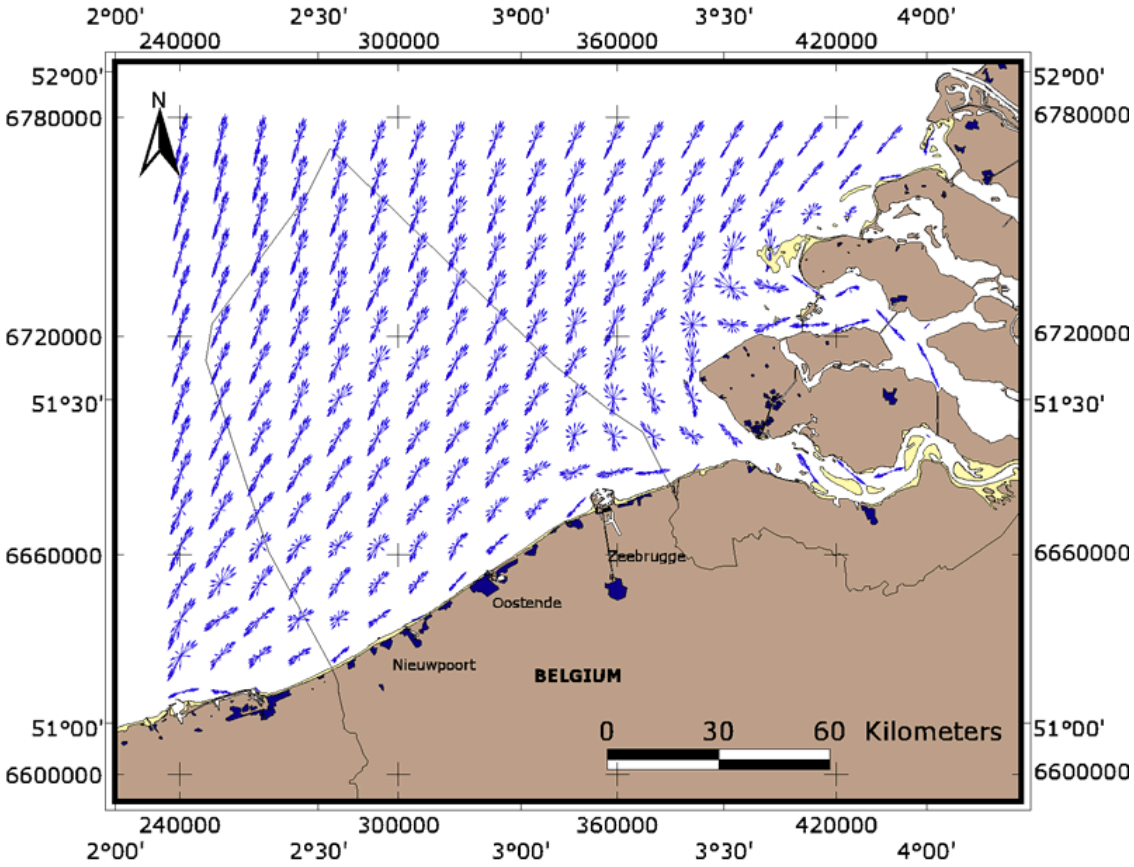

Figure 68: Tidal ellipses of the tidal currents on the BPNS (MUMM 2009).

So, when putting the above consideration together, the following synergies are possible:

- For the domain concession zone:
    - Wave energy resource is quite homogenuous on the domain concession zone and amongst the best locations to be found on the BPNS, especially in the northern concession zones (the *available* wave energy resource varies from 5.5 till 6.4 kW/m, or in the case of the *extractable* wave energy: a Straumekraft 25kW WEC would produce 4 to 4.1 kW on average, and a single 5m floater of the Wavestar would produce up to 8.6 kW);
    - Tidal energy: more heterogenouous than wave energy due to the changing bathymetry. The best locations are the Bligh Bank (up to 17 W/m² swept area extractable, depth is however a limiting factor for large turbines) or the region South of the Thornthon Bank (up to 15 W/m² swept area, deeper location than the Bligh bank).
- In general, the south-west region of the harbor of Zeebrugge seems favorable for the deployment of tidal current energy, especially if this could decrease the transverse flow in the navigation channel, making the entry and exit to the harbor easier and less dependent on tidal current windows. This nearshore region is however not interesting for wave energy.
- A new promising region, for offshore wind and tidal current is the Oostdyck bank (see Figure 47 for the location). It provides shallow waters, making installation and mooring relatively cheap, and has a good wind resource and acceptable tidal current resource. Wave power is relatively low compared to the more favorable conditions on the BPNS, but at the outer edge of the sandbank (especially at the north-west side, so orientated to the incoming waves) wave power exploitation might be possible.
- For the nearshore sandbanks, the Smalbank has the best *extractable* tidal current resource, in the order of 11 W/m², which is similar to most locations of the domain concession zone (excluding the Bligh Bank and the region south of the Thornton bank). However, depth is a limiting factor for bigger turbines, and offshore wind deployment is unlikely due to the proximity of the coastline.

8 Conclusions and recommendations

This chapter provides the overall conclusion of the BOREAS project, and concludes this report, and the (internal) intermediate reports.

The first intermediate report (Mathys *et al.* 2011a) gave an overview of the state of the art of wave and tidal current energy convertors. The convertors were assessed for their suitability on the BPNS. Only publically available information was used for this assessment.

In order to do so, the generic and specific requirements for both WECs and TECs were listed. In order to assess the development of a specific WEC or TEC, the TRL (Technology Readiness Levels) methodology was used. Five TRL phases, ranging from conceptual phase to a pre-commercial phase were used according to the methodology proposed by HMRC (Holmes 2009) and were adopted by European research projects like Waveplam. The number of devices which have reached TRL5, the pre-commercial phase, are still limited. Recent studies showed that it took the wave energy pioneering companies a least 15 years to reach the pre-commercial phase, due to a combination of technical , financial and political reasons (e.g. few interest in renewable energy due to cheap oil after the first oil crisis). The leading technologies of today, indeed started their research several years ago. A lot of technologies are struggling in phases 3-4, to overcome both the technical problems as well getting funding for further deployment. Even the technology leaders with a high publicity exposure are all having difficulties to find funding to start demonstrator projects.

Some trends became clear during the study of the state of the art of wave and tidal current energy convertors:

- With the exception of the real industry leaders (like Pelamis and Marine Current Turbines), a lot of device developers are looking for synergies with offshore windenergy. Some do this very explicitly, like Ocean Green Renewables with Wavetreader, others just mention it as supplementary claim over the existing (production) claims. Some try to look for other synergies, like integration within coastal defence systems, or road or rail bridges over rivers or tidal estuaries. Another synergy is the production of desalinated water.
- The UK, and more specific Scotland, is the European country were most developments occur, without minimizing the efforts in other countries. Gifted by nature with an immense marine energy resource, the UK has awarded lease options of 1.2 GW in Pentland Firth and Orkney waters. Most developments occur there, this can be seen in the number of developers and devices, the (public) funding, the number of research institutes involved, and the very ambitious policy plans for marine energy.
- The number of test sites is growing rapidly, however a lot of test sites that should have been fully operational in 2010, aren't due to a variety of reasons. Problems with consenting and licensing, funding (underestimating the required budget, especially the submarine cable), withdrawal of some device developers delayed these test sites.
- International standards are not yet established, but are under construction. The standards shouldn't form at threat to the further development, but should be an opportunity to increase the credibility about the efficiency and production claims towards investors.
- Only few devices showed some interesting features for deployment on the BPNS. None of them were specifically designed for the conditions on the BPNS, since the resource is low to moderate and most devices focus on the high energetic environments. Very little

information on the performance and efficiencies of the devices is available. No existing device can be deployed as-is on the BPNS. For wave energy, Straumekraft Protech, the Seabased point absorber or the WaveStar show interesting features and might be scalable to the conditions to be found on the BPNS. The FlanSea project, which, specifically targets the BPNS, sounds a promising solution, but it is still in a early phase of development. For tidal energy, stand-alone systems will be unlikely. The solution of Ecofys' waverotor is a nice example of a combined exploitation of marine energy resources.

When the first intermediate report was written, end 2010, a lot of milestone projects for many developers were well underway. Any observer who looks at the current developments, must admit that the interest in marine wave energy has exponentially increased. This is reflected in the number of developers, the number of patents with regard to marine energy, the investments both from public and private funding and the interest from policy makers. Expectations are very high towards the cost competitiveness of these renewable energy source. Some developers may have made quite bold claims about their cost price of electricity or more general their cost competiveness and development time, in order to gain interest with investors and policy makers. The next 2-3 years will be crucial for the further development of the whole sector. If the marine energy sector cannot provide cost competitive success stories (supported with any form of subsidy), it is likely that investors and policy makers will lose interest and focus on other renewable energy sources.

The technology leaders will have to proof that their devices (and by extension, marine energy as a whole sector) can provide electricity with an acceptable Cost of Electricity (COE). 'Acceptable' in this context means a COE which that will be initially higher than current conventional (or even other renewable) energy technologies, but low enough to become 'competitive' in time due to the learning effect and scaling and competition advantage. The technology leaders are almost exclusively focused on the highly energetic zones, and none of them have explicitly communicated that they will develop – or scale down – their devices for conditions that can be found on the BPNS. However, while the technology leaders have the difficult task to prove the commercial viability of the marine energy sector as a whole (and not just for their own technology), new and interesting niche technologies are being developed at research groups who started later than the technology leaders. These 'niche' developers realize that it will be hard to make up the lag with the technology leaders. In this perspective, the BPNS can be seen as a niche market, due to the low to moderate marine energy resource. It is therefore unlikely that a contribution towards marine energy deployment will come of the industry leaders of today. It is more likely that this contribution will come from the niche developers, but this will take still some years to develop.

The second intermediate report (Mathys *et al.* 2011c) was a technical summary of four technical reports (each describing the set-up, calibration and validation of the numerical models). In case of the wave modelling (Fernández *et al.* 2010), the model results of SWAN provides a coherent database with 10 year of wave modeling, with good temporal and spatial resolution. Furthermore, the comparison with both buoy data and the Transformation Matrix (Delgado *et al.* 2010), indicated a reasonable level of accuracy, which makes it a very powerful and useful tool to further asses the wave energy resource. There are however, some limitations:

- Although the grid is quite fine, local effects, such as local sand dunes or artificial structures like harbors are not modelled and may influence the waves.

- This dataset provides the wave climate before the implementation of wave energy convertor farms. A - hypothetical- massive WEC farm placed at the BPNS, would influence the waves and vice versa. In the assessment of the extractable wave energy resource, this must be approached in a pragmatic way.

For the tidal current modelling, two spring-neap tidal cycles of tidal currents were validated (Van den Eynde *et al.* 2010). This model was compared with another model (LTV model) to verify its validity (Dujardin *et al.* 2010b). One can conclude that the numerical model gives satisfactory results and that the model is well suited to be used for the calculation of the tidal current climate on the BPNS and can be used for the assessment of good sites for exploitation of tidal current energy.

The third report (Mathys *et al.* 2011b) assessed the *available* and *extractable* wave and tidal current resource on the BPNS and made an economical analysis. This was based on numerical models, validated with buoy data.

The **wave model** consisted of 10 year hindcast between 1999-2008, which allowed to calculate the *available* wave power (Figure 36). Three corrections were applied to increase the accuracy of the results. These corrections were: buoy data correction, deep to spectral correction and the 17 year period extension. The available wave power in the domain concession zone varies from 5.5 kW/m (Southern part of the zone) to 6.4 kW/m (Northern part of the zone), and varies from 9 to 10.7 in January (Figure 38) till 2.2-2.9 kW/m in July (Figure 40). During the 10 year hindcast, yearly differences were observed, with an annual maximum of 6.4-7.5 kW/m in 1999 and an annual minimum of 4.3-4.9 kW/m in 2003. A good agreement with other studies (namely Anemoc and the UK Wave Atlas) was found (Figure 37).

Three power matrices of WECs were coupled to the wave model dataset of wave height and period (with buoy data correction), in order to obtain the extractable wave power. The three WECs were Pelamis (Figure 44), Straumekraft (Figure 45) and Wavestar (Figure 46) and had a respective capacity factor in the domain concession zone of 6.1, 17.9 and 22.4% based on the 10 year hindcast and assuming they were operational all time. The capacity factor is defined as the average production over the total installed capacity. The obtained capacity factors show clearly what we have to expect. The Pelamis is designed for higher sea states e.g. rough wave climate. The Pelamis, in its actual design, is not to be placed on the BPNS. The Straumekraft and Wavestar with a capacity factor around 20% may be interesting for the BPNS. Probably, adaptation to the local wave climate is advisable, in order to increase the capacity factor.

The **tidal current model** consisted of a detailed three-dimensional hydrodynamic model for a period of two tidal cycles in October 2006 (Figure 48). The available tidal current power over the full water column is 90-120 W/m² swept area in the domain concession zone. The harbor of Zeebrugge has the highest power with locally 330 W/m² at the western breakwater. The Oostdyck bank was detected as an interesting zone, with available powers up to 140 W/m².

The power curve of a generic TEC (Figure 50) was coupled with the tidal current model dataset to obtain the *extractable* tidal current power (Figure 54). In the domain concession zone, the extractable tidal current power in the upper half of the water column ranged from 2 to 17 (Figure 54) W/m² swept area. If a generic turbine would be deployed on the Bligh Bank (most favorable zone in the domain concession zone) in this upper half of the column and with 10 m diameter blades, the rated power would have to be 13.3 kW, dimensioned on peak load (not the economical optimum, as this is very technology specific). In this case, a capacity factor for the domain concession zone of 10% was obtained, assuming full time operationability. A higher

capacity factor is expected around the harbor of Zeebrugge, however the grid resolution, bathymetry and possible boundary effects of the currently used model did not allow a detailed analysis. Therefore, it is suggested to use a finer tidal current model (like the mu-Heist model of MUMM), to determine the capacity factors at the harbor of Zeebrugge.

The **cost assessment methodology** was similar to the OPTIEP study for offshore wind (Mathys *et al.* 2010). Although the current support for wave and tidal Tradable Green Certificate (TGC) is restricted to 10 years, it was assumed that the TGC support would be guaranteed for 20 year. The results are shown for a 5-6 MW WEC park or a generic 0.5 MW TEC park (Table 29). The difference in capacity factors again show the importance of a design that is capable of capturing the moderate wave (or tidal current) climate on the BPNS. Pelamis is designed for high wave climates, and has a capacity factor of only 6.1 %. On the other hand, Straumekraft and Wavestar achieve a capacity factor of 17.9 and 22.4% respectively. Wavestar gives a high initial investment cost, but these are likely very realistic whereas other costprices may be too optimistic. In order to achieve a zero Net Present Value (NPV), the necessary TGC support varied from 379 till 856 €/MWh. This is influenced by the fact that a very small WEC farm is considered.

Table 29: Summary table of the cost assessment.

Value	Pelamis	Straumekraft	Wavestar	Generic 13.3 kW TEC
Size	8*750 kW= 6MW	200*25kW = 5 MW	7*(20*37kW)[31] = 5.18 MW	40*13.3 kW =0.532 MW
Capacity factor at the domain concession zone	6.1 %	17.9 %	22.4%	10 %
Final investments cost	2904 €/kW	4654 €/kW	8420 €/kW[32]	4307 €/kW
Net Present Value with a TGC of 90 €/MWh (20 year)	- 15 639 k€	-14 150 k€	-29 752 k€	-11 727 k€
Necessary TGC for the NPV to become 0 (20 year)	856 €/MWh	379 €/MWh	575 € /MWh.	446 €/MWh

[31] A single floater of a Wavestar is 'clustered' in a jack-up platform with 20 floaters, thereby reducing the cable cost for connecting to the grid.

It is likely that if the technology development leads to feasible WECs, bigger WEC farms will be built. The analysis for bigger wave energy parks, up to 50 -200 MW is shown in Table 30. It clearly shows that Pelamis (in its actual design), due to the low capacity factor, would need unreasonably high support to become competitive. In all Straumekraft scenario's, the necessary TGC to achieve zero NPV is below the initial Flemish support for solar energy (450 €/MWh).

When increasing the installed capacity and simultanuosly increasing the technology factor *tf (*or in other words: decreasing learning rate which is defined as 1-tf), the level of TGC support to achieve a zero NPV for Wavestar (420 €/MWh) drops below the initial support that was foreseen for solar energy (450€/MWh). Increasing even further, to 200 MW, the effect becomes small for Straumekraft (265 compared to 278 €/MWh) but still significant for Wavestar (420 to 376).

Table 30: Level of necessary TGC support (20 year) to make the NPV zero, when all input parameters are the same except for the technology factor and the cable cost (33% reductions in cost, based on €/kW installed, for both the 50 and 200 MW scenario compared to the 5-6 MW scenario).

Installed capacity (MW)	Technology factor *tf* (%)	Pelamis TGC (€/MWh)	Straumekraft TGC (€/MWh)	Wavestar TGC (€/MWh)
200	92	633	265	376
50	91	642	278	420
5-6	90	856	379	575

Scaling a device to meet the conditions found on the BPNS means increasing the capacity factor of the device. So, if the costs would remain the same (200 MW park), but the capacity factor would increase to 25% or 30% the necessary TGC support for a zero NPV would drop to be respectively 331 and 267 €/MWh for WaveStar, and to 174 and 136 €/MWh for the Straumekraft.

However, supporting wave and tidal current energy technologies with TGCs is most relevant in a later commercial stage. The main focus in the short term should be to fund research and development projects who specifically target the low to moderate wave and tidal current climate conditions that can be found on the BPNS. Currently, the available market technologies are developed for high energetic zones (both wave and tidal). These conditions are not present on the BPNS. Technologies that specifically aim this market would have a relatively moderate power production compared to the mainstream technologies, but, as mentioned before, capital costs would be lower because these convertors don't need to be extremely robust to withstand high storm forces.

Furthermore, synergies, especially in combining foundations, transformators and cabling need to be investigated in detail. This allows also the optimal use of the domain concession zone. These technologies are not solely usable for deployment on the BPNS, as other regions have similar power resources, for example the wave power at the Swedish western coast.

It is only in a second phase (precommercial phase), in the mid term, that higher TGC support would be recommended in order to support these pre-commercial technologies that are aimed for low to moderate wave or tidal current climates. It is certainly wishable that the guaranteed period would be extended to 20 years and that the level of TGC follows a high initial support, decreasing with time. In the OPTIEP report, the German system to support offshore wind (which takes into account the date of deployment, distance to shore and water depth) was presented as

a source of inspiration for the future offshore wind policy in Belgium. This system could also be used as a blueprint for the wave or tidal energy TGC policy in Belgium. And, a similar decreasing support system is already implemented for solar energy in Flanders.

Belgian companies already played a pioneering role in the construction of the so called 'far-shore' windmillparks in deep waters. Further research and development for conversion technologies for low to moderate wave and tidal current convertors is highly recommended, and could generate innovative knowledge to Belgian companies. Furthermore, synergetic effects by using combined foundations or electrical components could further reduce the overall capital cost, whilst insuring a more continuous supply of energy. This is due to the intermittent character of these renewable resources. Wave energy shows a phase shift on wind energy, which makes a very interesting source to be added to existing (offshore) windenergy. Tidal current energy has the very unique characteristic that it is completely predictable (with neglectable variations due to meteo effects) and is the only renewable source with this characteristic.

Today, with the current technology, it is still unlikely that wave or tidal current energy will be contributing significantly to the energy production in Belgium within the next 5 years. However, internationally big progress is made in the research of marine energy and demonstration sites are well underway. In the mid term (5-10 years), wave or tidal current energy (developed for moderate wave or tidal current climates) could contribute to the energy production, but only with the necessary investment in R&D for specific conversion technologies in a first phase, and a suitable TGC support level in a second phase.

9 Appendix

9.1 Factsheets of selected WECs

The Factsheet template was described in § 2.4. The first two presented WECs here, were selected because they have power matrices available (Pelamis and Wavestar). Note that for Straumekraft, very little information was available apart from the power matrix, so no Factsheet was made. The others WECs were selected because they show interesting features for deployment on the BPNS (Seabased, WaveTreader and Wavegen).

9.1.1 Pelamis

Current corporate profile	
Pelamis Wave Power	Pelamis
http://www.pelamiswave.com/	1998, UK
• Over 70 employees, arguably the biggest pure wave energy developper worldwide • Technology leader, however problems with a financial partner (Babcock and Brown) with the Agucadouro demo projext made bad publicity	Quoting Pelamis: "lowest on the market", without exactly specifying
Norsk Hydro, Technology VCs, Scottish Enterprise,…	

Pictures	
	
The second prototype of Pelamis, called P2	The second prototype of Pelamis, called P2

Device specifications

AT	Hydraulic	Anchored, quick release connection for towing back to harbour
• Shallow draft • Good survivability due to hydrostatic clipping: Pelamis dives 'under' big waves • Emergency release connection, device can be towed in harbor and dry docked		50-70m
		180m long, 3 m dia, 859 ton
		Yes, full power matrix available, giving Power output for a 750 kW device in function of T_p and H_s

Device Development history and future strategy

- Phase 1: 1:80 Edinburgh Uni. Scotland ('98-'01)
- Phase 2: 1:35 Edinburgh Uni. Scotland ('99-'01)
- Phase 3: 1:7 ECN, Nantes, France ('01-'03)
- Phase 3: 1:7 Firth of the Forth, Scotland ('01-'03)
- Phase 4: 1:1 EMEC, Scotland 750 kW ('04-'07)
- Phase 5: 1:1 Agucadoura, Portugal 3 x 750 kW ('08-'09)
- Phase 5: 1:1 EMEC, Orkney (EON + SPR), 1+1 x 750 kW ('10-)
- Commercial plans: Bernera Wave Farm (20 MW, Shetland, '13-'14) and Farr Point Wave Farm (50 MW, date unknown)

Device evaluation

- Agucadoura was the first commercial grid connected wave power plant at full scale (3* 0.75 kW)
- Commercially ready, although the new design (P2) will be further modified
- Broad project portfolio: P2 is currently at sea at EMEC for E.ON (Scotland); 20 MW ongoing in Shetland (Scotland), secured a tender from the UK Crown Estate for the Farr Point Wave Farm (UK) with at first phase of 7.5 MW and optionally a second phase of 50 MW; secured a second tender at Marwick Head (UK) for 50 MW
- Pelamis is now in a difficult and somehow ambigiuous position: on the one hand they are commercializing their device, but questions remain about the performance. An example is there participation cancellation in the Wavehub project to 'focus on testing'
- Pelamis was, and still is, an absolute forefront runner in the Wave Energy Industry, despite the problems at Agucadoura
- Other developers may catch up with Pelamis' leading position

Suitability for BPNS

- Very unlikely, depth requirements, developped for high wave climates

9.1.2 Wavestar

Current corporate profile	
Wave Star Energy ApS	Wave Star
http://www.wavestarenergy.com/	2003, Denmark
• Independent, 27 employees mostly engineers • Can be considered as one of the leading developpers	NA
The owners of Wavestar A/S are the brothers Jørgen Mads Clausen, Henrik Mads Clausen and Peter Johan Clausen of the Danfoss family	

Pictures	
	
Prototype of the Wavestar (with 2 of the 20 foreseen buoys). The platform can be lifted up for maintenance or survival	Concept of a full scale Wavestar

Device specifications		
PA	Hydraulic	Jackup platform
• Provides smooth output		Limited by jackup platform
• Using existing technology and knowledge from offshore industry		70 long, 6m height
• Proven efficient storm resistance (14 storms during 3 year operation with 1:10 prototype)		NA, 25-50 kW production per floater in 2.5 m Hs

Device Development history and future strategy
• Phase 1, 1:40, Aalborg University Danmark, ('04-'05)
• Collobaration with the Horns Rev windmillpark for further projects
• Phase 3, 1:10, Nissum Bredning, Denmark, 5.5 kW ('06-'10)
• Phase 4 1:1, First section of the 500 kW design (only 2 of 20 floaters), '09, full device (20 floaters) by '11-'12

Device evaluation
• Excellent track record, with clear milestones • Requires (expensive, but easily accesible) jackup platform • Dependent on wave direction

Suitability for BPNS
• Originally developped for a higher wave climate, so probably only in a scaled down or remodified design

9.1.3 Seabased AB - Linear generator (Islandsberg project)

Current corporate profile	
Seabased AB	Linear generator (Islandsberg project)
http://www.seabased.com/	2001, Sweden
• Spin-off of the Uppsala University, originally a 'sleeping' company to host the IP generated by the Uppsala University research	NA
• Investments from utilities like Vatenfall, Fortum, Statkraft and other private companies • The Swedish Energy Agency and Fortum granted a 10 MW wave farm in Sotenas, Sweden	

Pictures	
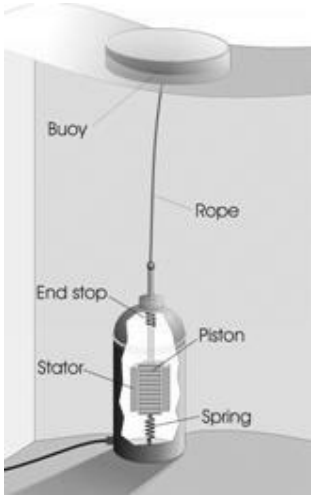	
Concept of the Seabased buoy, showing the linear generator PTO, mounted at the bottom	

Device specifications

PA	Linear generator (connected to bottom anchor)	Anchor, gravity based
• Simple conversion step to electricity		NA
		3m dia, 8m high
		NA

Device Development history and future strategy

NA

Device evaluation

- Long time development at Uppsala university (ongoing)
- All power producing component underwater make maintenance virtually impossible or extremely expensive
- Linear generator takes the full load during storms
- Simple conversion step to electricity
- Strong environmental monitoring programme, both at Lysekill (Sweden) and Ronde (Norway)
- Highly scalable and modular design

Suitability for BPNS

- Possibly: highly scalable and simple, but the tidal variation on the BPNS may form a a problem for the stroke length of the linear generator

9.1.4 GreenOcean energy Ltd - Wave Treader

Current corporate profile		
GreenOcean energy Ltd	Wave Treader	
http://www.greenoceanenergy.com/index.php/wave-treader	2005, Scotland	
• Spin off of engineering company consultancy firm	NA	
Not really specified, but partners include private companies like John M Henderson & Co Ltd, Prospect, Monitor Systems & Cadherent; investmunt funds likeNpower Juice Fund; reasearch instutions like NA-ME, EMEC, NaREC & Robert Gordon University and govern		

Pictures	
	
Concept of the WaveTreader	Concept of the WaveTreader

Device specifications		
PA	NA	Monopile of windmill foundation
• Explicitly designed for connection to offshore windmill foundations		NA
		NA
		NA

Device Development history and future strategy

- Phase 1: 1:50: Proof of Concept at NA-ME ('07);
- Phase 2: 1:12.5: Prototype testing at Narec ('09);
- Phase 3: 1:1 Construction of prototype in '10, to be deployed in '11

Device evaluation

- Explicitly designed to be designed on jacket foundations of offshore windmill farms; this provides a very unique characteristic;
- Seems to have a local (Scottish) network from private companies, research institutions and governments, so strong 'backbone';

Suitability for BPNS

- Connection to offshore windmill foundation sounds promising, however claim for accesibility needs verification. No information on efficiencies.

9.1.5 FlanSea

Current corporate profile		
Flansea	Flansea	
NA	2010, Belgium	
• Colloboration between Belgian industrial partners and the University of Ghent in order to apply the know-how obtained by the SEEWEC for moderate wave climates like the Belgian coast	NA	
IWT, DEME Blue Energy, Cloostermans, Electrawinds, Harbour of Ostend and Contec		

Pictures	
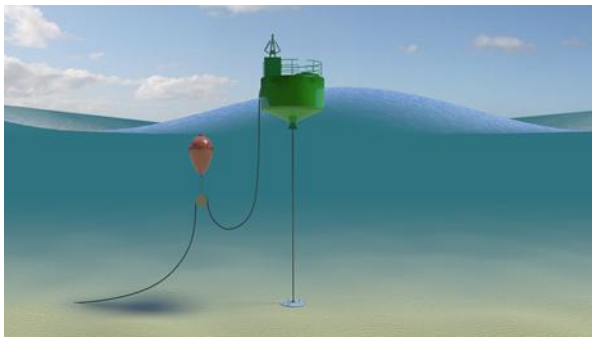	
Concept of the Flansea buoy, the red buoy holds the electricity cable whereas the straight rope is the anchoring cable which is attached to a drum inside the buoy	

Device specifications		
PA	Mechanical or electrical	Anchored, slack mooring
• Explicitly developed for wave climates like the BPNS		10-25m
		NA
		NA

Device Development history and future strategy
• Phase 1-2-3: SEEWEC project, European funded, (’05-’09).
• Phase 1-2: ’11-’12: testing and development in Flanders.
• Phase 3: ’12-’13: testing foreseen nearby the harbor of Ostend

Device evaluation
• Still in conceptual phase, since new design is under development

Suitability for BPNS
• Main design criterium is the low to moderate wave climate, and testing and optimization will be done at the BPNS, so yes

9.1.6 Wavegen (Siemens) – Limpet - Mutriku

Current corporate profile	
Wavegen (Siemens)	Limpet
http://www.wavegen.com/	UK
• Originally Applied Research & Technology ltd	NA
• Acquired by Voith Siemens Hydro in '05	

Pictures	
	
Onshore 500 kW OWC of Wavegen at Limpet, Islay, Scotland	Detail of the impuls air turbine

Device specifications		
OWC	Impuls air turbine	Anchored of onshore
• Completely accesible from land, independent on weather conditions		
• Built in breakwaters or coastal defence structures		
• Alternatively, separate structures can contain the OWC turbines, like the granted SIADAR project (Scotland)		NA, but website contains technical reports on the efficiencies and conversion losses of the components

Device Development history and future strategy
• Phase 4, 1:1, Dounreay, Scotland, 2 MW, '95
• Phase 3, 1:1.75, Islay, Scotland, 75 kW, ('88-'99)
• Phase 4, 1:1, Islay, Scotland, 500 kW, ('98-'07)
• Phase 5, 1:1, Mutriku, Spain, 16*18.5 kW ('98-'10), technically operational but administrative problems hindered the startup
• Phase 5/Commercial, 1:1, Siadar active breakwater, 4MW, planned

Device evaluation
• Long operational time, but tuneability remains difficult (achieving resonance conditions with a fixed air inlet chamber)
• Power producing components outside the water, but may suffer from seawater spray and corrosion
• Possible noise hindrance due to 'whistle' effect of the turbine: in Mutriku the noise was a design criterium

Suitability for BPNS
• Unlikely: tidal variation at BPNS is to high to be implemented onshore, nearshore versions will require high capital investments • If the turbines can be scaled down, and use existing structures to reduce capital costs, then perhaps possible

9.2 Factsheet of selected TECs

The Factsheet template was described in § 2.4. The 3 selected TECs discussed here were the ones that were selected because they show interesting features for deployment on the BPNS. None of these TECs gave a power curve (a generic efficiency curve was used to assess the *extractable* wave power).

9.2.1 Vortex Hydro Energy - VIVACE (Vortex Induced Vibrations Aquatic Clean Energy)

Current corporate profile	
Vortex Hydro Energy	VIVACE (Vortex Induced Vibrations Aquatic Clean Energy)
http://www.vortexhydroenergy.com/	2004, USA
• Spinoff of Michigan University	$ 55/MWh, quoted from an interview with the CTO, but not on the offical webpage
Privately held	

Pictures	
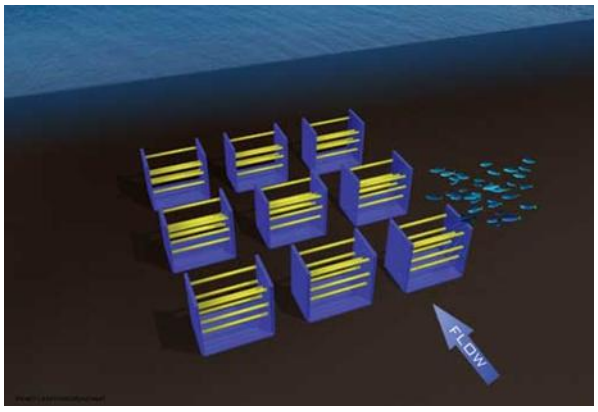	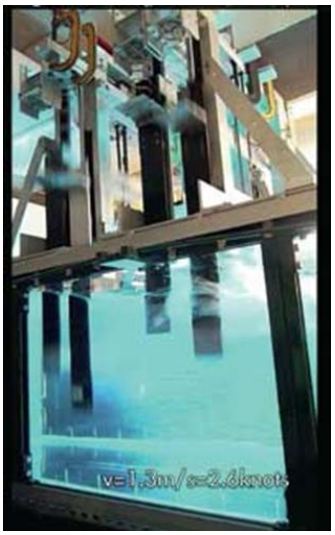
Conceptual, modular design of a Vivace park	Test set-up of 4 wave cilinders in a wave flume

Device specifications

Other, based on Vortex induced 'lock-in' phenomenon	NA	Gravity based
• Very compact design • Very wide efficient range, due to the underlying 'vortex lock in' phenomenon, which occurs over a wide range of flow characteristics		wide range
		NA
		NA

Device Development history and future strategy

- Phase 1: Michigan University, '06-'07
- Phase 2: Michigan University, wave flume testing of 4 cilinders, '09-'10
- Phase 3: Open water test at St Clair river, '10

Device evaluation

- No information on the future plans or the further development, still in research phase, not in a commercialization phase

Suitability for BPNS

- Likely, compact design, low cut-in speed and wide operating range are the most interesting features

9.2.2 Ecofys Wave Rotor

Current corporate profile		
Ecofys		Wave Rotor
http://www.ecofys.com/com/news/pressreleases2002/pressrelease02aug2002.htm		The Netherlands
• Now member of Eneco, which is one of the 3 leading energy utilities in the Netherlands		NA
• Subsidiary of Econcern, which was taken over after by Eneco after bankruptcy in may 2009		

Pictures	
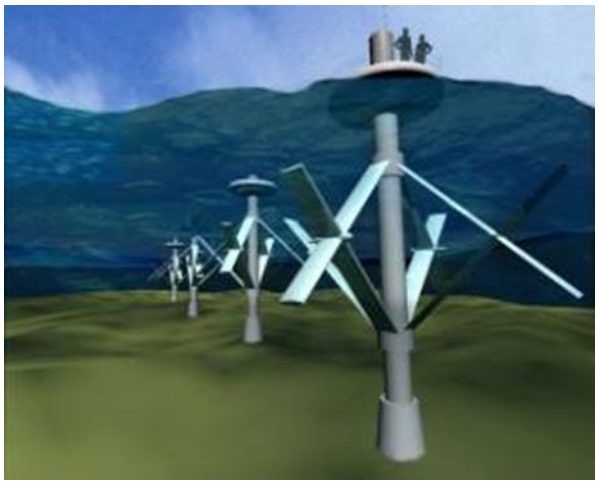	
Concept of the Ecofys Waverotor	Waverotor prototype at Borssele, the Netherlands

Device specifications		
Other, based on a Wells turbine, also captures tidal energy	Direct driven generator	Mounted on piles
• Can convert both wave and tidal current energy, in a single step by means of the wave 'rotor', which is a combination of a omnidirectional Darrieus rotor and a bi-directional Wells rotor. • Can be lifted up to account for difference in tidal range		NA
		NA, prototype has a swept area of 25m
		NA

Device Development history and future strategy
• Phases 1-2: serveral wave tank testing in Scotland and Denmark ('95 - '02)
• Phase 3: 1:10 scale model tested at Nissum Bredning ('02)
• Phase 3: 1:10, 30 kW, at Borssele (Scheldt Estuary) grid connected

Device evaluation
• Currently seeking funding for furhter deployment

Suitability for BPNS
• Combining wave, tidal current and wind energy could be very interesting in terms of optimal use of space

9.2.3 Blue Energy Canada Inc. - Davis Hydro Turbine

Blue Energy Canada Inc.	Davis Hydro Turbine
http://www.bluenergy.com/	Canada
NA	NA
Private	

Pictures	
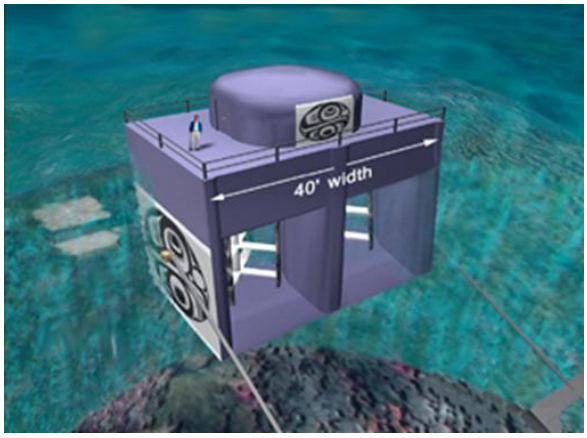	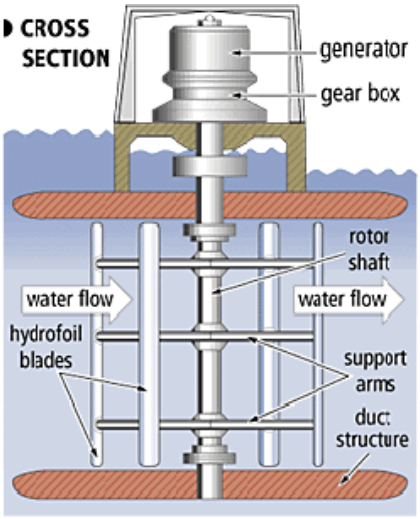
Concept of a floating Davis Hydro Turbine: Blue Energy turbines can be built in smal units. Blue Energy has developed a small modular 125KW design that can be combined into arrays of up to 4 units and used in free stream applications to provide community power.	Turbine schematics: Four fixed hydrofoil blades of the Blue Energy Turbine are connected to a shaft that drives a variable speed electrical generator assembly. This rotor is mounted in a durable concrete marine caisson which anchors the unit to the ocean floor, directs the water flow through the turbine and supports the coupler, generator, and electronic controls above it in a dry, climate controlled machinery room above the water surface. The hydrofoil blades employ a hydrodynamic lift principle that causes the turbine foils to move proportionately faster than the speed of the surrounding water. The turbine is designed to work through the entire tidal range with a typical cut-in speed of 1 m/s.

Device specifications

Ducted VATT ("Tidal Bridge")		Floating or fixed
• Scalable • Machinery and controls above the water • Strong potential synergy with bridges for road transport • High extraction efficiency		NA NA NA

Device Development history and future strategy

NA

Device evaluation

- Currently seeking capitcal with World Energy Research to build a 200 MW commercial dam
- The company has identified potential interesting sites, but no concrete plans are announced so far
- Two indepenent engineering firms, Halverson and RW Beck, assessed the Davis Hydro Turbine and were positive about the technology

Suitability for BPNS

- Focus on integrating tidal turbines in bridges over large estuaries, so not suitable for Belgium.

9.3 Monthly wave powers not shown in report

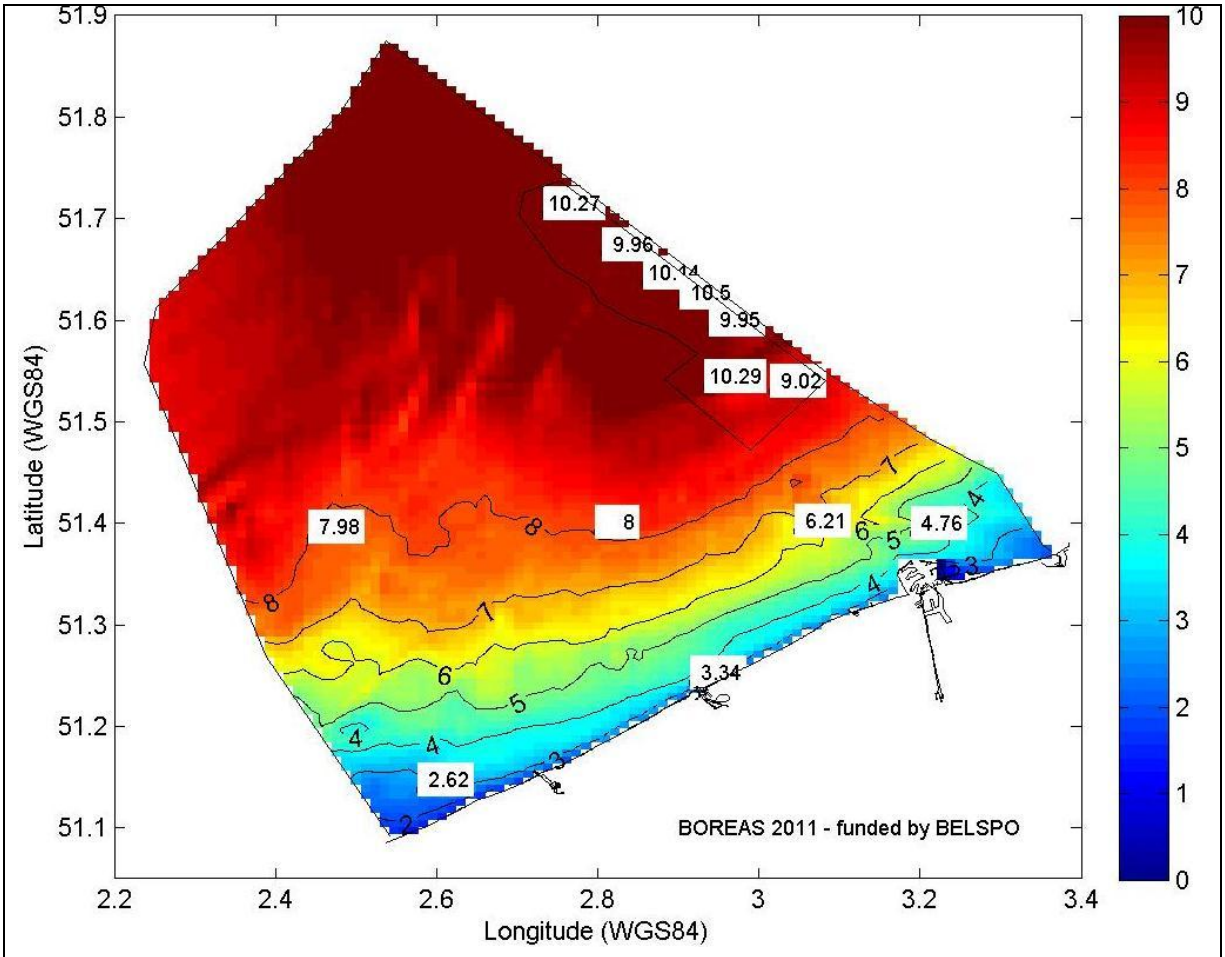

Figure 69: Average wave power (kW/m) for the month February (final, with the 3 corrections).

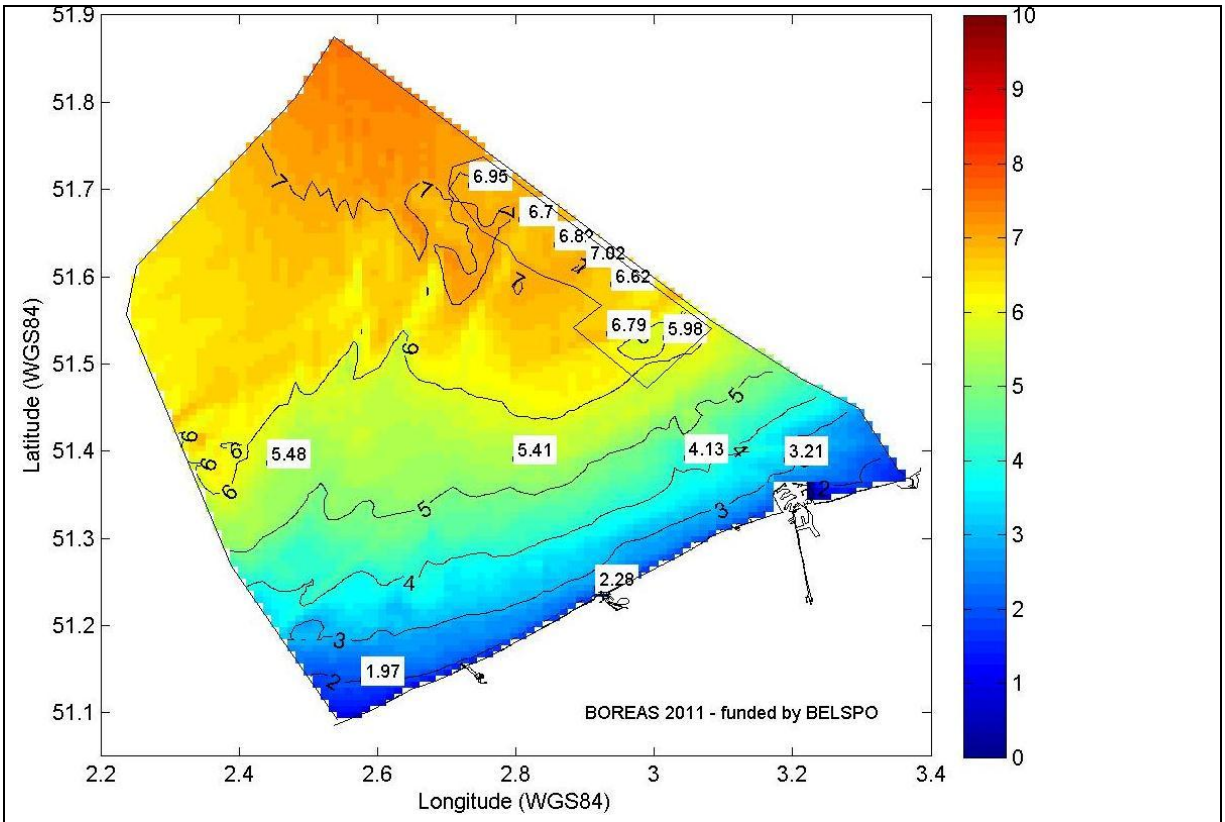

Figure 70: Average wave power (kW/m) for the month March (final, with the 3 corrections).

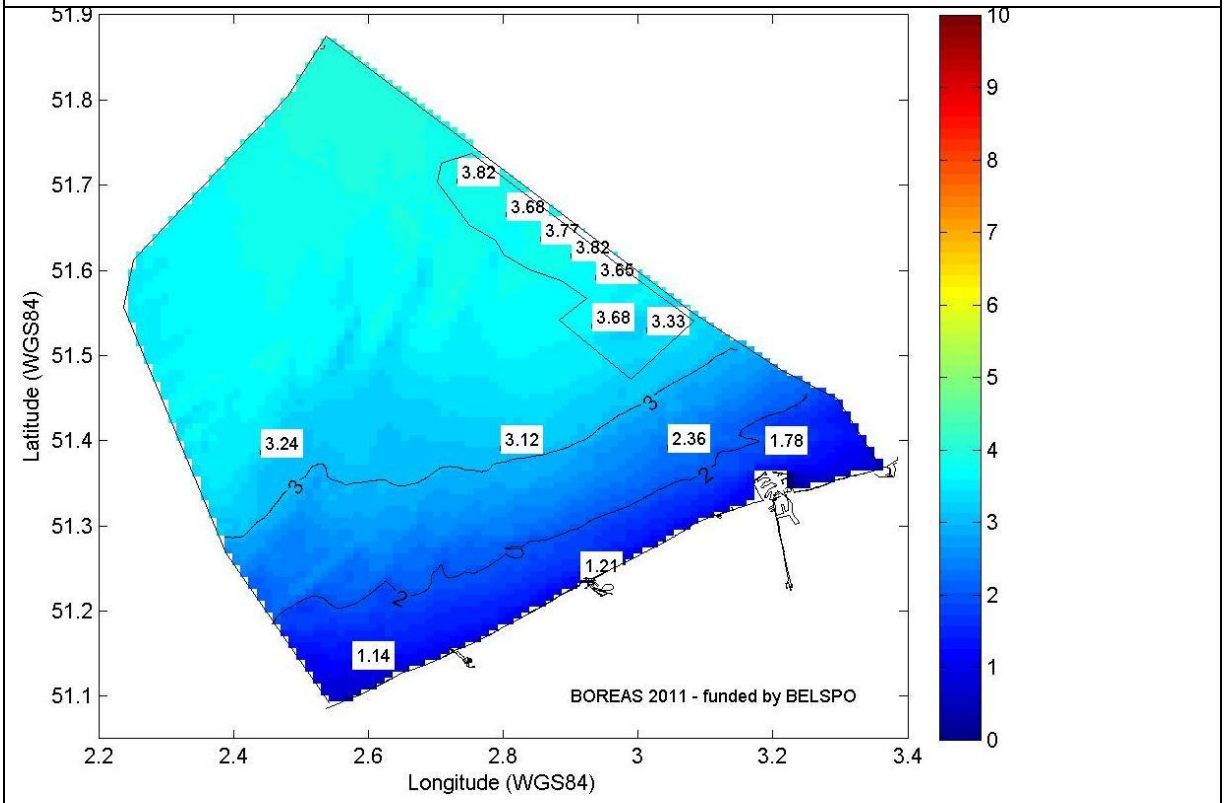

Figure 71: Average wave power (kW/m) for the month May (final, with the 3 corrections).

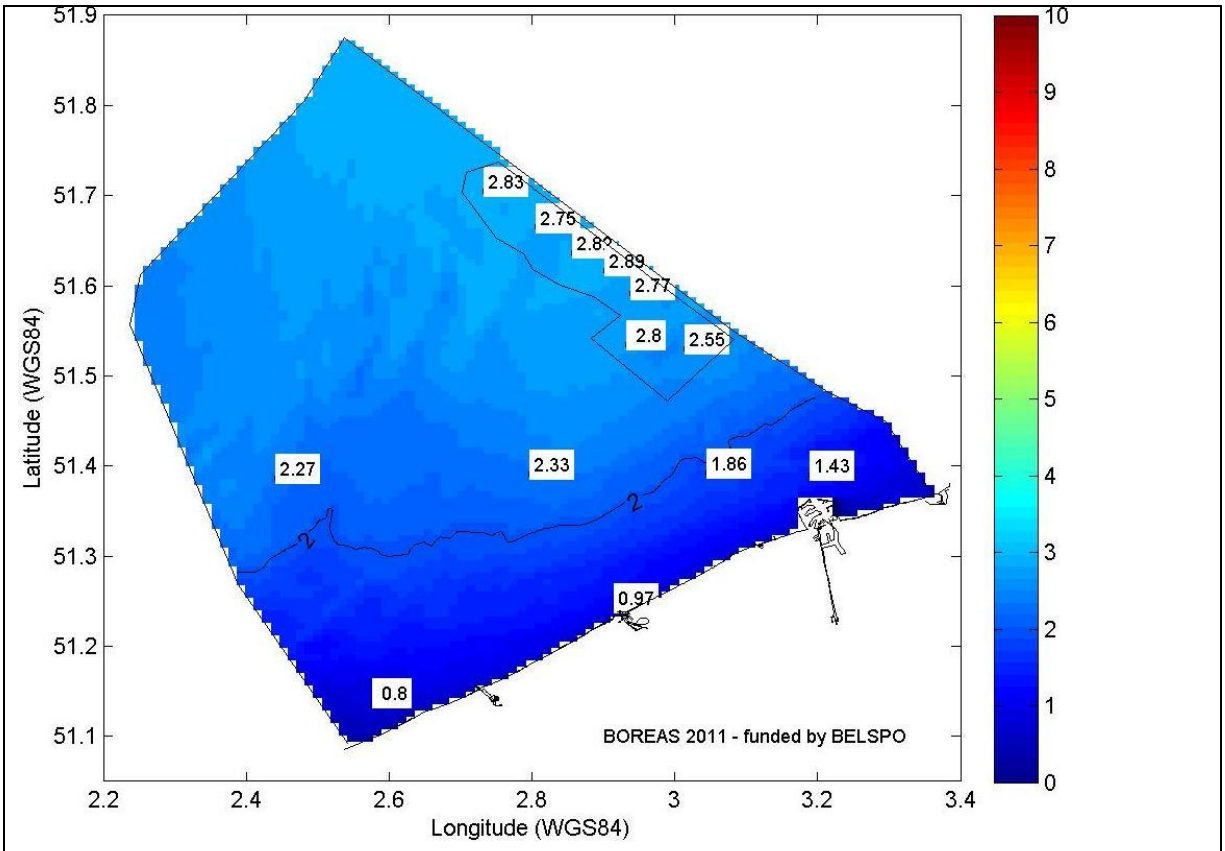

Figure 72: Average wave power (kW/m) for the month June (final, with the 3 corrections).

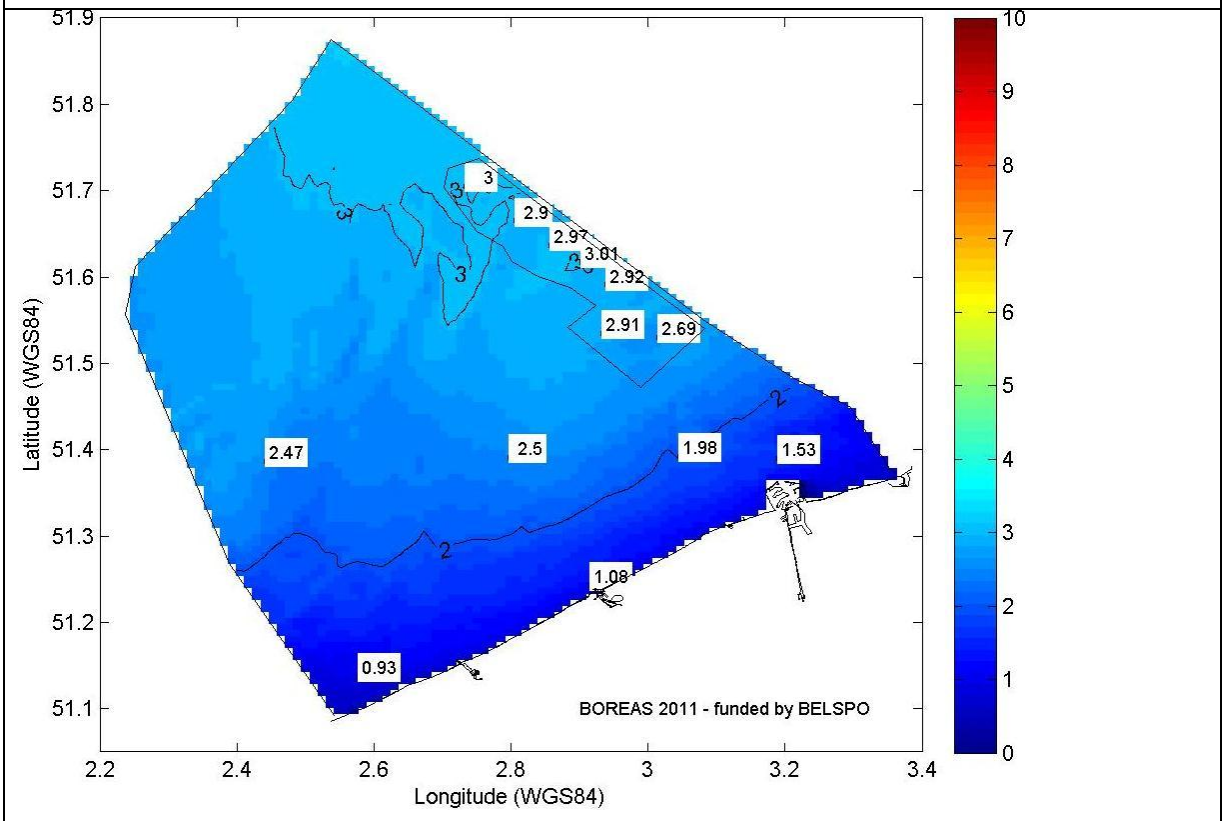

Figure 73: Average wave power (kW/m) for the month August (final, with the 3 corrections).

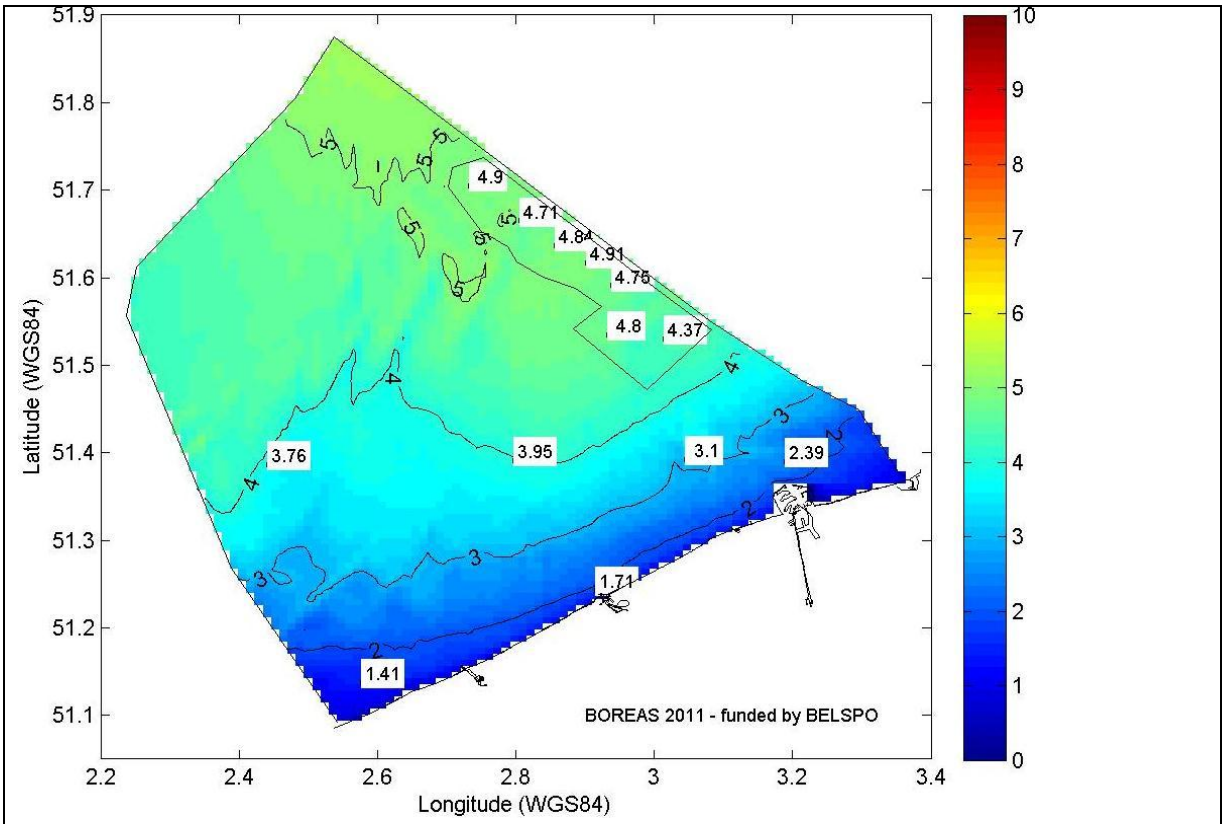

Figure 74 Average wave power (kW/m) for the month September (final, with the 3 corrections).

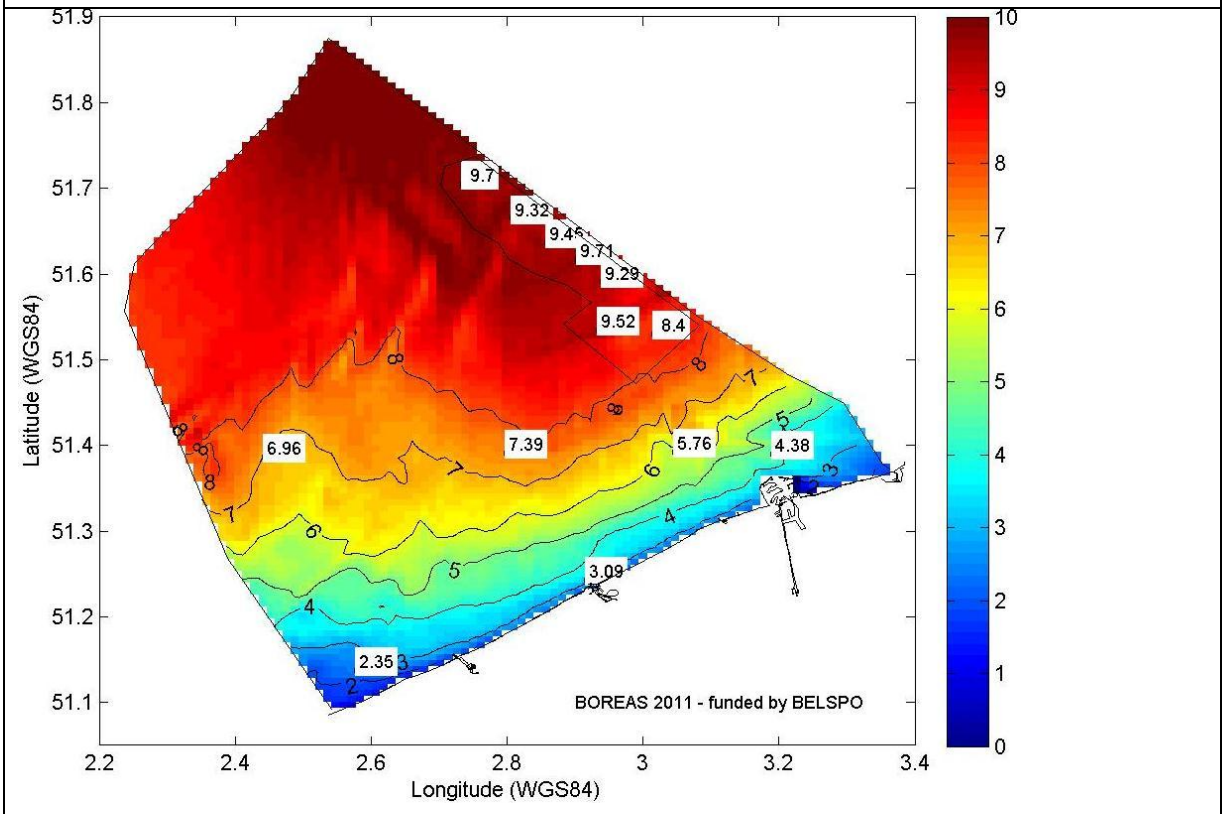

Figure 75: Average wave power (kW/m for the month November (final, with the 3 corrections).

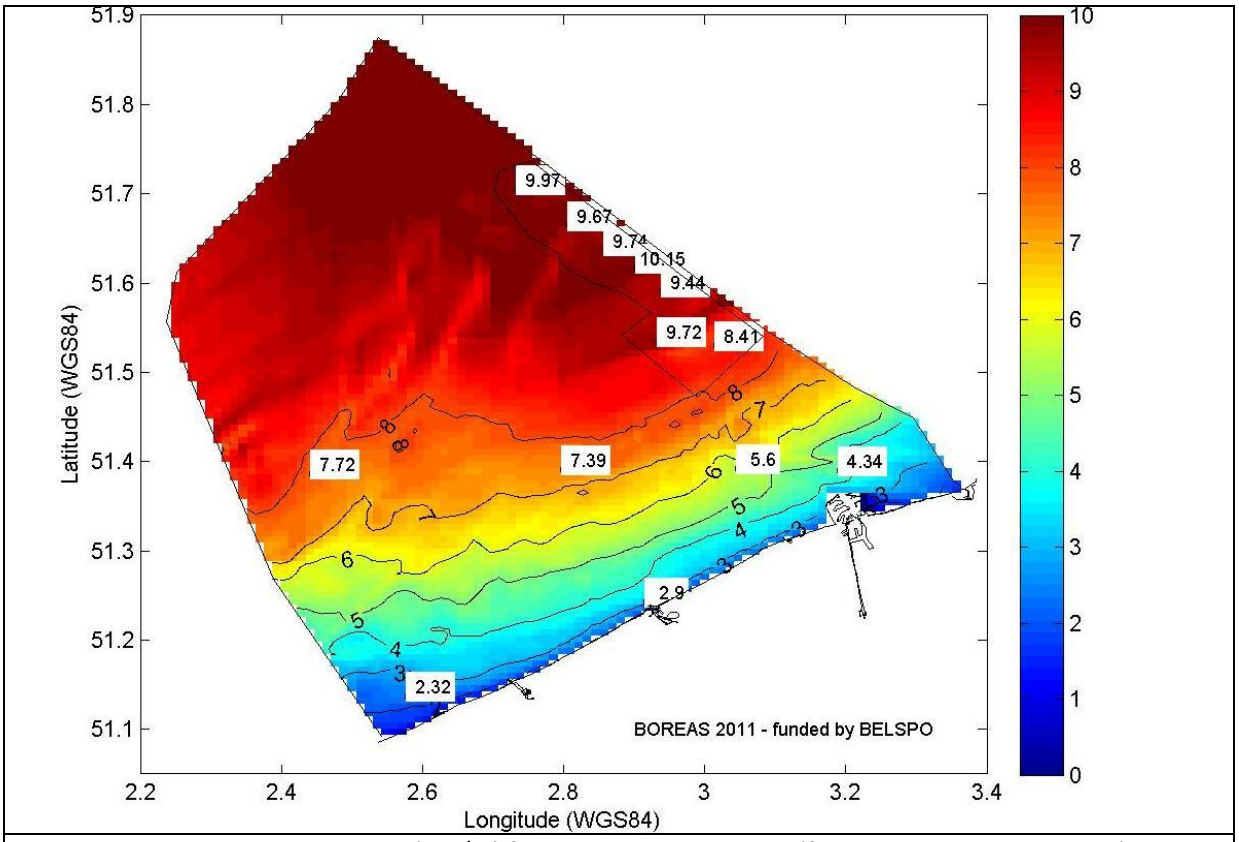

Figure 76 Average wave power (kW/m) for the month December (final, with the 3 corrections).

9.4 Yearly wave powers not shown in report

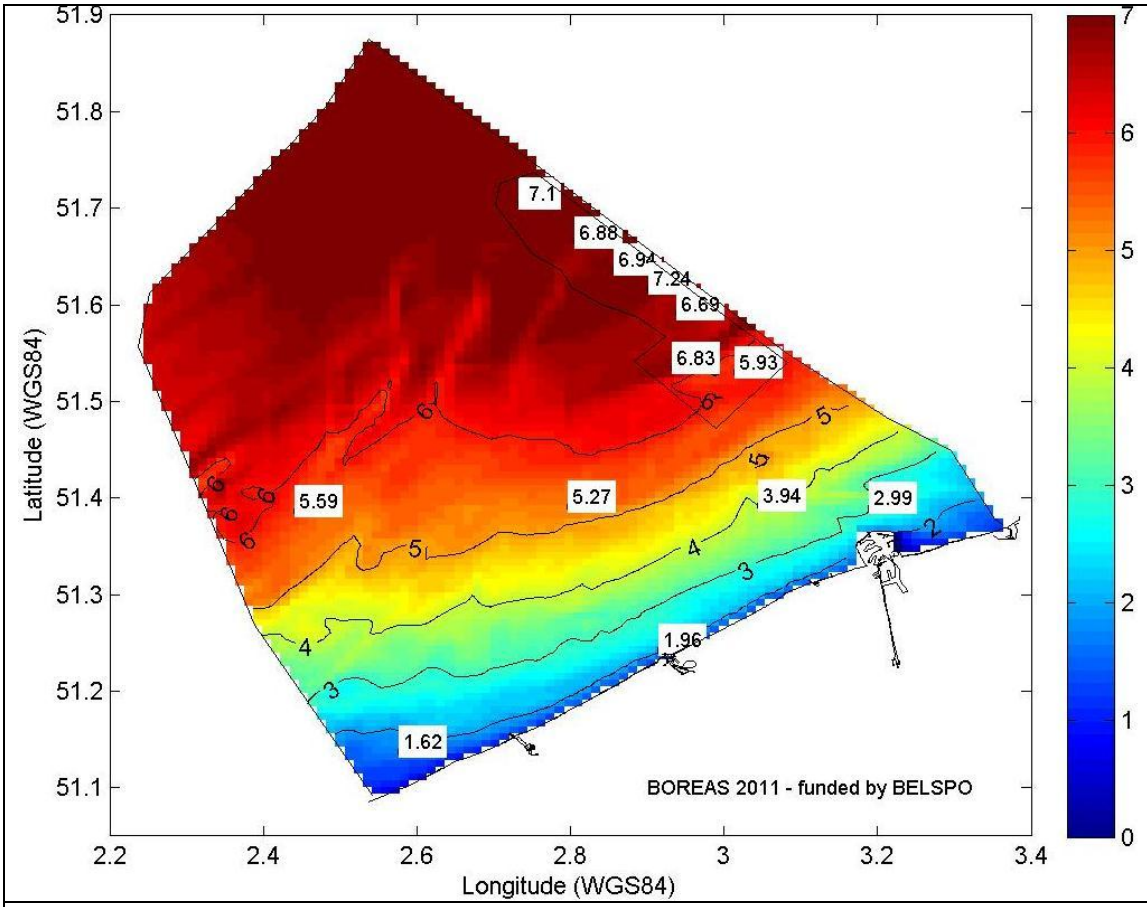

Figure 77: Average wave power (kW/m) for the year 2000 (final, with the 3 corrections).

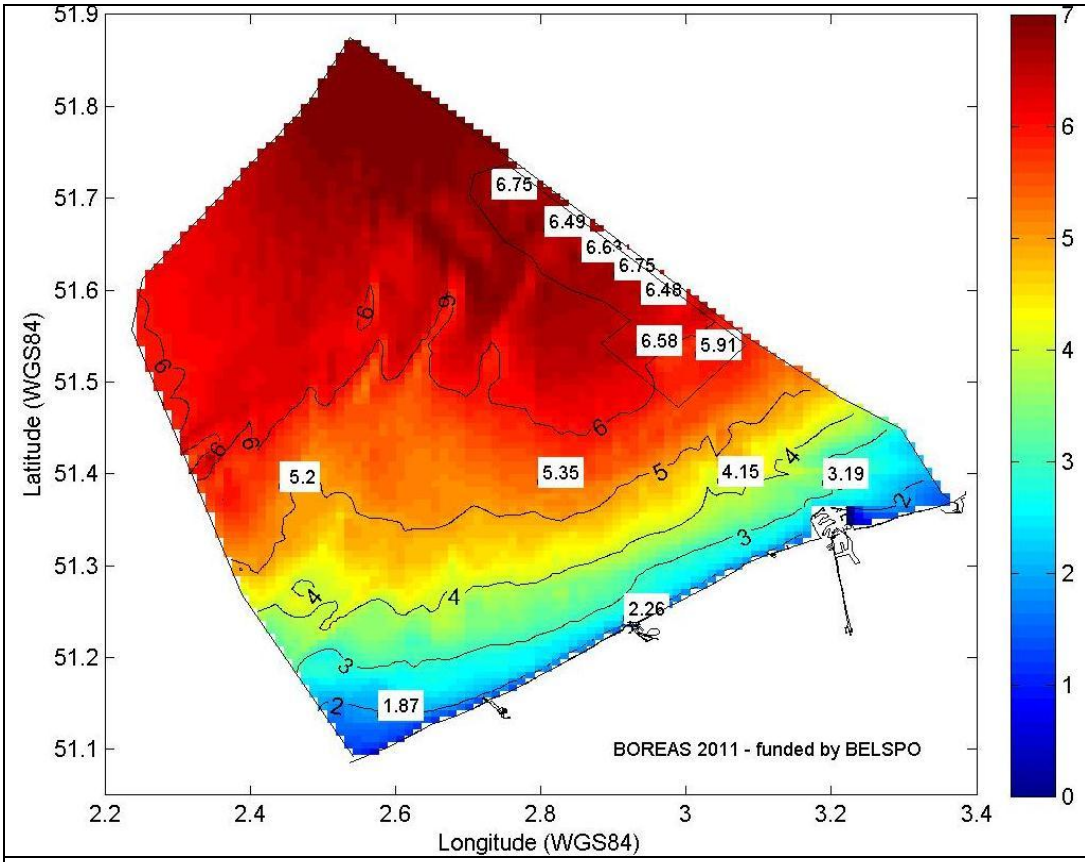

Figure 78: Average wave power (kW/m) for the year 2001 (final, with the 3 corrections).

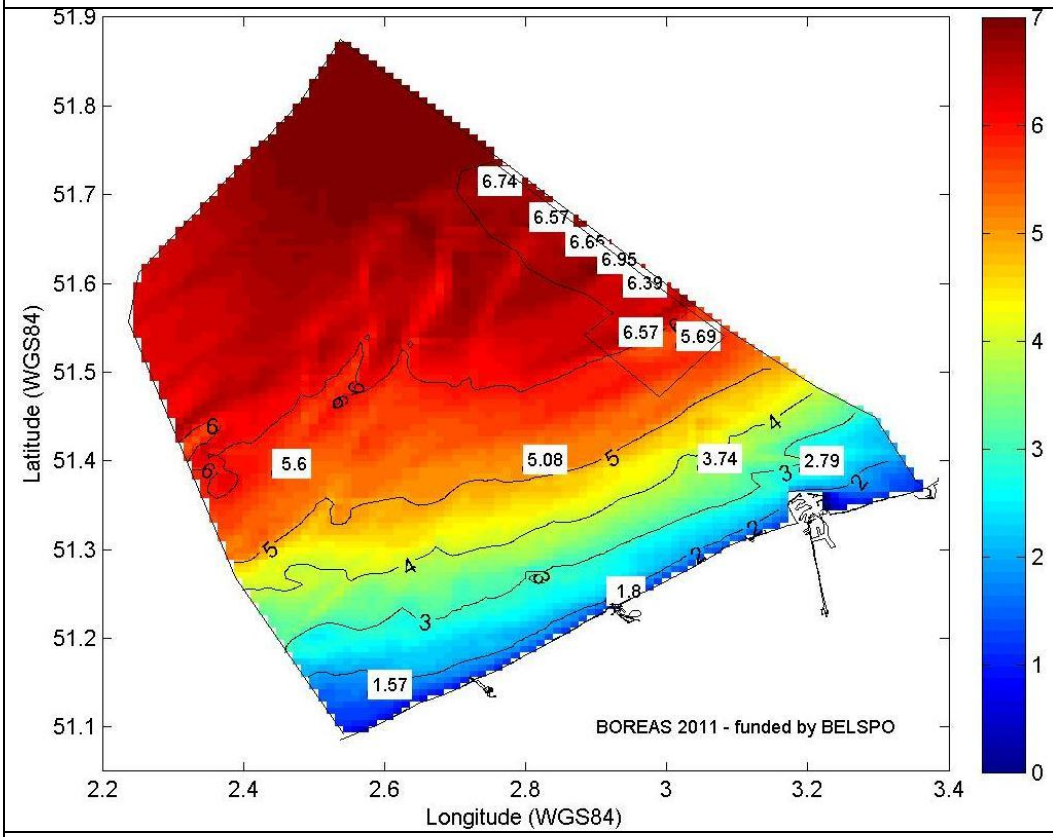

Figure 79: Average wave power (kW/m) for the year 2002 (final, with the 3 corrections).

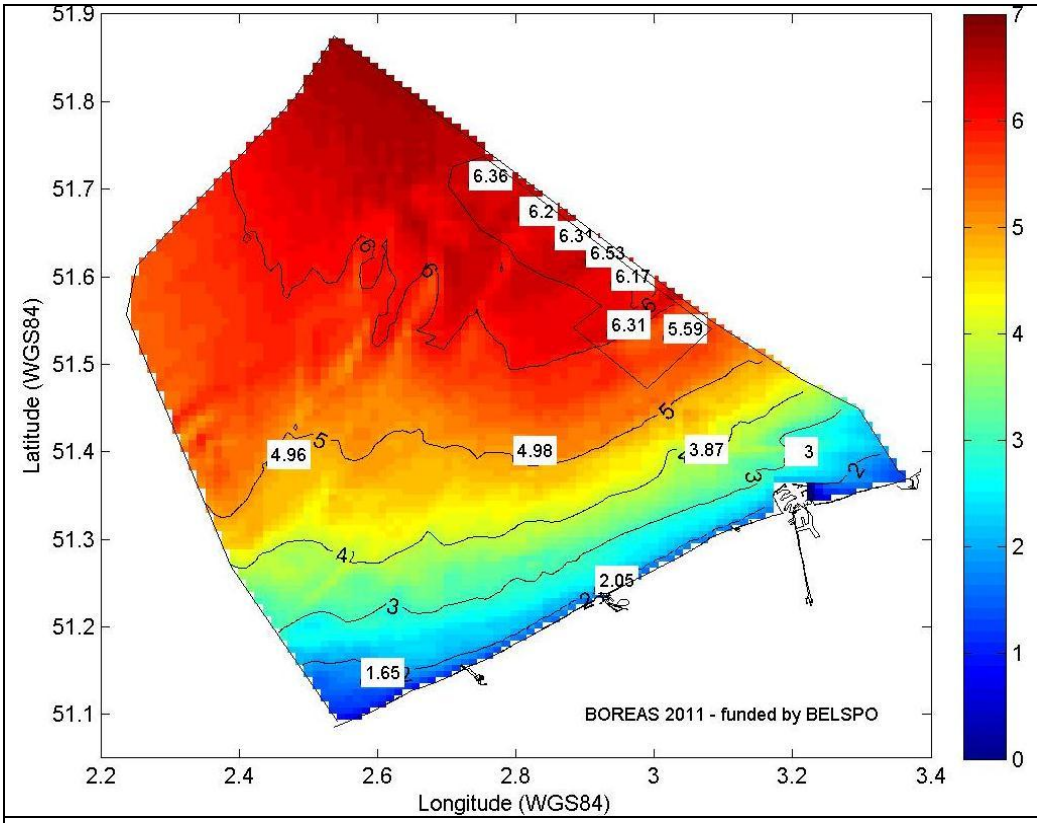

Figure 80: Average wave power (kW/m) for the year 2004 (final, with the 3 corrections).

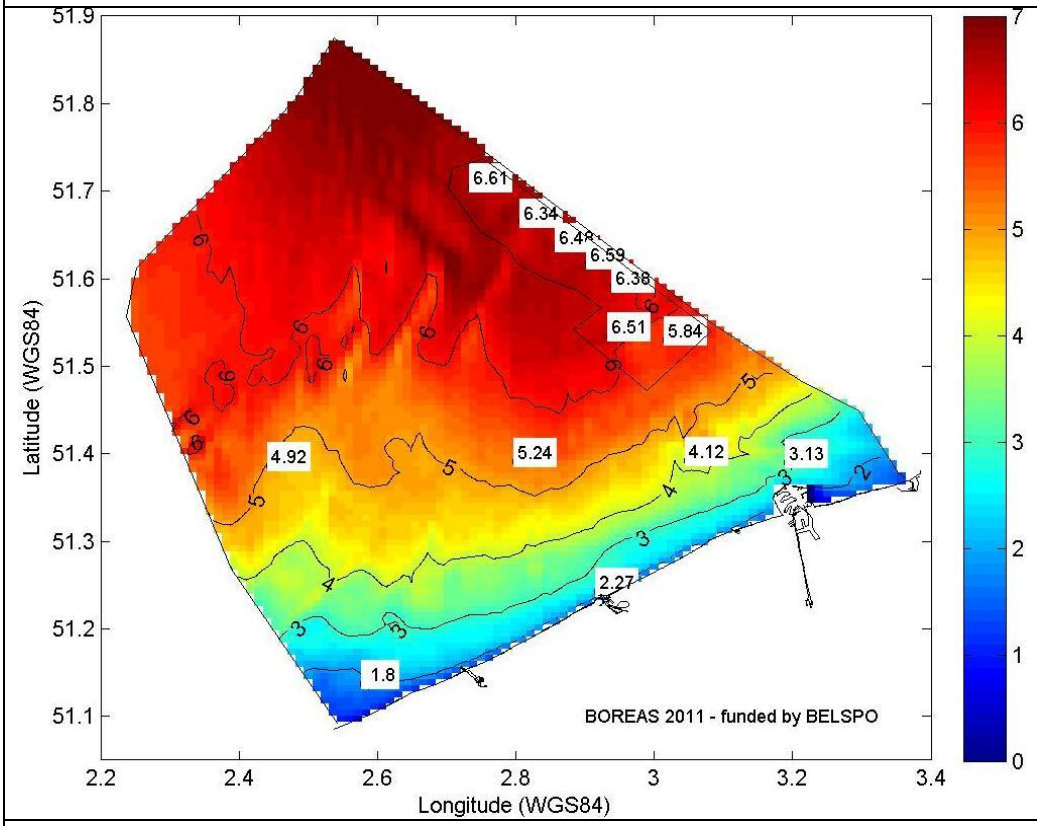

Figure 81: Average wave power (kW/m) for the year 2005 (final, with the 3 corrections).

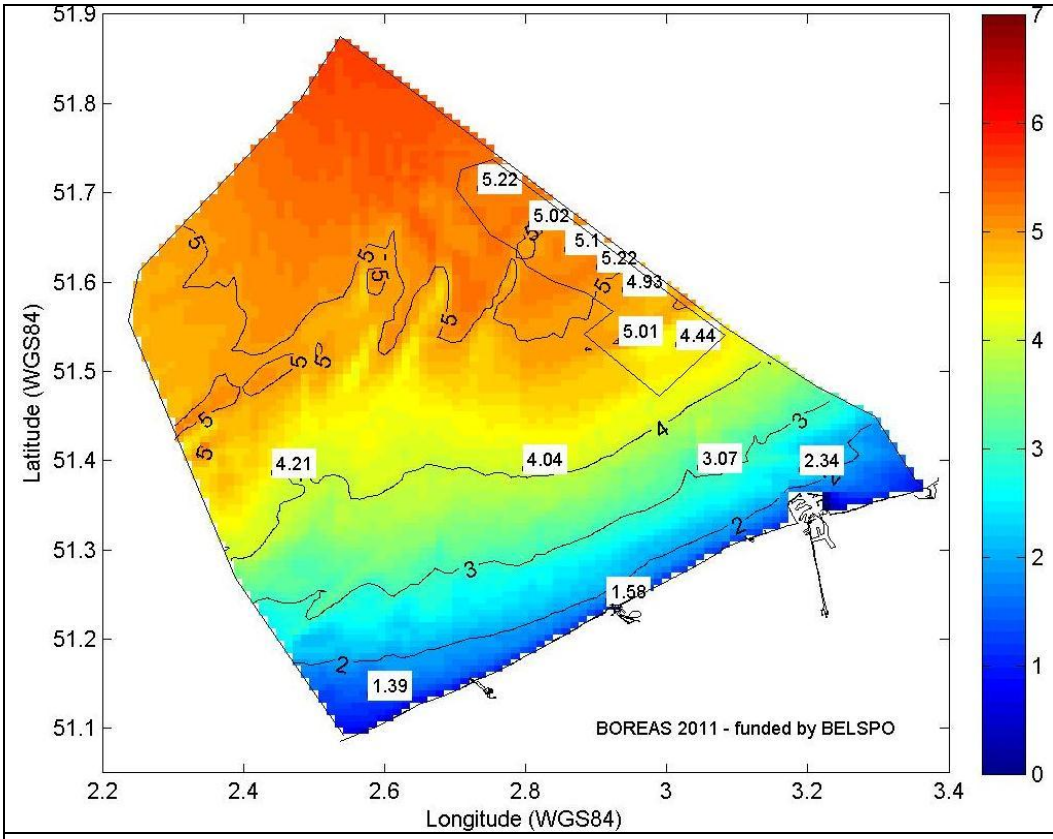

Figure 82: Average wave power (kW/m) for the year 2006 (final, with the 3 corrections) .

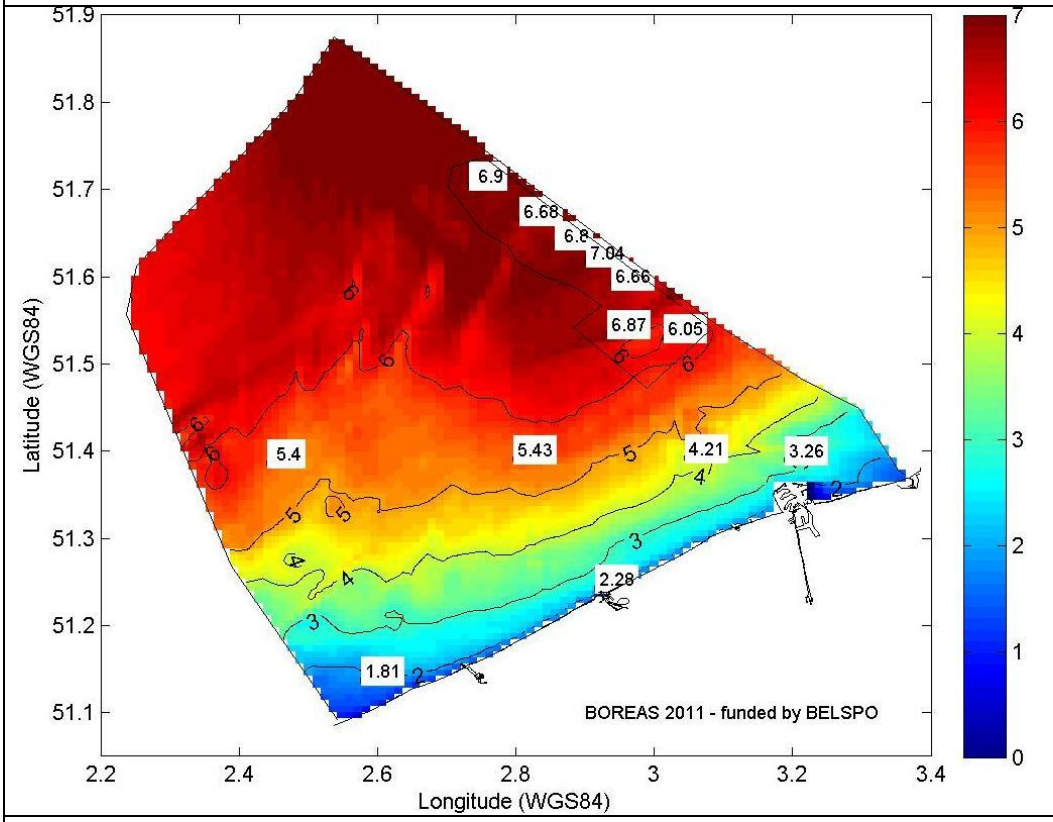

Figure 83: Average wave power (kW/m for the year 2007 (final, with the 3 corrections).

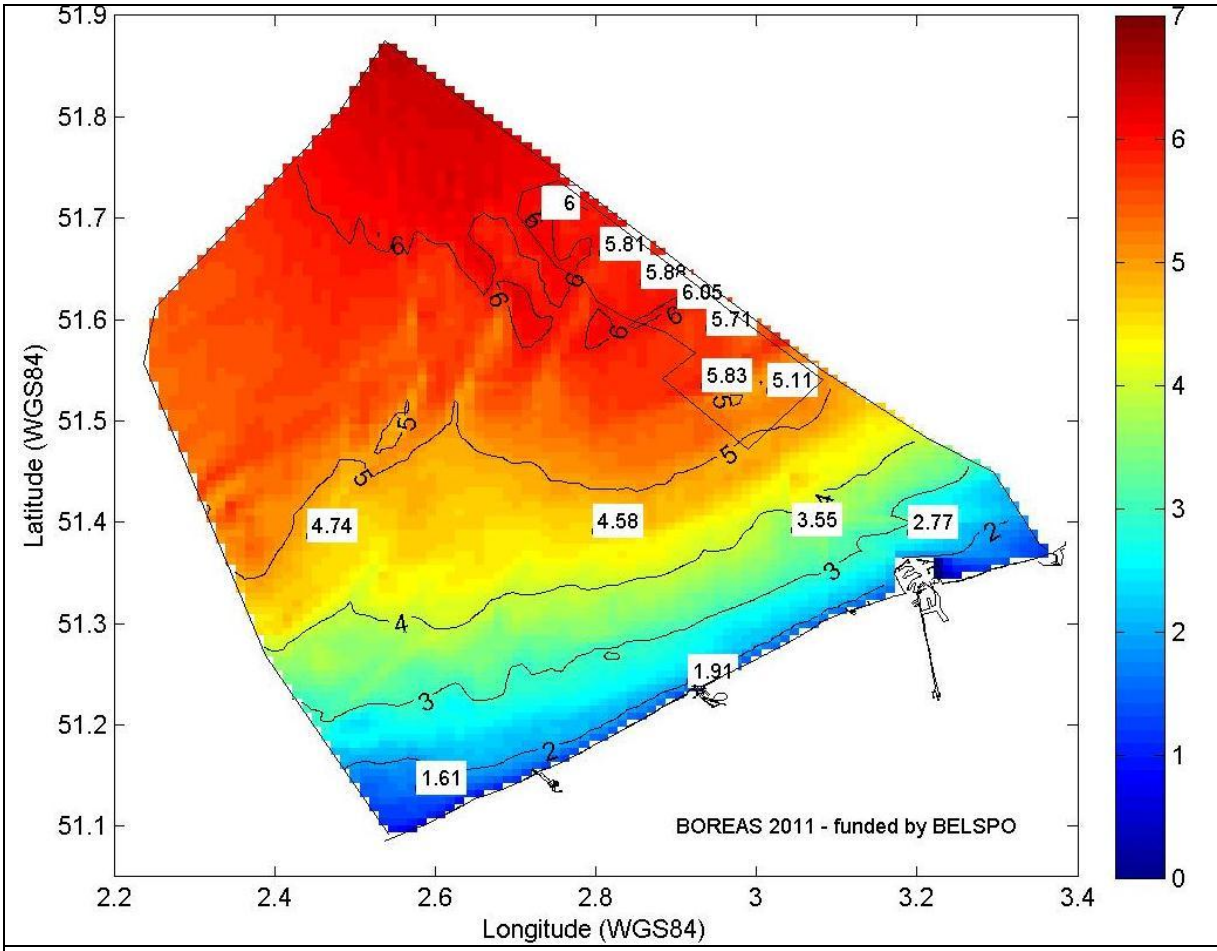

Figure 84: Average wave power (kW/m) for the year 2008 (final, with the 3 corrections).

9.5 Economical parameters (Mathys et al. 2010)

The Net Present Value (NPV) is calculated as:

$$NPV = -I_0 + \sum_{t=1}^{T} \frac{F_t}{(1+r)^t}$$

With :

- I_0 : Initial investment or capital cost
- F_t : Cash flows at time t (excluding the initial investment)
- t : Time
- T : Project time
- r : Disconto rate

A project may be accepted when the NPV > 0, and should be rejected when NPV < 0. When the NPV = 0, the project adds no monetary value to the investor. Decision should be based on other criteria, e.g. strategic positioning or other factors not explicitly included in the calculation (Wikipedia 2011).

The discontorate is determined as the WACC, of Weighted average of cost capital, which is the rate that a company is expected to pay on average to all its security holders to finance its assets:

$$r = k_{cp} \cdot \frac{CP}{CP+D} + (1-t) \cdot R \cdot \frac{D}{CP+D}$$

With :

- CP : Equity [%]
- D : Debts [%]
- t : Tax rate [%]
- R : Interest rate on debts [%]
- k_{cp} : cost of equity in the absence of debt

$$k_{cp} = R_f + (R_m - R_f) \cdot \beta$$

With (according to the Capital asset pricing model) :

- R_f : rate without risk [-]
- R_m : expected return on market [%]
- β : systematic risk [-]

After the determination of the discount rate, the inflation needs to implemented. The inflation is taken at 2.1% (based Eurostat data for '98'-'08 and based on STATBEL data for the period '85-'09 (EUROSTAT 2007; Eurostat 2009; NBB 2009). Hence the discontorate after inflation is calculated as:

$$r_{\text{after\_inflation}} = (1 + r_{\text{before\_inflation}}) \cdot (1 + Inflation) - 1$$

For the system of TGC the rate was calculated at 8.61% after inflation .

10 Bibliography

ABPMER Ltd, Garrad Hassan Ltd, MET Office and Proudman Oceanographic Laboratory (2008a). Atlas of UK Marine Renewable Energy Resources: Atlas pages.

ABPMER Ltd, Garrad Hassan Ltd, MET Office and Proudman Oceanographic Laboratory (2008b). Atlas of UK Marine Renewable Energy Resources: Technical Report.

Allan, G., Gilmartin M., McGregor P. and Swales K. (2011). Levelised costs of Wave and Tidal energy in the UK: Cost competitiveness and the importance of "banded" Renewables Obligation Certificates. Energy Policy **39**(1): 23-39.

Anemoc. (2011). Atlas Numérique d'Etats de mer Océanique et Côtier. from http://anemoc.cetmef.developpement-durable.gouv.fr/.

Aquaret (2008). Aquaret Manual.

ASME (2010). Out of the Vortex, Mechanical Engineering, The magazine of ASME.

Beels, C. (2007). Definition of Sea States - Internal report.

Beels, C. (2009). Optimization of the Lay-out of a Farm of Wave Energy Converters in the North Sea - Analysis of Wave Power Ressources, Wake Effects, Production and Cost., Department of Civil Engineering, Ghent University**:** 496p.

BELPEX. (2009). Website Belgian Power Exchange 5/09/2009, from www.belpex.be.

Blanco, M. I. (2009). The economics of wind energy. Renewable & Sustainable Energy Reviews **13**(6-7): 1372-1382.

Carbon Trust (2006). Future Marine Energy: Results of the Marine Energy Challenge: cost competitiveness and growth of wave and tidal stream energy.

CarbonTrust (2005). Marine Energy Glossary.

Cornett, A. and IEA-OES (2010). Guidance for assessing tidal current energy Resources Final Technical report. OES-IA document No: T02-1.2.

Cruz, J. (2008). Ocean Wave Energy - Current Status and Future Perspectives, Springer-Verlag.

Dalton, G. J., Alcorn R. and Lewis T. (2009). Case study feasibility analysis of the Pelamis wave energy convertor in Ireland, Portugal and North America. Renewable Energy **35**(2): 443-455.

De Vos, L., Mathys P. and De Rouck J. (2009). Rapport INSPA23.123 eindverslag - Studie 'Haalbaarheid kapping Paardemarkt'.

Degraer S. and Brabant R. (2009). Offshore wind farms in the Belgian Part of the North Sea - State of the art after two years of environmental monitoring

Delft University of Technology (2008). SWAN technical documentation and user manual Cycle III version 40,72.

Delgado, R., Fernández L., Monabliu J., Liste M., Verwaest T. and Mostaert F. (2010). BOREAS Technical report - A Comparison of numerical wave data at the Belgian Coast (SD/NS/13A) - Funded by Belspo.

Doorme and IMDC (2006). Afstemming Vlaamse en Nederlandse voorspelling golfklimaat op ondiep water - Deelopdracht 1: Voorbereiding tijdreeksen met randvoorwaarden in opdracht van WLH. Rapport Wetenschappelijke Bijstand.

Dujardin, A., De Clercq B., Vanlede J., Delgado R., van Holland G., De Mulder T. and Mostaert F. (2010a). Verbetering numeriek instrumentarium Zeebrugge: Bouw en afregeling detail model versie 2_0. WL rapporten, 753_08, Waterbouwkundig Laboratorium, Soresma en IMDC, Antwerpen, België.

Dujardin, A., Van den Eynde D., Vanlede J., Ozer J., Delgado R. and Mostaert F. (2010b). BOREAS Technical report - A comparison of numerical tidal models of the Belgian Part of the North Sea (SD/NS/13A) - Funded by Belspo.

EMEC. (2010). EMEC website. from http://www.emec.org.uk.

EquiMar. (2010). Equimar website. from http://www.equimar.org/.

EquiMar, Davey T., Venugopal V., Smith H., Smith G., Lawrence J., Cavaleri L., Bertotti L., Prevosto M., Girard F. and Holmes B. (2010). Equimar D2.7: Protocols for wave and tidal resource assesment.

EquiMar, Venugopal V., Davey T., Smith H., Smith G., Holmes B., Barrett S., Prevosto M., Maisondieu C., Cavaleri L., Bertotti L., Lawrence J. and Girard F. (2011). Equimar D2.2 Wave and Tidal Resource Characterisation.

EUROSTAT (2007). Europe in figures - Eurostat yearbook 2006-07.

Eurostat. (2009). Website. Retrieved 5/6/2009, from http://epp.eurostat.ec.europa.eu/.

Falnes, J. (2002). Ocean Waves and Oscillating Systems: linear interactions including wave-energy extraction., Cambridge University Press.

Fernández, L., Komijani H. and Monabliu J. (2010). BOREAS Technical report - Wave modelling (SD/NS/13A) - Funded by Belspo.

Frigaard, P., Marquis L., Kramer M. and Kofoed J. P. (2010). Wavestar - personal communication.

Giardino, A., Luyten P. and Monbaliu J. (2000). Implementation ot the Coherens parallel code for applications in the North Sea.

Goda, Y. (2000). Random Seas and design of Maritime Structures, World Scientific.

Green Ocean Energy (2010). Green Ocean Energy website.

Harris, R. E. H., Johanning L., Wolfram J. and OREG (2008). Mooring systems for wave energy converters: A review of design issues and choices.

Holmes, B. (2009). Marine Energy Device Development: A Structured Programme to Mitigate Technical & Financial Risk. IEA-OES Annual report 2009. IEA-OES.

Holthuijsen, L. H. (2007). Waves in Oceanic and Coastal Waters.

IEA-OES, Kahn J. and Bhuyan G. (2009a). Ocean energy: global technology development status - March 2009. A report prepared by Powertech Labs Inc. for the IEA-OES Annex I.

IEA-OES, Kahn J., Bhuyan G. and Moshref A. (2009b). Potential Opportunities and Differences Associated with Integration of Ocean Wave and Marine Current Energy Plants in Comparison to Wind Energy, a report prepared by Powertech Labs for the IEA-OES Annex III.

IMDC (2006). Afstemming Vlaamse en Nederlandse voorspelling golfklimaat op ondiep water – Deelopdracht 2: Voortzetting validatie numeriek model in opdracht van WLH. Rapport Wetenschappelijk Bijstand.

IMDC (2008). Afstemming Vlaamse en Nederlandse voorspelling golfklimaat op ondiep water – Deelopdracht 4: Technisch Wetenschappelijke bijstand – Traject Golfklimaat. Rapport Wetenschappelijk Bijstand.

IMDC (2009). Afstemming Vlaamse en Nederlandse voorspelling golfklimaat op ondiep water – Deelopdracht 4: Technisch Wetenschappelijke Bijstand – Traject Onderzoek. Rapport Wetenschappelijk Bijstand.

Khan, M. J., Bhuyan G., Iqbal M. T. and Quaicoe J. E. (2009). Hydrokinetic energy conversion systems and assessment of horizontal and vertical axis turbines for river and tidal applications: A technology status review. Applied Energy **86**(10): 1823-1835.

Lanckneus, J., Van Lancker V., Moerkerke G., Van den Eynde D., Fettweis M., De Batist M. and Jacobs P. (2001). Investigation of natural sand transport on the Belgian continental shelf, BUDGET (Beneficial Usage of Data and Geo-Environmental Techniques). Final report. Federal Office for Scientific, Technical and Cultural Affairs (OSTC).

Langhamer, O. (2009). Wave energy conversion and the marine environment - Colonization patterns and habitat dynamics. Faculty of science and technology, Uppsala University.

Leijon, M., Boström C., Danielsson O., Gustafsson S., Haikonen K., Langhamer O., Strömsted E., Stalberg M., Sundberg J. and Svensson O. (2008). Wave Energy from the North Sea: Experiences from the Lysekil Research Site. Surveys in Geophysics **29**: 221-240.

Luyten, P. J., Jones J. E., Proctor A. and BMM. (1999). COHERENS - A coupled hydrodynamical-ecological model for regional and shelf seas: User Documentation. MUMM Report, Management Unit of the Mathematical Models of the North Sea, 911pp., from http://www.mumm.ac.be/EN/Models/Coherens/index.php.

Luyten, P. J., Jones J. E., Proctor A. and BMM. (2011). COHERENS - A coupled hydrodynamical-ecological model for regional and shelf seas: User Documentation. MUMM Report, Management Unit of the Mathematical Models of the North Sea, version 2, RBINS-MUMM report, Royal Belgian Institute of Natural Sciences. 1177pp., from http://www.mumm.ac.be/EN/Models/Coherens/index.php.

Marquis, L., Kramer M. and Frigaard P. (2010a). First Power Production figures from the Wave Star Roshage Wave Energy Converter. ICOE, Bilbao.

Marquis, L., Kramer M. and Frigaard P. (2010b). Wave Star: First Power Production Results from the Wave Star Roshage Wave Energy Convertor - Presentation of the 3rd International Conference on Ocean Energy, 6 October, Bilbao., from http://wavestarenergy.com/sites/default/files/Wave%20Star%20Energy%20presentation%20ICOE%202010%20UPDATED%20After%20Conference.pdf.

Mathys, M. (2009). The Quaternary geological evolution of the Belgian Continental Shelf, southern North Sea, PhD thesis.

Mathys, P. and De Rouck J. (2011a). BOREAS Intermediate report - Wave and tidal energy energy convertors and their suitability for the Belgian Part of the North Sea.

Mathys, P. and De Rouck J. (2011b). BOREAS Technical report - Wave and tidal current resource assessment and Economical analysis.

Mathys, P., De Rouck J., Fernandez L., Muñoz M. L., Komijani H., Van den Eynde D., Monbaliu J., Ozer J., Delgado R., Dujardin A., Vanlede J., Verwaest T. and Mostaert F. (2011c). BOREAS Technical report: Summary of model set-up and validation.

Mathys, P., Meirschaert V., Portilla J., De Rouck J., De Volder G. and Dewilde L. (2010). OPTIEP-BCP: Optimalisering van de basiskennis over het energiepotentieel op het Belgisch Continentaal Plat (Contract AP/42 in opdracht van het Federaal Wetenschapsbeleid).

Mattarolo, G., Lafon F. and Benoit M. (2008). Wave energy resource off the French coasts: the ANEMOC database applied to the energy yield evaluation of Wave Energy Converters. ICOE, Brest.

Monbaliu, J., Padilla-Hernandez R., Hargreaves J. C., Albiach J. C. C., Luo W. M., Sclavo M. and Gunther H. (2000). The spectral wave model, WAM, adapted for applications with high spatial resolution. Coastal Engineering **41**(1-3): 41-62.

MUMM. (2009). Tidal Currents. Retrieved 10/09/2009, from http://www.mumm.ac.be/EN/Management/Atlas/tidalcurrents.php.

Nadeau, M. (2010). Personal communication regarding the integration of TRLs in the Technical Specifications of TC114.

NBB. (2009). Website Nationale Bank van België. from www.nbb.be.

Ozer, J., Padilla-Hernandez R., Monbaliu J., Fanjul E. A., Albiach J. C. C., Osuna P., Yu J. C. S. and Wolf J. (2000). A coupling module for tides, surges and waves. Coastal Engineering **41**(1-3): 95-124.

Pelamis Wave Power (2010). Power Matrix of Pelamis.

Raghaven, K., Bernitsas M. and Maroulis D. E. (2007). Effect of bottom boundary on VIV for energy harnessing. OMAE 2007, San Diego, USA.

SBB. (2011). World steel price tracker on http://www.steelbb.com/.

Schwartz, A. (2008). "Fish" marine turns ocean vibrations into energy. from http://cleantechnica.com/2008/11/24/fish-machine-turns-ocean-vibrations-into-energy/.

SEEWEC, De Rouck J. and Meirschaert V. (2009). SEEWEC - Publishable Final Activity Report.

Spee, E. J. (2010). WAQUA / TRIWAQ – two- and three-dimensional shallow water flow model. Technical documentation. Version 3.15, march 2010. Ministry of Transport, Public Works and Water Management; Directorate-General for Public Works and Water Management, Netherlands.

Straume, I. (2010). Straumekraft AS: Durable and profitable wave power. ICOE, Bilbao.

USDOE (2008). Report to Congress - Potential Environmental Effects of Marine and Hydrokinetic Energy Technologies.

Van Damme, L., De Rouck J. and Mathys P. (2009). Zeebrugge outer harbor : the evolution of scouring over the past 20 years ICCE 2008.

Van den Eynde, D., Kerkhof F., Lauwaert B. and Pichot G. (2007). Ontwikkeling van de zandbank ter hoogte van de Heist - Eindrapport.

Van den Eynde, D. and Ozer J. (2010). BOREAS Technical report - Tidal current modelling (SD/NS/13A) - Funded by Belspo.

van Kessel, T. and Vanlede J. (2010). Impact of harbour basins on mud dynamics Scheldt estuary in the framework of LTV. Deltares: Delft, Netherlands.**:** 29.

Van Lancker, V., Deleu S., Bellec V., Le Bot S., Verfaillie E., Fettweis M., Van den Eynde D., Pison V., Wartel S., Monbaliu J., Portilla J., Lanckneus J., Moerkerke G. and S. D. (2004). Management, research and budgetting of aggregates in shelf areas related to end-users (Marebasse). Scientific Report Year 2. Belgian Science Policy**:** 144.

Van Lancker, V., Du Four I., Verfaillie E., Deleu S., Schelfaut K., Fettweis M., Van den Eynde D., Francken F., Monbaliu J., Giardino A., Portilla J., Lanckneus J., Moerkerke G. and Dergraer S.

(2007). Management, research and budgetting of aggregates in shelf seas related to end-users (Marebasse). Final Scientific Report. Belgian Science Policy, 125pp.

Vlaamse Baaien. (2010). Vlaamse Baaien 2100: multifunctioneel eiland. from http://www.vlaamsebaaien.com/09-multifunctioneel-eiland.

Waters, R., Engström J., Isberg J. and Leijon M. (2009). Wave climate off the Swedish west coast. Renewable Energy **34**(6): 1600-1606.

Waveplam (2009). State of the Art Analysis - A Cautiously Optimistic Review of the Technical Status of Wave Energy Technology.

Yago, T. E. (2009). Planta de Energia de las olas de Mutriku. 3ª Jornada Internacional de Energía Marina, Bilbao.